Durham E-Theses

Molecular characterisation of neurotransmitter receptors in the CNS of the stargazer mutant mouse

Tiwari, Priyanka

Molecular Characterisation of Neurotransmitter Receptors in the CNS of the Stargazer Mutant Mouse

Priyanka Tiwari

A thesis submitted to the University of Durham in accordance with the requirements for the degree of Doctor of Philosophy

School of Biological and Biomedical Sciences,

University of Durham.

December 2002

1 2 DEC 2003

Abstract

The mutant mouse stargazer shows both ataxia and absence epilepsy from P14 onwards. A PCR amplification strategy was utilised to identify adult (i.e. > 3 months) +/stg from +/+ mice, which share the same phenotype, for use for breeding purposes. The same technique was employed to identify +/+, +/stg and stg/stg neonates (i.e. < 7 days old) for cell culture purposes, since the stargazer phenotype is not apparent at this age.

GABA$_A$ receptor α_6 subunit expression levels were significantly decreased in adult stargazer (stg/stg) cerebella when compared to control (+/+ and +/stg) cerebella. Interestingly, autoradiography using [^{3}H] Ro15-4513 revealed an apparent upregulation in $\alpha_4\gamma$-containing receptors in the adult stargazer dentate gyrus.

No significant differences in the expression of NMDAR subunits were detected between adult control and stargazer brain membranes.

A significant decrease was observed in AMPAR subunit expression within the adult stargazer cerebellum, particularly with the GluR2 subunit, which was reduced by 73 %. This decrease was replicated in cerebellar granule cells cultured from stargazer neonates, which also expressed at the cell surface only 18 % of the total GluR2 found in control granule cells.

Immunohistochemistry analyses using mouse anti-stargazin antibodies revealed stargazin to be found throughout the adult control brain, with highest levels of expression being within the hippocampus and cerebellum. Stargazin protein, however, was not expressed in adult stargazer forebrain nor in adult stargazer cerebellar membranes.

Finally, immunoaffinity columns using the anti-stargazin antibodies were prepared and demonstrated that stargazin could be purified from adult control mouse brain extracts. Moreover, AMPAR subunits co-immunoprecipitated, indicating an association *in vivo*.

Declaration

I confirm that no part of the material presented has previously been submitted for a degree in this or in any other university. If material has been generated through joint work, my independent contribution has been clearly indicated. In all other cases, material from the work of others has been acknowledged and quotations and paraphrases suitably indicated.

Part of this work has been publicised in the following manner:

Poster Presentations:

Ives JH, Drewery DL, Seighart W, Tiwari P, Wright MF, Lucocq JM, Payne H, Thompson CL (2002) Stargazin and its role in the expression, assembly and trafficking of cerebellar granule cell-specific GABA$_A$ receptor subtypes. Neuroscience North-East Conference, University of Sunderland.

Thompson CL, Ives JH, Drewery DL, Seighart W, Tiwari P, Wright MF, Lucocq JM (2002) Stargazin and its role in the expression, assembly and trafficking of cerebellar granule cell-specific GABA$_A$ receptor subtypes. SFN, USA.
Abstract published in Soc Neurosci Abstr (2002) 433.13

Tiwari P, Ives JH, Thompson CL (2001) Impaired AMPA receptor expression in stargazer mice: evidence of stargazin-AMPAR complexes *in vivo*. BNA, Harrogate, UK.
Abstract published in British Neurosci Assoc Abstr (2001) 16:77

Ives JH, Drewery DL, Tiwari P, Thompson CL (2001) Impaired GABA$_A$ receptor expression and trafficking in stargazer cerebellar granule cells. BNA, Harrogate, UK.
Abstract published in British Neurosci Assoc Abstr (2001) 16:78

Ives JH, Drewery DL, Tiwari P, Thompson CL (2000) Impairment of cerebellar GABA-A receptor expression in the ataxic mutant mouse, stargazer. FENS, Brighton, UK.
Abstract published in Eur J Neurosci (2000) 12 (11):45

Oral Presentations:

Kaja S, Wilton A, Bingley M, Tiwari P, Thompson CL (2002) Expression of cerebellar granule cell-specific GABA$_A$ receptors is impaired in the epileptic and ataxic tottering mouse. Neuroscience North-East Conference, University of Sunderland.

Manuscripts in preparation:

Tiwari P, Ives JH, Sieghart W, Wilkinson D, Wright M, Thompson CL; The stargazer mutation leads to abnormal expression of AMPA and $GABA_A$ receptors in the dentate gyrus.

Ives JH, Drewery DL, Lucocq J, Sieghart W, Tiwari P, Doran B, Wright M, Thompson CL; $GABA_A$ receptor assembly and trafficking is impaired in cerebellar granule cells of the ataxic mutant mouse, stargazer: evidence that stargazin directly interacts with receptor subtypes *in vivo*.

Acknowledgments

List of Tables

Materials

NMDA receptor expression in stargazer brain

Characterisation of AMPA receptor expression within stargazer mouse brain

Stargazin expression and solubilisation from mouse brains

List of Figures

Materials

GABA$_A$ receptor expression in stargazer mice

NMDA receptor expression in stargazer brain

Characterisation of AMPA receptor expression within stargazer mouse brain

Stargazin expression and solubilisation from mouse brains

Surface expression of GluR2 in cultured cerebellar granule cells

Abbreviations

ABP	AMPA receptor binding protein
AMPA	DL-α-amino-3-hydroxy-5-methylisoxazole-4-propinoic acid
AMPAR	AMPA receptor(s)
AMPS	Ammonium persulphate
AP5	2-amino-5-phosphonopropionic acid
aq.	Aqueous
BDNF	Brain derived neurotrophic factor
BDZ	Benzodiazepine
BDZ-IS	Benzodiazepine-insensitive
B_{max}	Maximum number of binding sites
bp	Base pair(s)
BS^3	Bis (sulfosuccinimidyl) suberate
BSA	Bovine serum albumin
^oC	Degrees Celsius
Ca^{2+}	Calcium (ion)
$CaCl_2$	Calcium chloride
CaMKII	Calcium/calmodium-dependent protein kinase II
cAMP	Cyclic-adenosine 3',5'-monophosphate
cDNA	Complimentary DNA
CGCs	Cerebellar granule cells
CHAPS	3-[(3-cholamidopropyl)-dimethylammonio]-1-propanesulfonate
cm	Centimetre
CNQX	6-cyano-7-nitroquinoxaline-2,3-dione
CO_2	Carbon dioxide
ctl	Control
Da	Daltons
DAB	3,3' diaminobenzidine tetrahydrochloride

dH2O	Distilled water
DIV	Day(s) in vitro
DMEM	Dulbecco's Modification of Eagle's Medium
DMP	Dimethylpimelimidate
DMSO	Dimethyl sulphoxide
DNA	Deoxyribonucleic acid
dNTPs	Deoxynucleotide triphosphates
dpm	Disintegrations per minute
DTT	Dithiothreitol
ECL	Enhanced chemiluminesence
EDTA	Ethylenediamine-tetra-acetic acid
EGTA	1,2-di(2-aminoethoxy)ethane-NNN'N'-tetra-acetic acid
ELISA	Enzyme-linked immunoabsorbent assay
EPSC	Excitatory post-synaptic current
FCS	Foetal calf serum
FDA	Fluorescein diacetate
FDU	5-fluoro-2'-deoxyuridine
g	Gram
g	Gravitational force
GABA	γ-amino-butyric acid
GABAR	GABA$_A$ receptor
GAERS	Genetic Absence Epilepsy Rats from Strasbourg
GRIP	Glutamate receptor interacting protein
GYKI 52466	1-(4-aminophenyl)-4-methyl-7,8-methylenedioxy-5H-2,3-benzodiazepine
H2O2	Hydrogen peroxide
H2SO4	Sulphuric acid
HCl	Hydrogen chloride
HEBSS	HEPES-containing Earle's balanced salt solution

HEK	Human embryonic kidney (cell)
HEPES	N[2-hyroxyethyl]piperazine-N'-[2-ethanesulfonic acid]
hr	Hour
HRP	Horse radish peroxidase
IgG	Immunoglobulin G
K^+	Potassium (ion)
K_D	Dissociation constant
kDa	KiloDaltons
KCl	Potassium chloride
KH_2PO_4	Potassium dihydrogen orthophosphate
KSCN	Potassium thiocyanate
L	Litre
Luminol	5-amino-2,3-dihydro-1,4-phthalazinedione
M	Molar
MAGUK	Membrane associated guanylate kinase
MBS	3-maleimidobenzoic acid N-hydroxysuccinimide ester
mEPSC	Miniature excitatory post-synaptic current
mg	Milligram
Mg^{2+}	Magnesium (ion)
$MgSO_4$	Magnesium sulphate
mIPSC	Miniature inhibitory post-synaptic current
ml	Millilitre
MK-801	Dilozcipine, (+)-5-methyl-10,11-dihydro-5H-dibenzo-[a,d]cyclohepten-5,10-imine maleate
mM	Millimolar
M_r	Molecular weight
mRNA	Messenger RNA

N₂	Nitrogen
Na⁺	Sodium (ion)
NaCl	Sodium chloride
NADPH	Reduced nicotinamide adenosine dinucleotide phosphate
NGF	Nerve growth factor
NHS-ss-biotin	Sulfosuccinimidyl 2-(biotinamido)ethyl-1,3-dithiopropionate
NaHCO₃	Sodium hydrogen carbonate
NaH₂PO₄	Sodium dihydrogen orthophosphate
Na₂HPO₄	Disodium hydrogen orthophosphate
NaNO₂	Sodium nitrite
NaOH	Sodium hydroxide
NBQX	2,3-dihydroxy-6-nitro-7-sulphamoylbenzo[f]quinoxaline-2,3-dione
nM	Nanomolar
NMDA	N-methyl-D-aspartate
NMDAR	NMDA receptor(s)
NSB	Non-specific binding
NSE	Neuron-specific enolase
NSF	N-ethylmaleimide-sensitive factor
NT-3	Neurotrophin 3
O₂	Oxygen
OD	Optical density
P	Postnatal (day)
PBS	Phosphate buffered saline
PBS-T	PBS-Triton X-100
PCR	Polymerase chain reaction
PDZ	Postsynaptic density 95/disc large/zonula occludens-1
PEI	Polyethyleneimine
PICK1	Protein interacting with C kinase-1
PMSF	Phenylmethanesulphonyl fluoride
PSD-93	Postsynaptic density protein of 93 kDa
PSD-95	Postsynaptic density protein of 95 kDa

SAP97	Synapse associated protein of 97 kDa
SAP102	Synapse associated protein of 102 kDa
SDS	Sodium dodecyl sulphate
SDS-PAGE	Sodium dodecyl sulphate polyacrylamide gel electrophoresis
sEPSC	Spontaneous excitatory post-synaptic current
SS	Iso-osmotic saline solution
stg	Stargazer
SWD	Spike-and-wave discharges
TBE	Tris-boric acid-EDTA
TBPS	t-butylbicyclophosphorothionate
TBS	Tris buffered saline
TE	Tris-EDTA
TEMED	N,N,N',N'-tetramethylethylenediamine
Thimerosal	(Mercury-[(o-carboxyphenyl)thio]ethyl)sodium salt
TM	Transmembrane domain
Tris	Tris(hydroxymethyl)methylamine
Triton X-100	iso-octylphenoxypolyethoxyethanol
Tween-20	Polyoxyethylenesorbitan monolaurate
μl	Microlitre
μM	Micromolar
UV	Ultraviolet
VOCC	Voltage operated calcium channel
v/v	Volume/volume
w/v	Weight/volume
YM90K	6-(1H-imidazol-1-yl)-7-nitro-2,3(1H,4H)-quinoxalinedione hydrochloride

Introduction

The amino acid glutamate is a major excitatory neurotransmitter within the central nervous system, where it is involved in synaptogenesis, synaptic plasticity and in the pathogenesis of neuropsychiatric diseases. It may also be further metabolised to produce the inhibitory neurotransmitter, γ-amino-butyric acid (GABA). As this work involved studying the potential roles of the $GABA_A$ and glutamate receptors in the brain of the mutant mouse stargazer, a brief review of the published literature on the stargazer and an overview of the current understanding of these receptors are below.

1.1 The mutant mouse, stargazer

The stargazer mutation (stg) arose spontaneously in the A/J inbred strain of mice at The Jackson Laboratory, MA, USA, and was subsequently bred onto the $B6C3Fe^{+}$ background strain. The mutation was found to reside on mouse chromosome 15 and due to a recessive mutation (Noebels et al., 1990). The stg mutation consists of an early viral transposon insertion into intron 2 of the stargazin gene (*Cacng2*) that leads to its premature transcriptional arrest (Letts et al., 1998). The stargazin gene encodes for a brain-specific $36 - 41$ kDa glycosylated protein (Letts et al., 1998; Sharp et al., 2001), which shows structural and amino acid similarity to the previously identified $\gamma 1$ subunit of the skeletal muscle-specific voltage-operated calcium channel (VOCC). The distribution of both stargazin mRNA and protein is discussed in chapter 6.

1.1.1 The CACNG family of γ subunits

The discovery of stargazin expanded the γ family of neuronal calcium channels – to γ_1 and γ_2 (stargazin) – whilst subsequent work by others led to the identification of further γ subunits. Currently, eight γ subunits, γ_1 to γ_8, along with their genes, *CACNG1* to *CACNG8* respectively, have been identified.

1

Rousset et al. (2001) found that transfection of human γ_2, γ_3 or γ_4 cDNA into cells revealed a strong expression of each of the three subunits which was localised to the cell membranes, indicating that their putative secondary structure involved transmembrane segments. Analyses of the structures of the γ subunits have confirmed the presence of four transmembrane domains, along with intracellular carboxyl and amino termini (Moss et al., 2002; Burgess et al., 2001; Klugbauer et al., 2000; Letts et al., 1998).

The tissue expression of each γ subunit gene has been determined by both Northern blotting and by PCR. Whilst γ_1 mRNA expression has been shown to be present in skeletal muscle (Jay et al., 1990), it has also been detected at very low levels in the human brain (Burgess et al., 2001). Expression of γ_2 and γ_8 mRNAs have been detected in the brain and in the testes whilst that of γ_3 was found only in the brain. γ_{4-7} mRNAs show a more extensive expression, being detected in the brain, the testes, the heart and in the lungs (Burgess et al., 2001; Chu et al., 2001; Green et al., 2001; Klugbauer et al., 2000). Regional differences in the expression of the various subunits within the brain is discussed in chapter 6.

1.1.2 The phenotype of the stargazer mouse

Stargazer mice exhibit ataxia, epilepsy and a distinctive upwards gaze, from which the mouse obtained its name ('star-gazing'). Electrocorticography revealed spontaneous recurrent spike-wave discharges, characteristic of absence epilepsy, and which were accompanied with behavioural arrest. These seizures, which occur in the neocortex, thalamus and hippocampus, are first manifest around P16-18 and remain throughout the normal lifespan of the mouse (Nahm and Noebels, 1998; Di Pasquale et al., 1997; Qiao and Noebels, 1993; Noebels et al., 1990).

The ataxia, which develops around P14, is mild, affecting the hindlimbs. Subsequent behavioural testing revealed an impaired motor co-ordination in stargazer mice. The mice were unable to stay on a stationary rod for more than 5 seconds and fell off immediately when either initiating movement or when the rod was rotated. Swimming tests revealed that the mice had disturbed righting responses and required rescuing to prevent drowning (Qiao et al., 1996; Noebels et al., 1990). Stargazer

mice also showed a severe impairment in the acquisition of classical eye-blink conditioning, which is a model of learning involving the cerebellum (Qiao et al., 1998; for a review of classical eye-blink conditioning, see Kim and Thompson, 1997).

Whilst the stargazer cerebellum has a normal foliation and laminar structure, a delayed migration of granule cells from the external to the internal layers was observed. In the adult stargazer cerebellum, granule cells with elongated nuclei, resembling migrating immature granule cells, were also detected. Although mRNA levels of the neurotrophins NGF (nerve growth factor) and NT-3 (neurotrophin 3) were normal in stargazer cerebella, BDNF (brain derived neurotrophic factor) mRNA was reduced in cerebellar granule cells (Qiao et al., 1998; Qiao et al., 1996).

Within the dentate gyrus of the hippocampus, mossy fibre axon sprouting has been described in the inner molecular layer, 4-6 weeks following the onset of the seizures. No corresponding cell death, gliosis or cellular injury, which have all been associated in other mossy fibre sprouting models, or increase in the intermediate early genes c-Fos, c-Jun and Zif/268, which are involved in mossy fibre synaptic reorganisation, have been found (Nahm and Noebels, 1998; Chafetz et al., 1995; Qiao and Noebels, 1993).

Although stargazin interacts with calcium channel subunits in BHK cells (Letts et al., 1998), *Xenopus* oocytes (Kang et al., 2001), and in mouse forebrain (Sharp et al., 2001), no changes in calcium currents in cerebellar granule cells were observed (Chen et al., 2000). However, Chen et al. (2000) indicated a role for stargazin in the trafficking of AMPA receptors and this is discussed further in chapter 6.

1.2 Glutamate receptors

The glutamate receptors can be divided into two classes: ionotropic and metabotropic glutamate receptors, both of which can be further subdivided. The former are involved in the opening of potassium/sodium/calcium permeable ligand-gated ion channels and were initially pharmacologically distinguished as *N*-methyl-

3

D-aspartate (NMDA) and non-NMDA receptors. The development of more selective ligands allowed the identification of the non-NMDA α-amino-3-hydroxy-5-methylisoxazole-4-propionic acid (AMPA) and kainate receptors. The metabotropic glutamate receptors are linked to G-proteins and, subsequently, to the second messengers inositol triphosphate and cyclic adenosine 3', 5'-monophosphate (cAMP). As the work undertaken here involved the ionotropic NMDA and AMPA glutamate receptors, these shall be further discussed below.

1.2.1 NMDA receptors

The ligand-gated NMDA receptors are multimeric complexes containing an integral cation-selective channel. Both glutamate (or other agonists) and glycine are required for the NMDA receptor (NMDAR) channel to open (Mayer et al., 1989; Kleckner and Dingledine, 1988; Collingridge et al., 1983). At resting membrane potentials, magnesium (in the form of Mg^{2+} ion) binds within the channel, however, membrane depolarisation removes the Mg^{2+} block (Nowak et al., 1984).

The receptor itself consists of NR1 and NR2 subunits (also known as ζ and ε, respectively, in the mouse); eight splice variants of the NR1 subunit have been described (NR1a-h) (Hollmann et al., 1993; Durand et al., 1993; Sugihara et al., 1992; Durand et al., 1992) whilst four NR2 subunits have been identified (NR2A-D) (Monyer et al., 1994; Ishii et al., 1993; Monyer et al., 1992; Kutsuwada et al., 1992; Meguro et al., 1992). A third class of NMDAR subunit, NR3, also exists, of which the NR3A and NR3B subunits have been identified (Nishi et al., 2001; Ciabarra et al., 1995; Sucher et al., 1995).

The subunits consist of an extracellular N-terminus, four membrane associated domains and an intracellular C-terminus. Of the membrane domains, three span the membrane whilst one (TM2) forms an intramembrane loop (Hollmann et al., 1994). The amino terminal contains multiple predicted glycosylation sites whilst the carboxyl terminal contains several predicted phosphorylation sites. All the NR1 and NR2 subunits share an overlap in the final eight amino acids, which contain binding sites for synaptic binding proteins such as PSD95 (Niethammer et al., 1996; Kornau

et al., 1995). The NR3 subunits, however, do not exhibit these consensus sequences (Nishi et al., 2001; Sun et al., 1998).

The NMDAR is composed hetero-oligomers composed of NR1, NR2 and NR3 subunits. Current evidence suggests that the receptor complex is either a trimer of one NR1 subunit and two NR2 subunits; Dunah et al., 1998; Chazot et al., 1994; Luo et al., 1997), a tetramer composed of two NR1 subunits and two NR2 subunits (Laube et al., 1998) or a pentamer of NR1 subunits and NR2 subunits (Hawkins et al., 1999; Premkumar and Auerbach, 1997; Ferrer-Montiel and Montal, 1996). A small number of receptor complexes, however, appear to be comprised of one NR1 and one NR2 subunits (Dunah et al., 1998; Luo et al., 1997). As little is known about the NR3 subunit, the exact subunit composition of these receptors is still unknown. However, NR3A has been shown to co-immunoprecipitate with NR1 and NR2B subunits and that co-assembly of NR1/NR2A/NR3A subunits were required for the formation of functional NR3A-containing receptors (Perez-Otano et al., 2001; Das et al., 1998).

The exact subunit composition of the NMDAR complex does, however, depend on both age and region of the brain. The NR1 subunit is ubiquitously distributed throughout the brain. The NR2 subunits have a more select distribution, with the NR2A and NR2D subunits found throughout the brain, the NR2B is found mainly in the forebrain and the NR2C subunit is found in the cerebellum. The distribution of NMDAR subunits is discussed further in section 4.3.

The NR1 subunit is regarded as being obligatory as it is required for the formation of a functional receptor channel. The NR2 subunits modulate the receptor and expression of the individual subunits confers the biophysical and pharmacological properties associated with the different receptor subtypes (Monaghan and Larsen, 1997; Ishii et al., 1993; Ikeda et al., 1992). The NR3 subunits are also regulatory subunits but act in a dominant-negative manner, depressing the whole cell current (Nishi et al., 2001; Perez-Otano et al., 2001; Das et al., 1998).

5

The binding site for glutamate is formed by the NR2 subunits (Anson et al., 1998; Laube et al., 1997). Whilst the binding site for glycine is found on the NR1 subunit, the NR2 subunits modify the interaction between NR1 and glycine (Honer et al., 1998; Wafford et al., 1995; Wafford et al., 1993). Agonists and antagonists exist for both the glutamate and glycine binding sites. Agonists at the glutamate-binding site include L-aspartate (Patneau and Mayer, 1990) and 2-(carboxycyclopropyl)glycine (L- and D-CCG-IV) (Kawai et al., 1992; Kudo et al., 1991). A wide range of competitive antagonists have been developed, and these include 2-amino-5-phosphopentaoic acid (also known as D-AP5) (Olverman et al., 1988; Murphy et al., 1987), 3-[(±)-2-carboxypiperazin-4-yl]propyl-1-phosphonic acid (CPP) (Hatta et al., 1991; Lehmann et al., 1987; Harris et al., 1986) and ifenprodil, which is a high affinity antagonist in NR2B-containing receptors (Gallagher et al., 1996; Priestley et al., 1995; Williams, 1993).

Glycine site agonists include the amino acids D-serine and D-alanine (Mothet et al., 2000; Matsui et al., 1995; Wroblewski et al., 1989; Fadda et al., 1988). Kynurenate and its derivatives, for example, 7-chloro-kynurenate and 5-iodo-7-chlorokynurenate (which is also known as L-683,344), act as antagonists at the glycine site (Foster et al., 1992; Kessler et al., 1989; Kemp et al., 1988) as do the 2-carboxyindoles (Leeson et al., 1991; Huettner, 1989) and GV 150526A (Mugnaini et al., 2000; Mennini et al., 1997).

Non-competitive antagonists at the NMDA receptor include phencyclidine, ketamine and MK-801, which all act within the ion channel of the receptor (Porter and Greenamyre, 1995; Huettner and Bean, 1988; Wong et al., 1988). The NMDA receptor also contains binding sites for zinc, lead and redox agents such as dithiothreitol (Hollmann et al., 1993; Guilarte et al., 2000; Aizenman et al., 1989).

NMDARs have been implicated in a number of physiological conditions such as pain (for review, see Chizh et al., 2001), long-term potentiation, which is a model of learning and memory (for reviews, see Kullmann et al., 2000, and Nicoll and Malenka, 1999), and excitotoxicity (for review, see Lynch and Guttmann, 2002; Sattler and Tymianski, 2001). NMDA receptors have also been implicated in ataxia

and in absence epilepsy, which are both seen in stargazer mice. These roles of the NMDA receptor shall be discussed further in chapter 4.

1.2.2 AMPA receptors

AMPA receptors (AMPARs), like NMDARs, are hetero-oligomeric receptors containing an ion channel. The receptor itself consists of four subunits – GluR1, GluR2, GluR3 and GluR4, which are also known as GluRA-D (Boulter et al., 1990; Keinanen et al., 1990). They share the same structure as NMDAR subunits; i.e. three transmembrane domains and one re-entrant membrane loop (TM2). The N-terminus is extracellular whilst the C-terminus is intracellular (Sutcliffe et al., 1996; Bennett and Dingledine, 1995). Furthermore, each subunit can exist in a flip or flop version, created by alternative splicing of a 115 bp region of mRNA (Monyer et al., 1991; Sommer et al., 1990). RNA editing of the GluR2 subunit results in a glutamine residue being changed to an arginine residue, thereby rendering edited GluR2-containing receptors relatively calcium impermeable (Sommer et al., 1991; Hume et al., 1991).

Various studies have been undertaken to determine the stoichiometry of the AMPARs. Whilst some have suggested that they are pentameric structures (Archibald et al., 1998; Ferrer-Montiel and Montal, 1996; Wenthold et al., 1992), other studies have suggested that the receptor complex is a tetrameric structure, comprising of two different subunits (Mansour et al., 2001; Robert et al., 2001; Mano and Teichberg, 1998).

Early in development, electrophysiological approaches have revealed some synapses containing functional NMDARs lack AMPAR-mediated responses. As NMDARs are blocked by magnesium at physiological resting potentials, no currents are mediated by the receptors following application of glutamate, thereby leading these synapses to be referred to as 'silent synapses'. Later in development, these synapses subsequently acquire AMPARs (Pickard et al., 2000; Petralia et al., 1999; Gomperts et al., 1998; Isaac et al., 1997; Wu et al., 1996). A similar redistribution of AMPARs to the synapse can be observed following activation of synaptic NMDARs (Lu et al., 2001; Pickard et al., 2001; Shi et al., 1999).

7

The subunit expressions of the AMPARs show a developmental switch in a number of brain regions. Within the neocortex, P16-21 pyramidal neurons show an increased expression of GluR2 when compared to P13-15 neurons. Levels of GluR1 and GluR4 did not change, suggesting that GluR2 levels are developmentally upregulated relative to both GluR1 and GluR4 (Kumar et al., 2002). A similar selective upregulation of GluR2 subunits was also observed in cultured hippocampal neurons (Pickard et al., 2000). Hippocampal GluR4 levels, however, show a decrease in expression over the same time period; whilst high levels of GluR4 were detected by immunoblotting in P1-5 hippocampal slices (and low levels of GluR1, GluR2 and GluR2/3 subunit proteins), protein levels soon decrease to undetectable levels by P15 (Zhu et al., 2000). In the cerebellum, whilst levels of GluR1 increased only moderately with development, GluR4 expression increased 15-fold (Ripellino et al., 1998). The subunit compositions of AMPARs in the adult brain are discussed further in chapter 5.

A number of AMPAR agonists and antagonists have been developed. Agonists selective for AMPARs are based on either the structure of AMPA or of willardiine. Analogues of AMPA with agonist properties include (RS)-2-amino-3-(3-carboxy-5-methyl-4-isoxazolyl)propionic acid (ACPA) (Stensbol et al., 1999; Wahl et al., 1996) and (S)-2-amino-3-(3-hydroxy-5-phenyl-4-isoxazolyl)propionic acid ((S)APPA) (Ebert et al., 1994a; Ebert et al., 1994b). Willardiine compounds that show agonist activity at AMPARs include 5-fluorowillardiine and 5-ionowillardiine (Hawkins et al., 1995; Wong et al., 1994). Cyclothiazide potentiates the responses at AMPARs by reducing or inhibiting the desensitisation of the receptor (Donevan and Rogawski, 1998; Wong and Mayer, 1993; Trussell et al., 1993) whilst potassium thiocyanate promotes receptor desensitisation (Donevan and Rogawski, 1998; Arai et al., 1995).

Competitive antagonists include the quinoxalinedione compounds CNQX and NBQX, however, these compounds also bind to kainate receptors but to a much lower degree (Wilding and Huettner, 1996; Sheardown et al., 1990; Honore et al., 1988; Fletcher et al., 1988). An analogue of CNQX, YM90K, has also been shown to be a competitive AMPAR antagonist (Shimizu-Sasamata et al., 1996; Ohmori et al.,

1994). Similarly, the Eli Lilley compound LY293558 has been shown to be a competitive AMPAR antagonist, however, it is also has some antagonistic activity at kainate receptors (Bleakman et al., 1996, Schoepp et al., 1995).

The development of AMPAR antagonists has led to the suggestion that they may have therapeutic potential in a number of neurodegenerative disorders involving glutamate. Both NBQX and YM90K show neuroprotection in models of ischaemia (Kawasaki-Yatsugi et al., 1998, Umemura et al., 1997, Graham et al., 1996; O'Neill et al., 1996, Pellegrini-Giampietro et al., 1994, Sheardown et al., 1993). Indeed, antisense oligonucleotides targeted to GluR2 mRNA led to a decrease in both GluR2 mRNA and protein levels before causing neurodegeneration in the hippocampus. Administration of CNQX protected against this cell death (Oguro et al., 1999). GluR2 subunits have also been shown to be decreased in hippocampal pyramidal neurons following kainate-induced status epilepticus, prior to the degeneration of these cells (Grooms et al., 2000). Absence seizures, which are observed in stargazer mice, lead to a decreased expression of GluR2 subunits in the cerebral cortex, implying that a similar decrease may be observed in stargazer (Hu et al., 2001). The levels of expression of the AMPAR subunits in stargazer are discussed further in chapters 5 and 7.

Finally, AMPARs have also been implicated in classical eye-blink conditioning, which is impaired in stargazer, and ataxia, which is seen in the stargazer mouse. These roles of the AMPAR are discussed further in chapter 5.

1.3 GABA receptors

GABA is the major inhibitory neurotransmitter within the mammalian central nervous system. Three types of GABA receptor have been identified on the basis of their pharmacology and electrophysiology: the predominant type, termed $GABA_A$, and a recently identified type, $GABA_C$, are linked to chloride channels, whereas $GABA_B$ receptors are G-protein coupled receptors affecting K^+ or Ca^{2+} channels (for reviews, see Rudolph et al., 2001; Billinton et al., 2001; Zhang et al., 2001).

The GABA$_A$ receptor (GABAR) is a pentameric receptor comprising of $\alpha_1 - \alpha_6$, $\beta_1 - \beta_4$, $\gamma_1 - \gamma_3$, δ, ϵ, π, θ and $\rho_1 - \rho_3$ subunits (for reviews, see Sieghart and Sperk, 2002; Barnard et al., 1998). All GABAR subunits consist of a large extracellular N-terminus and four transmembrane domains, with a large intracellular loop between TM3 and TM4, and a short extracellular C-terminus (Schofield et al., 1987). Co-expression of α, β and γ subunits are required for a fully functioning receptor and most native GABARs appear to be composed of these subunits (Tretter et al., 1997; Araujo et al., 1996; Benke et al., 1994; Hadingham et al., 1992; Fritschy et al., 1992; Benke et al., 1991b). The δ, ϵ, π and θ subunits appear to form functional receptors when they are co-expressed with α and β subunits (Neelands and Macdonald, 1999; Bonnert et al., 1999, Whiting et al., 1997; Saxena and Macdonald, 1994).

The preferred subunit stoichiometry of the GABAR varies throughout the adult brain. The $\alpha_1 - \alpha_5$ subunits are all expressed in the hippocampus and the cerebral cortex, yet only the α_1 subunit is present in the cerebellum in any significant amount. The α_6 subunit, however, is found only within cerebellar granule cells and the cochlear nucleus. β subunits are found in the cortex, the hippocampus and the cerebellum, where the predominant subunit is the β_2 subunit. The δ subunit is located in the cerebellum, the thalamus and the dentate gyrus of the hippocampus. Whilst the γ_2 subunit is found throughout the brain, the expression of the γ_1 and γ_3 subunits is more restricted (Pirker et al., 2000; Sur et al., 1999; Endo and Olsen, 1993; Wisden et al., 1991; Benke et al., 1991a). The adult cerebellum expresses GABARs comprising of $\alpha_1\beta_2/\beta_3\gamma_2$ subunits, $\alpha_6\beta_2/\beta_3\gamma_2$ subunits and $\alpha_1\alpha_6\beta_2/\beta_3\gamma_2$ subunits at granule cell synapses with both Golgi cells and mossy fibres. These receptors are also present on the extrasynaptic membranes, along with receptors containing the δ subunit (i.e. $\alpha_6\beta_2/\beta_3\delta$ receptors) (Jechlinger et al., 1998; Nusser et al., 1998a; Somogyi et al., 1996; Nusser et al., 1996; Khan et al., 1996; Pollard et al., 1995; Baude et al., 1992).

Immature granule cells express α_2 and α_3 subunits; however, these subunits are replaced by the α_6 subunit, an indicator of a mature cell (Thompson et al., 1996; Thompson and Stephenson, 1994). This switching on and off of the various GABAR subunits may be influenced by factors such as NT-3 and BDNF (Bao et al., 1999;

Yamada et al., 2002; Hyman et al., 1994). Immature granule cells show a dependence upon NT-3, however, when the granule cells mature, the levels of NT-3 decrease whilst the levels of BDNF, which are expressed at low levels at birth, increase to reach adult levels by P20 (Gao et al., 1995; Maisonpierre et al., 1990).

The GABAR contains binding sites for picrotoxin, barbiturates, neurosteroids and benzodiazepines, which are governed by the expression of various subunits within the receptor. The interface between α and β subunits is important for GABA and muscimol binding (Zezula et al., 1996; Schofield et al., 1987) whilst the β subunit is necessary for the picrotoxin site, which is also the binding site for the convulsant t-butylbicyclophosphorothionate (TBPS) (Zezula et al., 1996; Slany et al., 1995). Barbiturates act on the ion channel and it has been suggested that they bind to the TM2 region of β subunits (Serafini et al., 2000; Birnir et al., 1997). Multiple subunits regulate the action of neurosteroids: β subunits are required for steroid potentiation whereas α subunits regulate potency and efficiency (Belelli et al., 1996; Hadingham et al., 1993; Shingai et al., 1991). The δ subunit is also thought to be involved in regulating the function of neurosteroids (Hevers et al., 2000; Zhu et al., 1996). The benzodiazepine-binding site is located at the interface between α and γ_2 subunits, however, benzodiazepines such as diazepam and flunitrazepam do not bind to α_4– and α_6–containing receptors, leading to these receptors being labelled as diazepam-insensitive GABARs (Benke et al., 1997; Huh et al., 1996; Yang et al., 1995).

Work was undertaken to confirm previously published results and to further characterise the regulation and subunit expression of GABARs in stargazer brain. The results of such experiments are discussed in chapter 3.

Methods

2.1 Animals

Wild-type (C3B6Fe+, +/+), heterozygous (C3B6Fe+, +/stg) and homozygous stargazer mutant mice (C3B6Fe+, stg/stg) were derived from heterozygous breeding pairs obtained from The Jackson Laboratory (Bar Harbor, Maine, USA).

Brain tissues derived from +/+ and +/stg mice were combined and used as 'control' material in experiments in which stg/stg parameters were compared.

New Zealand white rabbits were obtained from Harlan, UK.

The animals were maintained in the Life Sciences Support Unit (LSSU), University of Durham. Animals had unlimited access to food and water and were on a 12 hour light/dark cycle. All animal husbandry, breeding and experimental procedures were performed in accordance with the Animals (Scientific Procedures) Act 1986.

2.2 Materials

All reagents and chemicals used, unless indicated otherwise, were either from BDH or Sigma and were of the highest quality available.

2.2.1 Antibodies and peptides

The anti-AMPA receptor subunit-specific antibodies were from Oncogene (GluR1) and Santa Cruz Biotechnology (GluR2-4). The anti-NSE antibodies were from Affiniti Research Products whilst the anti-β-actin antibodies were from Sigma.

The anti-GABA$_A$ receptor α_1 subunit-specific antibodies were a kind gift from Prof. F.A. Stephenson, School of Pharmacy, University of London.

The anti-NMDA receptor subunit-specific antibodies, anti-stargazin and anti-$GABA_A$ receptor α_6 subunit-specific antibodies were generated within the lab. The peptides for these antibodies were commercially synthesised by Immune Systems Limited

Rabbit anti-mouse IgG-HRP and donkey anti-rabbit IgG-HRP linked secondary antibodies were from Amersham Pharmacia whilst the anti-goat IgG secondary antibody was from Pierce.

Both Freund's complete adjuvant and Freund's incomplete adjuvant were obtained from Difco.

2.2.2 Radioligands

[^{3}H] AMPA, [^{3}H] MK-801, [^{3}H] muscimol and [^{3}H] Ro15-4513 were all obtained from NEN Life Sciences.

MK-801 was obtained from Tocris.

Flunitrazepam and Ro15-1788 were a kind gift from Hoffman La Roche, Switzerland.

The [^{3}H] hyperfilm used for the autoradiography was obtained from both Amersham Pharmacia and from ICN.

2.2.3 Cell culture solutions

Dulbecco's Modification of Eagle's Medium (DMEM) and L-glutamine were obtained from ICN.

The foetal calf serum was obtained from TCS Biologicals.

2.2.4 PCR reagents

The nuclei lysis solution, protein precipitation solution and the dNTPs were all obtained from Promega.

13

The primers (109F, E/Ht7 and ETN-OR) and DNA ladders (100 base pair markers) were from Gibco. Ultrapure agarose and ultrapure tris were also obtained from Gibco.

The TAQ polymerase, SuperTAQ storage buffer and SuperTAQ PCR buffer were all supplied by HT Biotechnology.

2.3 Antibody production

Affinity-purified anti-peptide-directed anti-stargazin (CACNγ2) (309 – 323) polyclonal antibodies and anti-NMDA receptor NR1 (17 – 35), NR2A (1381 – 1394) NR2B (46 – 60), and NR2C/D (1307 – 1323) subunit-specific antibodies were generated as described by Pollard et al. (1993) and Chazot et al. (1994).

Briefly, the protein sequence-specific peptides were chemically coupled to the carrier protein, thyroglobulin, using methods outlined below (section 2.3.2). The carrier-coupled peptides were emulsified and used to immunise rabbits (section 2.3.3). The sera from the immunised rabbits were collected and screened by enzyme-linked immunosorbant assay (ELISA) (section 2.3.4) and peptide-directed antibodies were subsequently affinity-purified from ELISA-positive sera using peptide-affinity columns (section 2.3.6). These methods are a modification of those published in Stephenson and Duggan (1991).

2.3.1 Preparation of dialysis tubing

Two types of dialysis tubing were used in the production and purification of the antibodies generated within the lab. Visking tubing with a molecular weight cut off between 12,000 to 14,000 Daltons (Da), hereafter referred to as high molecular weight tubing, was supplied by Philip Harris. CelluSep H1 dialysis tubing, which has a nominal molecular weight cut off of 1,000 Da, was supplied by Membrane Filtration Products Incorporated.

2.3.1.1 Preparation of high molecular weight tubing

High molecular weight tubing was placed into 1 L of 1 mM EDTA, 2 % (w/v) NaHCO$_3$, which had been heated to a temperature greater than 80°C (in a microwave oven), for 10 minutes. A 1 mM solution of EDTA (1 L) was then prepared and also heated to above 80°C. The tubing was placed into the EDTA solution and left for a further 10 minutes. The solution and tubing were then allowed to cool. The tubing was stored in this solution, at 4°C, until required. Immediately before use, a length of dialysis tubing (approximately 10 cm long) was cut and extensively washed in dH$_2$O.

2.3.1.2 Preparation of CelluSep H1 dialysis tubing

CelluSep 1H dialysis tubing comes ready prepared and was stored in its own storage buffer at 4°C. Lengths of tubing ($\sim$ 5-10 cm) appropriate for the experiment were excised and extensively washed in dH$_2$O prior to use.

2.3.2 Coupling of peptides used for immunisations

Peptides corresponding to the amino sequences of the NMDA receptor subunits NR1 (amino acid sequence 17 − 35), NR2A (amino acid sequence 1381 − 1394), NR2B (amino acid sequence 46 − 60) and NR2C/D (amino acid sequence 1307 − 1323) and to the stargazin protein (Cys-309 − 323) (Letts et al., 1998) were custom sequenced by Immune Systems Limited.

2.3.2.1 MBS coupling of peptides to thyroglobulin

This method was used to couple peptides to the carrier protein, thyroglobulin, through cysteine groups. Peptides to the NMDA receptor (NMDAR) subunits NR1 and NR2B and the stargazin peptide were coupled to thyroglobulin using this method.

Thyroglobulin (20 mg/ml) was dissolved in phosphate buffered saline (PBS), pH 7.2, before dialysing, using high molecular weight tubing, against the PBS overnight at 4°C. The high molecular weight tubing was prepared as described in section 2.3.1.1. The dialysed thyroglobulin was stored at −20°C, until required.

15

3-maleimidobenzoic acid N-hydroxysuccinimide ester (MBS) was dissolved in dimethylformamide (3 mg/ml) and stored at -20°C, until required.

The carrier protein was prepared by adding 50 µl of 10 mM phosphate buffer, 100 mg KH_2PO_4, 1 g Na_2HPO_4, pH 7.2, to 4 mg (200 µl) dialysed thyroglobulin. MBS (85 µl) was then added, drop-wise, whilst mixing. The mixtures were allowed to react at room temperature for 30 minutes, before dialysis in high molecular weight tubing, in the dark, in 2 x 1 L of phosphate buffer for 2 hr at room temperature. This was to ensure that any unreacted MBS was dialysed out.

A 4 mg/ml solution of peptide in phosphate buffer was prepared. Dithiothreitol (DTT, 200 mM) was then added drop-wise and the DTT/peptide mixture was allowed to incubate for 2 hr at room temperature. This step ensured that all cys-cys couplings were reduced so that $>CH_2-SH$ bonds were formed instead.

The peptide was then dialysed against 2 x 1 L of phosphate buffer, for 2 hr at 4°C, using the CelluSep H1 dialysis tubing (prepared as described in section 2.3.1.2). The dialysed carrier protein (MBS/thyroglobulin) was then added drop-wise to the dialysed peptide (340 µl carrier protein/ml peptide). The mixture was allowed to react overnight at room temperature. The product was then dialysed in high molecular weight dialysis tubing for 2 hr, against 2 x 1 L phosphate buffer. Once dialysed, the protein-coupled peptide was flash frozen in 40 µl aliquots, using liquid nitrogen, and stored at -20°C until required.

2.3.2.2 Glutaraldehyde coupling of peptides to thyroglobulin

This method was used to couple peptides to the carrier protein, thyroglobulin, through primary amines. The NMDAR subunit NR2A and NR2C/D peptides were coupled by this method.

Peptides (NMDAR NR2A or NR2C/D) were dissolved in PBS at a concentration of 4 mg/ml.

Dialysed thyroglobulin was prepared as described above, in section 2.3.2.1.

16

Thyroglobulin and dissolved peptide were mixed in a volume : volume ratio of 1:1.

Glutaraldehyde (0.2 % v/v in PBS) was added drop-wise whilst stirring. The peptide-thyroglobulin-glutaraldehyde mixture was allowed to react at room temperature, with stirring, for a minimum of 2 hr.

Unreacted glutaraldehyde was quenched by adding glycine (1 M, pH 7.2) to the peptide mixtures, giving a final glycine concentration of 20 % (v/v). This was incubated, with stirring, at 4°C, overnight.

Unreacted peptide was dialysed away using high molecular weight dialysis tubing, against 4 x 1 L PBS, at 4°C. The dialysed coupled peptides were removed from the dialysis tubing, aliquoted into 300 µl fractions, flash frozen in liquid N_2 and stored at –20°C.

2.3.3 Immunisation and collection of sera

Adult New Zealand white rabbits were immunised in the following manner. The rabbit was first bled from the marginal ear vein and the pre-immune blood was collected in universal tubes.

300 µl of the coupled peptide was added to 300 µl of Freund's complete adjuvant. The adjuvant and peptide were mixed by forcibly ejecting, through a needle and syringe, against the bottom of an eppendorf tube, until a cream-like consistency had formed. The emulsion was then left for one hour at 4°C, to ensure that a stable emulsion had formed; if the mixture separated into 2 layers, it was re-emulsified.

The coupled peptide-adjuvant emulsion (100 µl) was then injected, intramuscularly, into the rabbit. The rabbit was monitored, to ensure that it suffered no adverse effects to the injection.

Subsequent injections were performed in a similar manner, however, the coupled peptide was emulsified in Freund's incomplete adjuvant. The first booster was given

17

7 days following the primary immunisation with subsequent boosters being administered at 3 week intervals.

The rabbit was bled (~ 10 ml) from the marginal ear vein, 7-10 days following each injection. To extract the serum, the blood samples were incubated at 37°C in a water bath for 30 minutes. A glass Pasteur pipette was then rolled around the inside of the Perspex container, to ensure that the blood clot did not adhere to the surface of the Perspex container. The blood was then left at 4°C, overnight.

The blood clot was then removed from the Perspex container and discarded. The remainder was aliquoted into 1 ml fractions in eppendorf tubes. The tubes were centrifuged in the bench-top centrifuge (Eppendorf 5415c centrifuge) for 5 minutes, at 16,000g.

Following the centrifugation, the blood separates so that the serum is found at the top of each of the eppendorfs. The sera were removed from the eppendorfs and pooled together, into a 50 ml Falcon tube. The pooled sera were then aliquoted into 1 ml fractions, flash frozen using liquid N_2 and stored at -20°C, until required.

2.3.4 Screening of serum by ELISA

Serum derived from rabbits immunised with peptides was screened by ELISA, in order to monitor the responses of the NMDA R1, R2A, R2B and R2C/D antibodies. Briefly, lanes in a 96 well plate were coated with bicarbonate buffer, 50 mM $NaHCO_3$, 10 mM NaOH, pH 9.5, alone or with 100 µl of the respective peptide (1 µg peptide/ml bicarbonate buffer) per well and allowed to incubate at 4°C, overnight.

The wells were subsequently washed 3 times with 0.25 % (w/v) gelatin in PBS (200 µl), hereafter referred to as PBS-gelatin. PBS-gelatin (200 µl) was then added to each well and the plate left to incubate for 1 hr at room temperature in order to block any non-specific binding sites present. The PBS-gelatin was then aspirated.

Serum was serially diluted in PBS-gelatin, to give a semi-log dilution series ranging from 1:10 dilution to 1:31,600 dilution. Serially diluted serum (100 µl) was added to each well and the plate left to incubate, with agitation, overnight at 4°C.

The sera were then discarded and the plate washed 3 times with PBS-gelatin. PBS-gelatin (200 µl) was finally added to each well and the plate left to incubate for 10 minutes at 37°C. The PBS-gelatin was then discarded.

Anti-rabbit IgG-HRP, 100 µl of a 1:1000 dilution of the HRP-linked antibody in PBS-gelatin, was applied to each well and the plate left to incubate, in the dark, for 1.5 hr at 37°C. The wells were then washed 3 times using PBS-gelatin, followed by 2 washes with PBS.

HRP substrate, 100 µl of 4 mM O-phenylenediamine, 250 mM Na_2HPO_4, 20 mM citric acid, 0.004% (v/v) H_2O_2, was then applied to each well and the plate left to incubate, in the dark, at room temperature, for 5 minutes. The reaction (i.e. the development of the coloured product) was stopped by the addition of 50 µl of 20% (v/v) H_2SO_4 to each well. The plate was read on a plate reader at a wavelength of 492 nm.

2.3.5 Preparation of peptide-affinity columns

Antibodies were affinity purified on peptide-coupled affinity columns. The NR2A and NR2C/D peptides were coupled to the inert column matrix by the glutaraldehyde method described below (section 2.3.5.1). The NR1, NR2B and stargazin peptides were coupled to affinity columns using the MBS protocol described below (section 2.3.5.2).

2.3.5.1 Coupling of peptides to the column matrix through amino groups

Activated 6-aminohexanoic acid N-hydroxy succinimide ester Sepharose–4B (0.35 g) was swollen using dH_2O, before being washed, on a sintered glass funnel, using 100 ml of 1 mM HCl. The washed gel was equilibrated with 0.1 M $NaHCO_3$, 0.5 M NaCl, pH 8.0, for 1 hr at room temperature, before being washed again on the

sintered glass funnel using the same buffer. The NR2A or NR2D/C specific peptides (5 mg) were dissolved in 1 ml of NaHCO₃/NaCl buffer. They were then added to the gel matrix and allowed to incubate for a further 1 hr at room temperature, on the roller mixer (Stuart Scientific roller mixer SRT1).

The gel was washed with 25 ml of NaHCO₃/NaCl buffer before being incubated for 1 hr at room temperature, with 3 ml of 0.1 M tris-HCl, 0.5 M NaCl, pH 8.0.

The gel was subsequently washed in 10 ml of 0.1 M acetic acid, 0.5 M NaCl, pH 4.0, followed by 10 ml of 0.1 M tris-HCl, 0.5 M NaCl, pH 8.0. This procedure was repeated a further three times, in order to ensure that all non-covalently bound peptide was washed off. Following the acetic acid/tris-HCl washes, the gel was washed further with 100 ml PBS. The gel was then transferred to a chromatography column (0.8 x 4 cm Poly-Prep Chromatography Column, BioRad) and washed with 100 ml PBS. The column was then equilibrated with PBS containing 0.01 % (w/v) thimerosal before sealing and storing at 4°C.

2.3.5.2 Coupling of peptides to the column matrix through cysteine groups

Peptides were reduced essentially as described previously, in section 2.3.2.1. Briefly, 5 mg peptide (NR1, NR2B or stargazin) were dissolved in 1 ml PBS, pH 7.4, containing 30.8 mg DTT and left to incubate for 1 hr at room temperature. The reduced peptide was then dialysed using CelluSep 1H dialysis tubing against 4 changes of degassed wash buffer, comprising of 0.1 M tris-HCl, 0.3 M NaCl, 1 mM EDTA, pH 8.0, at 4°C.

Activated Thiol-Sepharose 4B, 0.35 g, was swollen in dH₂O. The gel was then washed on a sintered glass funnel using 100 ml of degassed wash buffer. The washed gel was then suspended in 2 ml wash buffer before the dialysed peptide was added. The peptide was allowed to incubate with the Thiol-Sepharose gel for 2 hr at room temperature, on the rolling shaker. The gel was then washed, on a sintered glass funnel, with 25 ml wash buffer followed by 10 ml of 0.1 M citric acid, pH 4.5 with KOH.

2-mercaptoethanol (20 mM final concentration in 0.1 M citric acid buffer) was then added to the gel, which was left to incubate for 1 hr at room temperature. The β-mercaptoethanol was used in order to block any unreacted thiol groups present in the gel; unreacted thiol groups may potentially couple to the antibody when the immune serum is exposed to the gel. The gel was then washed on the sintered glass funnel using 25 ml of 100 mM citric acid, to terminate the blocking reaction, before being placed into the column and washed with 100 ml of degassed PBS. PBS containing 0.01 % (w/v) thimerosal was then added to the column, which was sealed and stored at 4°C.

2.3.6 Purification of sera

Pre-immune sera were obtained from immunised rabbits as described previously, in section 2.3.3. A Watson Marlow 101U/R low-flow peristaltic pump and Watson Marlow silicone tubing with a bore of 0.8 mm were used in order to either circulate sera through or to introduce the buffers onto the peptide-affinity columns.

The columns were washed through with 3 ml of pre-immune sera for either 2 hr at room temperature or overnight at 4°C. Columns were washed with 100 column volumes of PBS at room temperature. The column was then washed with 10 volumes of 50 mM glycine-HCl, pH 2.3, followed by one wash of approximately 50 column volumes of PBS.

Immune serum (3 ml) was added to the affinity column and circulated, via the peristaltic pump, for either 2 hr at room temperature or overnight at 4°C. The circulated antibody-depleted serum was then allowed to run off the column. The column was subsequently washed with 100 volumes of PBS, at room temperature.

Glycine-HCl (50 mM, pH 2.3, 10 ml) was used to elute the antibody from the peptide-affinity column. Fractions (1 ml) were collected in eppendorfs containing 1 M tris. The volume of 1 M tris used was determined prior to each elution so that the pH of the antibody-containing glycine-HCl-tris mixture was returned to pH 7.4. The volume of tris required to neutralise the glycine-HCl varied from 30-70 μl.

The column was then washed with ~ 50 volumes of PBS, before being finally washed and stored in PBS-thimerosal at 4°C. The eluted fractions were read on a UV spectrophotometer (Pharmacia Biotech Ultrospec 2000) at 280 nm, using glycine-HCl-tris as the spectrophotometric 'blank' and semi-micro disposable polystyrene 2.5 ml cuvettes (Philip Harris).

A typical example of the results obtained are presented below:

Fraction	A_{280}
1	0.017
2	0.794
3	1.241
4	0.191
5	0.088
6	0.047
7	0.146
8	0.014
9	0.014
10	0.008
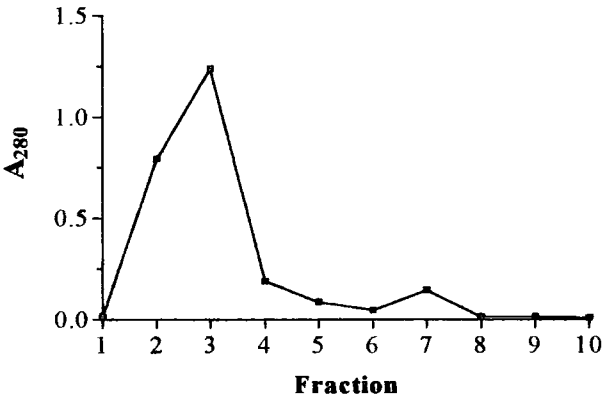
Table and figure 2.1 Absorbance (A_{280}) of fractions eluted from the purification of NR1 antibody affinity purification column. The table shows the values of the A_{280} of each of the eluted fractions. The absorbances of the fractions are represented as a line graph in figure 2.1. The spectrophotometer was blanked using 1 ml of 50 mM glycine-HCl, 1 M tris, pH 7.0, before measuring the collected eluate fractions.

The fractions giving the highest absorbance readings were then collected and pooled. The amount of protein was determined by calculating the average absorbance reading and dividing the value by the A_{280} value for IgG (1 mg/ml IgG gives a value at A_{280} of 1.35 absorbance units).

Using the values in the table above as an example, the amount of protein (i.e. antibody) present was calculated thus:

Average absorbance of fractions 2 – 7 =

$$(0.794 + 1.241 + 0.191 + 0.088 + 0.047 + 0.146)/6$$

$$= 2.507/6$$

$$= 0.418$$

Amount of protein $\qquad = 0.418/1.35$

$$= 0.3095$$

Concentration of antibody $\qquad = 310 \; \mu g/ml$

The antibody-containing fractions were then dialysed, in high molecular weight dialysis tubing, in 4 x 1 L PBS, pH 7.4, containing 0.02 % (w/v) sodium azide, at 4°C. The dialysed antibody was then aliquoted out and either stored at 4°C or flash frozen in liquid N_2 and stored at –20°C. If the antibody was being frozen, the concentration of the antibody was made up to 1 ml/ml using BSA as a cryoprotectant.

2.4 Purification of stargazin from membranes

2.4.1 Preparation of anti-stargazin antibody immunoaffinity column

The antibody immunoaffinity column was prepared using the Pierce Immunopure IgG Orientation kit according to the manufacturer's instructions.

The antibody was prepared by combining the antibody with an equal volume of antibody binding buffer, 50 mM sodium borate, pH 8.2. Four 3.5 ml aliquots were prepared and stored at 4°C, until required.

The supplied ImmunoPure Immobilized Protein A column was drained and washed with 5 volumes of wash buffer comprising of 50 mM sodium borate, pH 8.2. The base of the column was sealed and the first antibody aliquot was applied. The column was sealed and the gel, ImmunoPure immobilised protein A, was suspended by inversion before mixing for 30 minutes at room temperature, on the roller shaker.

The first antibody aliquot was then drained from the column and the second antibody aliquot applied. The gel was suspended by inversion before mixing for a further 30 minutes, at room temperature, on the roller shaker. This process was repeated twice more, using antibody aliquots three and four. The column was then washed in 10 volumes of wash buffer.

The antibody was covalently bound to the immobilised protein A by the application of the crosslinker dimethylpimelimidate (DMP) to the column. The DMP was prepared by dissolving 13.2 mg of the DMP in 2 ml of a crosslinking buffer, comprising 0.2 M triethanolamine, pH 8.2. The gel was mixed for 1 hr at room temperature, on the roller shaker, before the DMP-containing crosslinking buffer was drained from the column. The column was then washed in 5 volumes of crosslinking buffer.

Two volumes of blocking buffer, 0.1 M ethanolamine, pH 8.2, were then applied to the column and the gel was mixed for 10 minutes on the roller shaker. This allows the blocking buffer to block any remaining unreacted imidate groups present. The column was then washed with 5 volumes of elution buffer, ImmunoPure IgG elution buffer, pH 2.8, containing primary amine. This elution buffer will elute any IgG from the gel that is not covalently attached to the immobilised protein A. The gel was then washed with 5 volumes of wash buffer. A porous disc was inserted into the column and placed within a few millimetres of the gel surface. The column was then washed with a further 5 volumes of wash buffer followed by 15 volumes of PBS.

Uncoupled anti-stargazin antibody was then eluted off the column. The column was washed in 20 volumes of PBS before 5 volumes of 50 mM glycine/HCl, pH 2.8, was applied. The column was washed with PBS until the pH of the eluate returned to pH 7.0. Five volumes of glycine/HCl were again applied to the column, which was then washed with PBS until the pH of the eluate returned to pH 7.0. This elution/washing process was repeated once more so that it was undertaken three times in total. Sodium azide, 0.02 % (w/v) in PBS, was then applied to the column, which was then sealed, wrapped in foil and stored at 4°C until required.

2.4.2 Immunoaffinity purification of brain tissue

Detergent-solubilised control (+/+ and +/stg) forebrain and stargazer (stg/stg) forebrain membranes were applied to separate anti-stargazin antibody immunoaffinity columns, respectively. This method is a modification of that published by Duggan et al. (1991).

2.4.2.1 Preparation of brain membrane homogenate

Forebrains from both control (+/+ and +/stg mice) and stargazer (stg/stg) mice were used to prepare P2 membrane homogenates. The forebrains were homogenised in buffer A, which was comprised of 50 mM tris-acetate, pH 7.4, 5 mM EDTA, 5 mM EGTA, 320 mM sucrose, 1 mM PMSF, 1 mg/100 ml trypsin inhibitor, 1:1000 dilution of protease inhibitor cocktail (for constituents, see appendix 1). The tissue was then centrifuged in a Beckman JS-HC centrifuge, using a JA-20 rotor, at 1000g for 12 minutes, at 4°C. The pellet was discarded and the supernatant was centrifuged at 40,000g for 40 minutes, at 4°C. The supernatant was then discarded and the pellet was resuspended and homogenised in buffer B, which was comprised of 50 mM tris-acetate, pH 7.4, 5 mM EDTA, 5 mM EGTA, 1 mM PMSF, 1 mg/100 ml trypsin inhibitor, 1:1000 dilution of protease inhibitor cocktail. The homogenate was centrifuged for 40 minutes at 40,000g and 4°C. The supernatant was discarded and the pellet was resuspended and rehomogenised in 10 ml buffer B, before being flash frozen in liquid N_2 and stored at –20°C.

2.4.2.2. Detergent solubilisation of forebrain membrane proteins

The membrane homogenates were rapidly thawed by warming to 37°C. Solubilisation buffer, 50 mM tris-HCl, pH 9.0, 150 mM NaCl, 1 mM EDTA, 1 mM EGTA, 0.62 % (w/v) sodium azide, 1 mg/100 ml trypsin inhibitor, 1 µg/ml aprotinin, 1 µg/ml pepstatin A, 1 µg/ml leupeptin, 1 mM PMSF, was prepared and warmed to 37°C.

The solubilisation buffer (9 ml) was added to 10 ml of the homogenates. Sodium deoxycholate (20 % w/v) was added drop-wise to give a final concentration of 1 % (w/v) and the mixture was left to incubate, stirring, for 30 minutes at 37°C.

The mixture was then centrifuged in a Beckman Ultracentrifuge, using a 70Ti rotor, at 100,000g, for 70 minutes, at 4°C. The pellets were resuspended and rehomogenised in 10 ml of solubilisation buffer, flash frozen in liquid nitrogen and stored at -20°C.

The pHs of the supernatants were determined and returned to pH 7.0 with the addition of HCl. The volumes of the supernatants were then estimated and an equal volume of dilution buffer, 10 mM KH_2PO_4, pH 7.4, 0.5 M KCl, 10 % (w/v) sucrose, 0.02 % (w/v) sodium azide, 0.2 % (v/v) Triton X-100, was added.

2.4.2.3 Purification of forebrain membrane proteins

The anti-stargazin antibody immunoaffinity columns were allowed to come up to room temperature and drained. Elution buffer, 50 mM triethylamine, pH 11.5, 0.5 M KCl, 10 % (w/v) sucrose, 0.02 % (w/v) sodium azide, 0.2 % (v/v) Triton X-100, 10 ml, was applied to each of the columns. The columns were then washed with wash buffer, 10 mM KH_2PO_4, pH 7.4, 0.5 M KCl, 10 % (w/v) sucrose, 0.02 % (w/v) sodium azide, 0.2 % (v/v) Triton X-100, until the pH of the eluates returned to pH 7.0. The dilute solubilised homogenates were then added to the columns and circulated, via a peristaltic pump, for approximately 18 hr.

Subsequently, the columns were washed with ~ 75 volumes of wash buffer before the immunopurified protein was eluted by addition of 10 ml of elution buffer to each of the columns. The eluate was collected in 650 µl fractions, which were neutralised by the addition of 350 µl of 50 mM glycine/HCl, pH 2.3. The eluted fractions were stored at 4°C, until required for analysis by SDS-PAGE. The columns were washed with ~ 80 volumes of wash buffer and stored at 4°C, in the dark, with thimerosal, 0.01 % (w/v) in PBS.

2.5 SDS-solubilisation of brain tissue

The tissue prepared using this protocol was used mainly for immunoblotting.

Age-matched adult control (+/+ and +/stg) and stargazer (stg/stg) mice were killed by rising CO_2. The heads were decapitated and stored on ice whilst the brain sections (forebrains and cerebella) were dissected. These were then flash frozen in liquid N_2 and stored at $-80°C$ until required.

The frozen brain tissue was allowed to thaw before solublising. Tris-EDTA, 50 mM tris, 2mM EDTA, pH 6.8, was added to the brain tissue, which was then homogenised using a Potter glass/Teflon homogeniser. An equal volume of tris-SDS, 50 mM tris, 2 mM EDTA, pH 6.8, 4 % (w/v) SDS, was then added and the mixture homogenised further. Foaming occurred during the homogenisation process, which was dispersed by puncturing with a glass Pasteur pipette that had been heated in a Bunsen burner flame.

The homogenate was then transferred into eppendorf tubes and heated at 95°C for 5 minutes. The eppendorfs were then centrifuged, using the bench-top centrifuge, at 16,000g for 1 minute. The supernatants were pooled and kept on ice whilst the pellets were discarded. Protein concentration was determined using the method of Lowry (Lowry et al., 1951). The proteins were either immediately precipitated using chloroform and methanol (as below) or the supernatants were aliquoted, flash frozen in liquid N_2 and stored at $-20°C$ until required.

2.6 Chloroform – methanol precipitation of proteins

Proteins were precipitated from solubilised brain tissue and from solubilised cultured cells using chloroform and methanol. The method followed was devised by Wessel and Flugge (1984).

Essentially, 4 volumes of methanol were added to the membrane solution, mixed and centrifuged for 10 seconds at 16,000g in the Eppendorf bench-top centrifuge. 1 volume of chloroform was added, mixed and centrifuged. 3 volumes of dH_2O were then added, mixed and centrifuged as before.

The proteins form a precipitate at the interface between the two liquid layers so the top layer was removed and discarded. Three volumes of methanol were then added and the solutions were mixed by tapping before centrifuging, at 16,000g, for 5 minutes. The supernatant was removed and the pellet placed in the vacuum dessicator. Once dry, the pellet was suspended in SDS-PAGE sample buffer, 20 mM DTT, 283 µl dH$_2$O and 167 µl of 3 x SDS-PAGE sample buffer stock (30 mM NaH$_2$PO$_4$, 30 % (v/v) glycerol, 0.05 % (w/v) bromophenol blue, pH 7.4, 7.5 % (w/v) SDS). The suspended pellet was heated at 95°C for 5 minutes, vortexed and centrifuged in the benchtop centrifuge, at 16,000g. The sample was then allowed to cool and stored at –20°C until required.

The NMDAR subunit cDNAs for NR1, NR2A and NR2C, were transfected and translated in HEK 293 cells by Dr Paul Chazot, University of Sunderland. The expressed recombinant subunits were supplied for screening of antibodies by the calcium phosphate preparation method as described in Chazot et al. (1994). NR1 and NR2C recombinants, 100 µl aliquots, were precipitated using the method outlined above and resuspended in 100 µl SDS-PAGE sample buffer. The NR2A recombinant sample, 250 µl aliquot, was precipitated and resuspended in 50 µl of SDS-PAGE sample buffer.

2.7 Immunoblotting

Gel electrophoresis of proteins was carried out in order to dissociate proteins into their individual polypeptide subunits. This was undertaken using polyacrylamide gels and proteins that had been pre-treated with SDS and heated, as outlined in section 2.5.

2.7.1 Preparation of gels

The Hoefer Mighty Small II mini-gel system, which was used for the immunoblotting, comes with a multi-gel caster, which allows the casting of 10 resolving gels at once. All components of the gel casting system were cleaned with detergent, 70 % (v/v) ethanol and acetone before use.

Polyacrylamide resolving gel solutions were prepared thus according to whether 6 %, 7.5 % or 10 % resolving gels were required:

	6 %	7.5 %	10 %
dH$_2$O	29.5 ml	27.6 ml	24.47 ml
Acrylogel-3	7.5 ml	9.4 ml	12.53 ml
Running Buffer	12.5 ml	12.5 ml	12.5 ml
TEMED	40 μl	20 μl	20 μl
10 % (w/v) AMPS	0.5 ml	0.5 ml	0.5 ml

Table 2.2. Volumes of the various solutions required to prepare either 6 %, 7.5 % or 10 % resolving gels. The Acrylogel-3 is a 40 % solution of acrylamide, which has to be adjusted to prepare resolving gels containing the different concentrations of acrylamide. For the composition of the running buffer, see appendix 1. The solution was degassed, for a minimum of 15 minutes in the vacuum dessicator, before the application of the AMPS, which causes the acrylamide to start crosslinking and a gel to be formed.

The solution was then poured into the gel caster and ~ 150 μl water-saturated isobutanol applied to the top of each gel plate. The isobutanol was added to stop the gels from drying whilst they were cross-linking.

The gels were left to set at room temperature, for approximately 1 hr. The isobutanol was then removed and the gels rinsed with dH$_2$O. The gels were carefully removed from the gel caster, wrapped in running buffer-soaked tissue paper and stored in running buffer, which had been diluted 1:4 with dH$_2$O, at 4°C, until required.

Stacking gels were prepared immediately before use. The stacking gel solutions were prepared as indicated in table 2.3 below:

	3.5 %	5 %
dH₂O	3.759 ml	3.558 ml
Acrylogel-3	0.446 ml	0.638 ml
1 M Tris, pH 6.8	0.625 ml	0.625 ml
10 % (w/v) SDS	0.05 ml	0.05 ml
TEMED	0.01 ml	0.01 ml
10 % (w/v) AMPS	0.1 ml	0.1 ml

Table 2.3. Volumes of the various solutions required to prepare either 3.5 % or 5 % stacking gels. The Acrylogel-3 is a 40 % solution of acrylamide, which has to be adjusted to prepare stacking gels containing the different concentrations of acrylamide. The solution was degassed, for a minimum of 15 minutes in the vacuum dessicator, before the application of the AMPS, which causes the acrylamide to start crosslinking and a gel to be formed.

A 3.5 % stacking gel was prepared for use with both 6 % and 7.5 % resolving gels whereas a 5 % stacking gel was used with 10 % resolving gels. The stacking gel solution was poured on to the resolving gel and allowed to cross-link. Once cross-linked, the gel was loaded with protein and used for immunoblotting (section 2.7.2).

2.7.2 Quantitative immunoblotting

Protein (10 μg/10 μl unless otherwise indicated) and molecular weight markers were loaded on appropriate percentage acrylamide mini-resolving gels and separated by electrophoresis (SDS-PAGE) under reducing conditions with electrode buffer, using the Hoefer Mighty Small II Mini gel system and a Pharmacia Biotech Electrophoresis Power Supply EPS300. The prestained SDS-markers (BioRad) were broad range standards with weights between 6.7 kDa and 212 kDa. The proteins were separated at 80 V for approximately 2 – 2.5 hours, until the protein front reached close to the bottom of the resolving gel.

The proteins were then electrophoretically transferred onto 0.45 μm nitrocellulose membranes using the Hoefer Mighty Small Transphor Unit and transfer buffer. If a 6 % resolving gel was used, the transfer process would take 2 hr 30 minutes at 50 V. If a 7.5 % resolving gel was used, the transfer process would take 2 hr 20 minutes at

50 V. If a 10 % resolving gel was used, the transfer process would take 2 hr at 50 V. (See appendix 1 for electrode and transfer buffers).

Nitrocellulose membranes were then transferred into 50 ml Falcon tubes before incubating in blocking buffer, which comprised of 5 % (w/v) skimmed milk powder and 0.02 % (w/v) Tween-20 in PBS, for 1 hr, at room temperature, on the roller mixer. The blocking buffer was then removed and discarded. The nitrocellulose membranes were incubated with primary antibody in incubation buffer, which comprised of 2.5 % (w/v) skimmed milk in PBS, overnight, at 4°C, on the roller mixer.

The concentrations of the primary antibodies used are listed in table 2.4 below.

Antibody	Concentration
anti-NR1	$1 - 2$ μg/ml
anti-NR2A	2 μg/ml
anti-NR2B	2 μg/ml
anti-NR2C/D	4 μg/ml
anti-stargazin	$0.5 - 1$ μg/ml
anti-GluR1	0.5 μg/ml
anti-GluR2, anti-GluR3, anti-GluR4	$1:100 - 1:1000$
anti-β-actin	$1:100 - 1:1000$
anti-GAB$_A$ receptor α_1	0.5 μg/ml
anti-GAB$_A$ receptor α_6	1 μg/ml
anti-NSE	1:20,000

Table 2.4 Table showing the concentrations of the various primary antibodies used for immunoblotting purposes.

The primary antibodies were removed and the nitrocellulose membranes were subsequently washed three times in wash buffer, comprising of 2.5 % (w/v) skimmed milk powder, 0.02 % (w/v) Tween-20 in PBS. Secondary antibody, in 2.5 % (w/v) skimmed milk powder in PBS, was used at a dilution range of 1:100 − 1:5000. Donkey anti-rabbit Ig HRP secondary antibody was used when the primary antibody was of rabbit origin (the anti-NMDA receptor subunit-specific antibodies,

31

the anti-GABA$_A$ receptor subunit-specific antibodies, the anti-stargazin antibody, the anti-GluR1 antibody, the anti-β-actin antibodies and the anti-NSE antibodies). Rabbit anti-goat Ig HRP secondary antibody was used when the primary antibody was of goat origin (the anti-GluR2, anti-GluR3 and anti-GluR4 antibodies).

The membranes were incubated with the secondary antibody for two hours, room temperature, on the roller mixer The secondary antibody was then discarded and the membranes washed three times in wash buffer followed by two washes with PBS.

Immunoreactive species were detected using the enhanced chemiluminesence (ECL) Western blotting system. The ECL reagent was composed of 10 ml luminol, 680 μM p-coumaric acid (in DMSO) and 3 μl of H$_2$O$_2$ (30 % stock) and was prepared immediately before required. The immunoblots were incubated in the ECL reagent for approximately one minute before being wrapped in Saran-wrap. The immunoblots were then exposed to ECL Hyperfilm (Amersham Pharmacia) for 1 minute. The films were then manually developed in Kodak GBX developer, until a signal could be detected at the lowest concentration of protein used, and fixed using Kodak GBX fixer. The films were then washed in running H$_2$O and allowed to dry at room temperature. Immunoblots were then exposed to the hyperfilm for 10 seconds to 5 minutes, depending upon the strength of the signal.

2.7.3 Analysis of immunoblots

Immunoblots were quantified using the BioRad Quantity One System. Briefly, the films were scanned using the BioRad GelDoc 2000 system and the image intensities of the immunoreactive signals were obtained with the Quantity One (4.0.3) software. With all films, the background intensity was subtracted before the intensity of the immunoreactive signals was obtained. Conditions where a linear relationship between the amount of protein applied and the intensity of the immunoreactive signal were identified. Signals lying within this range were used to compare expression with the anti-NMDA/GABA$_A$ subunit-specific antibodies or anti-stargazin antibodies and the expression with the antibodies anti-β-actin or anti-NSE.

The image intensity of the NMDA receptor subunit / GABA receptor subunit / AMPA receptor subunit signal was divided by that of the actin/NSE signal. This was performed for both control proteins and stargazer proteins. The value of the stargazer signal was then divided by that of the control signal, to obtain a percentage value for each exposure time used. The average percentage value was then determined, to reveal the percentage change of the appropriate protein level between stargazer and control brain membranes. This process was repeated for each experiment. The average percentage values for each experiment were then combined and expressed as mean ± sem.

2.8 P2 membrane preparation

This protocol was used to prepare a synaptic membrane preparation for use in radioligand binding experiments. This preparation was also used for immunoblotting, once the proteins had been chloroform/methanol precipitated.

Age-matched adult mice were killed using rising CO_2 and decapitated, in accordance with schedule I killing regimes specified within the Animals (Scientific Procedures) Act 1986. The heads were kept on ice whilst the brain sections (forebrains and cerebella) were dissected out. The brain sections were immediately frozen in liquid N_2 and stored at $-80°C$, until required.

Frozen brain tissue (from both control (i.e. +/+ and +/stg) and stg/stg mice) was placed into excess ice-cold buffer 1, 50 mM tris-HCl, pH 7.4, 5 mM EDTA, 5 mM EGTA, 200 mM sucrose, 1 mM PMSF, trypsin inhibitor (1 mg/100 ml), 1:1000 dilution of protease inhibitor cocktail, until it had thawed out. The tissue was homogenised in ice-cold buffer 1 using a mechanical Potter glass/Teflon homogeniser before being centrifuged for 10 minutes at 1,000g, 4°C, using a JA-20 rotor in a Beckman JS-HC centrifuge. The pellets were discarded while the supernatants were centrifuged for 20 minutes at 20,000g, 4°C.

The supernatants were then discarded and the pellets suspended in ice-cold, hypotonic buffer 2, 50 mM tris-HCl, pH 7.4, 5 mM EDTA, 5 mM EGTA 1 mM

33

PMSF, trypsin inhibitor (1 mg/100 ml), 1:1000 dilution of protease inhibitor cocktail. The suspended pellets were rehomogenised and the homogenate re-centrifuged for 20 minutes at 8,000g, 4°C.

The supernatants and pellets were separated and stored on ice. The pellets were resuspended in a small volume of ice-cold buffer 2, whilst the supernatants were re-centrifuged for a further 20 minutes at 48,000g, 4°C. The supernatants were then discarded and the pellets resuspended in a small volume of ice-cold buffer 2 and combined with the previous pellet suspension, before being rehomogenised. The homogenate was re-centrifuged for 20 minutes at 48,000g, 4°C. The supernatant was discarded, the pellet resuspended in 5 ml ice-cold buffer 2 and stored at −20°C for at least 12 hr.

The pellet suspension was thawed on ice and an excess of assay buffer was added. The suspension was rehomogenised and re-centrifuged for 20 minutes at 48,000g, 4°C. The supernatant was discarded and the suspension, homogenisation, centrifugation steps repeated a further four times. The final pellet was resuspended in 5 ml assay buffer and stored at −20°C until required, with a fraction being removed so that the protein concentration could be determined by the method of Lowry (Lowry et al., 1951).

2.9 Radioligand binding assays

MK-801 is a non-competitive antagonist of the NMDA receptor, binding to the receptor in its ion channel. Radiolabelled MK-801, [³H] MK-801, was employed to study the binding characteristics of MK-801 to the NMDA receptor within both control and stargazer brains. Remacemide, an anticonvulsant that is also an NMDA receptor antagonist binding to the ion channel of the receptor (Ahmed et al., 1999; Palmer et al., 1992), was used to displace the binding of the [³H] MK-801. [³H] AMPA was used to determine parameters of AMPA receptors in control and stargazer brains.

2.9.1.1 [^{3}H] MK-801 binding

Control and stargazer forebrains and cerebella were homogenised as described in section 2.8, with the final pellet suspended in 5 mM tris-acetate, pH 7.5. The protein concentrations of the final homogenates were determined using the method of Lowry (Lowry et al., 1951). A 1 mg protein/ml tris-acetate solution of each tissue homogenate was prepared and aliquoted into test tubes.

Equal volumes of total binding mix or non-specific binding mix (see appendix 1) were added to the test tubes containing 100 µl of the membrane preparation. The tubes were left to incubate at room temperature for 2 hours. Preliminary experiments had determined that these were the optimal conditions for [^{3}H] MK-801 binding to brain membranes. Whatman GF/B filter paper strips were left to incubate with polyethyleneimine (PEI), 0.1 % (v/v) in 5 mM tris-acetate, pH 7.5.

The reactions were quenched with excess (2 ml) wash buffer, containing 5 mM tris-acetate, pH 7.5, 0.02 % (w/v) sodium azide, and the membranes transferred onto the PEI-treated filter paper, using a 24 well Brandel Cell Harvester. The test tubes were washed a further two times with the wash buffer before the filter paper was allowed to dry, for a minimum of 30 minutes at room temperature.

The filter papers were placed into scintillation vials and 4 ml scintillation fluid (Ecoscint) added. The vials were allowed to stand in the dark at room temperature for 30 minutes – 1 hr before being placed into a Packard 1600TR Liquid Scintillation Analyzer and the disintegrations per minute (dpm) calculated. These data were used to determine the parameters of [^{3}H] MK-801 binding sites in forebrain and cerebellar membranes.

2.9.1.2 Remacemide displacement of [^{3}H] MK-801

Remacemide displacement of [^{3}H] MK-801 binding was performed essentially as described above for [^{3}H] MK-801 binding (section 2.9.1.1). However, the total binding and non-specific binding solutions contained 10 nM [^{3}H] MK-801 and 100 nM to 10 mM remacemide (see appendix 1). Again, equal volumes of the

binding solutions (100 μl) were added to P2 membrane homogenates (100 μl), prepared as described in section 2.8.

The remacemide/radioligand/membrane mixtures were incubated for 2 hr at room temperature before the ligand-bound membranes were transferred to the Whatman GF/B PEI-coated filter paper using the cell harvester. The filter paper was left to dry at room temperature before placing into scintillation vials. To each vial, 4 ml Ecoscint was added and the scintillation vials were left to incubate for ~ 1 hr. The dpm for each vial was ascertained and ligand-binding analyses were performed to calculate the IC_{50} for remacemide in control and stargazer brain membranes.

2.9.2 [^{3}H] AMPA binding

2.9.2.1 Preliminary binding experiments

[^{3}H] AMPA binding to mouse brain membranes was performed essentially as described by Hawkinson and Espitia (1997), Kurschner et al. (1998) and Olivera et al. (1999), with minor modifications. Briefly, cerebellar and forebrain homogenates were prepared as described earlier (section 2.8), with the final pellet being resuspended in 5 mM tris-acetate, pH 7.5, to a final protein concentration of 2 mg/ml.

Equal volumes (100 μl) of ice-cold total binding mix, containing 5 mM tris-acetate, 10 nM [^{3}H] AMPA, with/without 50 mM KSCN or ice-cold non-specific binding mix, which contained 5 mM tris-acetate, 10 nM [^{3}H] AMPA, 1 mM glutamate with/without 50 mM KSCN, were added to the test tubes containing the membrane preparation (100 μl).

The tubes were left to incubate on ice for up to 1 hr. GF/B filter paper strips were pre-incubated with PEI, 0.1 % (v/v) in 5 mM tris-acetate, pH 7.5.

The reactions were rapidly quenched with excess wash buffer (~ 2 ml), 5 mM tris-acetate, pH 7.5, containing 0.02 % (w/v) sodium azide. Membranes with bound ligand were separated from unbound ligand by filtration onto the PEI-treated filter paper, using a Brandel Cell Harvester. The test tubes were washed a further two

times with the wash buffer before the filter paper was allowed to dry for a minimum of 30 minutes at room temperature.

The filter papers were placed into scintillation vials and 4 ml scintillation fluid (Ecoscint) added. The vials were allowed to stand, in the dark at room temperature, for 30 minutes – 1 hr, before being placed into a Packard 1600TR Liquid Scintillation Analyzer and the disintegrations per minute (dpm) calculated. The data were used to calculate specific binding of [^{3}H] AMPA to the brain membranes.

2.9.2.2 Triton-treatment of membranes

Further experiments were undertaken following the method described by Hawkinson and Espitia (1997). Briefly, control mouse forebrains were homogenised in 0.32 M sucrose, 1 mM EGTA, pH 7.0, and centrifuged at 800g, 4°C for 10 minutes. The supernatant was removed and centrifuged at 48,000g for 30 minutes. The pellet was the resuspended in 20 ml 0.04 % (v/v) Triton X-100, 1 mM EGTA, pH 7.0, and left to incubate for 30 minutes at 37°C before centrifuging again for 30 minutes at 48,000g. The pellet was then resuspended in 20 ml EGTA (1 mM, pH 7.0) and left to incubate for 20 minutes on ice. The suspension was then centrifuged at 48,000g for 30 minutes. The supernatant was removed and discarded. The pellet was frozen in liquid N_2 and stored at -80^oC before being resuspended in 100 mM tris-acetate, pH 7.2, 50 μM EGTA.

A 2 mg/ml forebrain homogenate was prepared using 100 mM tris-acetate, pH 7.2, 50 μM EGTA, and 100 μl fractions were incubated for 1 hr at 20°C with 100 μl buffer. The buffers used all contained 10 nM [^{3}H] AMPA and contained 100 mM tris-acetate, pH 7.2, 50 μM EGTA, or tris-acetate and EGTA plus 1 mM glutamate, or tris-acetate and EGTA plus 50 mM KSCN or tris-acetate and EGTA plus glutamate and KSCN. The PEI was prepared using the tris-acetate and EGTA buffer.

Membrane bound ligand was separated from unbound ligand using the cell harvester, onto PEI-coated filter paper. The wash buffer used was 100 mM tris-acetate, pH 7.2, with 0.02 % (w/v) sodium azide. The filter papers were dried, incubated with

scintillation fluid and the dpms obtained. The data were used to calculate the binding of the radioligand to the forebrain membranes.

2.9.2.3 Effect of calcium on binding

In order to determine the effect of calcium on the binding of [^{3}H] AMPA to brain membranes, CaCl$_2$ and the calcium chelator EGTA were added to the buffers (Stensbol et al., 1999; Nielsen et al., 1998; Hawkinson and Espitia, 1997). Membranes were prepared essentially as described in section 2.8, with the following modifications. The method outlined in section 2.8 was followed as far as the freeze-thaw step.

The pellet suspension was thawed and homogenised in 50 mM tris-acetate, pH 7.4, 50 μM EGTA. The homogenate was centrifuged at 48,000g, 4°C for 20 minutes and the supernatant was then discarded. The pellet was homogenised and centrifuged twice more using the tris/EGTA buffer and then with dH$_2$O. The pellet was then suspended in dH$_2$O and stored at –20°C, for at least 12 hrs.

The suspension was then thawed, homogenised in dH$_2$O and centrifuged at 48,000g, 4°C for 20 minutes. The supernatant was removed and the pellet suspended in 5 ml dH$_2$O. Protein concentration was determined by the method of Lowry (Lowry et al., 1951) and 2mg/ml dH$_2$O solutions prepared.

The forebrain homogenate, 100 μl, was incubated for 1 hr at room temperature with 10 nM [^{3}H] AMPA in tris buffers. These buffers were 50 mM tris-acetate, pH 7.4, or 50 mM tris-acetate, pH 7.4, and 100 μM EGTA or 50 mM tris-acetate, pH 7.4, and 2.5 mM CaCl$_2$. At the same time, GF/B filter paper was incubated with PEI, which was prepared using the 50 mM tris-acetate buffer.

The ligand-bound membranes were transferred onto the filter paper and washed using the 50 mM tris-acetate buffer plus 50 mM KSCN. The filter papers were allowed to dry before placing into scintillation vials and the addition of 4 ml scintillation fluid. The papers were left to incubate before the dpms were calculated and analysed to determine the amount of binding.

2.9.2.4 Quick homogenisation protocol

As neither the $CaCl_2$ nor the EGTA potentiated the binding seen above that observed with just the 50 mM tris-acetate +/- KSCN buffers, these were no longer used in the tris buffers. However, as the homogenisation protocol had increased in length to 3 days, a shorter protocol was adopted. The protocol followed was that described by Sigel et al. (1983), with minor modifications.

Briefly, the control and stargazer brains were homogenised in ice-cold buffer 1, consisting of 50 mM tris-acetate, pH 7.4, 5 mM EDTA, 5 mM EGTA, 320 mM sucrose, 1 mM PMSF, trypsin inhibitor (1 mg/100 ml), 1:1000 dilution of protease inhibitor cocktail, using the mechanical Potter glass/Teflon homogeniser and centrifuged for 12 minutes at 1,000 g, 4°C. The pellet was discarded and the supernatant was centrifuged at 40,000 g for 40 minutes, 4°C. The supernatant was discarded and the pellet rehomogenised in ice-cold buffer 2, which consisted of 50 mM tris-acetate, pH 7.4, 5 mM EDTA, 5 mM EGTA, 1 mM PMSF, trypsin inhibitor (1 mg/100 ml), 1:1000 dilution of protease inhibitor cocktail. The homogenate was then centrifuged at 40,000 g for 40 minutes, 4°C. The pellet was then rehomogenised in dH_2O and centrifuged at 40,000 g for 40 minutes, 4°C, a further three times. The final pellet was resuspended in dH_2O before being separated into three aliquots. One aliquot was used to determine the protein concentration using the Lowry's assay (Lowry et al., 1951); the second aliquot was stored at 4°C whilst the third aliquot was stored at –20°C.

Radioligand binding was determined using 100 mM tris-acetate, pH 7.4, 10 nM [^{3}H] AMPA buffers containing 1 mM glutamate, 50 mM KSCN or glutamate and KSCN. A 2 mg protein/ml dH_2O solution was prepared from the stored aliquots and 100 μl placed into test tubes. These were incubated with 100 μl of each of the buffers for 1 hr at room temperature. The ligand-bound membranes were then separated from unbound ligand onto PEI-coated GF/B filters, which were allowed to dry. The filter papers were then incubated with 4 ml scintillation fluid in scintillation vials and the dpm for each sample obtained. This protocol was repeated to obtain dose-response graphs for [^{3}H] AMPA binding in control and stargazer brain membranes.

2.10 Receptor autoradiography

Mice were anaesthetised with a lethal dose of Sagatal (sodium pentobarbitone); the stock concentration was 60 mg/100 ml but a lethal dose was induced with a dose of 100 μl/100 μg animal weight. The anaesthesia was determined by testing for a pressure reflex activity in the footpad and the nictating reflex of the eye of the mouse. The mouse was then transcardially perfused for 3 minutes with ice-cold $NaNO_2$, 0.1 % (w/v) in PBS, followed by perfusion with ice-cold sucrose, 10 % (w/v) in PBS, for 10 minutes. The perfusions were done at a rate of 10 ml/min.

Whole brains were dissected from the mice and immediately frozen in isopentane (−40°C) for 1 minute. Sections (16 μm) were cut on a Leica CM3050S cryostat (−21°C) and immediately thaw mounted onto polysine-coated glass slides (BDH). Two control and stargazer sections were mounted onto each slide. The slides were dried at room temperature for a minimum of 12 hr. Sections were then stored at −20°C under desiccant, until required.

Autoradiography was performed essentially as described by Jones et al. (1997), with minor modifications outlined below. Slide-adhering sections were incubated in the appropriate pre-incubation buffer (detailed below for each ligand), at 4°C, for 15-20 minutes. The slides were then incubated in [³H]-labelled buffer or NSB buffer for 1 hr, at 4°C, as this was deemed a sufficient amount of time for the binding to reach equilibrium. The slides were then washed by immersion (for 15 seconds) in three 1 L changes of wash buffer followed by 1 L dH_2O, all at 4°C. The slides were dried under cool air (the cool setting of a hairdryer) and stored at room temperature.
The buffers used are outlined below:

- [³H] AMPA autoradiography

Preincubation buffer – 30 mM tris-HCl, pH 7.4

Ligand-containing buffer – 30 mM tris-HCl, pH 7.4, 100 mM KSCN, 20 nM [³H] AMPA

NSB buffer – 30 mM tris-HCl, pH 7.4, 100 mM KSCN, 20 nM [³H] AMPA, 1 mM glutamate

Wash buffer – 30 mM tris-HCl, pH 7.4, 100 mM KSCN

- [^{3}H] MK-801 autoradiography

Preincubation buffer – 5 mM tris-acetate, pH 7.5, 100 µM glycine, 100 µM glutamate

Ligand-containing buffer – 5 mM tris-acetate, pH 7.5, 100 µM glycine, 100 µM glutamate, 20 nM [^{3}H] MK-801

NSB buffer – 5 mM tris-acetate, pH 7.5, 100 µM glycine, 100 µM glutamate, 20 nM [^{3}H] MK-801, 10 µM MK-801

Wash buffer – 5 mM tris-acetate, pH 7.5, 100 µM glycine, 100 µM glutamate

- [^{3}H] muscimol autoradiography

Preincubation buffer – 0.31 M tris-acetate, pH 7.1

Ligand-containing buffer – 0.31 M tris-acetate, pH 7.1, 20 nM [^{3}H] muscimol

NSB buffer – 0.31 M tris-acetate, pH 7.1, 20 nM [^{3}H] muscimol, 1 mM GABA

Wash buffer – 10 mM tris-HCl, pH 7.4

- [^{3}H] Ro15-4513 autoradiography

Preincubation buffer – 50 mM tris-HCl, pH 7.4, 120 mM NaCl

Ligand-containing buffer (A) – 50 mM tris-HCl, pH 7.4, 120 mM NaCl, 20 nM [^{3}H] Ro15-4513

Ligand-containing buffer (B) – 50 mM tris-HCl, pH 7.4, 120 mM NaCl, 20 nM [^{3}H] Ro15-4513, 10 µM flunitrazepam

NSB buffer – 50 mM tris-HCl, pH 7.4, 120 mM NaCl, 20 nM [^{3}H] Ro15-4513, 10 µM Ro15-1788

Wash buffer – 10 mM tris-HCl, pH 7.4

The slides were placed into an autoradiography cassette and exposed to [^{3}H]-hyperfilm. The film was left to expose for between 5 days ([^{3}H] muscimol) to 10 weeks ([^{3}H] AMPA). The exposed films were developed manually using Kodak GBX developer and fixer solutions. Images were obtained by scanning the films using a Canon CanoScan N1220U scanner and analysed using Scion Image software, Scion Corp (downloaded from the website http://www.scioncorp.com).

2.11 Toluidine blue staining of sections

The sections used for autoradiography were hydrated by incubating for 5 minutes each, at room temperature, in decreasing concentrations of ethanol – 100 % (v/v) followed by 90 % (v/v) followed by 70 % (v/v) followed by 50 % (v/v). The slides were then incubated in dH$_2$O for 3 minutes before incubating in 0.02 % (w/v) toluidine blue (aq.) for 10 minutes. Any excess toluidine blue was rinsed off by dipping the slides, briefly, in dH$_2$O. The slides were then dehydrated by incubating, for 5 minutes each, in increasing concentrations of ethanol – 50 % (v/v) followed by 70 % (v/v) followed by 90 % (v/v) followed by 100 % (v/v). The slides were left to dry at room temperature for at least 24 hr before mounting DPX mountant and overlaid with a glass cover slip. Images were taken using the Digital Camera RT Slider Spot (Diagnostic Instruments Incorporated) attached to an Axiovert 135 microscope (higher magnification sections) or a Zeiss Stemi SVII microscope (whole sections). The software used to interface with the digital camera was the Spot Advanced Imaging program, which came with the camera.

2.12 Immunohistochemical localisation of receptor subunits

Adult control (+/+ and +/stg) and stargazer mice were anaesthetised with a lethal dose of Sagatal, applied by intraperitoneal injection using a 1 ml syringe and a 25G needle. The chest cavities were then opened and the mice were transcardially perfused through the ascending aorta with ice-cold NaNO$_2$, 0.1 % (w/v) in PBS, for 3 minutes.

The perfusate was then replaced with ice-cold 4 % (w/v) paraformaldehyde (see appendix 1) for a further 20 minutes. The mice were initially perfused with the paraformaldehyde in PBS (some of the horizontal sections were from mice perfused with this). However, later experiments showed that the PBS appeared to be deleterious to the staining. For this reason, the later fixations were done with the paraformaldehyde in phosphate buffer, pH 7.4, without saline. All the sagittal sections were fixed with this paraformaldehyde solution.

The brains were then dissected out and were post-fixed by immersion in 4 % (w/v) paraformaldehyde in phosphate buffer, pH 7.4, for 24 hr. They were then transferred to 10 % (w/v) sucrose in PBS for 48 hr at 4 C. The sucrose solution was exchanged for fresh sucrose solution every 12 hr.

The brains were frozen for 2 minutes at $-70^\circ C$ in isopentane in an aluminium carriage suspended over liquid N_2. The brains were then transferred to the cryostat and once thermally equilibrated (to $-21^\circ C$), they were sectioned (30μm). Brain sections in the horizontal and sagittal planes were prepared. The sections were transferred to the wells of 24-well plates containing 0.02 % (w/v) sodium azide in PBS and either used immediately or stored at $4^\circ C$.

The free-floating brain slice sections were immunochemically stained using a modification of the VectaStain ABC Elite protocol as described by Thompson et al. (2000).

Briefly, cryostat cut, free-floating sections were incubated in a methanol-peroxide solution, comprising of 10 % (v/v) methanol and 3 % (v/v) H_2O_2 in PBS, for 30 minutes, at room temperature, to destroy endogenous peroxidase activity in the tissue. All the incubations were done on a Stuart Scientific 3D rocking platform STR9 or a Stuart Scientific platform shaker STR6. The methanol-peroxide solution was removed and the sections were washed three times with 0.2 % (v/v) Triton X-100 in PBS, hereafter known as PBS-T.

The slices were then incubated in 0.2 % (w/v) glycine in PBS, for 30 minutes, at room temperature, to quench any residual active fixative by binding to any unreacted paraformaldehyde.

The sections were then incubated with blocking buffer, which comprised of 10 % (v/v) blocking serum in PBS-T, for 1 hr at room temperature. This incubation ensured that the serum blocked any non-specific IgG binding sites. The species of animal from which the blocking serum was obtained was governed by the secondary IgG-biotinylated conjugate used as a reporter. For example, if the secondary IgG was

from goat, goat serum was used as the blocking serum; if donkey IgG was used, the blocking serum was obtained from horse.

Primary antibody, 1:100 – 1:1000 dilution or 0.125 – 1 µg/ml of primary antibody and 1 % (v/v) blocking serum in PBS, was applied and the sections were left to incubate at 4°C, overnight.

The sections were then washed three times for 5 minutes each with PBS-T before incubating with biotinylated secondary antibody, 50 µl biotinylated secondary antibody in 10 ml PBS with 1 % (v/v) blocking serum, for 1 hr, room temperature.

The sections were washed three times, for 5 minutes each, with PBS-T and incubated with the ABC reagent for 1 hr. The ABC reagent was prepared at least 30 minutes before it was required by adding 2 drops of solution A and 2 drops of solution B to 5 ml PBS. The ABC reagent was mixed for 30 minutes on the roller mixer.

The sections were washed three times with PBS-T followed by two washes with PBS before incubating with HRP substrate, which comprised of 1 ml of 5 mg/ml 3,3'-diaminobenzidine, 6.67 µl H_2O_2 (30 % v/v stock) and 9 ml PBS. The sections were left to incubate with the HRP substrate in the dark until the stain reached the desired intensity, at which point they were washed with multiple changes of dH_2O before mounting onto glass slides. The sections were left to dry on the slides for at least 12 hr at room temperature before DPX mountant and glass cover slips were applied. Images were taken with the digital camera and Spot Advanced Imaging software as described above for the toluidine blue stained slides.

2.13 Genomic PCR

A genomic PCR protocol was followed in order to determine whether a mouse was a control, wild-type mouse (i.e. +/+), a heterozygote mouse (i.e. a +/stg) or whether it was a stargazer mouse (i.e. stg/stg). This was important for determining which mice could be used for breeding purposes as, phenotypically, heterozygotes, which were used in the breeding programme, and wild-type mice were indistinguishable from

each other. The ability to determine the genotype of a mouse was also important for cell culture purposes as the mice were used at P5-7, an age when the stargazer phenotype is not apparent.

2.13.1 Preparation/isolation of DNA

Tail samples from tagged mice were incubated with ice-cold lysis buffer, containing 96.8 mM EDTA, pH 8.0, 500 µl Nuclei Lysis Solution, 0.35 mg proteinase K, at 55°C, until digested. This digestion step could take from 2 hr for samples from mouse neonates aged P3-4, to overnight for samples from adults.

The digested samples were allowed to cool before the addition of 200 µl Protein Precipitation Solution. The samples were then vortexed and chilled on ice for 5 minutes before centrifuging for 4 minutes at 14,000g using the Eppendorf 5415c microcentrifuge.

Supernatant (600 µl) removed from each of the samples, was placed into a fresh, eppendorf tube and mixed with 600 µl isopropanol by inversion. During the mixing, the DNA strands become visible to the naked eye, as the DNA precipitates. The samples were then centrifuged for 1 minute at 14,000g, at the end of which the DNA formed a pellet at the bottom of the eppendorf tubes.

The supernatant was removed and 600 µl of 70 % (v/v) ethanol was added to the DNA pellets. Each eppendorf tube was then inverted, in order to wash the DNA, before centrifuging for a further 1 minute at 14,000g.

The DNA formed a loose pellet at the bottom of the each eppendorf tube. The supernatant was removed and the DNA pellet was air-dried. TE, 10 mM tris, 1 mM EDTA (100 µl), was added to each sample, which were left to incubate for 1 hr at 65°C. The samples were then stored at 4°C until required for the polymerase chain reaction (PCR).

2.13.2 PCR

The following PCR mix was prepared for each sample as below:

10X SuperTAQ PCR Buffer	5 µl
10 mM dNTPs	1 µl
25 pM/µl 109F Primer	2 µl
25 pM/µl E/Ht7 Primer	2 µl
25 pM/µl ETN-OR Primer	1 µl
1 unit/µl TAQ	1 µl

The PCR reactions were performed in thin walled PCR tubes, which contained 12 µl PCR mix, 12 µl autoclaved dH_2O and 1 µl DNA sample. Positive controls were prepared using DNA from mice of known genetic background such that samples from +/+, +/stg and stg/stg were assayed alongside the unknown test samples; negative controls were prepared using 12 µl PCR mix and 13 µl autoclaved dH_2O.

The samples were placed into the PCR machine (Perkin-Elmer GeneAmp PCR System 2400) and run on a programme consisting of 1 cycle of 95°C for 5 minutes, followed by 30 cycles of 94°C for 1 minute, 55°C for 2 minutes and 72°C for 2 minutes. The programme is then held at 4°C until the PCR products can be removed from the machine and run on an agarose gel. The 95°C temperature causes the primer and the template to dissociate whilst the 55°C temperature will cause the primer and template to anneal. The 72°C temperature allows the extension of the products by the TAQ polymerase.

The agarose gel was prepared using 1.2 g agarose and 80 ml TBE (1X). PCR product (5 µl) was combined with 7 µl of PCR sample buffer, 2 µl PCR loading buffer and 5 µl autoclaved dH_2O, and loaded onto the agarose gel. Markers, 1 µl of 100 base pair DNA ladder in 2 µl PCR loading buffer and 9 µl autoclaved dH_2O, were also loaded and the gel was run at 70V for ~ 2 hr. The gel was then incubated with ethidium bromide, 10 µl ethidium bromide in 200 ml dH_2O, for ~ 15 minutes before destaining in multiple changes of dH_2O. The DNA bands were visualised under UV light using the BioRad GelDoc 2000 system. Photos of the gels were taken using the printer supplied with the system. These photos were scanned to provide the images used in the figures in the following chapters.

2.14 Primary cerebellar granule cell cultures

+/+, +/stg and stg/stg mouse neonates were identified by the genomic DNA PCR amplification strategy outlined above, using DNA obtained from tail biopsies from the mice at P3. +/+ and +/stg cerebella were combined and used to derive age-matched littermate control cerebellar granule cells (CGCs), which were used to compare against CGCs from stg/stg cerebella.

Cell culture, polylysine-coating of the dishes and dissection of the brains were all undertaken in a sterile laminar flow hood.

2.14.1 Poly-L-lysine treatment of plastic culture dishes

Sterile plastic petri dishes (35 mm, Nunc) were polylysine coated before using for primary cell culture. Poly-L-lysine hydrobromide was prepared to a concentration of 50 μg/ml in dH_2O. The polylysine solution, 2 ml per dish, was sterile filtered directly onto the dishes using a sterile syringe and a sterile 0.20 μm membrane disposable syringe filter (Nalgene, BDH). The petri dishes were left to incubate overnight, at room temperature.

The polylysine was then aspirated off the dishes, which where then left to dry in the laminar flow hood, for 30 minutes, at room temperature. Each dish was then washed three times with 2 ml of sterile, autoclaved dH_2O. The dishes were then left to dry in the flow hood, until required for plating of the cells.

2.14.2 Cell culture

The method adopted was that previously described by Thompson and Stephenson (1994). All solutions used are found in appendix 1 and were filter sterilised using sterile disposable syringe filters attached to sterile syringes before use.

Briefly, cerebella were dissected from neonatal mice aged P5-P7, under aseptic conditions, and minced using sterile scalpel blades. The tissue was then incubated in trypsin solution for 15 minutes at $37^{\circ}C$, with agitation, in a Grant SUB6 water bath.

Dilute trypsin inhibitor, containing DNAse I, was then added and the tissue was centrifuged at 100g for 2 minutes, using a Harrier 15/80 centrifuge.

The supernatant was removed and concentrated trypsin inhibitor (~ 8 ml) was added in two tranches and the pellet was triturated, using fire-polished sterile glass Pasteur pipettes. The cell suspension was overlaid onto the bovine serum albumin (BSA) and centrifuged at 200g for 5 minutes.

The supernatant was removed and discarded and the cell pellet was suspended in culture media, Dulbecco's Modification of Eagle's Medium (DMEM), 10 % (v/v) foetal calf serum, 2 mM glutamine, 50 µg/ml gentamycin, supplemented with 0.033 M glucose.

The total number of cells was estimated using an improved Neubauer haemocytometer (BDH) and a Nikon TMS microscope. Cells were plated out at a density of 2.5 x 10^6 cells per 35 mm plastic culture dish. The cells were stored in an LEEC incubator at 37°C, 95 % O_2/5 % CO_2, high humidity, which was maintained by the addition of sterile, autoclaved water to the base of the incubator.

Sterile 5-fluoro-2'-deoxyuridine (FDU), final concentration of 8 mM, was applied to the cells 24 hr after plating, in order to inhibit the mitosis of non-neuronal cells. Media was subsequently supplemented with sterile water and glucose, as required.

2.15 Cell surface expression of GluR2 receptors

Determination of surface expression of the AMPAR GluR2 subunit was performed essentially as described in Hall and Soderling (1997) and Ives et al. (2002). The impermeable cross-linker bis (sulfosuccinimidyl) suberate (BS^3) (Pierce) was dissolved in iso-osmotic saline solution (SS), 137 mM NaCl, 5.3 mM KCl, 0.17 mM Na$_2$HPO$_4$, 0.22 mM KH$_2$PO$_4$, 10 mM HEPES, 33 mM glucose, 44 mM sucrose, pH 7.2. Cultured cerebellar granule cells, 15 DIV, were washed 3 times with SS before being treated with/without BS^3 for 10 minutes at 37°C. Cells were then washed 3 more times with SS before the cross-linker was quenched using serum-

containing culture media. The cells were washed a further 2 times with SS before being collected in SDS-containing solubilisation buffer, 50 mM tris, 2 mM EDTA, 2 % (w/v) SDS, pH 6.8, for analysis by SDS-PAGE.

Following immunoblotting, where the blots were screened for GluR2 and β-actin expression, the films of the immunoblots were analysed using the GelDoc 2000 and the Quantity One software. The data were then incorporated into the following equations, adapted from Ives et al. (2002), to determine the extent of cell surface expression:

Total GluR2 expression $\quad = SS_{GluR2} / SS_{Actin}$

Intracellular GluR2 $\quad = BS^3_{GluR2} / BS^3_{Actin}$

Extracellular GluR2 $\quad =$
[(Total GluR2 − Intracellular GluR2) / Total GluR2] * 100

The level of expression of the GluR2 protein was determined in both cultured control (+/+ and +/stg) and stargazer (stg/stg) cerebellar granule cells.

2.16 Statistical analyses

Prism (version 3.0, GraphPad Software Incorporated) was used to generate the graphs used throughout. Statistical analyses (Student's t-tests) were also undertaken using Prism; with the null hypothesis being rejected if P was less than 0.05.

Chapter 3

GABA$_A$ receptor expression in stargazer mutant mice

3.1 Introduction

3.1.1 The stargazer mutation

Although the stg/stg cerebellum is mildly hypoplastic, the overall pattern of cerebellar foliation appeared normal and no major structural or anatomical abnormalities were observed (Qiao et al., 1996). However, whilst the layout of the cerebellar cortex and the deep cerebellar nuclei in adult stargazer mice was the same as in wild-type controls, a greater number of external granule cells was found to still reside in the external germ layer at postnatal day 15 (P15) in stg/stg cerebellum compared to controls. This difference was no longer apparent by P20, indicating a delayed migration of the granule cells. Furthermore, some of the granule cells in the stg/stg cerebellum appeared to have elongated oval-shaped nuclei with clumps of coarse chromatin, a morphology reminiscent of immature cerebellar granule cells (Qiao et al., 1998).

3.1.2 The GABA$_A$ receptor in stargazer mice

The α_6 subunit, which is exclusively expressed by cerebellar granule cells (CGCs), begins to appear in the cerebellum from P7 – P14. However, as mentioned above, maturation of the CGCs in the cerebellum of stargazer mice appears to be compromised as they have a delayed phase of migration and a sub-population of CGCs in the adult stargazer cerebellum that have morphological features of immature neurons (Qiao et al., 1998). Interestingly, adult stargazer mice have been reported to express much less of the GABAR α_6 (and β_3) subunit, a marker of CGC maturity (Thompson et al., 1998).

Ro15-4513 is a partial agonist at GABAR with high affinity for the α_4 and α_6 subunit-containing receptors. It had previously been shown that the number of total specific Ro15-4513 binding sites (a measure of total number of γ_2 subunit-containing GABAR) was not significantly different between control and stargazer cerebella.

50

The benzodiazepine-insensitive subtype, one of two components of the γ_2 subunit-containing population of GABAR, was, however, severely reduced in stargazer cerebellum (down to 30 % of controls). As the cerebellum does not contain the α_4 subunit, the decreased binding seen in the stargazer cerebellum was in accordance with the lower levels of α_6 expressed in stargazer (Thompson et al., 1998).

3.1.3 Work carried out

The work in this chapter was undertaken firstly to repeat the previous published work on stargazer and secondly, to further characterise GABAR expression within the brain of stargazer mice. Previous published work used the C57BL/6J strain of mice as the background control strain to the B6C3Fe$^+$ strain of stargazer mouse (Thompson et al., 1998). However, published studies have indicated that different strains of mice account for differences seen in both electrophysiological traits and survival of cultured cerebellar granule cells (Fujikawa et al., 2000; Bampton et al., 1999).

A genomic PCR amplification strategy was utilised to identify the genotype of the mice used (+/+, +/stg or stg/stg). Subsequently, the expression levels of the GABAR α_1 and α_6 subunits were quantified in +/+, +/stg and stg/stg cerebellar membranes by semi-quantitative immunoblotting. The anatomical expression profile of the α_6 subunit throughout the brain was investigated using immunohistochemistry. Finally, autoradiography was employed to determine the pharmacological profile of the assembled GABAR expressed in control and stargazer brain sections.

3.2 Results

3.2.1 Genomic Screening

A PCR amplification strategy, as outlined in section 2.13, was utilised to identify +/+, +/stg and stg/stg mice. Genomic DNA was obtained for this strategy was obtained from tail biopsies removed from adult mice: +/+ tissue was obtained from wild-type (B6C3Fe$^+$) mice; stg/stg tissue was obtained from adult stg/stg mice identified by their phenotype; +/stg tissue was obtained from the initial breeding pairs (+/stg mice) received from Jackson Laboratories. This genomic screen was

51

applied to genomic DNA derived from adult mice, to identify suitable breeding pairs (+/stg) in order to maintain the breeding programme, and to genomic DNA obtained from neonatal mice at P3, for primary cerebellar granule cell culture purposes.

As illustrated in figure 3.1, a predicted single PCR product of 600bp was generated from DNA from +/+ mice; amplification of DNA obtained from stg/stg mice resulted in a predicted single PCR product of 300bp. Genomic DNA of +/stg mice, as expected, produced two PCR products of both 300 and 600bp. A minor ethidium bromide intercalated species of 800bp product was also obtained but this was only ever present in DNA from +/stg mice. These results (i.e. the sizes of the DNA fragments in +/+, +/stg and stg/stg mice) were seen in both young and adult mice.

The validity of the genomic PCR screen was tested by allowing the screened neonates to mature and test for genomic background by their subsequent phenotype (stg/stg progeny) or as a consequence of mating assays. Mice showing just the 300bp product on the agarose gel do indeed go on to develop the stargazer phenotype. Mice showing both the 300bp and 600bp products (i.e. the heterozygotes) do not show any of the characteristics associated with stargazer mice. When mated, however, they produce offspring showing stargazer characteristics, in roughly mendelian ratios of 1 +/+ : 2 +/stg : 1 stg/stg. The mice with only the 600bp products show neither stargazer characteristics nor produce offspring with the stargazer phenotype.

Figure 3.1 Agarose gel analysis of amplicons obtained from a genomic PCR amplification of adult mouse tail biopsy, using UV light following ethidium bromide staining. A 100 base pair marker is in lane M, and the 300 base pair, 600 base pair and 800 base pair products indicated. The low molecular weight band identified by the red arrow was due to excess PCR primers. Lanes 1-10 were products from 10 adult mice. Negative control was in lane 11 whilst positive controls, from mice of a known genetic background, were in lanes 12-14. The key below indicates whether the sample came from a +/+, +/stg or stg/stg mouse:

Sample	Genotype	Sample	Genotype
1	+/stg	6	+/stg
2	+/stg	7	+/stg
3	stg/stg	8	+/stg
4	+/+	9	+/+
5	+/+	10	stg/stg

Sample	Control	
11	Negative	No DNA
12	Positive	DNA from known +/+
13	Positive	DNA from known +/stg
14	Positive	DNA from known stg/stg

800 →
600 →
300 →

M 1 2 3 4 5 6 7 8 9 10 11 12 13 14

Samples   Controls
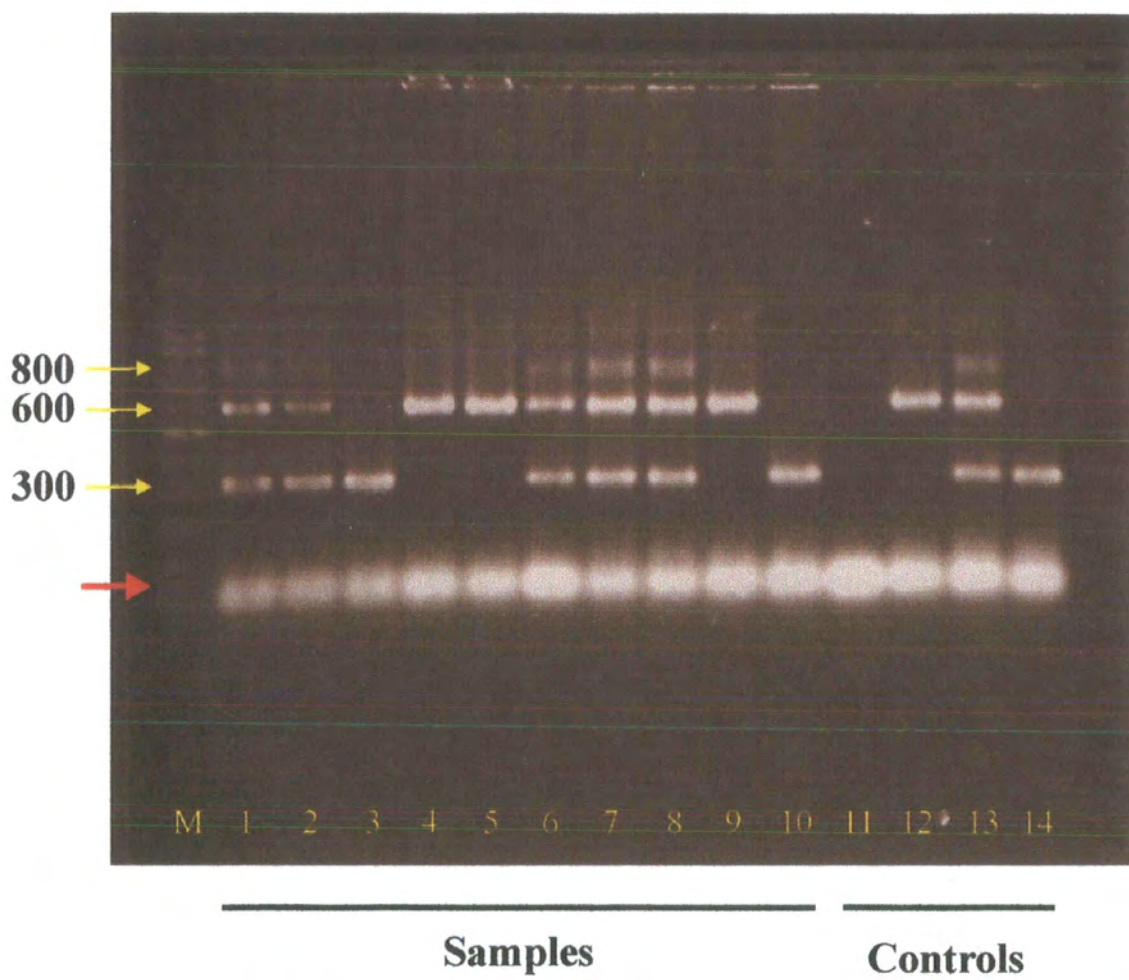
3.2.2 Semi-quantitative immunoblotting of $GABA_A$ receptor subunits

It has previously been shown that the expression levels of the $GABA_A$ receptor (GABAR) subunits α_6 and β_3 are both reduced in cerebellar membrane homogenates prepared from adult stargazer cerebella when compared to control cerebella. The levels of expression of the α_1 and β_2 subunits, however, were not different to control levels (Thompson et al., 1998).

The C57BL/6J strain was employed as the background strain of mice and was used for control tissue. It is a distinct possibility that the differences observed in the expression levels of GABAR subunits were due to stain differences between the mice used and not a consequence of the stargazer mutation. Therefore, the expression levels of the GABAR α_1 and α_6 subunits were determined in +/+, +/stg and stg/stg mice that had been identified by genomic PCR, as described in section 3.2.1. Cerebellar membranes taken from adult +/+, +/stg and stg/stg mice were probed with both GABAR anti-α_1 and anti-α_6 subunit-specific antibodies, as previously described (section 2.7).

3.2.2.1 Expression of α_1 and α_6 subunits in cerebellar membranes

As can been seen in figure 3.2, there was no significant difference in the levels of α_1 expressed in +/+, +/stg and stg/stg cerebellar membranes. However, when probed with the anti-α_6 antibody, α_6 levels were clearly lower in membranes prepared from cerebella taken from stg/stg mice. No decrease was seen in cerebella from +/+ and +/stg mice.

The levels of the α_1 and α_6 subunits were quantified by probing stg/stg and control cerebella membranes with anti-α_1, anti-α_6 and anti-NSE subunit-specific antibodies. The control membrane preparation now comprised of a mixture of +/+ and +/stg cerebellar membranes as no significant differences in any parameter so far investigated had been observed. This was supported by other studies that showed that there was no difference in BDNF mRNA expression between +/+ and +/stg cerebella (Qiao et al., 1996). Similarly, no significant differences were found in the

Figure 3.2 Immunoblot showing the expression of GABAR α_1 and α_6 subunit proteins in adult wild-type (+/+), heterozygote (+/stg) and stargazer (stg/stg) cerebellar membranes.

Broad range (20.5 kDa – 210 kDa) molecular weight markers were used and have been indicated to the left of the immunoblot. The α_1 protein has a molecular weight of 51 kDa and was the lower band present on the immunoblot; the α_6 protein has a molecular weight of 56 kDa and was the upper band present on the immunoblot. As can be seen, both the α_1 and α_6 proteins were present in the +/+, +/stg and stg/stg cerebellar membranes, although the α_6 protein was much reduced in the stg/stg membrane.
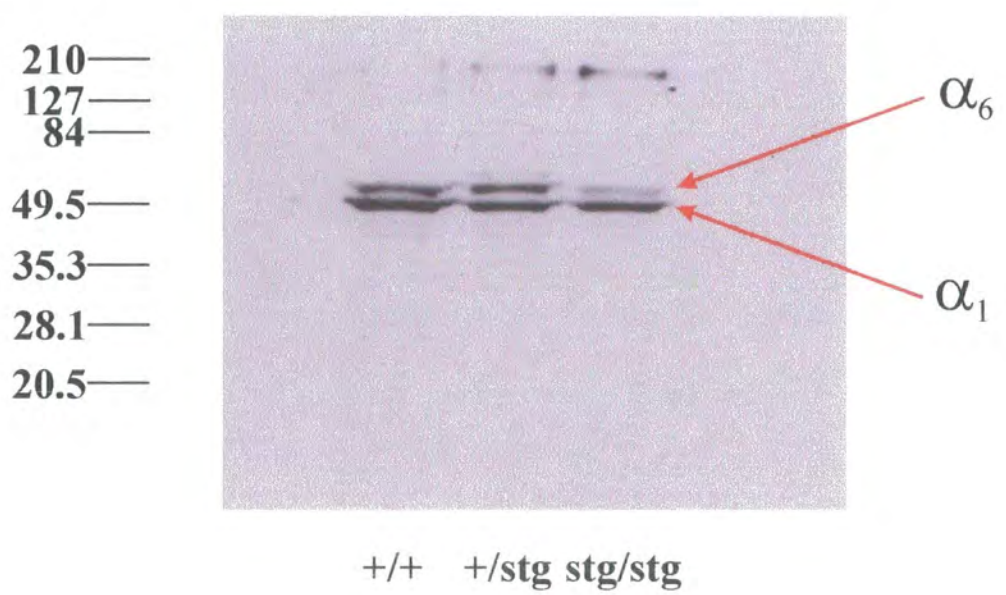
phenotype (Qiao et al., 1998) or following electrophysiological analyses (Hashimoto et al., 1999) of +/+ and +/stg mice.

3.2.2.2 Quantification of α_1 subunit levels

Control and stg/stg cerebellar membrane homogenates were probed with anti-α_1 antibody (0.5 µg/ml) and subsequently with anti-NSE antibody (1:20,000 dilution), as outlined previously. Figure 3.3A shows the expression of the α_1 subunit in differing concentrations of both control and stargazer cerebellar membrane homogenates. As mentioned above, the membrane was then reprobed for NSE expression (figure 3.3B).

The comparative expression levels of the α_1 subunit were then determined and this was normalised against the levels of NSE expressed, using computer-assisted densitometry (section 2.7.3). No significant differences between the expression levels of α_1 in stargazer cerebellar membranes and control cerebellar membranes were observed (figure 3.5). The relative levels were 100 % for control homogenate and 101.2 ± 6.4 % for stg/stg homogenate (values are means ± sem).

3.2.2.3 Quantification of α_6 subunit levels

The expression levels of α_6 and NSE in cerebellar membranes from stargazer and control were determined by immunoblotting using a concentration of membrane proteins to aid quantification (figure 3.4). SDS-PAGE mini-gels were loaded with control and stg/stg cerebellar membrane homogenates, along with control forebrain homogenates (at a protein concentration of 5 µg/10 µl). These were then probed with anti-α_6 subunit-specific antibody (1 µg/ml) and subsequently reprobed with the anti-NSE antibody (1:20,000 dilution), as outlined in (section 2.7.2).

The ratio of the α_6 subunit : NSE was determined using computer-assisted densitometry, as outlined in (section 2.7.3). By determining the levels of the GABAR subunits and then normalising against the levels of NSE expressed, it is possible to calculate the comparative levels of expression of the GABAR subunits.

Figure 3.3 Immunoblots showing levels of expression of the $GABA_A$ receptor α_1 subunit protein (A) and NSE protein (B) in control and stargazer cerebellar membranes. Also shown is the expression of both proteins in control forebrain membranes (5 µg/10 µl). A range of concentrations of the cerebellar membranes were used – 1.25 µg/10 µl, 2.5 µg/10 µl, 5 µg/10 µl and 10 µg/10 µl – as indicated on both immunoblots.

A

127 —
84 —
49.5 — ← α_1
35.3 —
28.1 —

10 5 2.5 1.25 10 5 2.5 1.25 5

control   stargazer   FB

B

127 —
84 —
49.5 — ← NSE
35.3 —
28.1 —

10 5 2.5 1.25 10 5 2.5 1.25 5
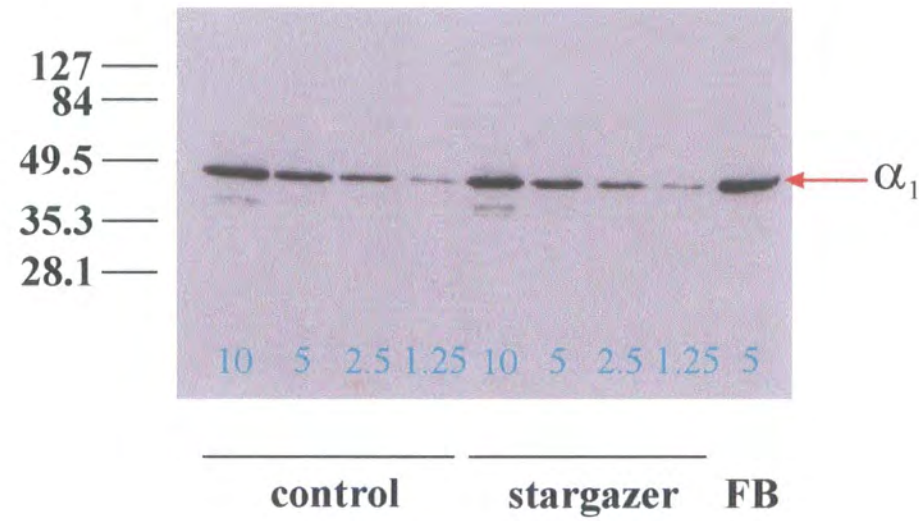
control   stargazer   FB
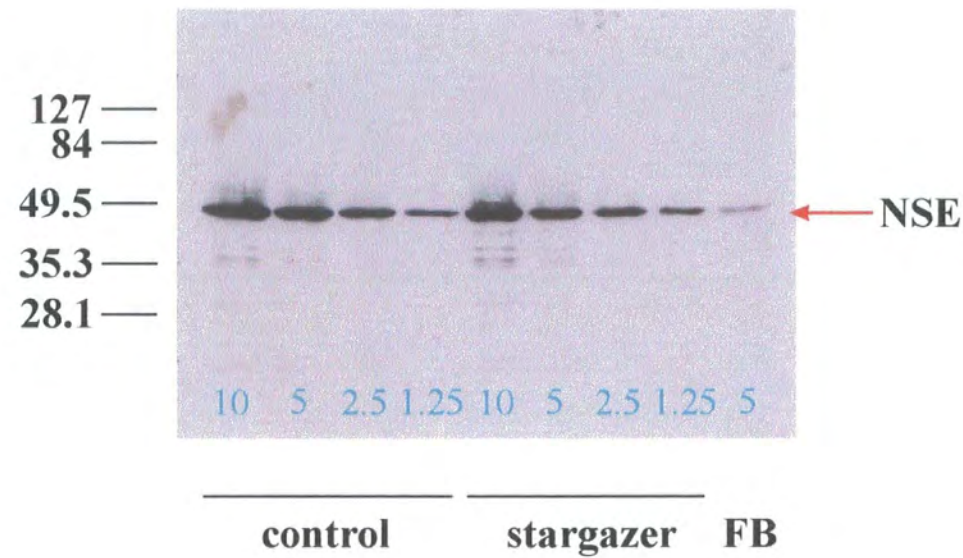
Figure 3.4 Immunoblots showing levels of expression of the GABAR α_6 subunit protein (A) and NSE protein (B) in control and stargazer cerebellar membranes. A range of protein concentrations were used – 1.25 µg/10 µl, 2.5 µg/10 µl, 5 µg/10 µl and 10 µg/10 µl – as indicated on both immunoblots. Also shown is the expression of both proteins in control forebrain membranes (5 µg/10 µl).

A

210 —
84 —
49.5 —
35.3 —
28.1 —

10 5 2.5 1.25 10 5 2.5 1.25 5

control   stargazer   FB

α₆

B

210 —
84 —
49.5 —
35.3 —
28.1 —

10 5 2.5 1.25 10 5 2.5 1.25 5

control   stargazer   FB

NSE
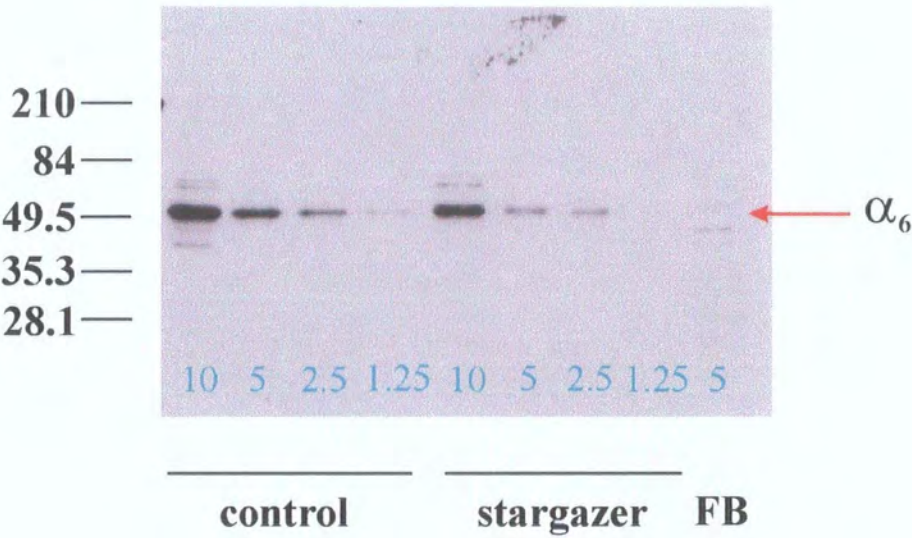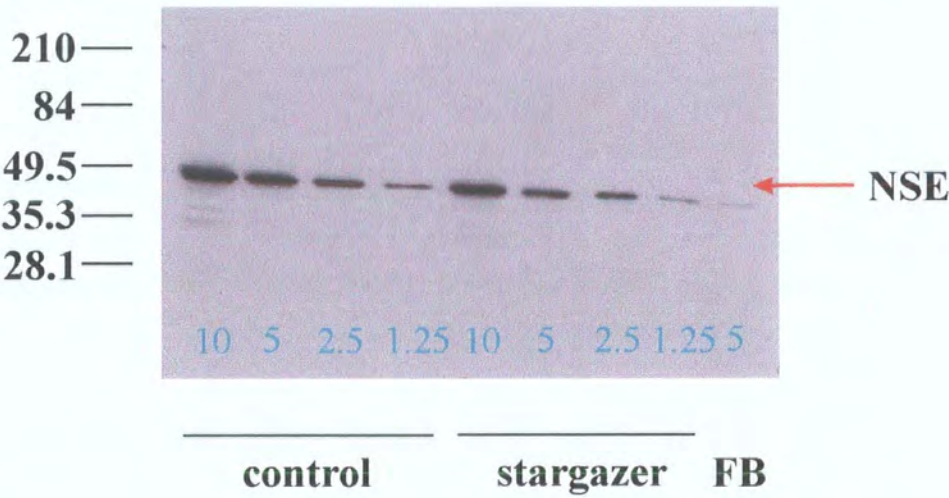
Using such calculations, the following figure was obtained:
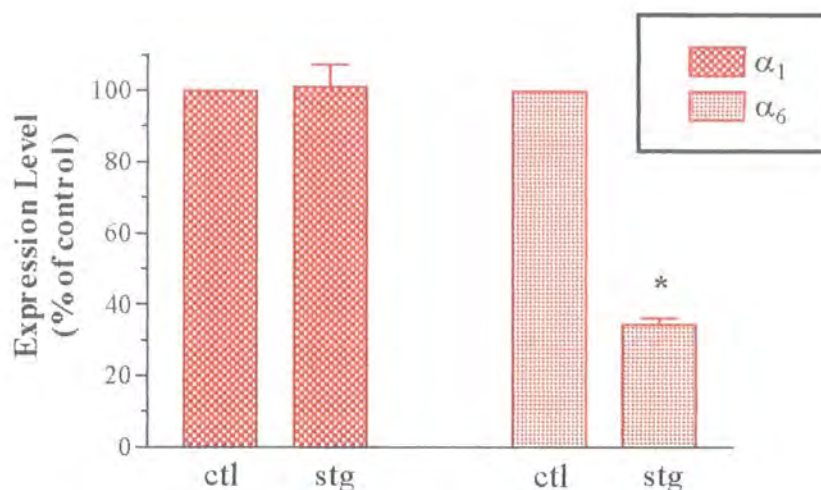
Figure 3.5 Bar graph showing the relative expression levels of the GABAR α_1 and α_6 subunits in control (ctl) and stargazer (stg) cerebellar P2 membranes. The levels were normalised to controls (100 %) using NSE as the normalising probe. As can be seen, there was no significant difference in the levels of the α_1 subunit whereas there was a significant decrease in the levels of α_6 expression in the stargazer cerebellum, as determined using Student's t-test (* = P < 0.02). Results expressed as mean ± sem; n = 3 – 4 samples from both control and stargazer cerebella; immunoblotting repeated twice.

From a visual inspection of the immunoblots in figure 3.4, it is clear that the GABAR α_6 subunit was under-represented in stg/stg cerebellum relative to controls. Immunoblots were quantified by image densitometry and NSE expression used as a normalising factor in the estimates. The levels of α_6 were arbitrarily assigned a value of 100 % in control membranes (figure 3.5). The expression level in stg/stg cerebellar membranes was only 34.4 ± 1.8 % (values expressed as mean ± sem).

3.2.3 Immunohistochemical localisation of GABAR α_6 subunit

In order to map the cellular expression patterns of the GABAR α_6 subunit, fixed control and stg/stg brain sections were subjected to immunohistochemical analysis using the GABAR anti-α_6 subunit-specific antibody as a probe (see figures 3.6 and 3.7).

Figure 3.6 Immunohistochemical expression of $GABA_A$ α_6 subunit protein within the forebrain of control (A) and stargazer (B) mice. Sections were incubated with anti-α_6 subunit-specific antibody before staining with DAB. Staining was not seen within either the control forebrain or within the stargazer forebrain, although staining was seen within the cerebellum attached to the control forebrain section.

Scale bars represent 1 mm.
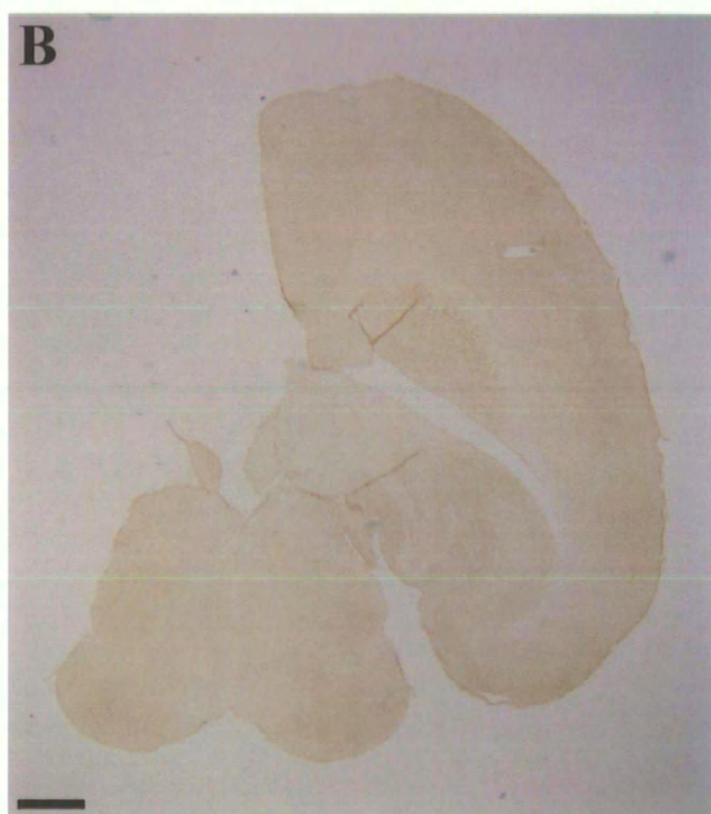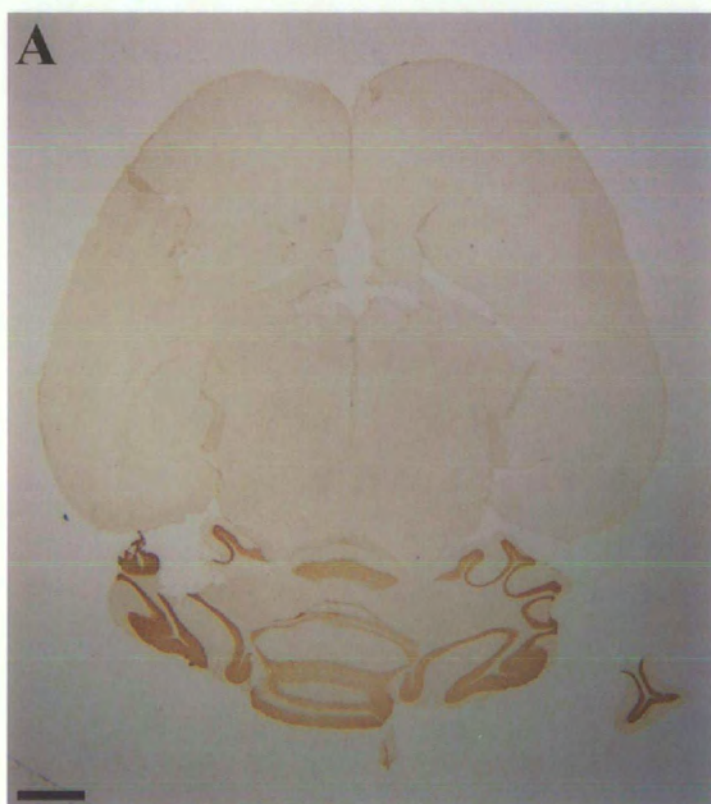
Control and stg/stg brain sections were incubated with 0.125 µg/ml GABAR anti-α_6 subunit-specific antibody. The distribution of bound primary antibody was revealed by conventional methods using the Vecta-stain ABC elite kit with 3,3'-diaminobenzidine horseradish peroxidase, as described in section 2.12. Both control and stg/stg sections were incubated with the HRP substrate for the same amount of time.

As illustrated in figure 3.6A, no specific staining was seen in any of the forebrain structures in the control forebrain. Note that, in figure 3.6A, a section of cerebellar tissue was attached to the control forebrain section and it can be clearly seen that the antibody has identified α_6 expression in cerebellar granule cells, in accordance with the known distribution of this subunit (Pirker et al., 2000; Mellor et al., 1998; Laurie et al., 1992; Thompson et al., 1992). Stargazer forebrain sections were also incubated with the α_6 antibody and, as was seen in figure 3.6B, no staining was evident in stargazer forebrain.

GABAR α_6 subunit-like immunoreactivity, however, was present in the cerebellum of both control and stg/stg brains (figure 3.7). In both tissue sections, the staining was specific to the granule cell layer, with no staining observed in the molecular layer. A decrease in staining intensity was seen in the stargazer cerebellar granule cell layer (figure 3.7D) when compared to the staining intensity seen within the control granule cell layer (figure 3.7B).

The results obtained by both the immunoblotting of cerebellar P2 membranes and immunohistochemistry appeared to imply a decrease in the numbers of α_6-containing $GABA_A$ receptors in the stargazer cerebellum.

Figure 3.7 Immunohistochemical analysis of the expression of α_6 subunit protein within the cerebellum. Control (A) and stargazer (C) horizontal cerebellar sections were incubated with anti-α_6 subunit-specific antibody before staining with DAB.

As can be seen in the whole sections, immunostaining was observed in both the control and stargazer cerebellum. Staining in the control cerebellum (B) was seen mainly within the granule cell layer (GL), with some staining within the Purkinje cell layer (PL). No staining was detected in the molecular layer (ML) or within the white matter (WM).

A similar expression pattern was seen within the stargazer cerebellum, although the staining intensity was reduced (D).

Scale bars represent 100 μm (B and D) or 1 mm (A and C).
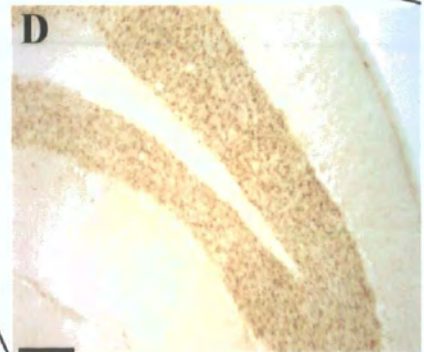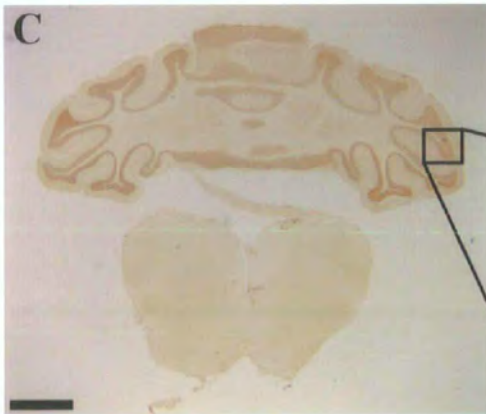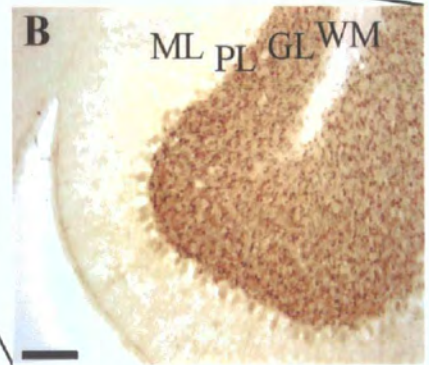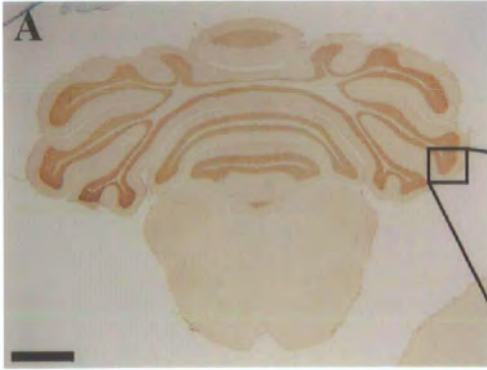
3.2.4 Autoradiography

Frozen whole brain sections were obtained from both control and stargazer mice and applied to polysine-coated slides. Each slide consisted of 2 x control slices and 2 x stg slices, allowing direct comparison of radioligand binding. The slides were incubated with [^{3}H] muscimol or [^{3}H] muscimol + GABA (specific and non-specific binding respectively), or with [^{3}H] Ro15-4513 only, [^{3}H] Ro15-4513 + flunitrazepam or [^{3}H] Ro15-4513 + Ro15-1788 (non-specific binding), as outlined in section 2.10. The treated slides were exposed to [^{3}H] hyperfilm for 5-10 days (for [^{3}H] muscimol binding) and 4-8 weeks (for [^{3}H] Ro15-4513 binding) before being stained with toluidine blue, as described in section 2.11.

3.2.4.1 [^{3}H] Muscimol Autoradiography

As can be seen in figure 3.8A, [^{3}H] muscimol binding was seen in most parts of the control brain, including the hippocampus, the caudate-putamen and the cortex, with the strongest signal obtained in the cerebellum. A similar labelling pattern was seen within the stargazer sections (figure 3.8E). However, the labelling seen in the stargazer sections appeared to be less than the labelling seen in the control sections. This was most apparent in the cerebellum, where the intensity of the signal seen in the control cerebellar sections was visibly decreased in the stargazer cerebellar sections. Non-specific labelling was at the level of film background in both the control (figure 3.8C) and stargazer sections (figure 3.8G).

3.2.4.2 [^{3}H] Ro15-4513 Autoradiography

Ro15-4513 is an inverse GABA agonist, which binds to the benzodiazepine-binding site of GABA$_A$ receptors containing the γ subunit. Flunitrazepam displaces Ro15-4513 bound to benzodiazepine (BDZ)-sensitive receptors, i.e. GABAR composed of α_1, α_2, α_3, or α_5 and β and γ_2 subunits. This displacement of the Ro15-4513 from the BDZ-sensitive receptors reveals labelling of the BDZ-insensitive (BDZ-IS) receptors, i.e. GABAR containing the α_4 and/or α_6 subunits. Ro15-1788 is a competitive antagonist at the BDZ binding site and will thus compete for specific Ro15-4513 binding sites, displacing the [^{3}H] Ro15-4513 from those GABARs to which it binds with high affinity, thereby identifying non-specific binding.

Figure 3.8 Autoradiography using [^{3}H] muscimol on frozen, unfixed control and stargazer brain sections. [^{3}H] muscimol-treated sections were exposed to [^{3}H] hyperfilm for 10 days before developing. The treated control (A) and stargazer (E) sections were then stained with toluidine blue (B and F respectively).

Non-specific binding on control and stargazer slices was done with [^{3}H] muscimol in the presence of GABA. No radiolabelling was seen with either the control (C) or stargazer slices (G), which were subsequently stained with toluidine blue (D and H respectively).
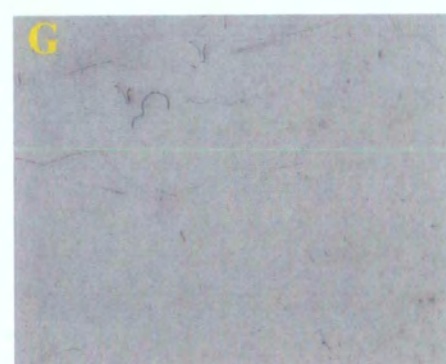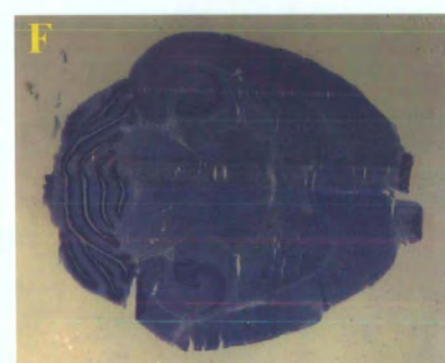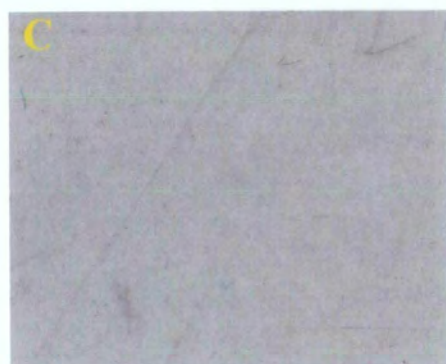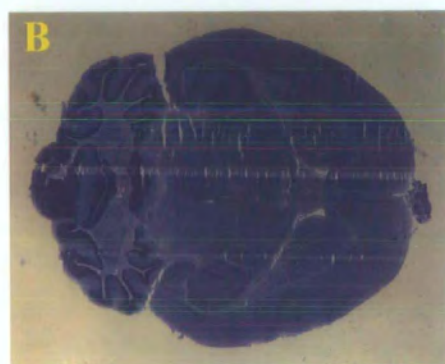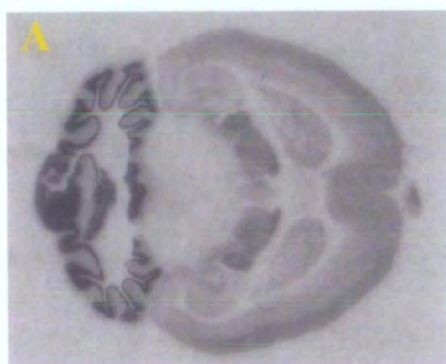
[^{3}H] Ro15-4513 binding was observed in most parts of the control brain, including the cerebellum, the hippocampus, the caudate-putamen and the cortex (figure 3.9A). The addition of flunitrazepam to the [^{3}H]-containing solution led to the displacement of the radioligand from flunitrazepam-sensitive subtypes of GABAR. Radiolabelling in the presence of flunitrazepam (BDZ-IS binding sites) was seen largely within the cerebellum, with labelling present but decreased within the forebrain areas mentioned above (figure 3.9C). This labelling pattern indicated the presence of α_4 and α_6 subunit-containing receptors. However, as no α_4 subunits are present in the adult cerebellum, any labelling seen here is due to the presence of the α_6 subunit.

The labelling pattern observed for total specific [^{3}H] Ro15-4513 binding sites in the stargazer slices appeared to be the same as that observed with control slices (figure 3.9G). That is, radiolabelling was seen within the cerebellum, the hippocampus, the caudate-putamen and the cortex. In the presence of flunitrazepam, the majority of labelling was seen within the cerebellum, with some labelling seen within the forebrain regions mentioned earlier (figure 3.9I).

Non-specific binding on control and stargazer slices was illustrated in figures 3.9E and 3.9K respectively. A small amount of radiolabelling was seen in both the non-specific binding figures, around the outline of the slices. This could be due to the length of time of exposure of the film to the slides.

72

Figure 3.9 Autoradiography using [^{3}H] Ro15-4513, flunitrazepam and Ro15-1788. Frozen, unfixed control sections were treated with [^{3}H] Ro15-4513 (A), [^{3}H] Ro15-4513 + flunitrazepam (C) or [^{3}H] Ro15-4513 + Ro15-1788 (E). The same sections were then stained with toluidine blue (B, D and F, respectively).

Frozen, unfixed stargazer whole brain sections were also treated with [^{3}H] Ro15-4513 (G), [^{3}H] Ro15-4513 + flunitrazepam (I) or [^{3}H] Ro15-4513 + Ro15-1788 (K) before being stained with toluidine blue (H, J and L respectively).
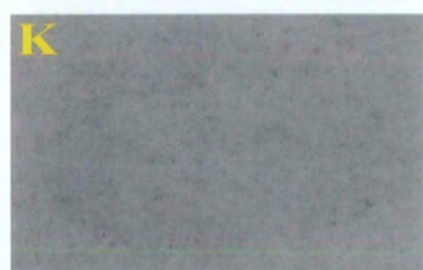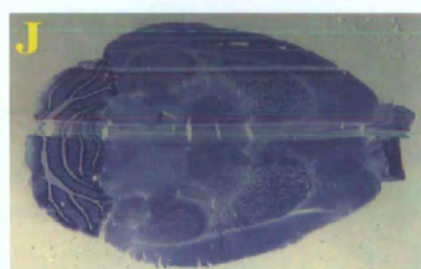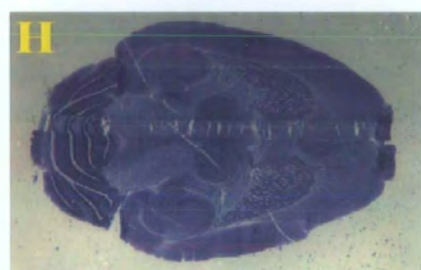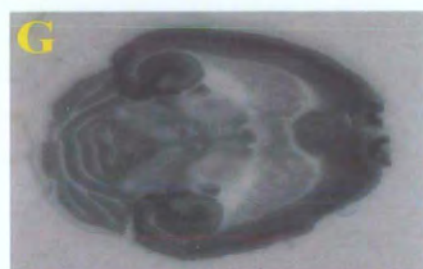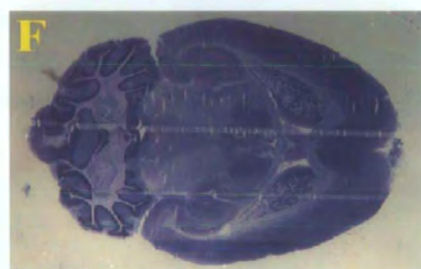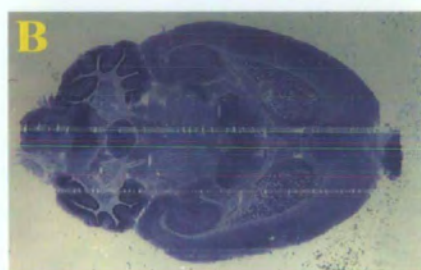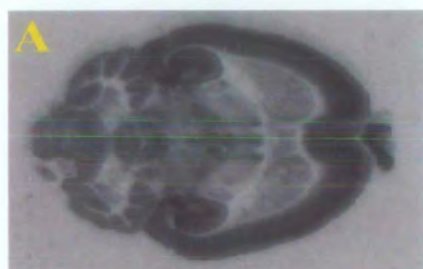
The amount of radiolabelling can be determined using Scion Image software. [³H]-standards were exposed to the [³H]-hyperfilm along with the treated slides. Using the ODs determined for the standards, the concentration of the radioligand bound to a particular tissue section can be calculated. Using this method, the concentrations of radioligand bound to both the control and stargazer cerebellar sections were determined.
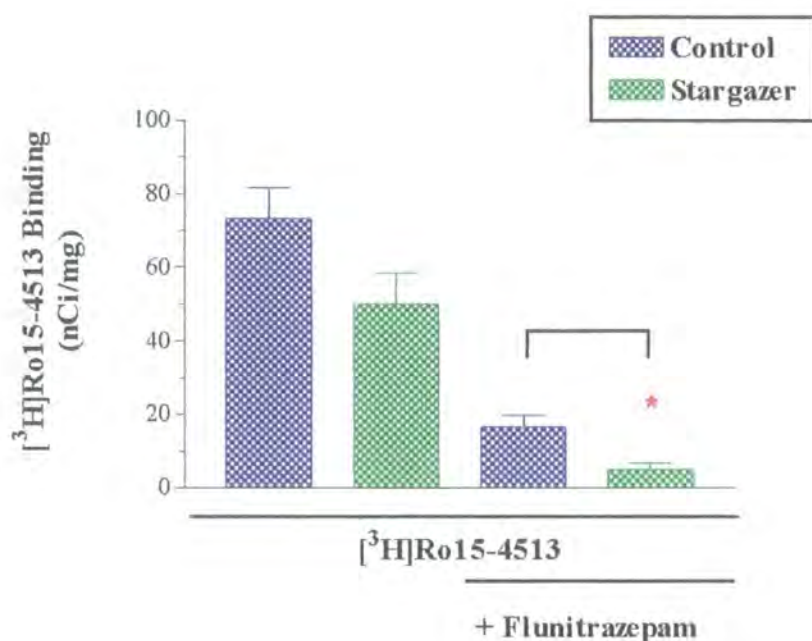
Figure 3.10 Bar graph showing the concentrations of [³H] Ro15-4513 binding in control and stargazer cerebellar sections, as determined by autoradiography following an 8 week exposure with [³H] hyperfilm. Binding of [³H] Ro15-4513 on stargazer cerebellum (49.9 ± 8.5 nCi/mg) was reduced when compared to control cerebellum (73.2 ± 8.4 nCi/mg). The amount of binding seen in the presence of flunitrazepam was significantly reduced in stargazer cerebellum (4.9 ± 1.8 nCi/mg) when compared to control cerebellum (16.7 ± 3.0 nCi/mg), as determined using the Student's t-test (* = P < 0.005). Results expressed as mean ± sem; n = triplicate measurements taken from 14 sections.

As can be seen in figure 3.10, there was a small decrease in the amount of total specific [³H] Ro15-4513 bound in the stargazer cerebellum, when compared to that in the control cerebellum. This decrease, however, was not significant (P > 0.05). Flunitrazepam displaced the radioligand from BDZ-sensitive GABAR in both

control and stargazer cerebella. In this instance, however, there was a significant decrease in the amount of [^{3}H] Ro15-4513 binding in the stargazer cerebellum, when compared to the binding observed within control cerebellum.

As illustrated in figure 3.9C, there was very little [^{3}H] binding, in the presence of flunitrazepam, in control dentate gyrus. The dentate gyrus was present in the control section as revealed after toluidine blue staining (figure 3.9D). Increased binding was apparent in the stargazer dentate gyrus (figure 3.9I). Due to limitations in the analysis method employed, however, it was not possible to obtain values for the amount of [^{3}H] binding within the dentate gyrus.

These results imply, therefore, that there was a decrease in the levels of the α_6 subunit in the stargazer cerebellum and are also comparable to previous studies employing [^{3}H] Ro15-4513 binding in control (obtained from C57BL/6J mice) and stg/stg membranes (Thompson et al., 1998).

3.3 Discussion

A genomic DNA PCR screen that was established in the lab enabled the identification of the normal (+) or mutated (stg) allele in the mice. This screen was employed to identify the genotype of the offspring arising from +/stg breeders, which were to be used either for breeding pairs (+/stg) or for cerebellar granule cell cultures. Furthermore, the GABAR expression profiles were reassessed to confirm earlier observations reported by Thompson et al. (1998), where cerebella from a C57 background strain was used as a control. Since stargazer mice are essentially a B6C3 line, the C57 strain was not the ideal background strain. In light of work describing mouse strain-dependent differences, it was important to confirm the authenticity of those earlier GABAR observations in stargazer.

When the adult +/+ and +/stg offspring of +/stg mice were used as controls, it was apparent that GABAR α_6 levels were significantly decreased in the cerebellum of stg/stg mice. These results confirmed that the impaired GABAR expression profiles in stg/stg cerebella were a consequence of the stg mutation and not mouse strain

76

variability. This decrease was selective to the α_6 subunit as no such decrease was observed in the α_1 subunit. Finally, autoradiographical analyses of frozen whole brain sections indicated a change in GABAR subunit expression in the dentate gyrus.

3.3.1 Use of a genomic screen to identify the genotype of mice

While stargazer mice older than P14-18 have a distinctive phenotype, comprising of absence epilepsy, ataxia, head tossing and a sustained upward gaze ('star gazing'), younger mice are indistinguishable from their normal littermates (+/+ and +/stg genotypes) (Noebels et al., 1990). Since the stargazer mutation is recessive, it was not possible to distinguish +/+ from +/stg mice on the basis of the phenotype alone.

The genetic locus of the stargazer mutation was found to reside on mouse chromosome 15 (Noebels et al., 1990) and was mapped to between *D15Mit30* and the parvalbumin gene (Letts et al., 1997). The identity of the mutated gene 'stargazin' was resolved and found to arise following an early transposon insertion that caused premature transcriptional arrest (Letts et al., 1998).

The DNA primers employed to identify the mutation by Letts et al. (1998) were then used here in the genomic screen, to identify the genotype of +/+, +/stg and stg/stg mice for use as breeding pairs and for the generation of primary neuronal cell cultures (section 3.2.1; section 7.2.1; Ives et al., 2003; Chen et al, 2000). For the former, it was necessary to be able to identify adult +/+ from +/stg mice since the stargazer mutation is recessive and so the phenotype of both strains was normal. For culture purposes, mice had to be sacrificed at P5/6, which was prior to the onset of a discernible stg/stg phenotype that would have allowed the segregation of +/+ and +/stg (control mice) from stg/stg (mutant mice).

The results obtained with the genomic DNA PCR amplification screen were verified by monitoring the behaviour of mature mice that had been screened prior to the onset of a discernible stg/stg phenotype, to ensure mice identified as stg/stg by the screen developed the stargazer phenotype. Further more, if the screen was effective, crossing mice identified as +/stg would be expected to yield stg/stg offspring. Neonatal mice subsequently classified as stargazers (stg/stg) did indeed show the

ataxic gait, the head tossing and the upward gaze, as would be expected. Heterozygote mice were confirmed as +/stg by the birth of stg/stg offspring whilst those identified as +/+ produced no offspring showing the stargazer phenotype.

Similar studies have been previously employed to identify a number of mouse mutants from their heterozygous and wild-type littermates, such as BDNF knockout mice (Henneberger et al., 2000), NMDA $\varepsilon2^{-/-}$ (NR2B) mice (Tovar et al., 2000), scrambler mice (Usman et al., 2000), dystrophia muscularis dy2J/dy2J mice (Vilquin et al., 2000) and wobbler mice (des Portes et al., 1994).

3.3.2 Mouse strain-dependent variability

A number of electrophysiological, pharmacological and biochemical properties of proteins have been found to differ between mouse strains. Bampton et al. (1999) found that differences occurred in maximal evoked EPSP slope and population spike amplitudes between 129 Ola mice and a number of other strains. They also found that DBA/2 mice not only showed a significantly reduced paired-pulse inhibition of population spike, a measure of inhibitory feedback, but also had a deficit in the maintenance of potentiation. Jones et al. (2001) also found that DBA/2 mice showed a lower, shorter potentiation of the population spike when compared to C57BL/6 mice. C57BL/6 mice also showed a much lower Ca^{2+} response to tetanic stimulation of the hippocampi when compared to the response observed with C57BL/10 mice (Shuttleworth and Connor, 2001).

Vulnerability of hippocampal neurons to kainate toxicity also differs between mouse strains. Hippocampal neurons from C57BL/6 mice are relatively resistant to kainate-induced excitotoxicity whereas neurons from C57BL/10 mice are vulnerable. Differences in dendritic calcium signalling following exposure to kainate was thought to underlie this vulnerability, with a large Ca^{2+} signal which led to a degenerative cascade and cell death being observed in the neurons of C57BL/10 mice. As the dendritic Ca^{2+} signals in C57BL/6 mice were smaller, the secondary responses leading to cell death did not occur (Shuttleworth and Connor, 2001).

The number of proliferating cells in the dentate gyrus also differs between strains, with C57BL/6 mice having a significantly larger number than Balb/C, CD1 (ICR) and 129Sv/J mice (Hayes and Nowakowski, 2002; Kempermann et al., 1997). Whilst proliferation in the dentate gyrus was similar in C3H/HeJ, A/J and DBA/2J mice, survival of the cells after 4 weeks was significantly higher in C3H/HeJ when compared to DBA/2J mice. Both C3H/HeJ and A/J mice produced significantly more 'new' neurons, compared to DBA/2J mice whilst the DBA/2J mice showed significantly more 'new' astrocytes (Kempermann and Gage, 2002).

With cultured cerebellar granule cells (CGCs), it has been reported that mice CGCs do not require a depolarising concentration of K^+ in the culture medium (Mogensen et al., 1994). However, it has subsequently been shown that this also depended on the strain of mouse from which the CGCs were obtained; CGCs from Balb/C mice did not require a depolarising concentration of K^+ in the culture medium whilst CGCs from C57BL/6 mice did not survive without an increase in K^+ concentration (Fujikawa et al., 2000).

The behavioural responses of mice in two anxiolytic tests, the light/dark choice test and the elevated plus-maze, were determined using nine strains of mice. The benzodiazepine diazepam reduced anxiety in the elevated plus-maze test in C57BL/6, DBA/2, NMRI and NZB mice. However, only the Balb/C and Swiss mice were responsive to diazepam in both tests (Griebel et al., 2000). Flumazenil, the competitive benzodiazepine antagonist, has been shown to induce partial agonist-like effects, by reversing behavioural responses in both the above mentioned tests in Balb/C mice but not in C57BL/6 mice (Belzung et al., 2000). These studies indicate that only certain strains of mice are suitable for investigating the effects of GABAR ligands.

Previous work looking at GABAR subunit expression in stg/stg cerebella relied on the C57BL/6J strain for control tissue (Thompson et al., 1998). The work was repeated here, using age-matched controls from +/+ and +/stg mice, in order to ensure that the differences observed were due to the mutation and not due to strain variabilities. No decrease in α_1 expression was observed in stargazer cerebellar

membranes (section 3.2.2.2), confirming the results obtained by Thompson et al. (1998). The decrease in α_6 expression observed in here in stargazer cerebella, using immunoblotting (section 3.2.2.3), immunohistochemistry (section 3.2.3) and receptor autoradiography (section 3.2.4), was comparable to that observed by Thompson et al. (1998), indicating that the decrease was indeed due to the stargazer mutation.

3.3.3 Consequences of GABAR α_6 subunit reduction

Cerebellar granule cells from B6C3Fe$^+$ mice, the background strain to stargazer, express 51 % of α_6 subunit at the cell surface (Ives et al., 2002). As it has been shown here that stargazer cerebellar membranes contain only 34 % of the α_6 expressed in control cerebella (section 3.2.2.3), it is likely that the amount expressed at the cell surface would also be decreased. This indeed has been shown in cultured stg/stg cerebellar granule cells (Thompson et al., 2002b; Ives et al., 2003). Since the α_6-containing GABAR also contains α_1, β_2, β_3, γ_2 and δ subunits (Hevers et al., 2000; Jechlinger et al., 1998; Pollard et al., 1995), there is the possibility that the levels of the other receptor subunits may also be affected.

β subunits have been shown to be associated with the α_6 subunit in cerebellar granule cells (Jechlinger et al., 1998; Pollard et al., 1995; Laurie et al., 1992). As the majority (83 %) of $\beta_{2/3}$ subunits are found on the cell surface in mouse cerebellar granule cells (Ives et al., 2002), any reduction in the surface expression of the α_6 subunit would also lead to a decrease in the expression of the $\beta_{2/3}$ subunits. Thompson et al. (1998) have indeed revealed a selective decrease in β_3 subunits of the stargazer cerebellar to 38 % of control levels. No such decrease was observed for β_2 subunits or in α_1 subunit expression (section 3.2.2.2; Thompson et al., 1998).

The distribution of [^{3}H] muscimol, a GABA agonist that binds to all GABARs, was revealed by receptor autoradiography in figure 3.8 (section 3.2.4.1). Binding within stargazer cerebellar sections, particularly within the granule cell layer, was reduced when compared to the binding observed with control sections. As specific [^{3}H] Ro15-4513 binding, which labels γ_2-containing receptors, was not significantly different between control and stargazer cerebella (section 3.2.4.2), it would appear that the γ_2 subunit was not decreased in stargazer cerebella. However, in the

cerebellum, under autoradiographic conditions, [^{3}H] muscimol selectively labels α_6-containing receptors (Jones et al., 1997). It would seem likely, therefore, that the reduction in stargazer granule cell layer binding was due to a decrease in the level of expression of the δ subunit.

Indeed, the expression of the δ subunit has been shown to be decreased in the stargazer cerebellar granule cell layer and at the surface of stg/stg CGCs. However, as similar amounts of δ protein were found in both control and stg/stg CGCs, the lack of cell surface δ expression implied an impairment in the surface trafficking of this subunit (Thompson et al., 2002b; Ives et al., 2003).

3.3.4 Inappropriate expression of GABARs in stargazer dentate gyrus

Ro15-4513 binds to the benzodiazepine-binding site on γ-containing GABARs and can be displaced from γ_2-containing receptors by diazepam and similar ligands. However, in a small subset of γ_2 receptors, i.e. those containing α_4 or α_6 subunits (diazepam-insensitive receptors), Ro15-4513 is not displaced (Benke et al., 1997; Benke et al., 1996; Yang et al., 1995; Khan et al., 1994). The use of [^{3}H] Ro15-4513 and its displacement by flunitrazepam allows the distribution of different GABAR subunits to be revealed as any binding in the presence of flunitrazepam is due to the presence of α_4 or α_6-containing receptors.

As can be seen in figure 3.9, very little [^{3}H] Ro15-4513 binding was apparent in control hippocampus in the presence of flunitrazepam, indicating the scarcity of $\alpha_4\gamma$-containing receptors. However, increased binding was observed in stargazer hippocampus, particularly within the dentate gyrus, indicating an upregulation in $\alpha_4\gamma$ receptors. Since spike-wave discharges characteristic of absence epilepsy can be recorded in stargazer hippocampus (Qiao and Noebels, 1993), it is possible that this upregulation in a specific subset of GABARs is involved.

Whilst some γ_2-containing GABARs have been shown to be extrasynaptic, the majority are concentrated at synapses in both hippocampal and cerebellar cells (Scotti and Reuter, 2001; Nusser et al., 1998b; Somogyi et al., 1996). This increase

81

in $\alpha_4\gamma$ receptors observed in the dentate gyrus of stargazer mouse would therefore imply an increase in the number of synaptic receptors. An increase in synaptic GABARs has been shown to occur in the dentate gyrus of a rat model of temporal lobe epilepsy, where an increase in the protein expression of the α_4 and γ_2 subunits were observed in the dentate gyrus (Nusser et al., 1998a; Brooks-Kayal et al., 1998; Schwarzer et al., 1997; Tsunashima et al., 1997). Within these models of temporal lobe epilepsy, increased δ subunit mRNA transcript and protein levels were also observed (Brooks-Kayal et al., 1998, Schwarzer et al., 1997).

The δ subunit has been shown to be associated with stargazin *in vivo* (Thompson et al., 2002; Ives et al., 2003). As neither stargazer forebrain membranes nor stargazer cerebellar membranes contained stargazin (section 6.2.2), it was suggested that stargazin was involved in the assembly and trafficking of the δ subunit in cerebellar granule cells (Thompson et al., 2002; Ives et al., 2003). It could, therefore, be proposed that δ-containing receptors are decreased elsewhere in stargazer brain, such as the dentate gyrus where it is co-localised with the α_4 subunit (Pirker et al., 2000; Sperk et al., 1997; Benke et al., 1991a).

The δ-/- mouse, whilst bearing the δ gene, is devoid of δ protein (Mihalek et al., 1999). Within the cerebellum, whilst no change was observed in the immunoreactivities for the α_6 and β_2 subunits, increased immunoreactivities were observed for the α_1, β_3, and γ_2 subunits, which showed the greatest increase. This was reflected in an increase in the number of $\alpha_6\beta\gamma_2$-containing GABARs (Tretter et al., 2001). As the δ subunit has been shown to be found at the extrasynaptic membrane of both mouse and rat cerebellar granule cells and the γ subunit mainly at the synapse, (Nusser et al., 1998b; Somogyi et al., 1996), it is likely that the localisation of the receptors had changed, to reflect their mainly synaptic distribution.

If the same theory were to be applied to stargazer dentate gyrus, we would expect no δ subunit protein or δ-containing receptors to be expressed at the extrasynaptic membrane. Instead, we would expect an increase in $\alpha\gamma$-containing receptors, particularly at the synaptic membranes. An increase in $\alpha_4\gamma_2$-containing receptors was

82

indeed observed, as evidenced by the increased [^{3}H] Ro15-4513 signal in the presence of flunitrazepam (section 3.2.4.2).

3.3.5 Conclusion

In conclusion, it has been shown that the genotype of +/+, +/stg and stg/stg mice can be determined using the genomic DNA screen employed. Cerebellar membranes from +/+, +/stg and stg/stg mice were probed for the expression of GABAR α_1 and α_6 subunits. No difference in subunit expression was observed between +/+ and +/stg membranes.

GABAR α_1 and α_6 subunit expression was then quantified in control (+/+ and +/stg) and stargazer (stg/stg) cerebellar membranes: no difference was observed in α_1 subunit protein however, α_6 levels, as expected, were significantly lower in stargazer. Receptor autoradiography also revealed a decrease in α_6-specific radiolabelling in stargazer cerebella. Interestingly, the same studies appeared to imply an increased $\alpha_4\gamma$ radiolabelling in stargazer dentate gyrus.

Work by other members of the group has revealed the subcellular distribution of the α_6 subunit to be different in stg/stg cerebellum, with little extrasynaptic and a reduction in synaptic α_6 observed. Within these cells, a decrease in the GABAR δ subunit, which has an extrasynaptic localisation, was also described. Further work is currently being undertaken to elucidate the exact role of stargazin in the assembly and trafficking of GABARs.

Chapter 4

NMDA receptor expression in stargazer brain

4.1 Introduction

The stargazer mutant mouse phenotype includes absence seizures and ataxia, both of which become apparent around P14 – P16 (Noebels et al., 1990; Qiao and Noebels, 1993; Qiao et al., 1996). Coincidentally, a developmental switch in the expression of the NMDA receptor (NMDAR) subunits is observed – expression of the NR2B subunit begins to decline in the cerebellum, expression of the NR2C subunit begins to increase in the cerebellum and expression of the NR2D subunit decreases in the forebrain (Didier et al., 1995; Akazawa et al., 1994).

Direct evidence for the possible involvement of NMDARs came from pharmacological studies on stargazer. The spike-and-wave discharges, which are observed during absence seizures, were suppressed in stargazer with the application of the non-competitive NMDAR antagonist, MK-801 (Aizawa et al., 1997). Other evidence implicating a role for the NMDARs in another model of absence epilepsy are outlined in section 4.1.2.

Both BDNF mRNA and protein levels are selectively decreased in the stargazer cerebellum (Qiao et al., 1996, and Qiao et al., 1998, respectively). BDNF has been shown to affect the expression levels of the NMDAR subunits in both the forebrain and cerebellum, as outlined below (section 4.1.1).

4.1.1 BDNF and NMDA receptors

Within the forebrain, BDNF has been shown to affect NMDA receptors. Application of BDNF to hippocampal synaptoneurosomes and postsynaptic densities increased phosphorylation of the NR1 subunit (Suen et al., 1997). Within cultured cortical neurons, exposure to BDNF for 24 hr caused a significant increase in the expression level of the NR2A subunit whilst decreasing the expression levels of the NR2B subunit (Small et al., 1998).

84

A role for BDNF in NMDAR-mediated synaptic transmission was shown in cultured embryonic hippocampal neurons, where in the presence of CNQX (6-cyano-7-nitroquinoxaline-2,3-dione), a non-NMDAR antagonist, BDNF depressed EPSCs (Song et al., 1998). BDNF was also shown to increase the amplitude of the inward current induced by glutamate in the same cell preparation, an increase that was reduced in the presence of AP5. Ifenprodil, an NDMAR antagonist which is selective for the NR2B subunit, was shown to reproduce the reduction seen with AP5, suggesting that BDNF enhanced the activity of NR2B containing NMDARs (Crozier et al., 1999).

In cultured cerebellar granule cells, application of NMDA increased BDNF mRNA levels, a response which was inhibited by MK-801 (Favaron et al., 1993). BDNF itself was shown to decrease the expression of NR2A and NR2C subunits and NMDA-mediated increases in intracellular calcium concentrations, indicating a possible downregulation of the NMDAR (Brandoli et al., 1998).

4.1.2 NMDARs have been implicated in a model of absence seizures

Like stargazer, the GAERS Wistar rat (Genetic Absence Epilepsy Rats from Strasbourg) presents with spontaneous recurrent absence seizures, which are characterised by bilateral, synchronous spike-and-wave discharges (SWD). The use of NMDA and NMDAR antagonists revealed that NMDA neurotransmission within the thalamus played a role in the control of absence seizures (Koerner et al., 1996). Injection of NMDAR antagonists into the substantia nigra and muscimol, a GABA agonist, into the subthalamic nucleus, which projects glutamatergic afferents to the substantia nigra, led to the suppression of seizures (Deransart et al., 1996). NMDA was shown to increase, in a dose-dependent manner, the number of SWD (Peeters et al., 1990) and MK-801 has been shown to both reduce the number and mean duration of SWD in this model (Peeters et al., 1989).

4.1.3 NMDAR subunits and motor coordination

Stargazer mice show a severe impairment of motor coordination and balance, as judged using a plastic rod test. Adult stargazer mice were unable to balance on the

stationary rod for more than 5 seconds and were unable to remain on the rotating rod for any significant length of time (Qiao et al., 1996).

Transgenic mice engineered with either truncated NMDAR subunits or lacking one or more subunits also show defects in motor coordination. Mice deficient in either the NR2A (NR2A$^{-/-}$) or the NR2C (NR2C$^{-/-}$) subunit showed no overt motor coordination problems, as measured using a wooden bar or in a rotarod test using a gritted roller. Mice deficient in both subunits, however, had trouble walking on the narrow wooden bar and failed to stay on the rotating rod (Kadotani et al., 1996).

NR2C$^{-/-}$ mice and mice with C-terminal truncation of NR2C (NR2C$^{\Delta C/\Delta C}$) were both able to balance on a rotating rotarod but had trouble balancing on a stationary plexiglass rod, leading the authors to speculate that this was due to a deficit in the fine-tuning of motor control (Sprengel et al., 1998).

Mice with C-terminal truncation of NR2A (NR2A$^{\Delta C/\Delta C}$) were unable to stay on either the stationary rod or the rotating rod for the same length of time as wild-type mice. These deficits in balance were reproduced by mice with truncated NR2A and NR2C C-terminals (NR2A/C$^{\Delta C/\Delta C}$) but not by NR2C$^{\Delta C/\Delta C}$ mice, indicating a dominance of the NR2A subunit and that more severe consequences arose from truncating the subunit than ablating it (Sprengel et al., 1998).

Finally, mice in which cerebellar Golgi cells were ablated also showed problems balancing on a thin wooden bar and on a rotating rod. Both GABA immunoreactivity and GABA-mediated feedback inhibition of granule cell excitation were abolished by the Golgi cell elimination. This elimination resulted in the attenuation of functional NMDARs in the granule cells, indicating that both GABA inhibition and NMDAR activation were essential for motor coordination (Watanabe et al., 1998a).

4.1.4 NMDAR antagonists and motor coordination

NMDAR antagonists are thought to have a therapeutic role in conditions such as epilepsy and stroke, however, they also show adverse side effects including effects on locomotion and ataxia. MK-801 protected against NMDA-induced seizures at

doses that produced ataxia and a stimulation of locomotor activity. Memantine, ibogaine and ADCI, all non-competitive NMDAR antagonists, also protected against NMDA-induced seizures. However, at higher concentrations, these compounds also produced ataxia (Geter-Douglass and Witkin, 1999). MK-801 acts as an anticonvulsant against kainate-induced seizures, however, in neonatal rats, the side effects included ataxia and limb cycling (Stafstrom et al., 1997). Intravenous injection of MK-801 into rats induced behaviours which consisted of hyperlocomotion, head-weaving and ataxia (Tortella and Hill, 1996) whilst subcutaneous administration of MK-801 also produced ataxia, stereotypy and changes in locomotion (Haggerty and Brown, 1996).

4.1.5 Work undertaken in this chapter

Since NMDAR have been implicated in both absence epilepsy and ataxia, which are both observed in stargazer, it is conceivable that the expression of the NMDAR in stargazer is disrupted.

In order to elucidate the role played by NMDAR in stargazer, antibodies against the principal NMDAR subunits (NR1, NR2A, NR2B and NR2C/D) were generated. These antibodies (NR1, NR2A, NR2B and NR2C/D) were then used to both quantify the levels and the distribution of the NMDAR subunits expressed in the stargazer brain. [^{3}H] MK-801 was also employed in pharmacological studies to deduce whether the number and type of NMDARs expressed in stargazer brain differed from those in control brain.

4.2 Results

4.2.1 Antibody production and purification

Peptides to the NMDAR subunits NR1 (17 – 35), NR2A (1381 – 1394), NR2B (46 – 60) and NR2C/D (1307 – 1323) were commercially synthesised and coupled to carrier proteins, as outlined in section 2.3.2. The rabbits were immunised against the respective coupled-peptides, bled and sera obtained (section 2.3.3). The sera were screened by ELISA, in order to determine the titres of the antibodies, as described in section 2.3.4.
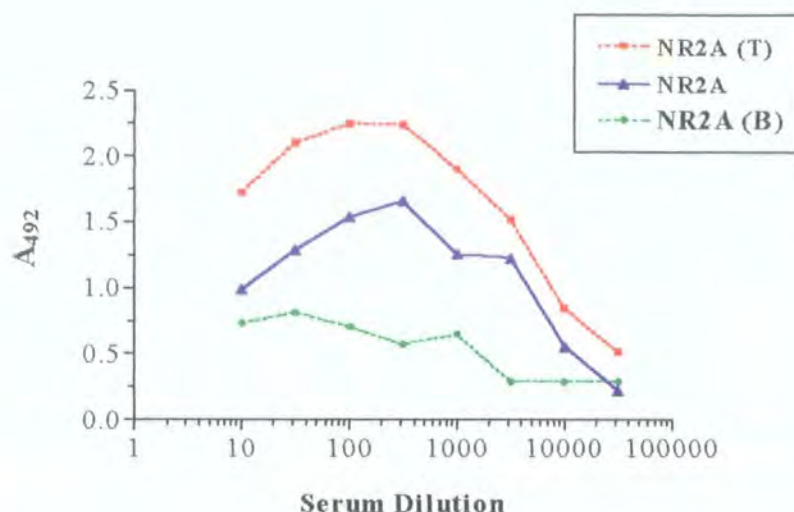
Figure 4.1 ELISA of NMDA receptor NR2A subunit-specific antisera, taken from the second bleed of a New Zealand White rabbit immunised against the peptide-thyroglobulin conjugate to the NR2A subunit. Absorbance was read at a wavelength of 492 nm (A_{492}). Total A_{492} for sera incubated in the presence (NR2A, 'T') and background A_{492} for sera incubated in the absence of the NR2A peptide (NR2A, 'B') are shown, along with the specific absorbance (NR2A). The titre for this particular batch of sera was 1:6000 dilution.

Immunogenic responses to the peptides were obtained in the bleeds taken from the rabbits. The size of the response varied from peptide to peptide and from bleed to bleed. Figure 4.1 shows a typical response obtained against the NR2A peptide. A large response was observed when the sera were incubated with the peptide. A much smaller response was observed when the sera were incubated with the vehicle alone, thereby producing the background absorbances. Specific absorbances of the sera over a dilution range (1/10 – 1/31600), and thus the titre, were deduced by subtracting the background value from the total values obtained.

Graphs, such as those in figure 4.1, were obtained for antisera directed against the NR1, NR2B and NR2C/D subunit peptides. From such graphs, the titres for each of antisera were calculated. The titre for the sera against the NR1 peptide was 1:38 dilution, the NR2A peptide was 1:6000 dilution, the NR2B peptide was 1:115 dilution whilst that for the NR2C/D peptide 1:15 dilution. Further immunisations were undertaken to boost the immune response. Typically, an immune response titre

of 1:1000 was considered feasible for further use and so immunisations were continued until this was achieved.

The immunised rabbits were bled and the immune sera collected, as described in chapter 2 (section 2.3.3). Antibodies were purified from the immune sera using the respective peptide-coupled affinity columns. Fractions (1 ml) were eluted from the columns and the antibody-containing fractions were determined by spectrophotometry. The peak antibody-containing fractions were combined and dialysed against PBS containing sodium azide (0.02 % w/v). The concentration of the combined antibody was determined and the antibodies were stored at either 4°C or –20°C, as detailed in section 2.3.6

Purified antibodies were generated from all bleeds obtained from the rabbits. The concentration of the purified antibodies varied both from bleed to bleed, from 109 µg/ml (for NR2B bleed 4) to 584 µg/ml (for NR1 bleed 4). The optimal concentrations of each antibody required for immunoblotting and immunohistochemistry were determined as described below, in sections 4.2.3 and 4.2.4 respectively.

4.2.2 Screening of antibodies against recombinantly expressed NMDAR subunits

NMDAR subunit cDNAs for NR1, NR2A and NR2C were individually expressed in HEK 293 cells, using the calcium phosphate precipitation method (Chazot et al., 1994). The expressed proteins were precipitated from detergent-solubilised cells and resuspended in SDS-PAGE buffer, as outlined in section 2.6.

The recombinantly expressed NMDAR subunits were analysed following SDS-PAGE on 7.5 % acrylamide resolving mini-gels and electrotransferred onto nitrocellulose, as described in section 2.7. The immunoblots were probed with 1 –

Figure 4.2: Recombinantly expressed NMDA NR1, 2A AND 2C subunits were probed with subunit-specific antibodies by immunoblotting. The recombinant proteins were probed with 1 µg/ml anti-NR1 antibody (A and B), 2 µg/ml anti-NR2A antibody (C) or 4 µg/ml anti-NR2C/D antibody (D). Control forebrain and cerebellar membranes were also probed with the anti-NR1 antibody (B). The molecular weights are shown to the left hand side of each immunoblot, in kDa.

The anti-NR1 antibody recognises a single band in the R1 lane, at approximately 120 kDa, corresponding to the NR1 subunit. This antibody also detected a signal of the same weight in both the membranes. The anti-NR2A antibody recognises a band at approximately 180 kDa in the 2A lane, which corresponds to the NR2A subunit. The anti-NR2C/D antibody recognises several proteins in the 2A and 2C lanes, however, it is only in the 2C lane that a protein corresponding to the NR2C subunit (with a molecular weight of ~140 kDa) is detected.
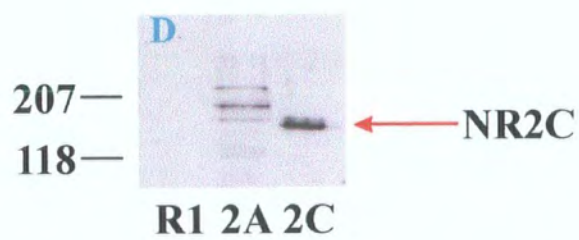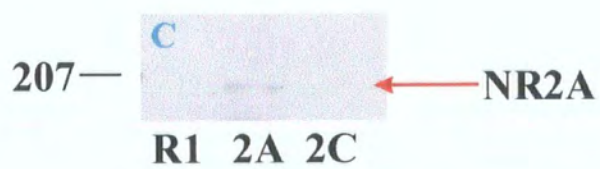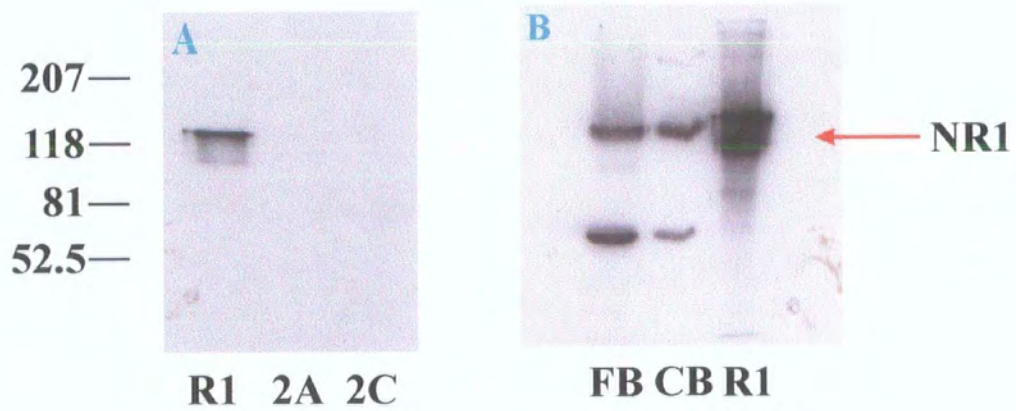
2 μg/ml anti-NR1, 2 μg/ml anti-NR2A or 4 μg/ml anti-NR2C/D subunit-specific antibodies (figure 4.2).

As can be seen in figure 4.2A, when the recombinantly expressed NR1, NR2A and NR2C proteins were probed with the anti-NR1 subunit-specific antibody, only the NR1 recombinant was identified, at approximately 120 kDa. This clearly showed that the anti-NR1 antibody recognised a single protein species with an M_r of 120 kDa, as predicted for NR1, confirming the specificity of the anti-NR1 antibody.

In figure 4.2B, the anti-NR1 antibody recognised a single band at ~ 120 kDa in the NR1 recombinant. This same band was visible in both the cerebella and forebrain samples. It would, therefore, appear that the NR1 protein was, as expected, present in both control cerebella and forebrain membranes and that the anti-NR1 antibody was able to recognise the native mouse protein.

The recombinantly expressed proteins were then probed with the anti-NR2A subunit-specific antibody (figure 4.2C). The anti-NR2A antibody recognised a band of M_r ~ 180 kDa only in the lane containing the NR2A recombinant protein. When brain membranes were probed with the anti-NR2A antibody, the ~ 180 kDa band was seen in both the control cerebellar and forebrain membranes, confirming that the antibody recognised the native NR2A protein.

Figure 4.2D shows an immunoblot where recombinant NR1, NR2A and NR2C were probed with the anti-NR2C/D subunit-specific antibody. No signal was detected with the NR1 recombinant protein. The anti-NR2C/D antibody recognised a band at approximately 140 kDa, which corresponded to the predicted weight for the NR2C protein, with the NR2C recombinant protein. Various bands were seen with the NR2A recombinant protein but none of these were of the correct size.

The anti-NR2C/D antibody also recognised the same sized band in the cerebellar membranes as in the NR2C recombinant protein thereby implying that the anti-NR2C antibody recognised the native protein. No band of the correct molecular weight was seen with the forebrain membranes. This is consistent with evidence that

the NR2C subunit is essentially absent from the adult forebrain but heavily expressed in cerebellar granule cells (Wenzel et al., 1995).

The anti-NR2C/D antibody was raised to a peptide sequence corresponding to the C-terminal 16 amino acids of NR2D. However, there is a high degree of sequence similarity at the C-termini of NR2C and NR2D, in that the final 7 amino acids of each subunit are identical. Subsequently, in cerebellar membranes, the anti-NR2C/D antibody recognised two immunoreactive species on immunoblots. The upper band at ~ 150 kDa corresponded to the NR2D subunit and was just above the band which corresponded to the NR2C subunit. A band of similar size was also observed in the forebrain membranes and also corresponded to the NR2D subunit.

4.2.3 Immunoblotting of mouse brain NMDAR subunits

4.2.3.1 Detection of mouse brain NMDAR subunit immunoreactive species

The optimal concentrations of each antibody were determined for immunoblotting by probing cerebellar and forebrain membranes (10 μg) derived from control mice with a range of antibody concentrations. Figure 4.3 is a representative immunoblot where forebrain and cerebellar membranes were probed with 0.125 μg/ml, 0.5 μg/ml or 2 μg/ml of anti-NR1 antibody. However, the antibody used came from two bleeds, bleeds three and four. As can be seen in figure 4.3, a strong NR1 signal was seen even with the lowest concentration of antibody from bleed 4. This process was repeated for each antibody purified from every bleed in order to optimise the concentration of each antibody to be used for immunoblotting.

The levels of the NR1, NR2B, NR2C and NR2D subunits were determined using the subunit-specific antibodies. A protein concentration range of control and stargazer cerebellar and forebrain membranes were loaded onto 6.5 % or 7.5 % SDS-PAGE resolving mini-gels. These were then transferred onto nitrocellulose, as described in section 2.7, and subsequently probed for the level of expression of the subunit of interest relative to β-actin, which was used as a normalising protein.

Figure 4.3 Determination of the optimal concentration of purified antibody. Control forebrain (FB) and cerebellar (CB) proteins were probed with anti-NR1 antibody purified from sera collected from either bleed 3 or bleed 4. The bleed 4 purified antibody was used at a concentration of 0.125 µg/ml, 0.5 ML/ml or 2 ML/ml, whilst the bleed 3 antibody was used at a concentration of 0.5 ML/ml. All the concentrations used detected the NR1 protein in both the cerebellar and the forebrain proteins.

The molecular weights are shown to the left of the immunoblot.

	212 —	
	122 —	←
	83 —	
	51.8 —	

CB FB	CB FB CB FB	CB FB
Bleed 3	**Bleed 4**	
0.5μg/ml	0.125 μg/ml 0.5 μg/ml	2μg/ml
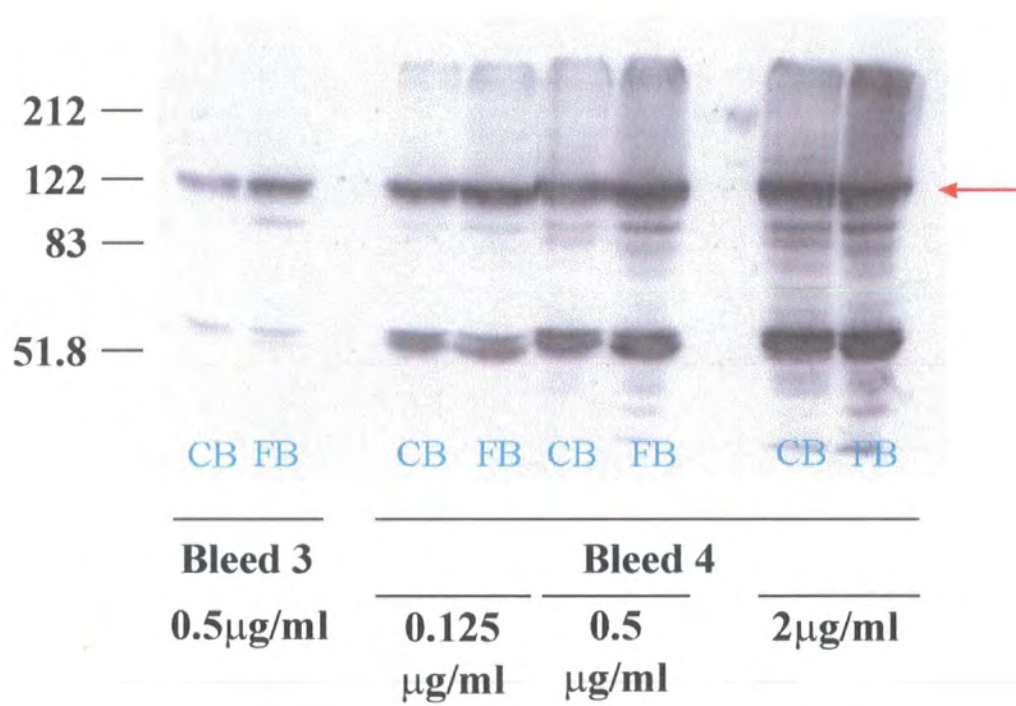
The NR1 subunit was present in both the control cerebellum and the forebrain, as can be seen in figures 4.4A and 4.4C. The NR1 subunit was also present in stargazer cerebellar and forebrain membranes (figures 4.4A and 4.4C respectively).

Figures 4.5A and 4.5B show the level of expression of the NR2B subunit and β-actin protein within control and stargazer cerebellar membranes. The NR2B subunit was present in control forebrain membranes (figure 4.5A). The NR2B subunit was also present within the stargazer forebrain. As can be seen in figure 4.5A, the levels of expression of the NR2B subunit were too low to be detected within both control and stargazer cerebellar membranes. The immunoblots were subsequently probed for the expression of β-actin and this was clearly detected (figure 4.5B), proving that these results are not due to protein loading errors.

The NR2C and NR2D subunits were both detected in control and stargazer cerebellar membranes (figure 4.5C). Although the NR2D subunit was clearly detected in both control and stargazer forebrain membranes, the NR2C subunit was not detected in either control or stargazer forebrains, or, at least, was below the level of sensitivity of detection by immunoblotting.

4.2.3.2 Quantitative immunoblotting of the NMDAR subunits

As cerebellar and forebrain membranes were probed for NMDAR subunit-specific immunoreactivities and subsequently for β-actin immunoreactivity, the levels of expression (in both control and stargazer tissue) could be determined by computer-assisted densitometry. The optical densities of the subunit signals were measured and adjusted, or normalised, according to the relative expression levels of the housekeeping gene protein product, β-actin. These signals were also determined by image densitometry. The results obtained from the stargazer membranes were normalised to those obtained from the control membranes, which were arbitrarily assigned a value of 100 %.

Figure 4.4 Expression of NR1 subunit protein and actin in control and stargazer forebrain and cerebellar membranes. Control (ctl) and stargazer (stg) cerebellar membranes were probed with anti-NR1 antibody (A) and anti-actin antibody (B). Control and stargazer forebrain membranes were also probed with the anti-NR1 antibody (C) and the anti-actin antibody (D).

Both antibodies detected the relevant proteins in the immunoblots (red arrows). A range of protein concentrations was used (1.25 µg/10 µl – 10 µg/10 µl) in order to be used for quantitative immunoblotting.
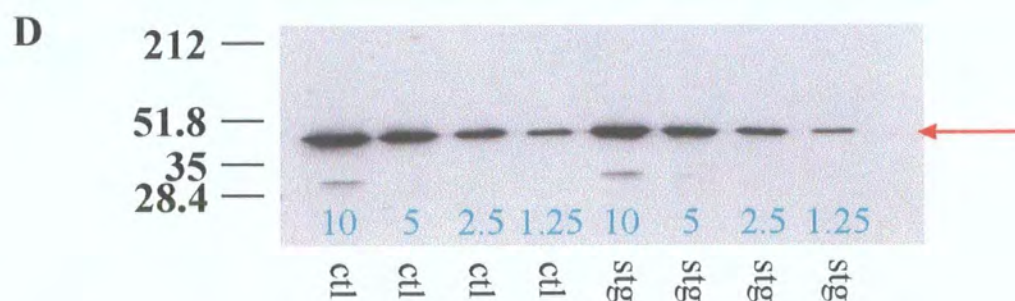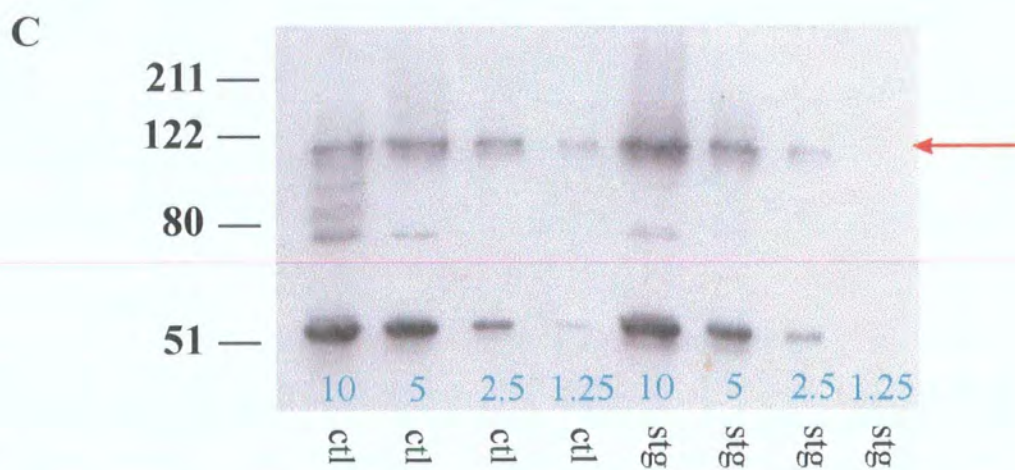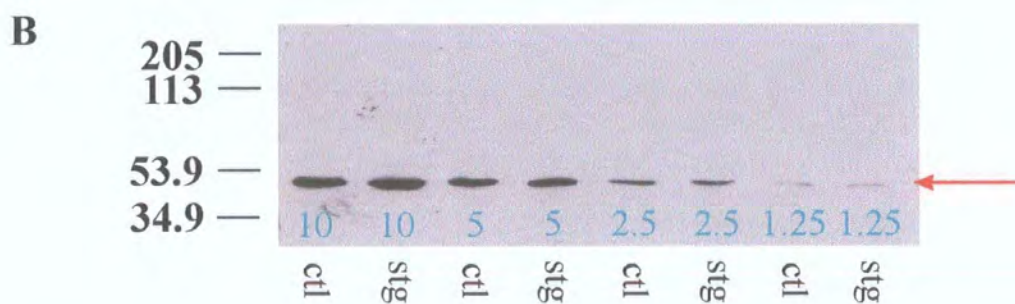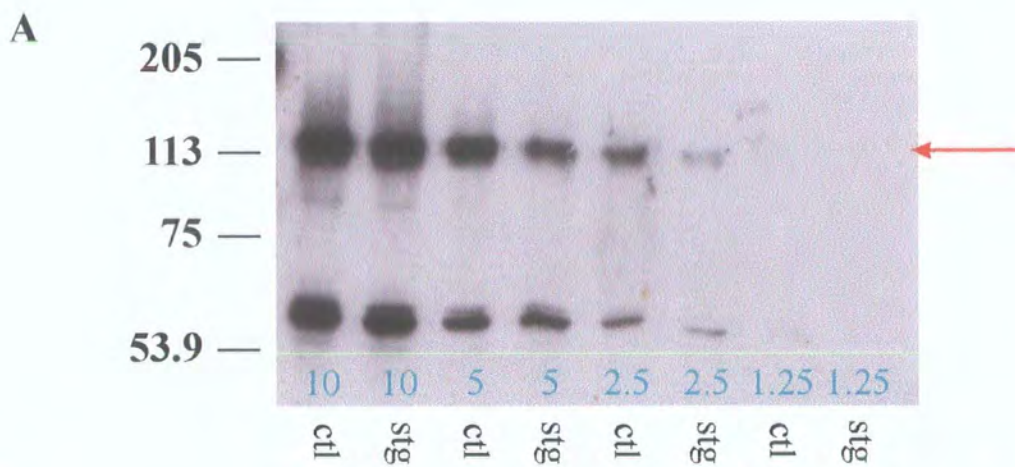
Figure 4.5 Immunoblot showing expression of NR2B and NR2C/D proteins in forebrain and cerebellar membranes. Control (ctl) and stargazer (stg) cerebellar proteins were probed with the anti-NR2B antibody (A) before being reprobed with the anti-actin antibody (B). Also probed were control forebrain membranes (FB). Whilst NR2B was detected in the forebrain membranes, no signal was obtained with either control or stargazer cerebellar membranes.

Control and stargazer cerebellar membranes were probed for the expression of NR2C and NR2D subunits (C), using the anti-NR2C/D antibody, before being reprobed for actin expression (D), using the anti-actin antibody.

A range of proteins was used in order to quantify the levels of expression of the subunits in the control and stargazer cerebellum.

The molecular weights are shown to the left of each of the immunoblots.
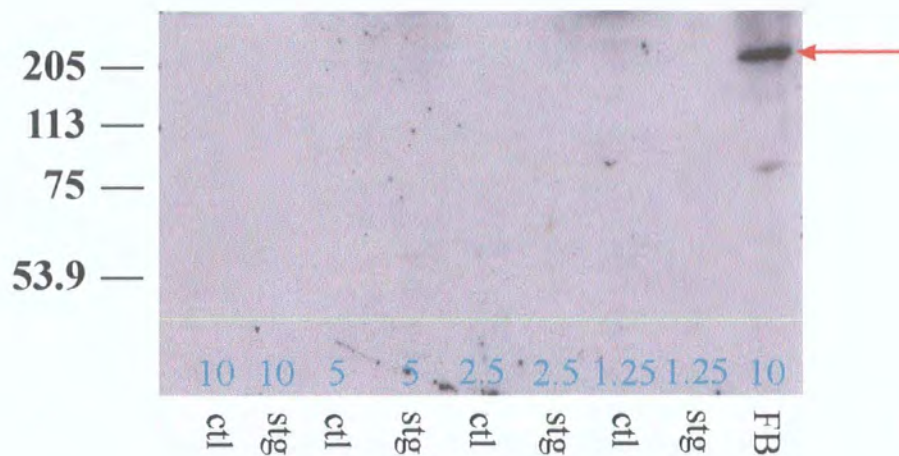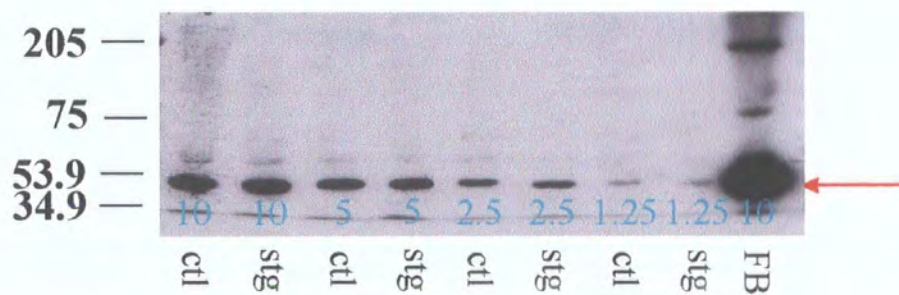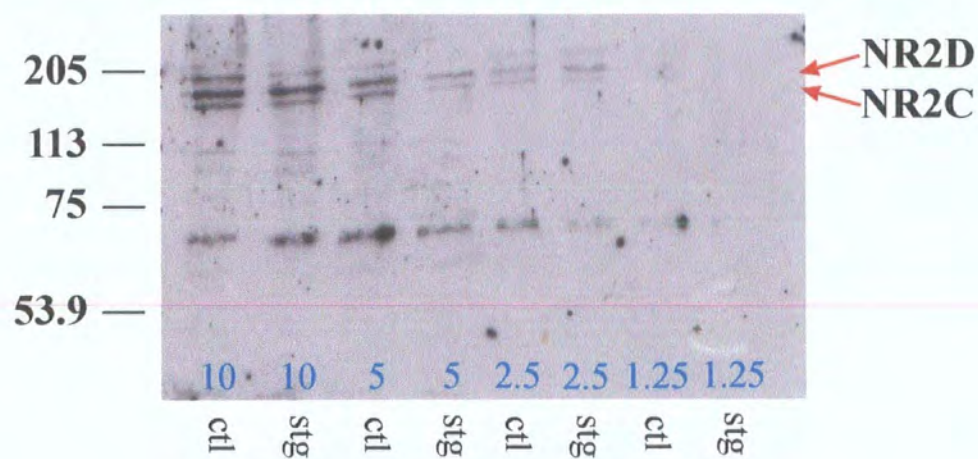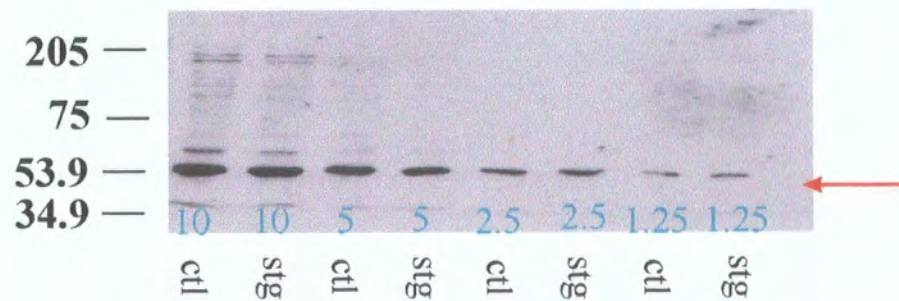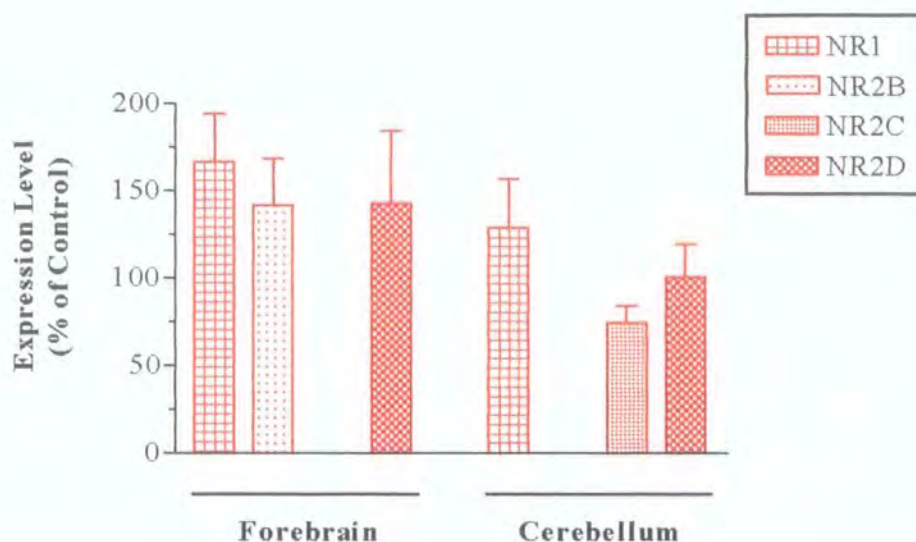
Figure 4.6 Bar chart showing comparative expression levels of the NMDAR subunits NR1, NR2B, NR2C and NR2D in stargazer forebrain and cerebellar membranes, relative to control tissues. Optical densities were obtained and normalised using those of corresponding β-actin immunoreactivities. The immunoreactive signal obtained with control cerebellar and forebrain membranes was assigned an arbitrary value of 100 %. For actual values, see table 4.1 below. n = 3 – 4 samples from both control and stargazer forebrains and cerebella membranes; immunoblotting conducted 4 times.

As can be seen in figure 4.6, the NR1 and NR2D subunits were detected in both stargazer forebrain and cerebellar membranes. NR2B protein, as expected, was only detected in both control and stargazer forebrain membranes; it was not detected in either control or stargazer cerebellar membranes. The NR2C subunit was detected in both control and stargazer cerebellar membranes whilst no NR2C protein was detected either in control or stargazer forebrain membrane.

	Forebrain	Cerebellum
NR1	166.5 % ± 27.1 %	128.6 % ± 28.0 %
NR2B	141.4 % ± 26.6 %	–
NR2C	–	74.3 % ± 10.0 %
NR2D	142.8 % ± 41.4 %	100.7 % ± 18.6 %

Table 4.1 Table showing levels of expression of the NMDA receptor subunits as percentages of control, where control = 100 %. Values are expressed as mean ± sem, n = 3 – 4 samples from control and stargazer forebrains and cerebella membranes; immunoblotting conducted 4 times. There were no significant differences in the expression levels of any of the NMDAR subunits in stargazer forebrain or cerebellar membranes when compared to tissue prepared from age-matched controls, as determined using Student's t-test (P > 0.05).

As can be seen in both figure 4.6 and table 4.1, whilst expression levels of the NR1 subunit in both the forebrain and cerebellum, the NR2B subunit in the forebrain and the NR2D subunit in the forebrain, were greater than the expression levels in control brain tissue, the expression levels of these subunits were not significantly increased. Similarly, although it appeared that the expression level of the NR2C subunit was decreased in stargazer cerebellum, this result was not significantly lower than control. Note also that NR2B, a marker of immature cerebellar neurons, was not detected in adult stargazer cerebellar membranes.

4.2.4 Immunohistochemical localisation of NMDAR subunits

Brain sections from paraformaldehyde-perfusion fixed adult control and stargazer mice were probed with the NMDAR subunit-specific antibodies, as described in section 2.12. Sections were originally incubated with a range of primary antibody concentrations (0.125 – 2 µg/ml) to optimise the specific versus non-specific signals obtained for each primary antibody. The anti-NR1 antibodies were used at a concentration of 0.5 µg/ml and the anti-NR2A antibody was used at 0.25 – 0.5 µg/ml. The anti-NR2B antibody was used at 0.5 – 1 µg/ml whilst the anti-NR2C/D antibody was used at 1 µg/ml.

Figure 4.7 Control (A and B) and stargazer (C and D) mouse brain sections were analysed by immunohistochemistry, using anti-NR1 subunit specific antibodies. Staining was seen within the control cerebellum (A), particularly within the granule cell layer (GL) and the cell bodies of the Purkinje cell layer (PL). Some staining was seen within the dendrites of the molecular layer (ML) whilst it was absent from the white matter (WM). Similar staining was observed within the stargazer cerebellum (D)

Scale bars represent 1 mm (A and C) or 100 μm (B and D).

WM
GL
PL
ML
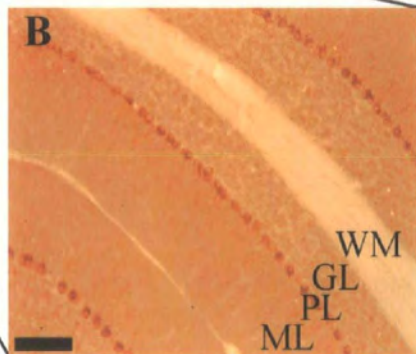
4.2.4.1 Immunostaining with the anti-NR1 antibody

Specific anti-NR1 immunostaining (figure 4.7A and table 4.2) in the cerebellum of control and stargazer mice was observed within Purkinje cell bodies and cerebellar granule cells (figure 4.7B). Staining patterns were qualitatively similar between control and stargazer cerebella (figures 4.7C and 4.7D and table 4.3).

NR1 staining was also observed within the forebrain of both control and stargazer mice (see tables 4.2 and 4.3). Both control and stargazer hippocampi were immunopositive for NR1 staining. Staining within the dentate gyrus was detected mainly within the molecular layer with some staining observed within the granule cell layer. Moderate staining was observed within the pyramidal cell layers of CA1-CA3 regions in both control and stargazer hippocampi.

4.2.4.2 Immunostaining with the anti-NR2A antibody

NR2A was present throughout most of both the control and stargazer forebrain. Areas of strong anti-NR2A immunostaining included the cerebral cortex and the hippocampus (tables 4.2 and 4.3). Within the hippocampus, the immunostaining was detected in the stratum alveole of the CA1-CA3 regions and within the molecular layer of the dentate gyrus. Immunostaining was observed within the control cerebellum, where the cerebellar granule cells and the Purkinje cell bodies both showed moderate to high cell staining (figure 4.8 and table 4.2). A similar staining pattern was observed within the stargazer cerebellum, although the staining appeared less intense than that within the control cerebellum (figure 4.8 and table 4.3).

4.2.4.3 Immunostaining with the anti-NR2B antibody

NR2B was thought not to be present within the adult cerebellum, although it is present in the adult forebrain. NR2B immunostaining has been shown to be prominent in the Purkinje cell bodies and dendrites and yet, absent from the granule cell layer (Thompson et al., 2000). In this study using the same antibodies, anti-NR2B-specific staining was observed within the cell bodies of the Bergmann glia, at the border of the Purkinje cell layer and the molecular layer, as well as within the dendrites of the Bergmann glia in the molecular layer of the control cerebellum

Figure 4.8 Immunohistochemical analysis of NR2A within the cerebellum of control (A and B) and stargazer (C and D) mice. Sagittal sections were stained using the anti-NR2A antibody and DAB. Staining was seen within control cerebellum (A), particularly within the granular layer (GL), within the cell bodies of the Purkinje cell layer (PL) and within the dendrites of the molecular layer (ML). No staining was seen within the white matter of the cerebellum (B). NR2A labelling was also observed within the stargazer cerebellum (C), where staining was detected within the granular layer and the cell bodies of the Purkinje cell layer (D). Some punctate staining was visible within the cell bodies of the molecular layer.

Scale bars represent 1 mm (A and C) or 100 μm (B and D).

A

B

GL   ML
WM PL

C

D
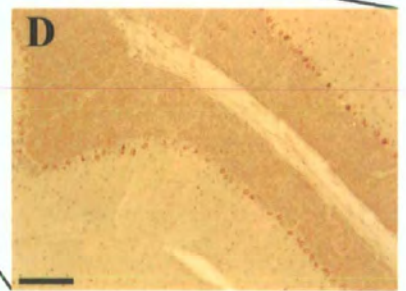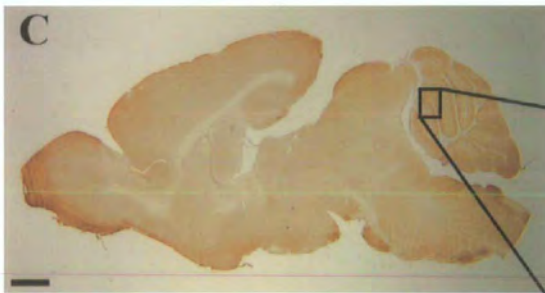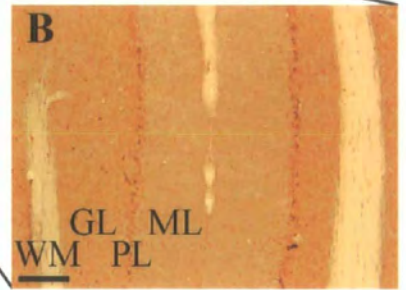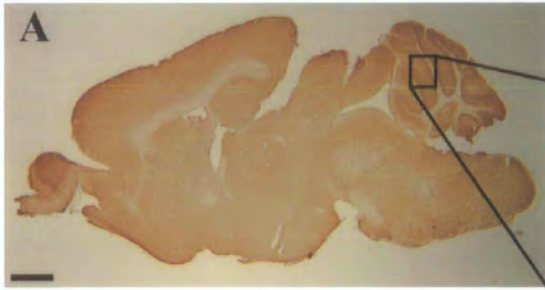
(table 4.2). A similar distribution was observed within the stargazer cerebellum (table 4.3).

Some immunostaining was observed within the control forebrain and within the stargazer forebrain (tables 4.2 and 4.3 respectively). Immunoreactivity was detected within the cortex, the thalamus and the hippocampus. Within the hippocampus, staining was observed within the CA1 and CA3 regions, mainly within the stratum radiatum. Within the dentate gyrus, specific immunostaining was observed in the molecular and polymorphic layers. This was observed in both control and stargazer forebrains.

4.2.4.4 Immunostaining with the anti-NR2C/D antibody

The anti-NR2C/D antibody also revealed immunostaining throughout the brain with the cerebellum, hippocampus, cerebral cortex and striatum stained. The CA1 and CA3 regions of the hippocampus showed a low level of staining in both control and stargazer, with no immunostaining evident within the pyramidal cell layer. Within the dentate gyrus, whilst staining was observed within the polymorphic layer, the most intense staining was observed within the molecular layer (see tables 4.2 and 4.3).

Specific immunostaining was observed throughout the control cerebellum (figure 4.9A and table 4.2) and stargazer cerebellum (figure 4.9C and table 4.3). Within the control cerebellum, immunoreactivity was detected in the cerebellar granule cells and the Purkinje cell layer. Within this cell layer, immunostaining appeared to be localised to basket cells. Some staining was also detected within the dendrites of the molecular layer (figure 4.9B). NR2C/D immunostaining was also detected within the granule cell layer in the stargazer cerebellum (figure 4.9D). However, the immunostaining observed within the Purkinje cell layer of control cerebellum was reduced in stargazer cerebellum.

Figure 4.9 Immunohistochemical analysis of NR2C and NR2D within the cerebellum of control (A and B) and stargazer (C and D) mice. Sagittal sections were stained using the anti-NR2C/D subunit-specific antibody and DAB. Staining was observed within the control cerebellum (A), where the majority of immunostaining was seen within the granule cell layer (GL); however, some staining was also seen within some of the dendrites of the molecular layer (ML). Immunostaining was also detected in the basket cells of the Purkinje cell layer (PL). No staining was detected within the white matter (WM) (B).

A similar staining pattern was observed within the stargazer cerebellum (C), with the majority of the staining been seen within the granular layer (D).

Scale bars represent 1 mm (A and C) or 100 μm (B and D).

GL ML
WM PL

	NR1	NR2A	NR2B	NR2C/D
Cerebral Cortex	+++	++/+++	++/+++	++
Hippocampus				
Ammon's horn				
CA1	+	+	+/++	+
CA3	+	+	+/++	+
Dentate Gyrus				
Molecular layer	++	+/++	++	+/++
Granule cell layer	+	+	−	−
Polymorphic layer	−/+	−/+	+	+
Caudate-Putamen	+++	++	++	++
Thalamus	++	++	++	++
Cerebellum				
Granule cell layer	++	++	−	+++
Purkinje cell layer	+++	+++	+	+++
Molecular layer	−/+	+	+	+

Table 4.2 Relative expression levels of the NMDAR subunits within control brain. Levels were estimated by visual comparison of DAB stained sections. − = staining at background levels; + = low staining; ++ = moderate staining; +++ = high staining; ++++ = very high level of staining. n = 4 – 8 sections from 2 – 4 mice.

	NR1	NR2A	NR2B	NR2C/D
Cerebral Cortex	+++	++/+++	++/+++	++
Hippocampus Ammon's horn				
CA1	+	+	+	+
CA3	+	+	+	+
Dentate Gyrus				
Molecular layer	++	+/++	+	+/++
Granule cell layer	−/+	−	−	−
Polymorphic layer	−/+	−/+	+	+
Caudate-Putamen	+++	++	+	++
Thalamus	+++	++	+	++
Cerebellum				
Granule cell layer	++	+	−	+++
Purkinje cell layer	++	++	+	+
Molecular layer	−/+	−/+	+	+

Table 4.3 Relative expression levels of the NDMAR subunits within stargazer brain. Levels were estimated by visual comparison of DAB stained stargazer sections with DAB stained control sections. − = staining at background levels; + = low staining; ++ = moderate staining; +++ = high staining; ++++ = very high level of staining. n = 4 – 8 sections from 2 – 4 mice.

4.2.5 Radioligand Binding

Both the previous experiments, i.e. quantitative immunoblotting and immunohistochemistry, revealed the expression levels and distribution of the NMDAR subunits within control and stargazer brains. This does not illustrate the expression of the final NMDA receptor complex. This was determined by radioligand binding experiments − by using both brain membrane preparations (see sections 4.2.5.1 and 4.2.5.2) and whole slices (see section 4.2.5.3).

4.2.5.1 [^{3}H] MK-801 Binding

Initial experiments were performed in order to optimise [^{3}H] MK-801 binding using homogenised control forebrain membranes. The forebrain membranes were prepared according to the protocol for the P2 membrane preparation (see section 2.8).

112

The binding parameters for [3H] MK-801 binding were determined by incubating control forebrain membranes with 200 nM [3H] MK-801, 15 µM glutamate, 5 µM glycine and with 10 µM MK-801 (for non-specific binding). The effects of temperature and incubation time were then determined. From these initial experiments, it was decided to perform the radioligand binding experiments at room temperature and with an incubation time of 2 hrs.

[3H] MK-801 binding, using a range of radioligand concentrations, was performed on control and stargazer forebrain membranes, as described in section 2.9.1.1, with the data then undergoing Rosenthal transformations in order to accurately determine K_D and B_{max} (figure 4.10).
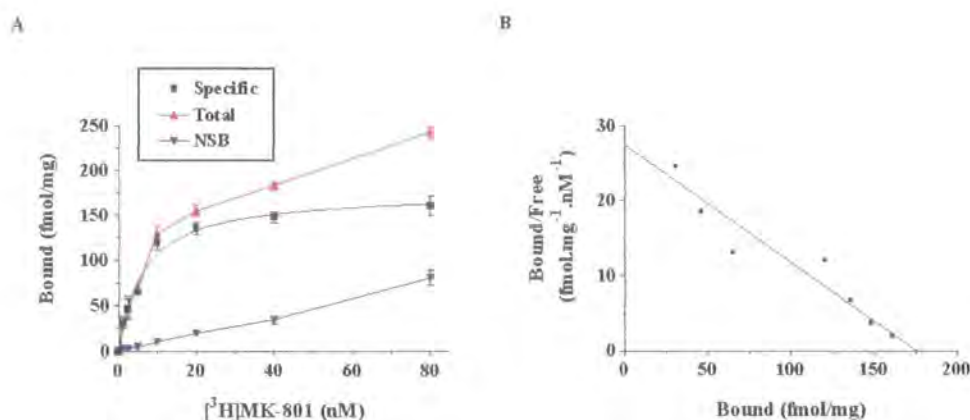
Figure 4.10 [3H] MK-801 binding on control forebrain membranes. (A) Binding isotherm showing total, non-specific and specific binding. (B) Rosenthal transformation of the specific binding results. n = 2 experiments, each consisting of tissue from 10 – 15 control forebrains.

Similar experiments were undertaken using stargazer forebrain membranes instead of control forebrain membranes (figure 4.11).
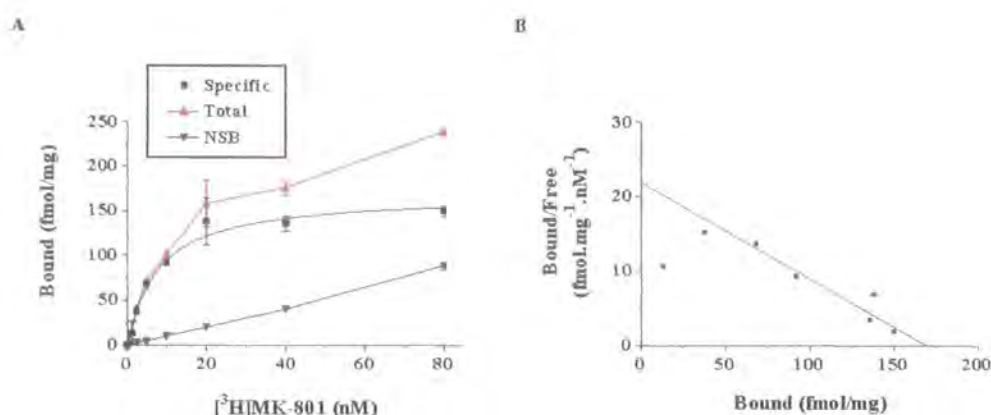
Figure 4.11 [³H] MK-801 binding in stargazer forebrain membranes. (A) Binding isotherm showing total, non-specific and specific binding. (B) Rosenthal transformation of the specific binding results. n = 2 experiments, each consisting of tissue from 10 – 15 stargazer forebrains.

B_{max} and K_D were determined for both control and stargazer forebrain membranes using Prism. The B_{max} for the control forebrain was 175.7 ± 7.3 fmol/mg protein whilst that for the stargazer forebrain was 169.3 ± 9.1 fmol/mg protein. The K_D for control forebrain was 6.4 ± 0.9 nM, whilst that for stargazer forebrain was 7.8 ± 1.4 nM. Neither the B_{max} nor the K_D for stargazer forebrain membranes were significantly different from those of control forebrain membranes.

As the B_{max} of control forebrain was the same as the B_{max} of stargazer forebrain, this would imply that the number of binding sites was unchanged in the two tissue preparations. The fact that the K_D was the same in both the control forebrain membranes and the stargazer forebrain membranes would imply that the affinity of the radiolabel for its receptor (i.e. the NMDA receptor) was unchanged.

Cerebellar membranes were also employed to determine the binding parameters of [³H] MK-801 in control and stargazer cerebella.

114
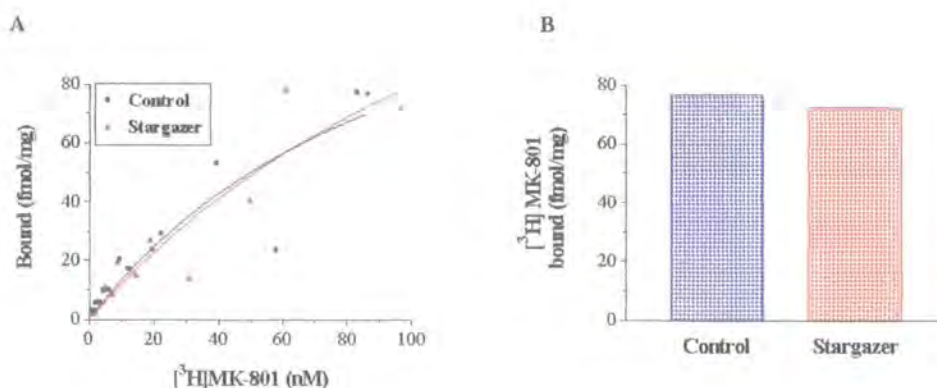
Figure 4.12 [³H] MK-801 binding in control and stargazer cerebellar membranes. (A) Binding isotherm showing specific binding of the radioligand in cerebellar membranes. (B) Specific binding of 90 nM [³H] MK-801 to 100 µg protein. n = 2 experiments, each consisting of tissue taken from 10 – 15 control and stargazer cerebella.

Figure 4.12A shows the amount of specific binding obtained with control and stargazer cerebellar membranes. These data were obtained from total and non-specific binding curves. As can be seen, the stargazer specific binding curve lies along the control specific binding curve.

Figure 4.12B shows the amount of binding with a single concentration of radioligand to stargazer and control cerebellar membranes. Saturation curves were plotted for both control and stargazer cerebellar membranes but these were unsatisfactory. Due to the amount of tissue required to obtain a full saturation curve, and the limited amount of tissue available, single point assays were undertaken instead. The amount of [³H] MK-801 bound to control membranes was 76.6 fmol/mg whilst the amount bound to stargazer cerebellar membranes was 72.3 fmol/mg.

The data were analysed using Prism to determine the maximum number of binding sites (B_{max}) and the dissociation constant (K_D); B_{max} was calculated to be 156.8 ± 80.1 fmol/mg protein in control cerebellar membranes and 442.5 ± 507.7 fmol/mg protein in stargazer cerebellar membranes; K_D was calculated to be 107.0 ± 85.8 nM and 396.9 ± 548.5 nM in control and stargazer cerebellar membranes respectively (results expressed as mean ± standard deviation).

It was thought that the small amount of specific binding was due to the cerebellar preparations having two binding sites for the radioligand. This was tested, in Prism, using an F-test. Testing the results from both control and stargazer cerebellar membranes revealed that both preparations fitted one-binding site models.

Due to the high standard deviations obtained with stargazer cerebellar membranes, it was not possible to use this tissue for further radioligand binding experiments. However, as satisfactory results were obtained with forebrain tissue (i.e. means with small standard deviations), these tissues were used for remacemide displacement assays (see section 4.2.5.2 below).

4.2.5.2 Remacemide displacement of [³H] MK-801

Remacemide, an anti-epileptic that binds to NMDA receptors and inhibits the binding of MK-801 to the NMDAR (Subramaniam et al., 1996), was then used to displace [³H] MK-801 from NMDA receptors. A range of concentrations of remacemide was used with 10 nM [³H] MK-801 and displacement curves obtained for both control and stargazer forebrain membranes, as described in section 2.9.1.2.
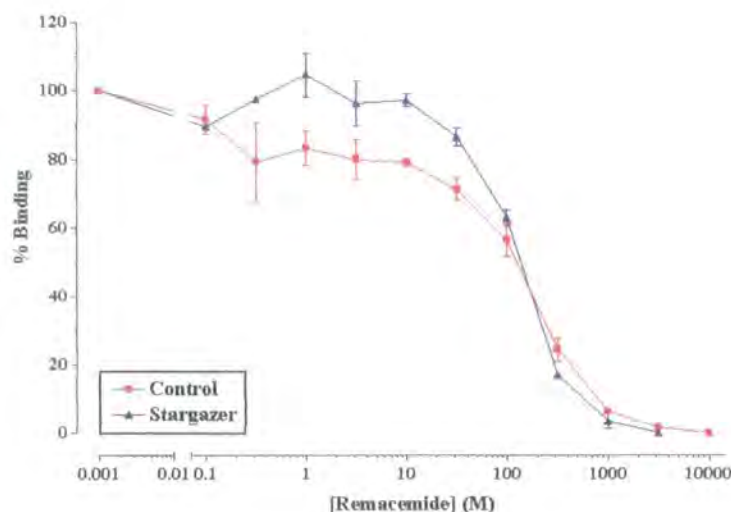
Figure 4.13 Remacemide displacement of [³H] MK-801 from control and stargazer forebrain membranes. The graph represents the combined results from 2 separate experiments with each membrane preparation.

Figure 4.13 shows the effect of increasing concentrations of remacemide on the binding of [^{3}H] MK-801 in both control and stargazer forebrain membranes. The IC_{50} was determined for both tissue preparations and was calculated to be $125.2 \pm 19.0 \, \mu M$ for control forebrain and $126.1 \pm 7.3 \, \mu M$ for stargazer forebrain (results expressed as mean $\pm$ standard deviation). Remacemide displaced the radioligand in both control and stargazer forebrains. As there was no difference between the IC_{50} for the remacemide in either tissue preparation, this implied that the pharmacology was the same in both the control and stargazer forebrains.

4.2.5.3 Autoradiographic localisation of NMDAR

[^{3}H] MK-801 was also used for autoradiographic binding on frozen whole sections taken from both control and stargazer brains (see figure 4.14). The slides were prepared and incubated as described in section 2.10. For the non-specific binding, a high concentration of the cold ligand (10 μM MK-801) was used to displace the radioligand (20nM [^{3}H] MK-801).

As can be seen in figure 4.14A, [^{3}H] MK-801 binding was seen in the control brain, mainly within the forebrain structures of the cortex and the hippocampus. A similar binding pattern was observed within the stargazer forebrain (figure 4.14E). In both cases, some [^{3}H] MK-801 binding was seen within the cerebellum, where the labelling appeared diffuse and weak. This radioligand, however, was not as specific as would be expected as some labelling was seen in both the control and stargazer non-specific binding slices (figures 4.14C and 4.14G respectively).

4.3 Discussion

Briefly, anti-NR1, anti-NR2A, anti-NR2B and anti-NR2C/D antibodies were generated and characterised using both recombinantly expressed NMDAR NR1, NR2A and NR2C subunits transiently transfected into HEK 293 cells and control brain membranes. The levels of expression of the NMDAR subunits were unchanged in control and stargazer forebrains and cerebella, as determined by the use of these antibodies in quantitative immunoblotting with brain membranes and immunohistochemistry with brain sections. The radioligand [^{3}H] MK-801 was

117

Figure 4.14 Autoradiographic exposure of control and stargazer whole brain sections to [³H] MK-801. Horizontal sections were cut from frozen, unfixed control (A-D) and stargazer brains (E-H). Control sections were incubated with either 20 nM [³H] MK-801 (A) or with the radioligand plus 10 μM MK-801 (C), to show non-specific binding. The sections were subsequently stained with toluidine blue (B and D respectively).

Stargazer sections were also incubated with the radioligand (E) or the non-specific binding buffer (G) before being stained with toludine blue (F and H) respectively.

The radiolabelled slides were exposed to [³H] hyperfilm for a total of 10 days before the film was developed and the slides stained with toluidine blue.
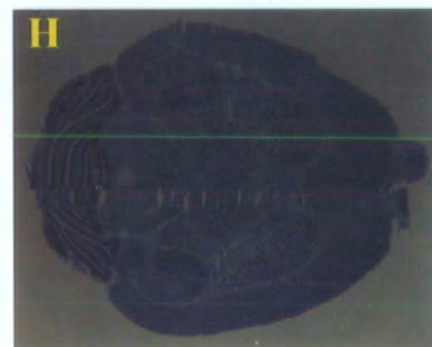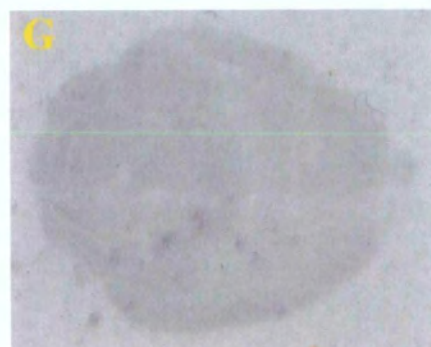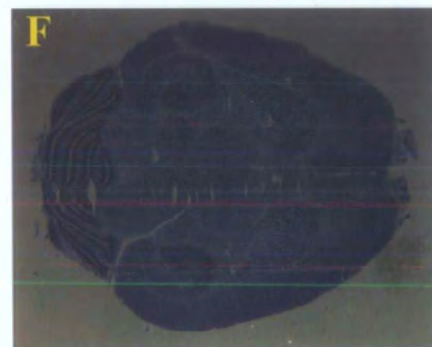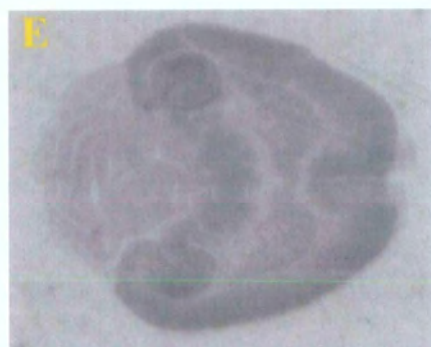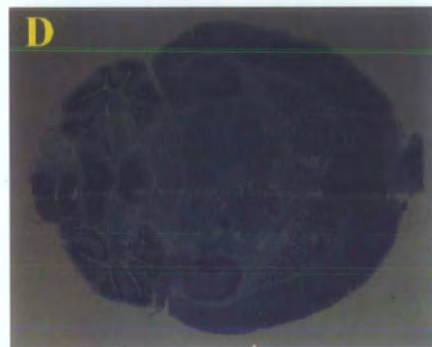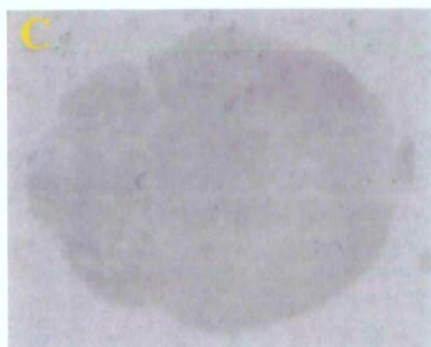
employed to determine whether the characteristics of assembled NMDA receptors were compromised by the mutation. No differences were observed between control and stargazer tissue. Similarly, the IC_{50} for remacemide-mediated displacement of $[^3H]$ MK-801 from NMDARs in control and stargazer forebrain tissue were not significantly different. As remacemide is an anti-epileptic agent targeting NMDA receptors, it is unlikely that this would be effective in controlling seizure activity in stargazer mice.

4.3.1 NMDAR subunit levels are unchanged in stargazer brain

No significant differences in the levels of NR1, NR2C and NR2D subunits were observed, by immunoblotting (section 4.2.3), between control and stargazer cerebellar membranes. Furthermore, no NR2B was detected by immunoblotting in control and in stargazer cerebella, indicating that this subunit had become developmentally downregulated to the levels expected in adult cerebella (Yamada et al., 2001; Wang et al., 1995; Wenzel et al., 1995). It is possible, however, that the lack of NR2B immunoreactive species was due to a very low level of expression within the cerebellum since faint signals have been obtained in membranes obtained from cerebella and cultured cerebellar granule cells (Jin et al., 1997; Portera-Cailliau et al., 1996; Janssens and Lesage, 2001).

Similarly, no differences in the level of expression of the NR1, NR2B and NR2D subunits were observed between by quantitative immunoblotting of control and stargazer forebrain membranes (section 4.2.3). The NR2C immunopositive signal was not perceived in either control or stargazer forebrain.

Qiao et al. (1998) reported that an unusually large number of cerebellar granule cells were still evident in the external granule cell layer at P15 and that granule cells with an immature morphology were detected in the granule cell layer of adult stargazer cerebellum. It could, therefore, be predicted that these granule cells would express an 'immature' complement of NMDAR subunits, characterised by the presence of the NR2B subunit.

In the cerebellum, the NMDAR subunits show a distinct developmental profile. NR1 mRNA was detected at low levels in neonatal rats (P0) but rapidly increased to reach adult levels by P14 (Akazawa et al., 1994). A similar increase was observed with the levels of NR1 subunit protein in both rat and mouse cerebella, where maximal levels of expression were detected after P21 (Luo et al., 1996; Didier et al., 1995).

NR2A mRNA transcript was detected at very low levels at P3-5 and increased in during development (Wenzel et al., 1997; Akazawa et al., 1994; Riva et al., 1994). The protein subunit also followed a similar pattern, with low levels detected by immunoblotting at birth (P0) and increasing levels of expression detected during the first three weeks of life, reaching a plateau by P21 (Laurie et al., 1997; Wenzel et al., 1997; Portera-Cailliau et al., 1996; Wang et al., 1995; Didier et al., 1995).

A distinct expression profile was displayed by NR2B mRNA with low levels of expression observed at P0. However, expression of NR2B mRNA increased, reaching a plateau around P10-21 after which levels decreased, becoming undetectable in the adult cerebellum (Wenzel et al., 1997; Akazawa et al., 1994). Similarly, protein levels of the NR2B subunit were low during the first postnatal week, increasing during the second week and subsequently decreasing to undetectable levels by P21-30 (Wenzel et al., 1997; Portera-Cailliau et al., 1996; Takahashi et al., 1996; Wang et al., 1995; Didier et al., 1995).

Whilst weak levels of NR2C mRNA were detected in the cerebellum around P5-8, the levels of the transcript increased to reach adult levels by P21 (Wenzel et al., 1997; Akazawa et al., 1994; Riva et al., 1994). Low levels of protein expression were also detected, by immunoblotting, at P5-9 and increased dramatically to reach adult levels by P15-21 (Wenzel et al., 1997; Laurie et al., 1997; Didier et al., 1995). Finally, whilst Akazawa et al. (1994) were able to detect NR2D mRNA in the cerebellum from P0 onwards in Purkinje cells, this signal had disappeared by P11. However, transcript expression was detected in the molecular and internal granule cell layers from P14 onwards. NR2D protein was detected in P7, P21 and P49 (adult) rat cerebella (Dunah et al., 1996; Wenzel et al., 1996).

121

If stargazer cerebellum did indeed contain immature cells, as suggested by Qiao et al. (1998), intermediate levels of NR1 and NR2A protein and low levels of NR2C and NR2D subunit proteins would be expected along with high levels of expression of the NR2B subunit. However, the results obtained here by quantitative immunoblotting revealed no significant differences in any of the NMDAR subunits between control and stargazer cerebella. These results, therefore, indicated that the expression of the NMDAR subunits in stargazer cerebella followed the predicted developmental profile.

4.3.2 Anatomical distribution of the NMDAR subunits does not differ between control and stargazer mice

Membranes from both forebrains and cerebella were probed for the expression of the NMDAR subunits by immunoblotting. Whilst this will reveal whether there are overall changes in the steady state level of expression of the proteins in the two brain tissues, it cannot reveal if the expression of the subunits is altered in any one anatomically distinct nucleus of cells or brain subregion. In order to establish if this was the case, the distributions of the subunits were determined, using the generated antibodies, by immunohistochemistry.

No significant differences in the distribution of each subunit were observed between control and stargazer brain sections. The NR1 subunit was shown to have a ubiquitous distribution, being found throughout the brain (section 4.2.4.1); a distribution which was consistent with those observed by others (Thompson et al., 2002; Thompson et al., 2000; Watanabe et al., 1998b; Hafidi and Hillman, 1997; Petralia et al., 1994; Brose et al., 1993). The pattern of immunostaining observed with the anti-NR2A antibody (section 4.2.4.2) was, as expected, similar to that of the NR1 subunit (Thompson et al., 2002; Thompson et al., 2000; Watanabe et al., 1998b). Whilst the anti-NR2C/D antibody detected both the NR2C and NR2D subunits in the cerebellum, it only detected the NR2D subunit in the forebrain (section 4.2.3.1). The immunostaining revealed by this antibody was comparable to published results (Thompson et al., 2002; Thompson et al., 2000).

Immunohistochemical studies, both here (section 4.2.4.3) and by others, have revealed NR2B subunit protein to be expressed within a number of brain regions, including the hippocampus, the olfactory bulb, cerebral cortex and the striatum (Thompson et al., 2002; Charton et al., 1999; Watanabe et al., 1998b). Similarly, immunoblotting studies have demonstrated the presence of the NR2B subunit within the forebrain (section 4.2.3; Laurie et al., 1997; Wang et al., 1995). In the cerebellum, immunohistochemical studies revealed NR2B immunoreactivity within the Purkinje and molecular layers, where it appeared to be localised to the Bergmann glia (section 4.2.4.3). Immunostaining has been reported previously in both mouse and rat cerebella where, unlike the results observed here, Purkinje cells were stained (Thompson et al., 2000).

These results indicated that the distributions of the NMDAR subunits are similar between control and stargazer brains. They also indicated that the distributions observed here are comparable to published findings.

4.3.3 Pharmacological properties of the NMDAR complex

Seizures induced in rats once a day for three consecutive days from P15 to P17, a time when stargazer mice begin to show the symptoms of absence epilepsy, led to a decease in the density of [^{3}H] MK-801 binding sites as well as a decrease in the receptor dissociation constant (Doriat et al., 1999). It could, therefore, be argued that stargazer mice would also exhibit alterations in NMDARs.

The immunoblotting and immunohistochemical studies undertaken here revealed similar levels of NMDAR subunits in both control and stargazer brains and that the subunits shared a similar distribution profile. However, these results did not reveal whether the subunits assembled into receptors or not.

The properties of NMDARs in control and stargazer brain tissue were analysed by measuring the binding of the selective non-competitive NMDAR antagonist [^{3}H] MK-801. Since the binding site for MK-801 is located in the NMDAR ion channel and so is dependent on channel activation (Kloog et al., 1988; Wong et al.,

1988; Foster and Wong, 1987), it can therefore be assumed to reflect the distribution of the functional receptor.

Both control and stargazer forebrains exhibited similar autoradiographical distributions of [^{3}H] MK-801 binding (section 4.2.5.3). In both cases, the highest amount of binding was observed within the forebrain; however, some binding was also perceived in the cerebellum. The binding was characterised using P2 synaptic membranes prepared from control and stargazer mice (section 4.2.5.1). No differences were quantified between control and stargazer forebrain tissue in either the number of binding sites or the affinity of [^{3}H] MK-801 for the NMDAR. The specific binding of [^{3}H] MK-801 appeared to be the same between control and stargazer cerebellar tissue, however, it is not possible to ascertain unequivocally if the number of binding sites or affinity were the same between these two tissues since the saturation point was not reached.

Remacemide, an anti-convulsant, has been shown to decrease the number of spike-wave discharges in a genetic rat model of absence epilepsy (van Luijtelaar and Coenen, 1995). Currently undergoing clinical trials as adjunctive therapy in patients with epilepsy (Chadwick et al., 2002; Hooper et al., 2001), remacemide has also been shown to be involved in an improvement in motor fluctuations in patients with Parkinson's Disease (Clarke et al., 2001; Shoulson et al., 2001) and in the motor deficits seen in both mouse models of and patients with Huntington's Chorea (Ferrante et al., 2002; Schilling et al., 2001; Kieburtz et al., 1996).

Studies have revealed that remacemide and its active des-glycine metabolite are non-competitive antagonists at the NMDAR ion channel, where they interact with the MK-801 binding site (Ahmed et al., 1999; Subramaniam et al., 1996; Palmer et al., 1992). This ability to interact with MK-801 binding was utilised to displace [^{3}H] MK-801 from control and stargazer forebrain synaptic membranes. Remacemide was able to displace the radioligand in both membrane preparations, with no significant differences apparent in the IC$_{50}$ (section 4.2.5.2). Interestingly, there appeared to be some divergence between the displacement observed in control and stargazer brain membranes, with low concentrations of remacemide. It is

124

possible, therefore, that the stargazer brain may be lacking in high affinity binding sites for remacemide. Further experiments will be needed, using radiolabelled remacemide, to determine whether this is true.

The results obtained here revealed no significant differences in the binding of [^{3}H] MK-801 and its displacement from the NMDARs in control and stargazer brain tissue, as measured by IC_{50}. There is some possibility, however, that the binding of remacemide differs between the two tissues, particularly at low concentrations.

4.3.4 Conclusion

Immunoblotting and immunohistochemical studies using anti-NMDAR subunit specific antibodies revealed the expression of NMDAR subunits in control (+/+ and +/stg) adult brains to be in correlation with published studies on the distribution of NMDAR subunits. The distributions and amounts of subunit protein did not differ significantly between control and stargazer brains.

[^{3}H] MK-801 and remacemide, both non-competitive antagonists that bind to the NMDAR ion channel, were used to determine the pharmacology of the NMDARs. No significant differences were observed in the binding of the radioligand or in its displacement by remacemide, between control and stargazer synaptic membranes.

These studies indicated no significant differences in NMDAR expression or pharmacology between control and stargazer. Further evidence for a lack of defect in NMDARs came from Hashimoto et al. (1999), who found normal NMDAR-mediated EPSCs at the cerebellar mossy fibre-granule cell synapse and in the hippocampal CA1 pyramidal cells in stargazer.

Characterisation of AMPA receptor expression within stargazer mouse brain

5.1 Introduction

As shown previously (chapter 4), no significant difference was observed in the expression of the NMDA receptor subunits between control and stargazer mice, by immunohistochemistry or by quantitative immunoblotting. No significant differences in [^{3}H] MK-801 binding were observed between control and stargazer brain membranes either. Similarly, Hashimoto et al. (1999) reported no apparent abnormality in NMDA receptor function at the mossy fibre-granule cell synapse in the stargazer cerebellum.

AMPA receptors (AMPARs), however, have been implicated in a number of characteristics also shown by the stargazer mutant mouse, including classical eye-blink conditioning, epilepsy and ataxia.

5.1.1 The role of AMPARs in classical eye-blink conditioning

The stargazer mutant mouse has been shown to be impaired in the acquisition of the classical eye-blink conditioning (Qiao et al., 1998). Classical eye-blink conditioning is a form of sensory-motor learning and has been used to study cellular mechanisms underlying learning and memory, particularly within the cerebellum. Basically, a puff of air is given to the cornea, causing the eye to blink. This blink reflex can be evoked to a tone when the tone is paired to the air puff to the eye (for review, see Kim and Thompson, 1997; Thompson and Kim, 1996; Yeo, 1991).

AMPARs have been implicated in the regulation of classically conditioned eye-blink reflex. CNQX (6-cyano-7-nitroquinoxaline-2, 3-dione), an AMPAR antagonist, has been shown to reversibly abolish conditioned responses in the rabbit following infusion of CNQX into the cerebellum (Attwell et al., 1999). [^{3}H] AMPA binding

was also shown to be decreased on the trained side of the cerebellar cortex following eye-blink conditioning elicited by paired electrical stimulation with an airpuff to the eye (Hauge et al., 1998). Conversely, [^{3}H] AMPA binding was increased within the hippocampus following classical conditioning (Tocco et al., 1991) and trace conditioning, which is a variation of the classical conditioning paradigm (Tocco et al., 1992).

5.1.2 AMPAR antagonists as anticonvulsants

There is evidence to suggest that AMPARs play a role in epilepsy in a variety of models and that AMPAR antagonists could play a role as anticonvulsants (for review, see Rogawski and Donevan, 1999). YM90K (6-(1H-imidazol-1-yl)-7-nitro-2,3(1H,4H)-quinoxalinedione hydrochloride), an AMPAR antagonist, was used in a rat amygdala-kindling model of epilepsy. Pre-treatment with YM90K retarded the evolution of the kindling whilst once kindling was established, the administration of YM90K led to a dose-dependent suppression of the seizures (Kodama et al., 1999). Application of NBQX (2,3-dihydroxy-6-nitro-7-sulphamoylbenzo[f]quinoxaline-2,3-dione), a competitive AMPAR antagonist, to the same model also inhibited the development of the kindling as well as suppressing the seizures in a dose-dependent manner (Namba et al., 1994). NBQX and GYKI 52466 (1-(4-aminophenyl)-4-methyl-7,8-methylenedioxy-5H-2,3-benzodiazepine), a non-competitive AMPAR antagonist, have both been shown to act as anticonvulsants against sound-induced seizures in DBA/2 mice and against AMPA-induced seizures in Swiss mice (Chapman et al., 1991).

5.1.3 AMPARs have been implicated in ataxia

Stargazer begins to show ataxia around P14 (Noebels et al., 1990). This ataxia consists of a mild ataxic gait and a severe impairment of both motor co-ordination and balance as determined by the length of time wild-type control and stg/stg mice remained on a stationary and a rotating rod (Qiao et al., 1996). It has been postulated that the deficits in motor learning, which led to the disturbances in motor co-ordination, were due to reduced AMPAR-mediated synaptic transmission within the cerebellum (Hashimoto et al., 1999).

Further evidence for a role of AMPARs in ataxia comes from studies employing antagonists to the AMPA receptor. NBQX, a competitive AMPAR antagonist, has been shown to cause ataxia in rats at doses over 30 mg/kg (Filliat et al., 1998; Mares et al., 1997). Administration of NBQX to mice also produced motor-impairment, as did administration of a non-competitive antagonist, GYKI 52466 (Swedberg et al., 1995; Yamaguchi et al., 1993). Ataxia is also produced in rats by YM90K, another AMPAR antagonist, in a dose-dependent manner (Katsumori et al., 1998).

There is also some evidence that the GluR2 subunit is involved in the regulation of motor co-ordination. GluR2-/- mice do not contain GluR2 protein, as shown by immunoblotting using crude synaptic plasma membrane preparations. However the length of time they manage to remain on a moving rod is significantly less than that of control mice (GluR2+/+). The levels of other AMPA receptor subunits, GluR1 and GluR4, kainate receptor subunits, GluR6 and GluR7, and NMDAR subunits NR1, NR2A and NR2B, in the GluR2-/- mice were comparable to the levels seen in GluR2+/+ mice. As only the GluR2 subunit was affected, a role for GluR2 in ataxia was implied (Jia et al., 1996).

5.1.4 AMPARs in the stargazer mutant mouse

Cultured cerebellar granule cells from stg/stg mice show few synaptic GluR4 puncta, although these can be clearly detected in cultured +/stg cerebellar granule cells. Electron microscopy of +/stg and stg/stg cerebella revealed that granule cell synapses in stg/stg cerebellum are devoid of GluR2/3 and GluR4 labelling, even though cytoplasmic GluR2/3 labelling was seen to the same extent in both +/stg and stg/stg granule cells (Chen et al., 2000).

Stargazin, transfected into COS cells, interacted with GluR1, GluR2 and GluR4 (Chen et al., 2000). GluR1 was also shown to co-immunoprecipitate with γ_2 in brain extracts derived from forebrains of control (B6EiC3H) mice (Sharp et al., 2001). As stargazer is a null mutant for stargazin, it could be postulated that there would be a decrease in the levels of the AMPAR subunits, as was seen at the cerebellar granule cell synapse.

Mossy fibre-granule cell synapses from the cerebellum of the stg/stg mutant are deficient in the AMPAR-mediated fast component of EPSCs. Similarly, synaptic transmission between parallel fibres and Purkinje cells and between climbing fibres and Purkinje cells were also reduced (Hashimoto et al., 1999). Spontaneous EPSCs, which are governed by the release of glutamate onto AMPARs, are essentially absent in cultured stg/stg granule cells. However, transfection of stargazin into stg/stg granule cells restored AMPAR function as evidenced by a large number and an increased frequency of sEPSCs (Chen et al., 2000).

Phosphorylation of stargazin could play a role in the modulation of AMPAR EPSCs. Cultured hippocampal neurons were transfected with a phosphomimetic construct of stargazin and mEPSCs were evaluated. The amplitude and frequency of AMPAR mEPSCs were significantly reduced in the transfected cells when compared to non-transfected cells (Chetkovich et al., 2002).

5.1.5 Work undertaken in this chapter

The work in this chapter was undertaken to determine the expression and characterisation of the AMPA receptor subunits within the control and stargazer brain. Subunit specific antibodies were used to determine the expression of the AMPAR subunits throughout the brain by immunohistochemistry and within the cerebellum by immunoblotting. Finally, binding of [^{3}H] AMPA was determined by both radioligand binding and autoradiography.

5.2 Results

5.2.1 Immunohistochemical distribution of AMPAR subunits

Paraformaldehyde-fixed whole brain sections from adult control and stargazer mice were probed with antibodies specific for the AMPAR subunits. Sections were originally incubated with a variety of primary antibody concentrations, ranging from 0.125 – 1 µg/ml for the anti-GluR1 antibody and 200 ng/ml – 2 µg/ml for the other AMPAR antibodies. The optimal antibody concentration was determined for both cerebella and forebrain sections using each of the primary antibodies. The concentrations used were 0.125 µg/ml (GluR1), 200 ng/ml (GluR2-stained cerebella

129

Figure 5.1 Immunohistochemical mapping of the distribution of GluR1 in control (A and B) and stargazer (C and D) forebrain. Horizontal sections were immunostained using the anti-GluR1 antibody and DAB as the hydrogen peroxide substrate. Immunostaining was prominent in the control hippocampus (A), particularly within the CA1, CA2 and CA3 areas and the molecular layer of the dentate gyrus (DG) (B). A similar staining pattern was observed within the stargazer forebrain (C) and hippocampus (D).

Scale bars represent 1 mm.
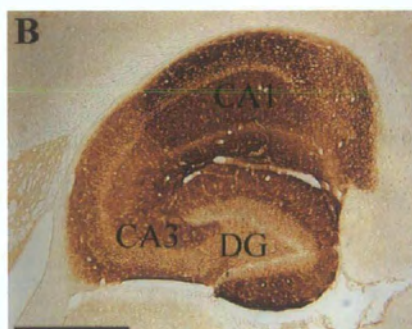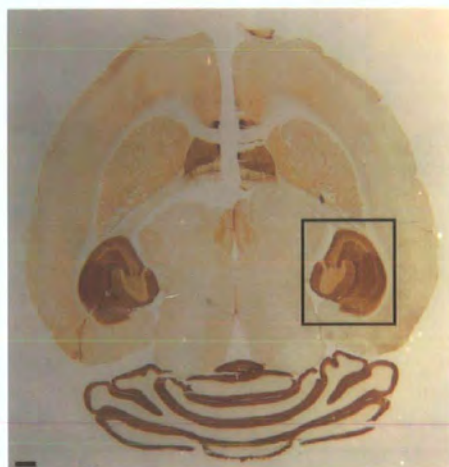
sections), 800 ng/ml (GluR2-stained forebrain sections), 2 μg/ml (GluR3) and 200 ng/ml (GluR4).

5.2.1.1 Immunostaining with anti-GluR1 antibody

Immunostaining with the anti-GluR1 antibody is seen in the same areas of the control (figure 5.1A and table 5.1) and stargazer brain (figure 5.1C and table 5.2). Strong immunostaining was observed within the hippocampus and within the septum. Within the hippocampus, staining is seen in within the CA1, CA2 and CA3, with the most intense staining being in the CA1 region (figure 5.1B for the control hippocampus). However, the staining in the stargazer CA1 region (figure 5.1D) is slightly less intense than that seen in the control CA1. Similarly, the stargazer dentate gyrus appears to contain slightly fewer immunostained GluR1 subunits than the control dentate gyrus.

Immunostaining was also observed within the cerebella of both stargazer and control brains (see figure 5.2). In both, the staining was confined to the molecular layer, with no staining being observed within the granule cell layer (figures 5.2B and 5.2D). Whilst the majority of Purkinje cells did not stain for the GluR1 subunit, there appeared to be some staining at the border of the Purkinje cell layer and the molecular layer, corresponding to basket cells (tables 5.1 and 5.2).

The distribution of the GluR1 protein within the control forebrain structures, the lack of staining within the granule cell layer of the control cerebellum and the intense staining within the control cerebellar molecular layer corresponds to the distribution of GluR1 mRNA (Sato et al., 1993; Keinanen et al., 1990).

5.2.1.2 Immunostaining with anti-GluR2 antibody

GluR2 immunostaining was found through out the control brain and the stargazer brain. Immunostaining was present within forebrain structures such as the cerebral cortex, the caudate-putamen and the hippocampus (tables 5.1 and 5.2 respectively). Within the hippocampi of both the control and stargazer, the staining appears to be the most intense within the stratum alveole of the CA1.

Figure 5.2 Immunohistochemical mapping of the distribution of GluR1 in the cerebellum of control (A and B) and stargazer (C and D) mice. Sagittal sections were stained using the anti-GluR1 antibody and DAB. Staining was seen within the control cerebellum (A), mainly within the molecular layer (ML). No staining was detected within the white matter (WM), the granule cell layer (GL) or the cell bodies of the Purkinje cell layer (PL) of the control cerebellum (B). A similar immunostaining pattern was revealed within the stargazer cerebellum (D)

Scale bars represent 1 mm (A and C) and 100 μm (B and D).

A

B

WM GL ML PL

C

D
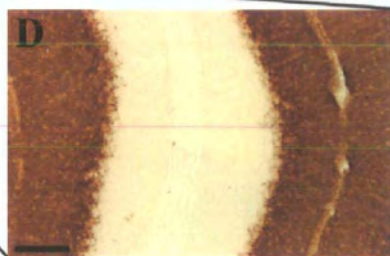
Figure 5.3 Immunohistochemical mapping of the distribution of GluR2 within the cerebellum of control (A and B) and stargazer (C and D) mice. Sagittal sections were immunostained using the anti-GluR2 antibody and DAB. Staining was seen within the control cerebellum (A), particularly within the cell bodies of the Purkinje cell layer (PL) and the dendrites of the molecular layer (ML) (B). Staining was detected within the stargazer cerebellum, however, less staining was observed than in the control cerebellum (C). Only some of the dendrites of the molecular layer showed GluR2 staining along with some of the cell bodies within the Purkinje cell layer (D). Scale bars represent 1 mm (A and C) and 100 μm (B and D).

GL
PL
ML
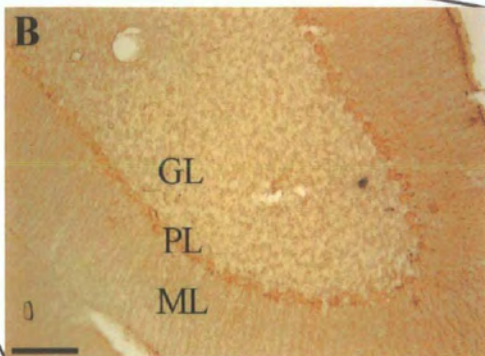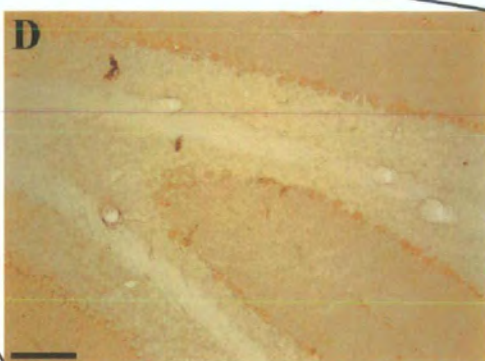
Immunostaining for GluR2 was also observed within the control cerebellum (figure 5.3A). As can be seen in figure 5.3B, specific immunostaining was visible within the cell bodies of the Purkinje cell layer and within the molecular layer, where staining was apparent within the dendrites of the Bergmann glia. Some staining was also apparent within the granule cell layer. GluR2 immunostaining was also observed within the stargazer cerebellum (figure 5.3C), where some staining was apparent in the granule cell layer. The Purkinje cells were also stained although not all the cell bodies were labelled (figure 5.3D). The staining observed in the dendrites of the Bergmann glia of the control cerebellum was not seen in the same cells of the stargazer cerebellum. The intensity of staining in stargazer cerebella was much reduced when compared to the staining obtained in control cerebella, despite the sections being stained in parallel. This reduction in staining intensity is reflected in the results obtained by quantitative immunoblotting (figure 5.12). The staining pattern visible within the control cerebellum and the reduction observed in stargazer cerebellum was similar to the immunostaining observed with anti-stargazin antibody (figure 6.3) possibly indicating an interaction between stargazin and GluR2.

5.2.1.3 Immunostaining using anti-GluR3 antibody

GluR3 staining was apparent throughout the control cerebellum (figures 5.4A and 5.4B). A similar staining pattern is seen within the stargazer cerebellum, as can be seen in figures 5.4C and 5.4D. Immunostaining is also seen in the control hippocampus (table 5.1) and within the stargazer hippocampus (table 5.2). Some staining was also observed within the cerebral cortex and the striatum and thalamus of the stargazer forebrain. Unfortunately, the high concentration of antibody required for immunostaining made it difficult to adequately determine staining above the level of background staining within the regions of the forebrain.

5.2.1.4 Immunostaining using anti-GluR4 antibody

GluR4 subunit-like immunoreactivity was exclusively found in the cerebellum of both control and stargazer mouse brains with little or no staining observed in the forebrain structures (see figure 5.5 and tables 5.1 and 5.2). Within the cerebellum, staining was restricted to the molecular layer of both the control (figure 5.5B and table 5.1) and stargazer brain sections (figure 5.5D and table 5.1). In the stargazer

Figure 5.4 Analysis of the expression of GluR3 within the cerebellum of control (A and B) and stargazer (C and D) mice by immunohistochemistry. Sagittal sections were immunostained using the anti-GluR3 antibody and DAB. Staining was seen within the control cerebellum (A), particularly within the granule cell layer (GL) and within the molecular layer (ML). Staining was absent from both the white matter (WM) and the Purkinje cell layer (PL) (B). Similar staining was detected within the stargazer cerebellum (D)

Scale bars represent 1 mm (A and C) and 100 μm (B and D).

A

B PL
ML GL WM

B

D
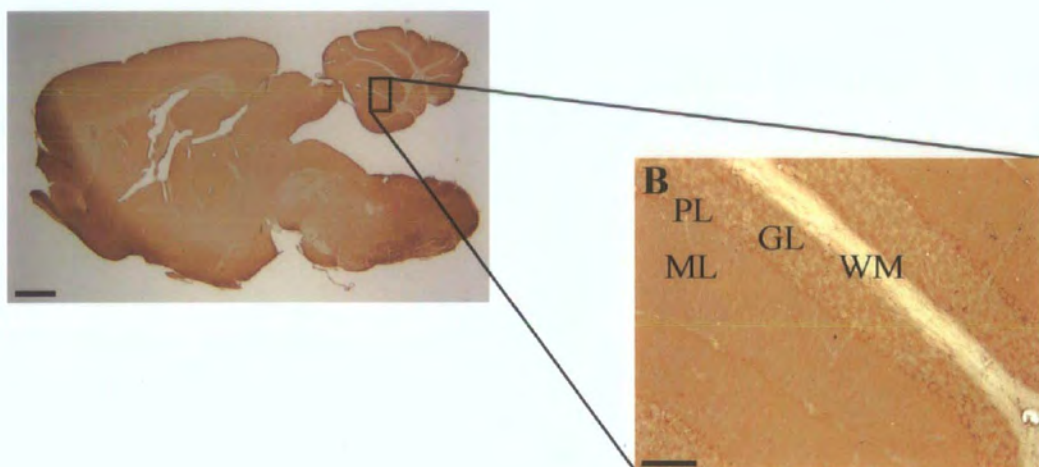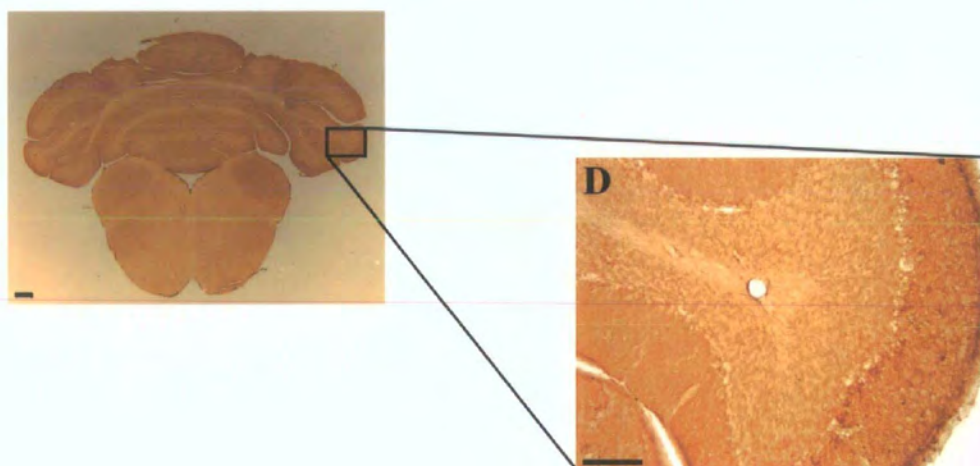
cerebellum, staining was less intense than in the control cerebellum, even though both sections were run in parallel. This result corresponds to the results obtained by quantitative immunoblotting, which showed that expression of the GluR4 subunit was decreased in stargazer (figure 5.12).

The pattern of immunostaining displayed by the anti-GluR4 antibody was completely abolished by pre-adsorption with the immunogenic (blocking) peptide (figure 5.6). This was also the case for the anti-GluR2 and anti-GluR3 antibodies used. No immunogenic peptide was available for the anti-GluR1 antibody. However, the distribution of immunoreactivity observed with the anti-GluR1 antibody was similar to that of GluR1 mRNA (Sato et al., 1993; Keinanen et al., 1990).

Figure 5.5 Immunohistochemical mapping of the distribution of GluR4 within the cerebellum of control (A and B) and stargazer (C and D) mice. Sagittal sections were stained using the anti-GluR4 antibody and DAB. Staining was observed within the control cerebellum (A), mainly within the molecular layer (ML). Some staining was also seen within the granule cell layer (GL) whilst it was absent in both the Purkinje cell layer (PL) and the white matter (WM) (B). A similar staining pattern was observed within stargazer cerebellum (C), although there was a decrease in the staining intensity within the molecular layer (D).

Scale bars represent 1 mm (A and C) and 100 μm (B and D).

A

B

ML
PL
GL
WM

C

D

Figure 5.6 Specificity of the anti-GluR4 antibody by using the GluR4 peptide and immunohistochemistry within brain sections of control mice. Sagittal sections were stained using the anti-GluR4 antibody (A) or anti-GluR4 antibody and peptide (B) and DAB. Staining was only seen within the control cerebellum (A). With the addition of the peptide to which the anti-GluR4 antibody was raised, the staining seen with the antibody alone was blocked.

Scale bars represent 1 mm.

A

B

	GluR1	GluR2	GluR3	GluR4
Hippocampus				
Ammon's horn				
CA1	++++	++	++	−
CA3	+++	++	++	−
Dentate Gyrus				
Molecular layer	++++	++	+	−
Granule cell layer	+++	+	−/+	−
Polymorphic layer	+++	+	−/+	−
Caudate-Putamen	+	+/++	+/++	−
Septum	++++	+/++	+	−
Cerebellum				
Granule cell layer	−	++	+/++	++
Purkinje cell layer	−/+	+++	++	+/++
Molecular layer	+++	++	++	++++

Table 5.1 Relative expression levels of the GluR subunits within control brain. Levels were estimated by visual comparison of DAB stained sections. − = staining at background levels; + = low staining; ++ = moderate staining; +++ = high staining; ++++ = very high level of staining. n = 4 − 8 sections from 2 − 4 mice.

	GluR1	GluR2	GluR3	GluR4
Hippocampus				
Ammon's horn				
CA1	+++	++	++	−
CA3	+++	+	+	−
Dentate Gyrus				
Molecular layer	+++	+/++	+	−
Granule cell layer	++/+++	+	−/+	−
Polymorphic layer	+++/++++	+/++	+	−
Caudate-Putamen	+	+/++	+/++	−
Septum	+++/++++	+/++	+	−
Cerebellum				
Granule cell layer	−	+	+/++	+
Purkinje cell layer	−/+	−/+	−/+	−
Molecular layer	+++	+	++	++

Table 5.2 Relative expression levels of the GluR subunits within stargazer brain. Levels were estimated by visual comparison of DAB stained stargazer sections with DAB stained control sections. − = staining at background levels; + = low staining; ++ = moderate staining; +++ = high staining; ++++ = very high level of staining. n = 4 − 8 sections from 2 − 4 mice.

145

5.2.2 Quantitative immunoblotting of AMPAR subunits

Cerebellar membranes were prepared from control and stargazer mouse brains and samples were precipitated, as described in sections 2.5 and 2.6, for analysis by SDS-PAGE using mini-gels. The immunoblots were probed with anti-GluR1 antibodies (0.5 μg/ml), anti-GluR2 antibodies (1:2000 dilution ≡ 100 ng/ml), anti-GluR4 antibodies (1:1000 dilution ≡ 200 ng/ml) or anti-β actin antibody (1:100 – 1:1000 dilution). The membranes were then incubated with the relevant anti-IgG-HRP linked secondary antibodies before developing for immunoreactive species using the ECL system and hyperfilm as described in the methods chapter 2.7.

5.2.2.1 Detection of the AMPAR subunits

As can be seen in figure 5.7A, a single band was seen with a molecular weight of approximately 104 kDa, which corresponded to the GluR1 protein. The GluR1 protein was detected in both the control and the stargazer cerebellar membranes. The samples were probed with the anti-actin antibody, a normalising probe to compensate for loading errors, as can be seen in figure 5.7B.

A single band was also seen with the anti-GluR2 antibody in both the control and the stargazer cerebellar membranes (figure 5.8A). This band has a molecular weight of approximately 105 kDa and corresponded to the GluR2 protein. The immunoblot was then reprobed using the anti-actin antibody and the result can be seen in figure 5.8B. Here, a single band is detected at approximately 42 kDa, the molecular weight for actin.

The cerebellar proteins were also probed for the expression of the GluR4 subunit in the same way, using the anti-GluR4 antibody as shown in figure 5.9A. A band at approximately 105 kDa, which corresponded to the molecular weight of the GluR4 subunit, was detected in both the control and stargazer cerebellar membranes. The same protein samples were run on a 10 % resolving gel and probed for the expression of actin, as can be seen in figure 5.9B.

The specificity of the antibodies was further confirmed by the distinct brain distributions of the respective proteins in immunohistochemically labelled sections.

146

Figure 5.7 Immunoblot showing the relative expression levels of GluR1 and actin in control and stargazer cerebellar membranes. A dilution series of control (ctl) and stargazer (stg) cerebellar membranes were probed with anti-GluR1 antibody (A) and anti-actin antibody (B).

Both antibodies detected the relevant proteins in the immunoblots (red arrows). The range of protein concentrations used was 1.25 μg/10 μl, 2.5 μg/10 μl, 5 μg/10 μl and 10 μg/10 μl.

The molecular weights (in kDa) are shown to the left of each immunoblot.

A

207 —
118 — ← GluR1
81 —

52.5 —

36.2 —

29.9 —

10   10   5   5   2.5   2.5   1.25   1.25

ctl   stg   ctl   stg   ctl   stg   ctl   stg

B

207 —
118 —
81 —

52.5 — ← Actin

36.2 —

29.9 —

10   10   5   5   2.5   2.5   1.25   1.25

ctl   stg   ctl   stg   ctl   stg   ctl   stg
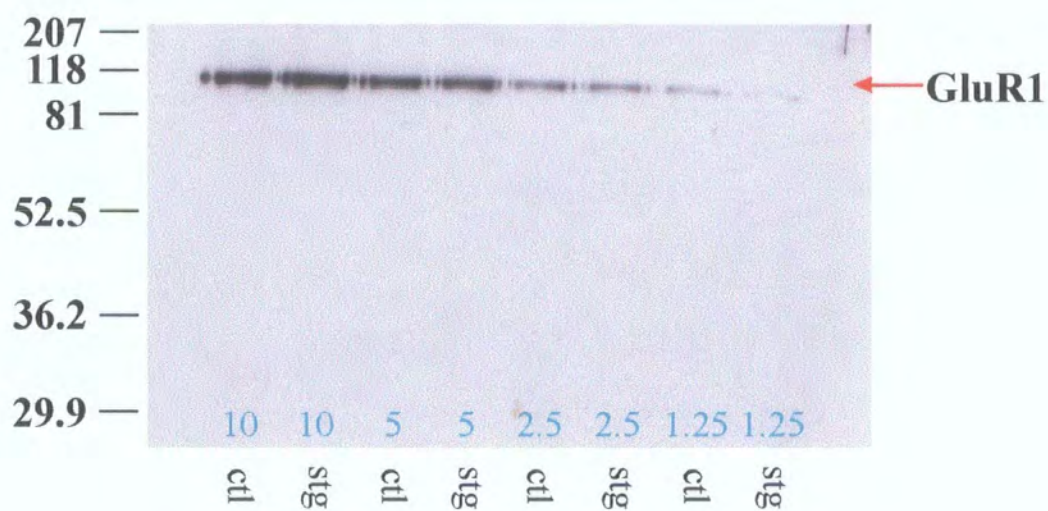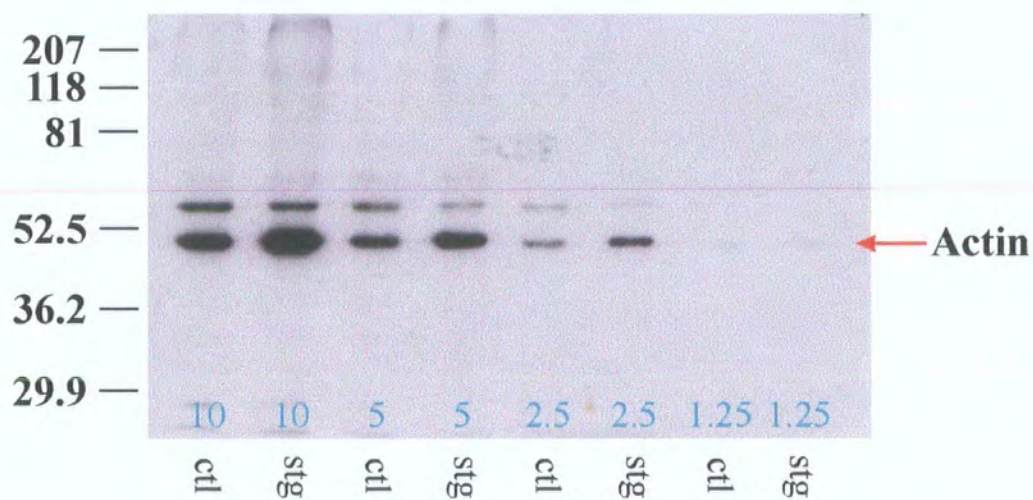
Figure 5.8 Immunoblot showing the relative expression of GluR2 and actin within control and stargazer cerebellar membranes. Control (ctl) and stargazer (stg) cerebellar membranes were probed with anti-GluR2 antibody (A) before being reprobed with the anti-actin antibody (B).

The anti-GluR2 antibody detected a 104 kDa protein, which corresponded to the GluR2 protein, whilst the anti-actin antibody detected a 45 kDa protein, which corresponded to the actin antibody. The range of protein concentrations used here was 1.25 µg/10 µl, 2.5 µg/10 µl, 5 µg/10 µl and 10 µg/10 µl.

The molecular weights, in kDa, are shown to the left of each immunoblot.

A

205 —

113 —

75 —

53.9 —

← GluR2

| 10 | 5 | 2.5 | 1.25 | 10 | 5 | 2.5 | 1.25 |

ctl ctl ctl ctl stg stg stg stg

B

205 —

113 —

75 —

53.9 —

34.9 —

← Actin

| 10 | 5 | 2.5 | 1.25 | 10 | 5 | 2.5 | 1.25 |

ctl ctl ctl ctl stg stg stg stg
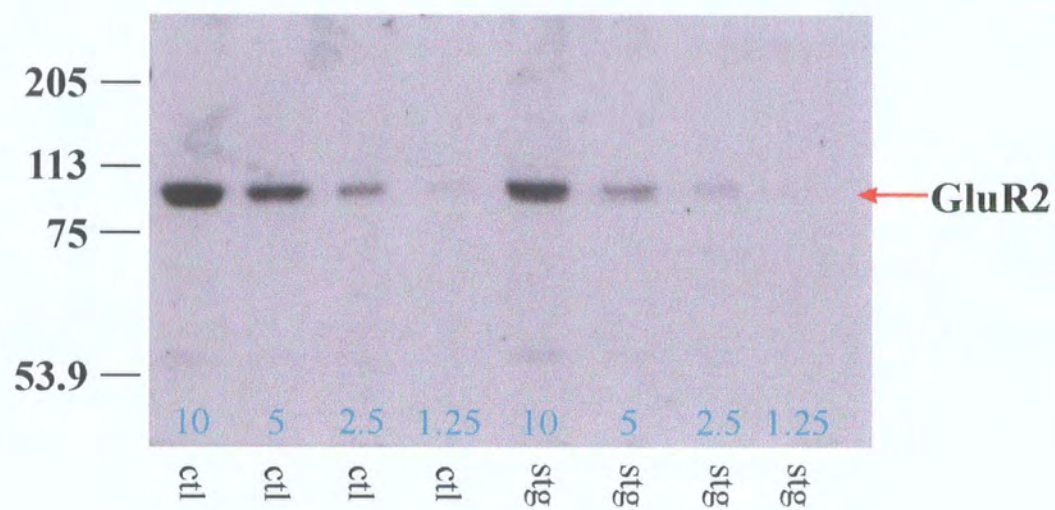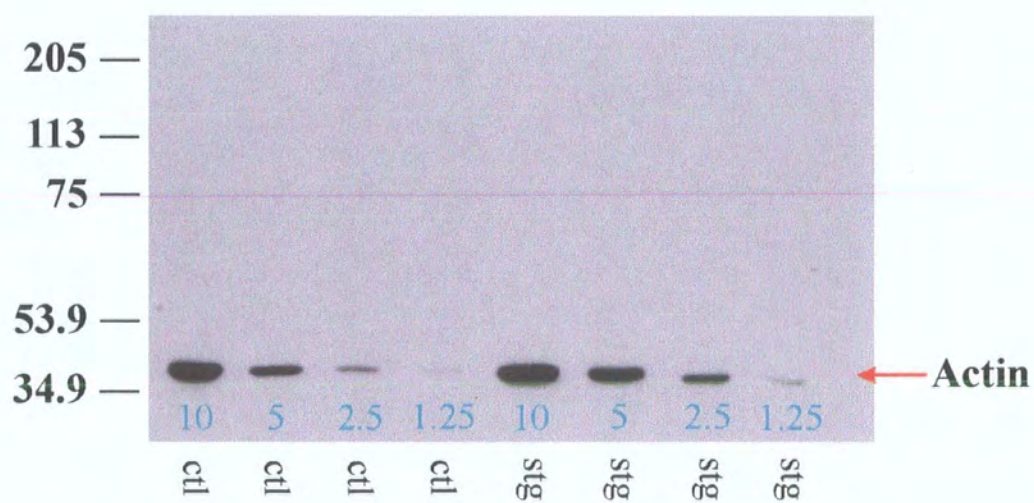
Figure 5.9 Immunoblot showing the relative expression levels of GluR4 and actin within control and stargazer cerebellar membranes. Control (ctl) and stargazer (stg) cerebellar membranes were probed with anti-GluR4 antibody (A) and anti-actin antibody (B).

Both antibodies detected the relevant proteins in the immunoblots (red arrows). A range of protein concentrations was used (1.25 µg/10 µl – 10 µg/10 µl) in order to be used for quantitative immunoblotting.

The molecular weights (in kDa) are shown to the left of each of the immunoblots.
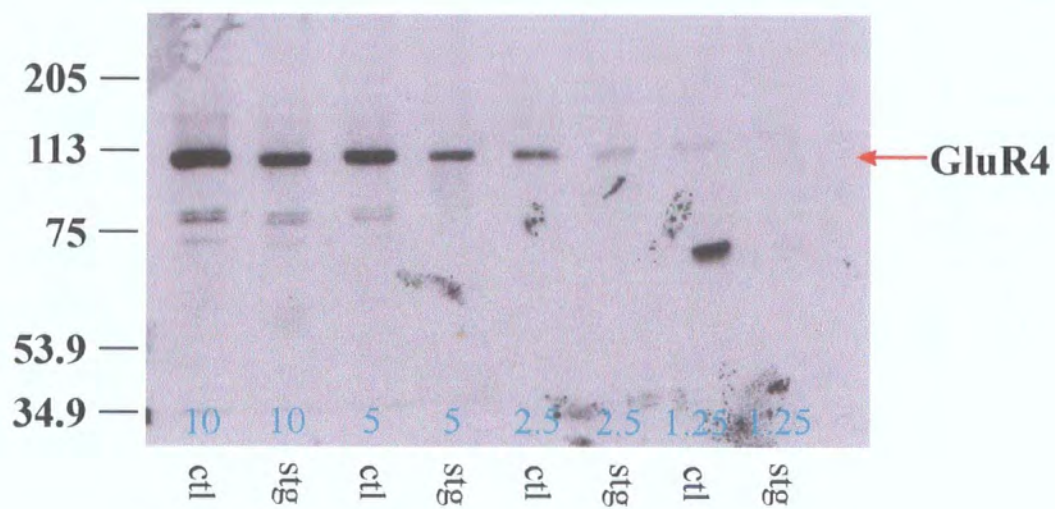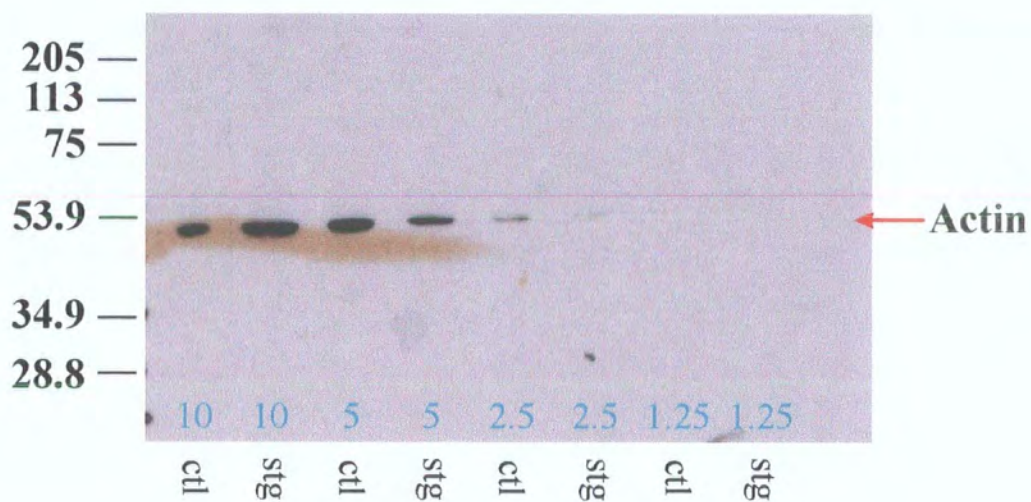
5.2.2.2 Specificity of the antibodies using peptides

Blocking peptides to the anti-GluR2 and anti-GluR4 antibodies were used to determine whether the signal was specific to the antibody. The primary antibodies were used at a concentration of 200 ng/ml (i.e. 1:1000 dilution) and incubated with either 1 μg/ml (5x) or 2 μg/ml (10x) blocking peptide overnight at 4°C. Proteins precipitated from control cerebellar membranes were analysed by immunoblotting using the anti-GluR2 or anti-GluR4 antibodies alone or following preadsorption with the respective immunogenic peptides.

The anti-GluR2 antibody produced a signal at approximately 105 kDa as can be seen in figure 5.10A. This signal was reduced in the presence of 5x blocking peptide and completely absent with the addition of 10x blocking peptide. The GluR4 signal, however, was completely blocked by the presence of 5x blocking peptide (figure 5.10B).

5.2.2.3 Quantification of subunit levels

Cerebellar membranes from control and stargazer mouse brains were analysed in this way to estimate the relative levels of expression of the various AMPA receptor subunits after normalising for actin levels. The immunoblots were analysed, using computer-assisted densitometry, as described in section 2.7.3.

Figure 5.10 Immunoblot showing expression of GluR2 (A) and GluR4 (B) with their respective peptides. Proteins from control cerebellar homogenates were probed with the antibodies alone or with the antibodies plus their peptides. Two concentrations of peptide were used – 5x (corresponding to 1 µg/ml) or 10x (corresponding to 2 µg/ml), which were equal to five times or ten times the concentration of the antibody.

As can be see in (A), the GluR2 antibody signal was blocked with the use of 10x peptide whilst the GluR4 signal was blocked with 5x peptide (B).

The molecular weights (kDa) are shown to the left of the immunoblots.

A

205 —
121 — ← GluR2
70 —
52.4 —

GluR2
Peptide
5x 10x

B

205 —
121 — ← GluR4
70 —
52.4 —
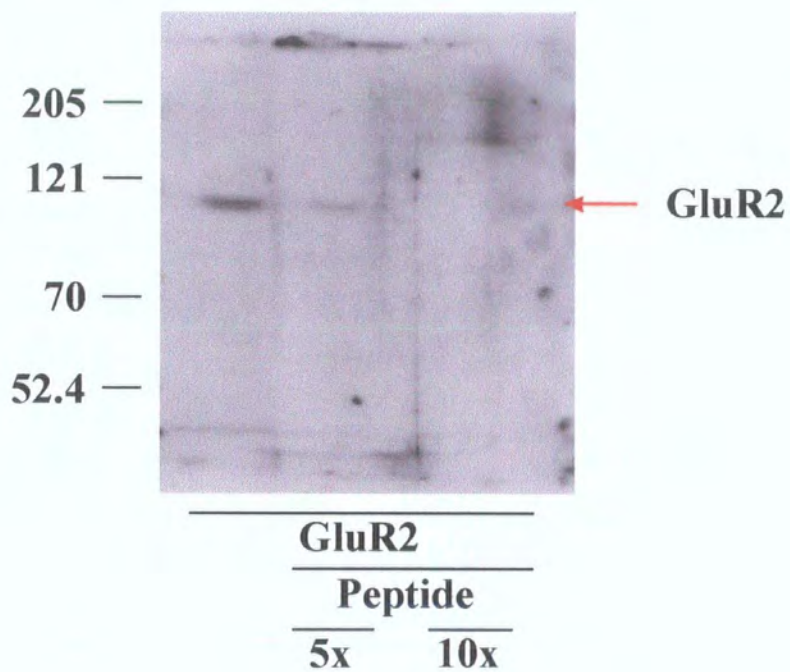
GluR4
Peptide
5x 10x
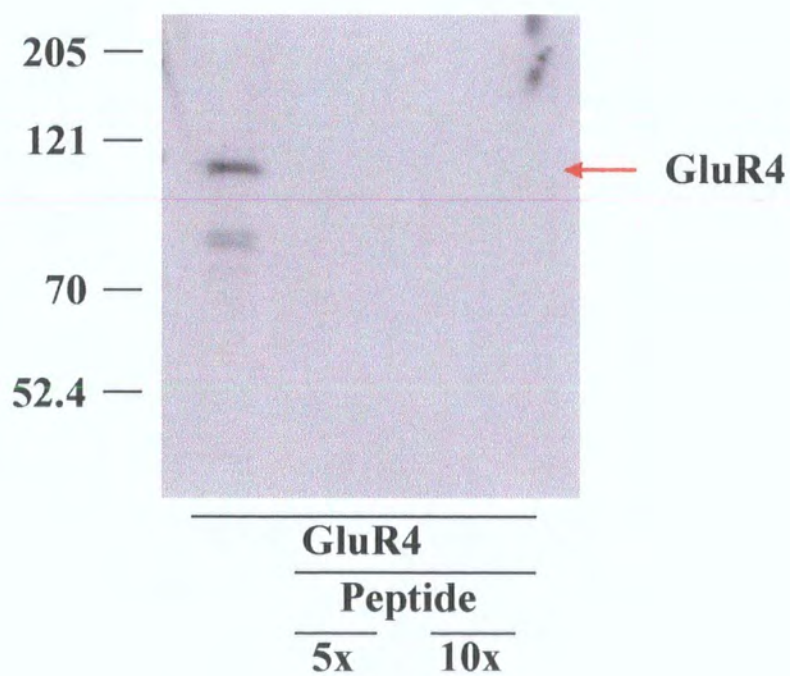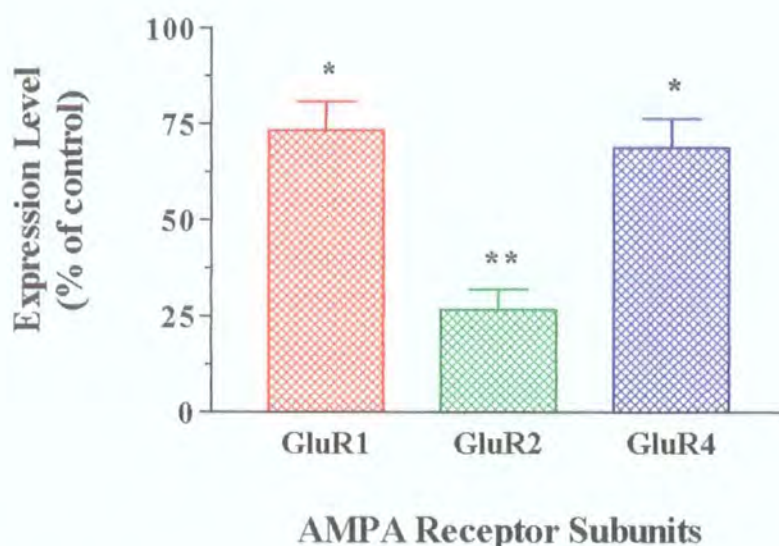
Figure 5.11 Comparative levels of expression of the AMPA receptor subunits, GluR1, GluR2 and GluR4, in the cerebellum of stargazer mice relative to control mice. The levels were normalised to actin levels. The GluR subunit levels in the stargazer cerebellum were expressed as a percentage of control expression. Results are expressed as mean ± sem. Student's *t*-tests were used to determine the level of significance:* = P < 0.05, ** = P <0.001. n = 3 − 4 samples for both control and stargazer cerebella membranes per immunoblot, immunoblotting repeated 4 (GluR1 and GluR4) or 5 (GluR2) times.

As can be seen in figure 5.11, the expression levels of GluR1, GluR2 and GluR4 subunits were significantly lower in stargazer mice cerebella, with respect to controls. GluR1 expression levels and GluR4 expression levels were 73.5 ± 6.6 % and 69.1 ± 6.5 % of control levels respectively. The level of expression of stargazer GluR2, however, was only 26.8 ± 4.7 % of control GluR2. This is evident in the immunoblots in figure 5.8 where, although the actin signal for the stargazer tissue was stronger than that of the control, implying a greater loading of cerebellar material from stargazer, the stargazer GluR2 signals were weaker than the control signals. The reduction in expression of GluR2 is not only detected both by immunostaining and immunoblotting of cerebellar membranes, but is also detected in cultured cerebellar granule cells (section 7.2.2.1).

5.2.3 Radioligand binding

[^{3}H] AMPA was used for radioligand binding experiments on forebrain and cerebellar membranes. Membranes allow a number of ligand concentrations to be used on the same preparation, thereby allowing the calculation of K_D and B_{max}, which would be more difficult to determine if only one concentration was used.

Initial experiments were performed in order to optimise [^{3}H] AMPA binding using control forebrain membranes. The forebrain membranes were prepared according to the protocol for the P2 membrane preparation (see section 2.8). The first experiment undertaken was to determine the binding parameters. Forebrain membrane was incubated for 30 minutes and for 60 minutes, at either 4°C or at 20°C and in 5 mM tris-acetate, pH 7.5, with 10 nM [^{3}H] AMPA and the radioligand-containing buffer with 1 mM glutamate (to show non-specific binding). The forebrain membrane was also incubated in the same radioligand-containing buffers with KSCN, as KSCN has been shown to potentiate AMPA binding (section 2.9.2.1).

From this experiment, it appeared as though KSCN did potentiate [^{3}H] AMPA in the forebrain membranes. Also, there appeared to be an increase in binding with an increase in incubation temperature, with the specific binding at 20°C being higher than that of the 4°C incubation. However, there appeared to be no difference in the amount of specific binding seen after a 30 minute incubation and the amount of specific binding seen after a 60 minute incubation.

Subsequent experiments were performed where both control cerebellar membranes and control forebrain membranes were incubated in the buffers. Both aliquots of the buffers used previously (stored at -20°C) and buffers prepared on the day were used. However, these experiments failed to show any difference in the level of binding seen at 4°C and that seen at 20°C. Even though in the initial experiment KSCN potentiated the level of binding seen with [^{3}H] AMPA, this finding could not be repeated in the subsequent experiments.

Following these experiments, it was decided to follow the protocol of Hawkinson and Espitia (1997), as the authors were able to both show [^{3}H] AMPA binding and

157

determine the saturation parameters (i.e. K_D and B_{max}) (see section 2.9.2.2). Briefly, control mouse forebrains were homogenised in sucrose/EGTA and centrifuged. The pellet was incubated with Triton X-100/EGTA before centrifuging. The pellet was then incubated with EGTA before centrifuging again. The pellet was stored at -80°C before being resuspended in 100 mM tris-acetate, pH 7.2, 50 μM EGTA.

Fractions of forebrain membrane were incubated for 60 minutes at 20°C with the buffers. The buffers were 100 mM tris-acetate, pH 7.2, 50 μM EGTA, 10 nM [^{3}H] AMPA (here after known as radioligand-containing buffer), radioligand-containing buffer plus 1 mM glutamate, radioligand-containing buffer plus 50 mM KSCN and radioligand-containing buffer plus glutamate and KSCN. As a control, forebrain membranes (P2 preparation) in 5 mM tris-acetate, pH 7.5, were incubated with the buffers used in the initial experiments, which were prepared on the day of use.

The control forebrain preparation showed a slight increase in binding in the presence of KSCN, however, the level of specific binding was still lower than expected. With the forebrain membrane in the 100 mM tris buffer, some specific binding could be seen and, even though it was still lower than expected, it was higher than that seen with the 5 mM tris buffer.

More control forebrain membrane was prepared according to the P2 membrane protocol, however, the buffers used for the protocol were all prepared using 50 mM tris-acetate, pH 7.4 (see section 2.9.2.3). The pellet was washed in ice-cold dH$_2$O and stored overnight at -20°C, in order to remove any endogenous glutamate still remaining. An extra overnight incubation step was included towards the end of the protocol.

In order to increase the level of binding seen, the buffer used to contain the radioligand was modified. Several groups have used tris buffers containing either EGTA (Hawkinson and Espitia, 1997) or CaCl$_2$ (Stensbol et al., 1999; Nielsen et al., 1998). [^{3}H] AMPA binding was determined using 10 nM [^{3}H] AMPA in 50 mM tris-acetate, pH 7.4, 50 mM tris-acetate, pH 7.4, with 100 μM EGTA or in 50 mM tris-

acetate, pH 7.4, with 2.5 mM $CaCl_2$. The forebrain membrane was incubated with the various radioligand-containing buffers alone or buffers containing 50 mM KSCN, 1 mM glutamate or KSCN and glutamate. The incubations were for 60 minutes and at 20°C.
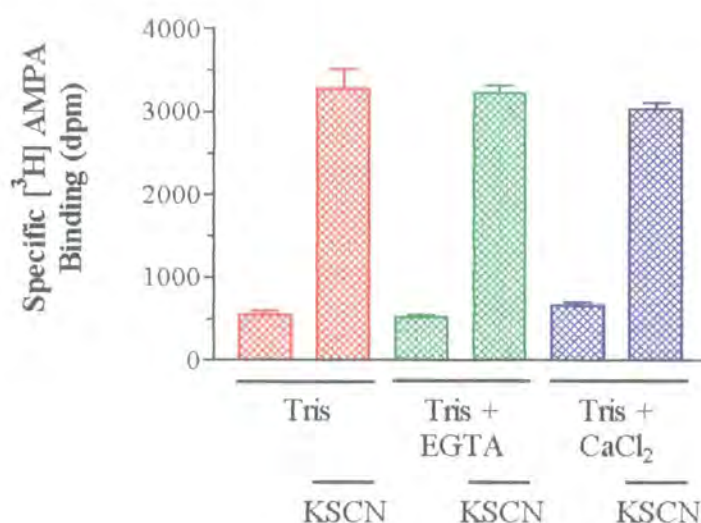
Figure 5.12 Specific [^{3}H] AMPA binding to control forebrain membranes, in the presence of 10 nM radioligand. Three tris buffers were used: 100 mM tris-acetate, pH 7.4 (tris), 100 mM tris-acetate, pH 7.4, 100 µM EGTA (tris + EGTA) and 100 mM tris-acetate, pH 7.4, 2.5 mM $CaCl_2$ (tris + $CaCl_2$). Specific binding was determined by subtracting the non-specific binding values (tris buffers + 1 mM glutamate) from total binding values (tris buffers). KSCN (50 mM) was added to each of the buffers (tris buffers alone and tris buffers + glutamate). Columns represent mean ± sem of 1 experiment done in triplicate.

As can be seen in figure 5.12, there was no difference in the amount of specific binding seen between each of the three tris buffers used. KSCN, however, potentiated [^{3}H] AMPA binding in all three buffers used. There was no significant difference in the specific binding levels seen between the tris buffers plus KSCN.

This protocol, with the extra freeze-thaw step, for the preparation of brain membranes was used to prepare control and stargazer cerebellar membranes. These were incubated, for 60 minutes and at 20°C, with 100 mM tris-acetate, pH 7.4, and 10 nM [^{3}H] AMPA alone, radioligand-containing buffer and 1 mM glutamate, radioligand-containing buffer and 50 mM KSCN or with radioligand-containing

buffer and 1 mM glutamate plus 50 mM KSCN. The KSCN potentiated the binding seen in both cerebellar membranes.

However, the protocol for the preparation of the membranes had now extended to being three days long before the protein concentration could be determined and the membrane used for binding. For this reason, a shorter protocol was attempted using control forebrain membranes (section 2.9.2.4).

Briefly, the forebrains were homogenised in 50 mM tris-acetate, pH 7.4, homogenisation buffers. The forebrains were homogenised in buffer 1 and then centrifuged for 12 minutes at 1,000 g, 4°C. The supernatant was then centrifuged at 40,000 g for 40 minutes, 4°C. The pellet was then homogenised in buffer 2 before being centrifuged at 40,000 g for 40 minutes, 4°C. The pellet was then homogenised in dH$_2$O and centrifuged at 40,000 g for 40 minutes, 4°C, a further three times. The final pellet was resuspended in dH$_2$O before being separated into three aliquots. The pellet was resuspended in dH$_2$O in order to minimise any interference of buffer components with the solutions employed in the Lowry's assay.

One aliquot was used for determining the protein concentration of the membrane, whilst the second aliquot was stored, overnight, at 4°C and the third was stored, also overnight, at -20°C. The second and third aliquots were used for radioligand binding using 10 nM [^{3}H] AMPA in 100 mM tris-acetate, pH 7.4 (radioligand-containing buffer), radioligand-containing buffer plus 1 mM glutamate, radioligand-containing buffer with 50 mM KSCN and radioligand-containing buffer plus glutamate and KSCN.

160
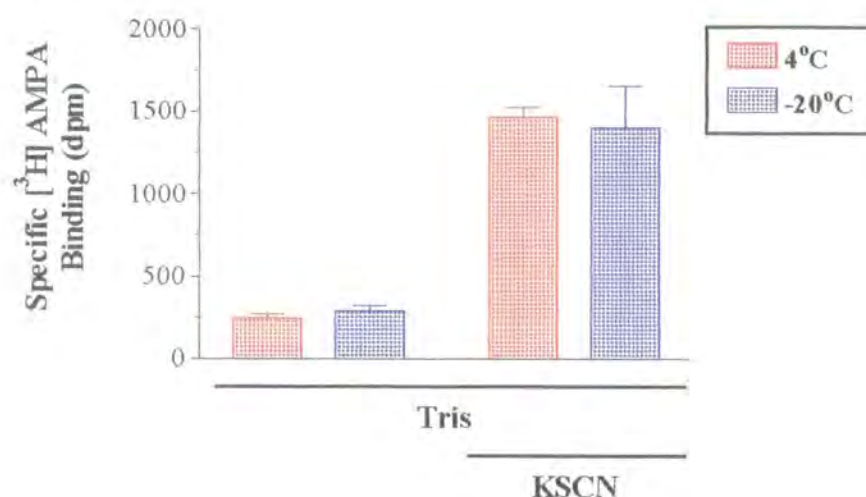
Figure 5.13 Specific binding in control forebrain membranes stored overnight at 4°C and at -20°C. The membranes were then incubated with 10 nM [^{3}H] AMPA for 60 minutes at 20°C. KSCN potentiated the binding seen with [^{3}H] AMPA. Storing the membrane overnight at 4°C did not significantly affect the amount of specific binding detected. Data obtained from the results of a single experiment, using membranes taken from 15 control forebrains.

As can be seen in figure 5.13, no difference was observed between the binding seen with the radioligand in control membranes stored overnight at 4°C and that seen with the control membranes stored overnight at −20°C. The KSCN potentiated the binding seen with the radioligand but, again, there was no difference between whether the membrane was stored at 4°C or whether it was stored at −20°C before use. This was repeated using more control forebrain membrane and a similar result was obtained.

Using this quick homogenisation protocol, control cerebellar membranes were prepared. This membrane was stored at 4°C whilst the protein concentration was determined, before being employed to perform a full dose-response analysis using varying concentrations of [^{3}H] AMPA in 100 mM tris-acetate, pH 7.4, with 50 mM KSCN and 1 mM glutamate (to determine non-specific binding).
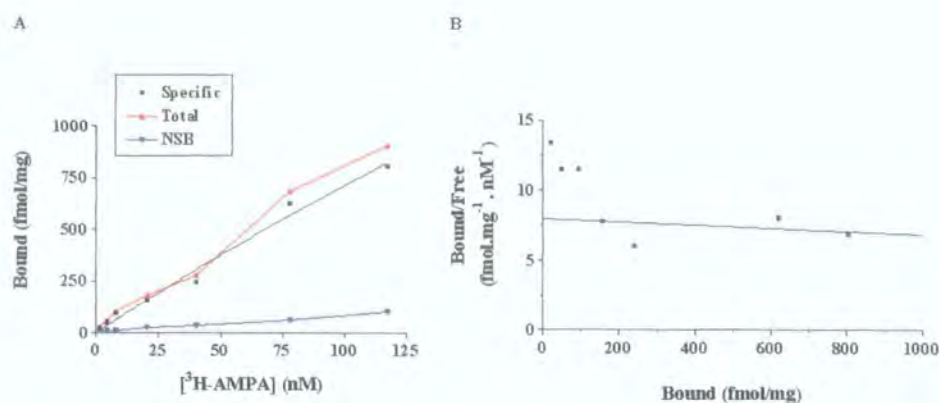
Figure 5.14 [³H] AMPA binding in control cerebellar membrane. (A) Binding isoform showing specific, non-specific and total binding of the radioligand in control cerebellar membrane. (B) Rosenthal transformation of the specific binding results. Data obtained from the results of a single experiment, using membranes taken from 12 control cerebella.

Prism was used to determine the values for B_{max} and K_D; B_{max} was calculated to be 6.9 pmol/mg protein whilst K_D was calculated to be 866.6 nM. The signal to noise ratio, that is specific binding to non-specific binding, was also calculated and this was determined to be 11.2 %. The data obtained was analysed using equations describing one and two binding sites for the (AMPA) receptor. An *F*-test was used to determine which equation fitted the data better and from this, it was calculated that the data fitted a one-binding site model.

However, due to the amount of tissue that was required for each Rosenthal transformation, it was not possible to repeat the previous experiment or to obtain data using stargazer cerebella.

5.2.4 Autoradiography

Due to the amount of tissue that was required in order to obtain data from radioligand binding studies, receptor autoradiography was employed. Autoradiography can also reveal the cellular distribution of the receptors in question whereas radioligand binding, with its use of brain membranes, cannot. In this respect, autoradiography is acting as a complementary assay to the radioligand-binding assay.

162

[^{3}H] AMPA was used for autoradiography on cryostat sectioned unfixed whole brains taken from control and stargazer mice (figure 5.15). Two control sections and two stargazer sections were mounted onto each polysine-coated slide and the slides were incubated in either the radioligand-containing buffer (tris-HCl containing KSCN and 20 nM [^{3}H] AMPA) or the non-specific binding buffer (ligand-containing buffer plus 1 mM glutamate). The slides were then exposed to [^{3}H]-hyperfilm for up to 10 weeks, as described in the methods (section 2.10).

An example of the results is presented in figure 5.15A, where [^{3}H] AMPA binding can be seen in the control brain. Binding is seen throughout the control brain, within structures including the cerebellum, the cortex, the caudate-putamen and the lateral septal nuclei. However, the maximum amount of binding was seen within the hippocampus. A similar binding pattern can be seen within the stargazer forebrain and cerebellum (figure 5.15E). Non-specific binding was insignificant, being at the level of film background in both control (figure 5.15C) and stargazer (figure 5.15G). All the major brain structures are present in the sections used for non-specific binding, as can be seen in figures 5.15D and 5.15H respectively, where the slides used were subsequently stained with toluidine blue.

The amount of radioligand bound was determined using the Scion Image software. The optical densities were determined for known standards, which were exposed to film for the same length of time as the radiolabelled sections. For each cerebellar section, three representative areas were selected and the mean intensity determined. The binding in the cerebellum appeared to be mainly in the molecular layer, with a small amount of binding apparent in the granule cell layer, and this was reflected in the areas chosen. The amount of [^{3}H] AMPA bound to the control and stargazer cerebellar sections could then be estimated.

Figure 5.15 [^{3}H] AMPA labelled adult whole brain sections as shown by autoradiography. Horizontal sections were cut from frozen, unfixed control (A-D) and stargazer brains (E-H). Control sections were incubated with either 10 nM [^{3}H] AMPA (A) or with the radioligand plus 1 mM glutamate (C), to show non-specific binding. The sections were subsequently stained with toluidine blue (B and D respectively).

Stargazer sections were also incubated with the radioligand (E) or the non-specific binding buffer (G) before being stained with toluidine blue (F and H) respectively.

The radiolabelled slides were exposed to [^{3}H] hyperfilm for a total of 8 weeks before the film was developed and the slides stained with toluidine blue.
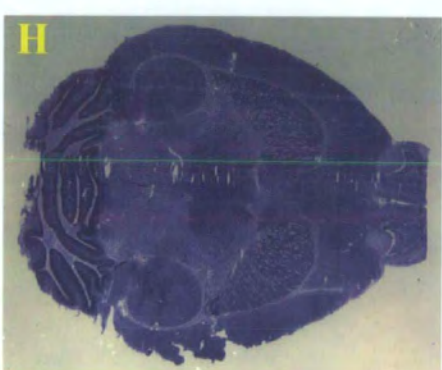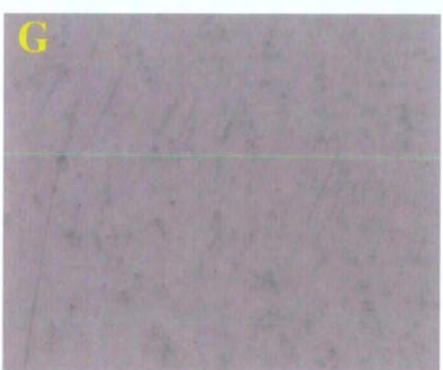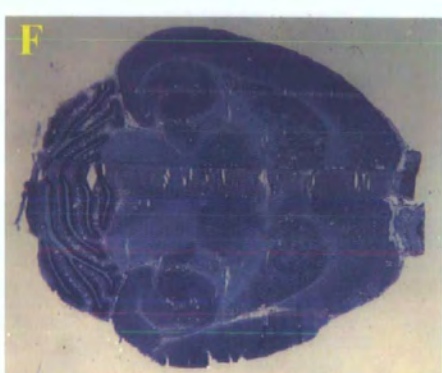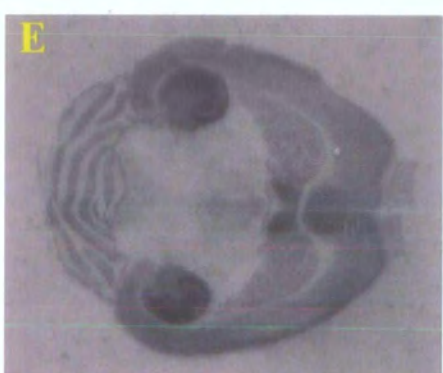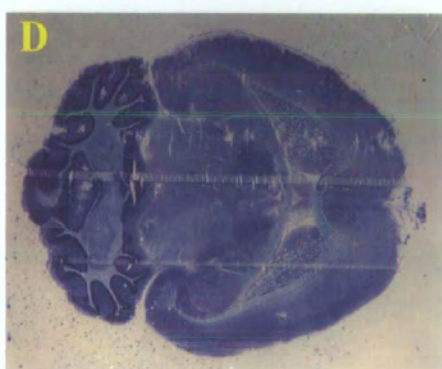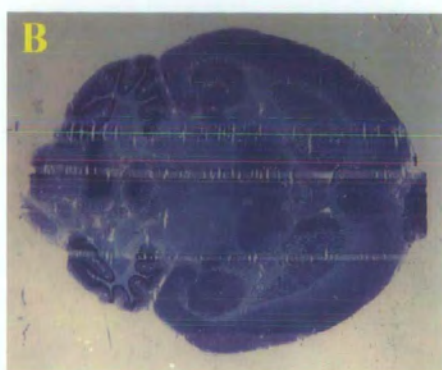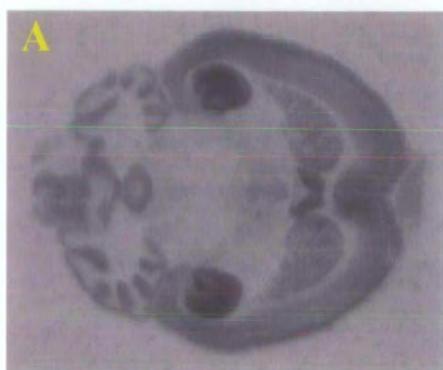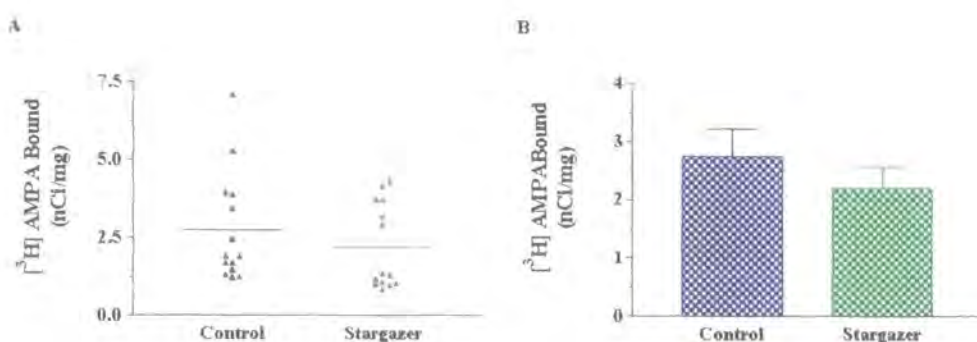
Figure 5.16 Quantification of [³H] AMPA bound to cerebellar sections as determined by autoradiography. Control and stargazer sections were incubated with 20 nM [³H] AMPA before being exposed to film for 8 weeks. (A) Amount of radioligand bound in each of the sections. All results are shown with the mean represented as a bar. (B) Radioligand bound shown as mean ± sem. n = triplicate measurements taken from 14 sections from 1 control and 1 stargazer mouse. No significant difference in binding between control and stargazer cerebellar sections was apparent, as determined using the Student's *t*-test (P > 0.05).

Figure 5.16 shows the results of densitometric analysis of [³H] AMPA autoradiography on control and stargazer cerebellar sections. The amount of radioligand bound to the control cerebellar sections was determined to be 2.40 ± 0.27 nCi/mg whilst the amount bound to stargazer cerebellar sections was 2.09 ± 0.24 nCi/mg.

Surprisingly, given the decrease in the subunit levels as determined by quantitative immunoblotting and as seen in figure 5.16, there was no significant difference in the amount of [³H] AMPA bound to the stargazer cerebellum when compared to the amount bound to the control cerebellum.

It has been suggested that synaptic AMPA receptors may be disrupted in hippocampal pyramidal cells of the stargazer mouse (Chen et al., 2000). If this is the case, then it is possible that there may be a difference in the binding of [³H] AMPA in the hippocampi of stargazer and control brains. Using the same autoradiographs as above and the Scion Image software, the amount of binding in both control and stargazer hippocampi was determined. In this instance, the binding in the whole hippocampus was measured.
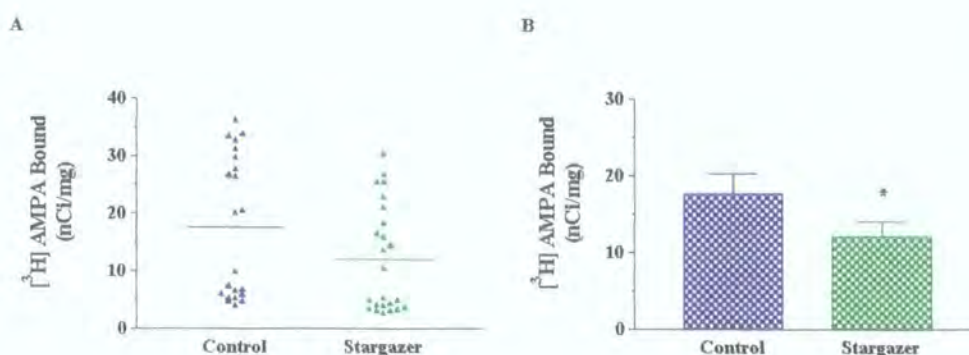
Figure 5.17 Level of [³H] AMPA bound in control and stargazer hippocampi. Control and stargazer brain sections were incubated with 20 nM [³H] AMPA before being exposed to film for 8 weeks. (A) Amount of radioligand bound in each hippocampus measured. All results are shown with the mean represented as a bar. (B) Radioligand bound shown as mean ± sem. Measurements taken from hippocampi in 14 sections from 1 control and 1 stargazer mouse brain. Binding was significantly reduced in stargazer hippocampi when compared to control hippocampi, as determined using the Student's *t*-test (* = P < 0.05).

Figure 5.17 shows the level of [³H] AMPA binding in control and stargazer hippocampi after exposing to film for 8 weeks. The level of binding in the control hippocampi was calculated to be 17.6 ± 2.6 nCi/mg whilst that of the stargazer hippocampi was calculated to be 12.1 ± 1.9 nCi/mg. A significant difference in the amount of [³H] AMPA binding was detected, with the binding observed in stargazer hippocampi being significantly decreased when compared to control hippocampi (P = 0.046), supporting the observation by Chen et al (2000).

5.3 Discussion

AMPAR subunit expression profiles were assessed in order to determine their levels in both control (+/+ and +/stg) and stargazer brain tissue. The anatomical distribution of the AMPAR subunits was shown to be the same in both control and stargazer brain sections, however, the intensity of immunostaining appeared to be decreased in stargazer. Analysis of cerebellar membranes by semi-quantitative immunoblotting revealed that expression of the AMPAR subunits GluR1–4 was significantly decreased in stargazer. Surprisingly, this did not correlate with assembled receptor expression as determined by autoradiography, where no significant difference was

167

observed between control and stargazer cerebella, however, a decrease in ligand binding was apparent in the hippocampus.

5.3.1 Regional distribution of AMPAR subunits is unchanged between control and stargazer mice

It was reported, during the course of these studies, that the stargazer cerebellar mossy fibre-granule cell synapse was devoid of AMPAR-mediated EPSCs, granule cells exhibited no AMPAR-mediated sEPSCs and that granule cells had a reduced sensitivity to AMPA (Chen et al., 2000; Hashimoto et al., 1999). However, expression of the AMPAR subunit mRNAs did not differ between control and stargazer, indicating the possibility of a defect in the expression of one or more AMPAR subunit proteins in stargazer cerebellum (Hashimoto et al., 1999). In order to determine if this was the case, the distributions of the four subunits were examined by immunohistochemistry.

Immunolabelling with the anti-GluR3 antibody revealed no apparent differences in the expression of the subunit between stargazer and control sections (section 5.2.1.3), which follows the expression of GluR3 mRNA (Sato et al., 1993; Boulter et al., 1990; Keinanen et al., 1990).

No significant differences were apparent in the distribution of GluR1 in stargazer and control sections. Specific staining was found in a number of forebrain regions; however, the strongest staining was evident in the cerebellum and the hippocampus (section 5.2.1.1). This is pattern of immunostaining was in accordance with that observed by others (Martin et al., 1998; Baude et al., 1994; Molnar et al., 1993; Martin et al., 1993; Rogers et al., 1991).

The distribution of the GluR2 subunit was the same in both stargazer and control brain sections (section 5.2.1.2). The distribution observed was comparable to published results (Petralia et al., 1997; Vissavajjhala et al., 1996). Similarly, the pattern of immunostaining was similar in both control and stargazer sections (section 5.2.1.4). Published results have shown that the GluR4 subunit is highly enriched in the cerebellum, a distribution which was also exhibited here (section 5.2.1.4)

168

(Ripellino et al., 1998; Bahr et al., 1996; Martin et al., 1993). However, GluR4 mRNA transcripts have been detected throughout the rat brain (Sato et al., 1993) and weak GluR4 immunoreactivity has also been exhibited in the rat forebrain (Bernard et al., 1997; Bahr et al., 1996; Baude et al., 1995; Martin et al., 1993). It is possible that the same cells were labelled here but were undetectable over the background staining.

Within the cerebellum, the levels of expression of both the GluR2 and GluR4 subunits were shown to be dramatically decreased in stargazer (figures 5.3 and 5.5 table 5.2). Few synaptic GluR4 puncta were detected in cultured stg/stg granule cells and in intact stargazer cerebellar glomeruli; electron microscopy also revealed that these synapses were devoid of GluR2/3 labelling (Chen et al., 2000). These results confirmed a decrease in immunolabelling of the GluR2 and GluR4 subunits in stargazer cerebella.

5.3.2 Decreased expression of AMPAR subunits in stargazer cerebellum

The GluR1, GluR2 and GluR4 subunits were all detected in the expected anatomical regions of control mouse cerebellum, as shown in section 5.2.1. These subunits were also shown to be located in the same cell types in stargazer cerebella; however, these qualitative immunohistochemical studies appeared to indicate a decreased expression of the GluR2 and GluR4 proteins. This was in contrast to Hashimoto et al. (1999), however, who reported that there were no differences in the level of expression of the GluR4 subunit between control and stargazer cerebellar membranes. In order to investigate whether the expressions of the GluR1, GluR2 and GluR4 subunits were indeed decreased, cerebellar membranes were analysed by semi-quantitative immunoblotting.

The levels of expression of GluR1 and GluR4 subunits were found to be slightly, yet significantly, decreased in stargazer cerebellar membranes (section 5.2.2.3). Levels of the GluR2 subunit were found to be dramatically reduced by 73 % in stargazer cerebellar membranes, when compared to the controls. This result confirmed the decrease observed by immunostaining (section 5.2.1).

Electrophysiological studies in various neuronal cell types and brain regions have identified the presence of a family of AMPARs with differing functional properties. Correlation of these properties with results obtained from subunit immunolabelling experiments and the PCR amplification of mRNAs has led to estimations of the subunit stoichiometry of these functionally distinct AMPAR subtypes. Homomeric native AMPARs have been shown to exist in the hippocampus (Wenthold et al., 1996) and in cortical neurons (Dai et al., 2001); however, the majority of native AMPARs are composed of heteromeric subunit combinations. In hippocampal neurons, functional receptors were found to be composed of GluR1 and GluR4 subunits (in non-pyramidal cells) and of GluR1 and GluR2 subunits (in CA1/CA2 neurons) (Bochet et al., 1994; Tsuzuki et al., 2000; Wenthold et al., 1996; Craig et al., 1993). However, a large number of receptor complexes were also found to consist of the GluR2 and/or GluR3 subunits only (Wenthold et al., 1996). Within the neurons of the subthalamic nucleus and the cortex, GluR1 was co-expressed with GluR2 and GluR2 was also found to be co-expressed with GluR4 (Dai et al., 2001; Tai et al., 2001).

Although no GluR1 was detected in the control granule cell layer, there was considerable overlap in the expression of the AMPAR subunits through out the cerebellum (table 5.1). The immunohistochemical studies undertaken here revealed the majority of GluR1 and GluR4 subunits to be expressed in the molecular layer (section 5.2.1). It is possible that these subunits were found in the same receptor complex and that a decrease in expression of one subunit would lead to a decrease in the expression of the other. Indeed, immunoprecipitation studies have shown these two subunits to interact in cerebellar membranes, although a fraction of GluR1 subunits did not bind to GluR4 (Ripellino et al., 1998).

It is possible, therefore, that the reduction in subunit expression observed here (section 5.2.2.3), could, therefore, be reflected in a decrease in the number of functional receptors.

5.3.3 The use of [³H] AMPA to determine changes in receptor expression

In order to determine whether AMPARs were altered in stargazer mice, brain sections were used for receptor autoradiography (section 5.2.4). Although only a single ligand concentration was used and so, full saturation analyses cannot be determined, it was possible to estimate whether there were differences in the binding of [³H] AMPA to its receptors.

No significant differences were apparent in the binding of [³H] AMPA to control and stargazer cerebella (figure 5.15). A decrease in binding would have been expected as the subunit proteins were shown to be significantly decreased in stargazer cerebellar membranes (section 5.2.2.3) and that functional AMPARs were also lacking in stargazer cerebella (Chen et al., 2000; Hashimoto et al., 1999). However, analysis of the autoradiographs indicated no significant decreases in binding (figure 5.16). It is possible that, since the majority of GluR2 subunits are intracellular (chapter 7; Hall et al., 1997; Hall and Soderling, 1997), that the numbers of surface expressed GluR2-containing receptors were only slightly decreased in stargazer cerebellum, thereby leading to the slight, yet insignificant, decrease in binding observed. However, it is not possible to determine the number of binding sites using this approach.

It is also possible that since a saturating dose of [³H] AMPA was not used, not all of the AMPA receptors were labelled. Indeed, if a higher dose were used, any differences in the binding of [³H] AMPA may have become more apparent and may reflect more accurately the levels of the AMPA receptor complexes within control and stargazer cerebella.

Since expression of the GABAR subunits were altered in stargazer hippocampus, as revealed by an increase in benzodiazepine-insensitive binding, hippocampal AMPARs were also examined. Surprisingly, analysis of hippocampal binding on the autoradiographs by the Scion Image software yielded a significant decrease in the amount of [³H] AMPA bound between control and stargazer sections (figure 5.17), indicating a possible decrease in AMPA receptor expression. This corresponded with

a slight decrease in [^{3}H] AMPA binding to stargazer hippocampi that was observed in the autoradiographs (figure 5.15).

The expression of the GluR2 subunit has been shown to be altered in a number of models of epilepsy. In kainate-induced status epilepticus, both GluR2 mRNA and protein levels were decreased in the CA3 of the hippocampus, with no change in GluR1 levels (Grooms et al., 2000; Friedman, 1998; Friedman et al., 1994). GluR2 knockdown by infusion of antisense oligodeoxynucleotides into the hippocampus of P13 rats, an age similar to when stargazer mice begin to show epileptic seizures, resulted in spontaneous seizure-like behaviour (Friedman and Veliskova, 1998). Amygdala-kindled animals show a selective decrease in GluR2 levels of 25 – 40 % in the piriform cortex and limbic forebrain (Prince et al., 1995) and an increase in the formation of GluR2-lacking AMPARs (Prince et al., 2000). In the γ-hydroxybutyrate model of absence epilepsy, a decrease in the expression of the GluR2 subunit was detected 72 hours after the induction of the seizures in crude brain cortex homogenates (Hu et al., 2001).

Interestingly, in the kainate-induced status epilepticus models, GluR2 was decreased in the CA3 and not the CA1. It is possible, therefore, that the decreased binding observed here with [^{3}H] AMPA could reflect a decrease in AMPARs in the CA3, an area that was shown to be lacking in the expression of stargazin protein (figure 6.4; (Sharp et al., 2001). Conversely, Hashimoto et al. (1999) found that AMPAR-mediated EPSCs were normal in stargazer CA1 pyramidal cells, an area where stargazin-like proteins were expressed in stargazer (figure 6.4; Sharp et al., 2001).

5.3.4 Conclusion

The anatomical distribution of the AMPAR subunits have been examined in both control (+/+ and +/stg) and stargazer mice, by immunohistochemistry. These studies revealed that the AMPAR subunits shared the same anatomical distribution, although expression was decreased in stargazer. Semi-quantitative immunoblotting using cerebellar membranes revealed significant decreases in the levels of expression of the GluR1, GluR4 and GluR2, with the largest decrease observed with the GluR2 subunit. Although autoradiography indicated a decrease in the binding of a single

concentration of [^{3}H] AMPA to cerebellar membranes, it was not significant. However, this same method revealed a significant decrease in binding in stargazer hippocampi.

It is possible that stargazin interacts with the AMPAR subunits and a lack of stargazin would lead to a decrease in AMPAR expression. This work was undertaken, the results of which are described in chapter 6. The level of GluR2 cell surface expression in cerebellar granule cells was determined and this is described further on in this thesis (chapter 7).

Stargazin expression and solubilisation
from mouse brains

6.1 Introduction
6.1.1 The *CACNG* genes

The stargazer mutation was identified as being on mouse chromosome 15 (Noebels et al., 1990). Later work by Letts et al. revealed the mutation to be an early transposon insertion into intron 2 of a novel gene termed *Cacng2* (Letts et al., 1998). This family of genes was later expanded to include *CACNG3*, *CACNG4*, *CACNG5* (Burgess et al., 1999), *CACNG6*, *CACNG7* and *CACNG8* (Chu et al., 2001). These genes were subsequently predicted to encode for a family of human, rat and mouse γ proteins, γ_2 (stargazin) – γ_8 (Chu et al., 2001; Green et al., 2001; Klugbauer et al., 2000; Black and Lennon, 1999).

6.1.2 mRNA distribution of the γ subunits

Stargazin (γ_2) mRNA was found to be expressed in adult mouse brain but not in heart, spleen, lung, liver, kidney, testis or skeletal muscle (which is where the γ_1 subunit is expressed) (Letts et al., 1998). *In situ* hybridisation studies revealed that stargazin mRNA was heavily expressed in the cerebellum, the CA3 and dentate gyrus of the hippocampus, the cerebral cortex, the thalamus, the nucleus accumbens and the olfactory bulbs (Chu et al., 2001; Green et al., 2001; Klugbauer et al., 2000; Letts et al., 1998).

γ_3 mRNA expression was observed mainly within the brain, with some expression within the testis. Within the brain, γ_3 mRNA was strongly detected within the hippocampus, the cerebral cortex, the amygdala, the putamen and the nucleus accumbens (Chu et al., 2001; Green et al., 2001; Klugbauer et al., 2000).

The distribution of the γ_4 mRNA was more widespread than that of the γ_2 and γ_3 mRNAs and included the brain, the heart, the lungs and the prostate. γ_4 showed a widespread distribution throughout the brain, with a high level of expression within the caudate-putamen and the olfactory bulb, with lower levels observed within the cerebellum, the thalamus and the hippocampus (Chu et al., 2001; Green et al., 2001; Klugbauer et al., 2000).

The mRNAs for γ_5 – γ_8 were all shown to be present with in the brain, as well as in other anatomical structures including skeletal muscle, liver, lungs and heart (Chu et al., 2001; Klugbauer et al., 2000).

6.1.3 The stargazin protein

The *Cacng2* gene was predicted to encode a membrane spanning protein (stargazin) which had 4 transmembrane domains and cytosolic amino and carboxy termini, and which shared low sequence similarity (~ 25 %) and a predicted secondary structure with the γ subunit of skeletal muscle voltage operated calcium channel (VOCC), γ_1. A synthetic peptide, CAA plus the stargazer C-terminal sequence DSLHANTANRRTTPV, was coupled to keyhole limpet hemocyanin and used to generate a rabbit anti-stargazin antibody. Using this antibody, stargazin was shown to be expressed in mouse brain synaptic plasma membranes and with a weight of 35-38 kDa (Letts et al., 1998).

HEK293 cells transfected with γ_2 cDNA and probed with an antibody raised against the human γ_2 subunit revealed a protein that migrated as a broad band between 33-38 kDa, and with a deglycosylated weight of approximately 26 kDa. Immunoblotting B6EiC3H mouse tissue showed the expression of the protein to be confined to the brain (Sharp et al., 2001).

γ_2 cDNA was also fused to the myc-epitope at its C-terminus, before transfecting into HEK293 cells. Immunoblotting with an anti-myc antibody revealed a protein with a weight of between 39 and 42 kDa (Klugbauer et al., 2000). Immunocytochemistry revealed the location of the protein to be at the cell surface (Green et al., 2001; Klugbauer et al., 2000).

Immunohistochemical localisation of the γ subunits revealed a high level of expression within the hippocampus, cortex and cerebellum and a moderate level of expression in the striatum, olfactory tubercle and amygdala. A lower level of expression was detected within the thalamus and brainstem. A decreased level of staining was observed throughout the stargazer brain, when compared to control brain (Sharp et al., 2001).

6.1.4 Proteins associating with stargazin

Because of its shared amino acid identity with the γ subunit of skeletal muscle VOCC (25 %) and a predicted secondary structure which resembled that of the γ_1 subunit, it was suggested that γ_2 was an auxiliary subunit of neuronal Ca^{2+} channels (Letts et al., 1998). Co-sedimentation and immunoprecipitation experiments have shown that γ_2 and γ_3 subunits bind to neuronal Ca^{2+} channel $\alpha_{1A/B}$, $\alpha_2\delta$ and β subunits (Kang et al., 2001; Sharp et al., 2001). However, immunofluorescence studies indicated that there was no direct interaction between the γ_2 and β_1 subunits (Rousset et al., 2001) and no difference in calcium channel function was observed between +/stg and stg/stg cultured cerebellar granule cells (Chen et al., 2000).

There is some evidence, however, to suggest that stargazin associates with the AMPAR subunits. Chen et al. (2000), using COS cells co-transfected with the various subunits and stargazin, were able to show that stargazin co-immunoprecipitated with GluR1, GluR2 and GluR4 but not with the NMDAR subunit NR1 or the potassium channel subunit Kv1.4. They were also able to show an interaction between stargazin and the PDZ-motif containing MAGUK proteins PSD-93, PSD-95, SAP-97 and SAP-102. Sharp et al. (2001) were also able to demonstrate the co-immunoprecipitation of stargazin with GluR1, but from mouse brain extracts.

6.1.5 Aims of this chapter

During the course of this work, the studies by Chen et al. (2000) and Sharp et al. (2001) were published. Although Chen et al. (2000) were able to show that granule cell synapses in stargazer were devoid of GluR2/3 and GluR4 labelling, and that

176

stargazin interacted with both of these subunits in transfected COS cells, they were unable to show an interaction between stargazin and the GluR subunits in brain extracts.

Sharp et al. (2001) were able to show that there was no stargazin protein in stargazer by immunoblotting and the distribution of stargazin by immunohistochemistry. Furthermore, immunoprecipitation studies using their anti-human stargazin antibodies, which also cross-reacted with other gamma isoforms, they were able to tentatively imply that GluR1 and stargazin co-associated in mouse brain.

Using the mouse peptide sequence as an immunogen, as outlined by Letts et al. (1998), we generated anti-stargazin antibodies. These antibodies were shown to be effective probes in both immunoblotting and immunohistochemical studies. Hence, they were used to characterise the expression of stargazin protein in both control and stargazer brain tissue. Control and stargazer forebrains were also solubilised and anti-stargazin antibody-specific immunoaffinity columns were prepared. The solubilised proteins were run down the columns, bound proteins eluted and probed, by immunoblotting, for the presence of the AMPAR subunits and the NMDAR subunit NR1, using solubilised stargazer forebrain proteins as a control.

6.2 Results

6.2.1 Preparation of anti-stargazin specific antibodies

A peptide corresponding to the C-terminus amino acid sequence of stargazin (amino acids 309 – 323, sequence DSLHANTANRRTTPV), which included an additional terminal cysteine residue for directional coupling to carrier and affinity purification column, was commercially synthesised. The cysteine-stargazin peptide was then coupled to thyroglobulin, using the MBS method, as outlined in section 2.3.2.1.

A New Zealand white rabbit was immunised with the thyroglobulin-coupled peptide and immune sera subsequently isolated, as described in section 2.3.3. The cysteine-coupled peptide was also used to prepare a Thiol-Sepharose peptide-affinity column

(section 2.3.5.2), which was used to purify the antibody from the sera taken from the immunised rabbit (as described in section 2.3.6).

6.2.2 Immunoblotting using the anti-stargazin antibody

The anti-stargazin antibodies were used to probe both control (+/+ and +/stg) and stargazer tissue (figure 6.1A). Forebrain (10 µg/10 µl) and cerebellar P2 synaptic membranes (10 µg/10 µl) were analysed by immunoblotting, as described in section 2.7.2. Immunoblots were probed with an optimised concentration of the anti-stargazin antibody, 1 µg/ml.

Three immunoreactive species were identified by the antibody in both the forebrain and cerebellum of control mice. These had molecular masses of 35-41 kDa ('stargazin-like'), 53 kDa (NS53) and 60 kDa (NS60), (figure 6.1A). The diffuse band at 35-41 kDa corresponds to stargazin and probably represents differentially glycosylated forms of the protein (Sharp et al., 2001; Letts et al., 1998). This immunoreactive species was not detected in either the forebrain or cerebellar membrane preparations derived from adult stargazer mice.

Immunoblots were subsequently reprobed with anti-β actin antibodies (1:500 dilution, figure 6.1B). In the control membranes, a signal corresponding to the actin protein was clearly evident. A similar robust immunopositive signal was obtained with the stargazer membranes, indicating that similar amounts of total membrane proteins had been loaded onto the gels. Note, however, that the actin immunopositive signal for the stargazer cerebellar membrane was stronger than that of the control cerebellar membrane, indicating an increased loading of stargazer cerebellar protein compared to control cerebellar protein.

The lack of an anti-stargazin signal in both the stargazer forebrain and cerebellar homogenates cannot, therefore, be explained by a lack of protein loading as an immunopositive signal to actin was detected. It is possible, however, that the full-length stargazin was either not translated or that it has an extremely rapid rate of turnover.

178

Figure 6.1: Immunoblot showing stargazin expression levels in forebrain and cerebellar membranes derived from control (+/+ and +/stg, ctl) and stargazer (stg). The membranes were probed with anti-stargazin antibody. The diffuse stargazin-like immunoreactive species (35-41 kDa) was clearly visible in both control forebrain and cerebellar membranes but not in those derived from stargazer mouse. The same membranes were then probed with anti-β-actin antibody (B). All four membrane preparations were found to be strongly immunopositive, indicating a proficient loading of membrane samples to the gels and efficient transfer.

A

84 —
52.2 —
36.3 —
30.2 —

ctl   stg   ctl   stg

FB   CB

← Stargazin

B

84 —
52.2 —
36.3 —
30.2 —

ctl   stg   ctl   stg

FB   CB

← Actin
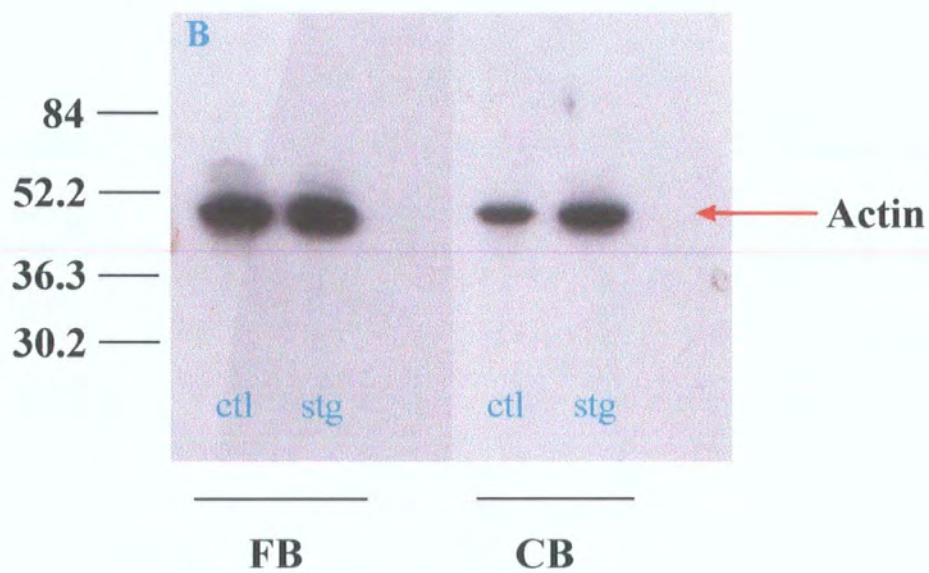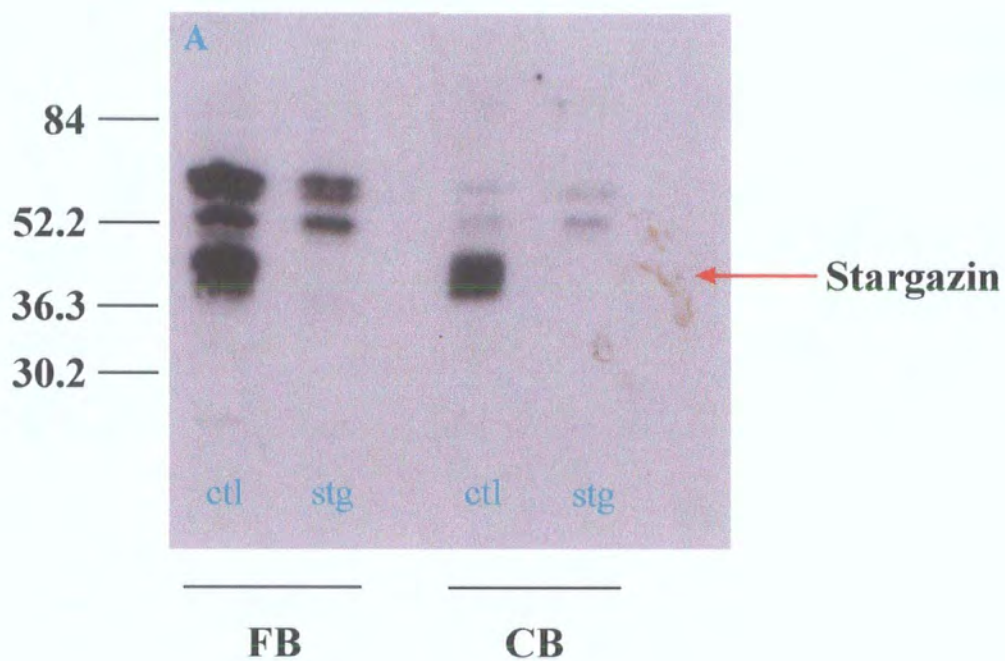
Figure 6.2 Immunoblot showing the specificity of the stargazin immunospecies in both control (ctl) and stargazer (stg) forebrain membranes in the presence or absence of the immunogenic peptide. The stargazin protein, along with minor bands at 53 kDa (NS53) and 60 kDa (NS60), were detected in the control forebrain. The stargazin signal was absent in the stargazer forebrain membranes although NS53 and NS60 were still visible. All the bands were absent when the antibody was pre-incubated with the peptide prior to application onto the control forebrain membrane. Refer to section 6.2.2 for concentrations of antibody and peptide used.

120 —

84 —

52.2 —

30.2 —

ctl   stg   ctl
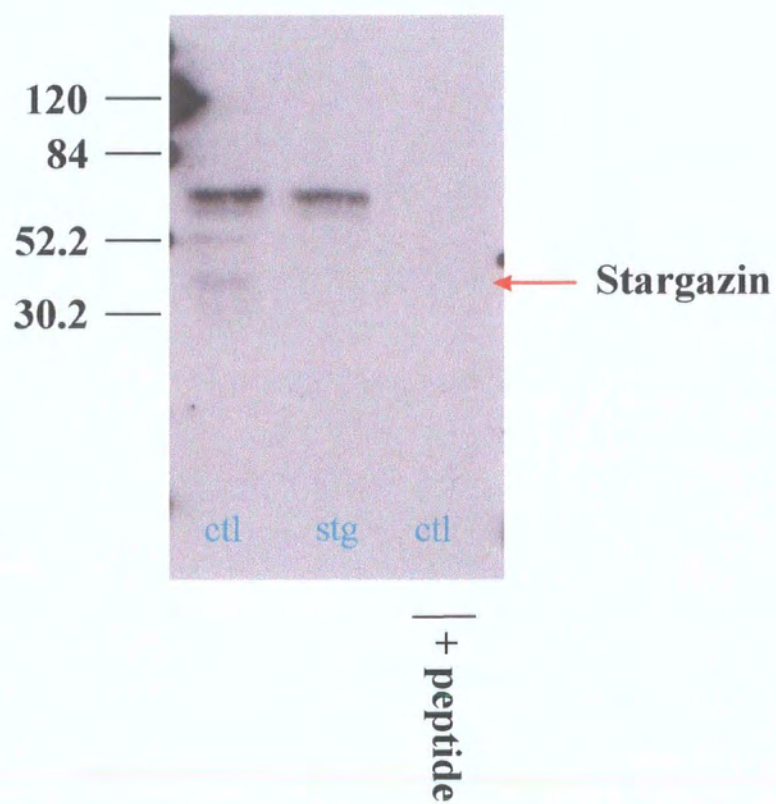
Stargazin

+ peptide

The specificity of the immunosignals obtained was tested by performing immunogen-blocking reactions. The anti-stargazin antibody was pre-incubated for a minimum of 1 hr at room temperature, with a saturating concentration of the peptide (1 μg/ml) to which the antibody was raised (peptide : anti-stargazin antibody molar ratio of ~ 100:1). This cocktail was then used to probe an immunoblot containing control synaptic membranes, as described in section 2.7.2.

As can be seen in figure 6.2, stargazin, NS53 and NS60 immunosignals were detected in control forebrain membranes whereas stargazin was not detected in stargazer forebrain. Control forebrain membrane was also probed with the peptide-blocked antibody. In this case, no stargazin immunosignal was observed nor were the NS53 and NS60 bands detected.

6.2.3 Immunohistochemical localisation of stargazin

Control and stargazer brain sections were incubated with 0.5 μg/ml anti-stargazin antibody in order to determine the immunohistochemical distribution of the stargazin protein. The method followed has been described earlier (section 2.12).

As can be seen in figures 6.3A and 6.3B, staining of cells is visible in all cell layers of cerebellar sections from control mice. Staining was observed within the granule cell layer and within the cell bodies (in the Purkinje cell layer) and dendrites of the Bergmann glia (in the molecular layer) (table 6.1).

The intensity of staining within stargazer cerebellum was decreased when compared to control cerebellum (figures 6.3C and 6.3D). Some staining was still evident in the granule cell layer, although it was not to the same extent as that observed in the control granule cell layer. The staining was almost completely absent from the Bergmann glia cell bodies in the Purkinje cell layers and processes within the molecular layer (table 6.1).

Immunostaining with the anti-stargazin antibody was also analysed within the forebrain of both control and stargazer mice (figure 6.4). Strong immunoreactive signals were observed in the various regions of the forebrain, including the

Figure 6.3 Immunohistochemical mapping of the distribution of stargazin within the cerebellum. Cerebellar sections were incubated with the anti-stargazin specific antibody before staining with DAB. Figures 6.3A and 6.3B show control sections, whilst a stargazer section is seen in figures 6.3C and 6.3D. Staining was clearly seen in the molecular layer (ML), the Bergmann glial bodies in the Purkinje Cell layer (PL) and granule cell layer (GL) of the control. No staining was seen within the white matter (WM) (figure 6.3B). The staining intensity was reduced in the granule cell layer of the stg cerebellum and appeared to be absent from the Purkinje Cell layer and molecular layer (figure 6.3D).

Scale bars represent 1 mm (A and C) or 100 µm (B and D).

A

B

PL   WM
ML   GL
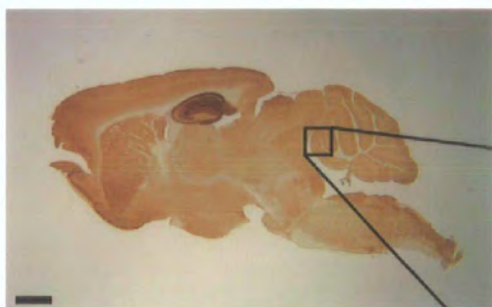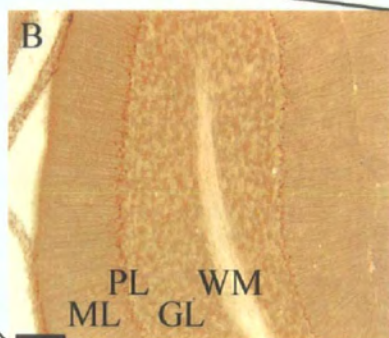
C

D

hippocampus, the striatum and the cortex (figure 6.4A). The hippocampal formation was very strongly labelled, with intense staining observed within the subiculum and the molecular layer of the dentate gyrus and the highest intensity of staining being within the CA1 region. (figure 6.4B and table 6.1).

Immunostaining was greatly reduced in stargazer forebrain (figure 6.4C). Whilst some staining was still evident, especially within the hippocampus and the cerebral cortex, it was essentially absent from the other regions of stargazer forebrain. The hippocampal subiculum and CA1 regions still expressed some staining with the anti-stargazin antibody, but it was much reduced when compared to control sections (figure 6.4D and table 6.1). As no stargazin protein is present in the brains of stargazer mice (section 6.2.2), it was likely that the staining present in the brain sections of stargazer mice was due to either cross-reactivity with unrelated proteins or that the antibody recognised other γ isoforms (Sharp et al., 2001).

Figure 6.4 Immunohistochemical mapping of the distribution of stargazin within the forebrain of adult control and stargazer mice. Sagittal sections were stained using the anti-stargazin antibody and DAB. Staining was observed throughout the control forebrain (A) but was most prominent within the regions of the hippocampal formation (B). Staining within the stargazer forebrain was much reduced, being seen essentially in the cerebral cortex and the hippocampus (C). Within the hippocampus, the highest levels of expression of stargazin-like proteins were in the CA1, with staining much reduced elsewhere.

Scale bars represent 1 mm.

A

B

CA1

DG

CA3
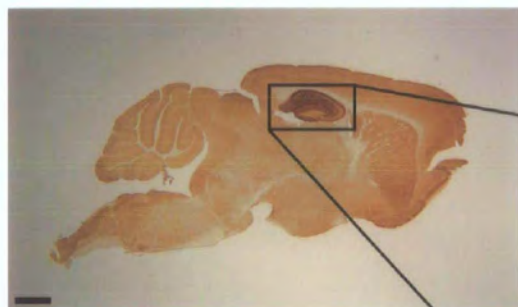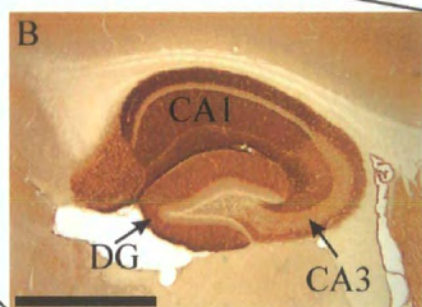
C
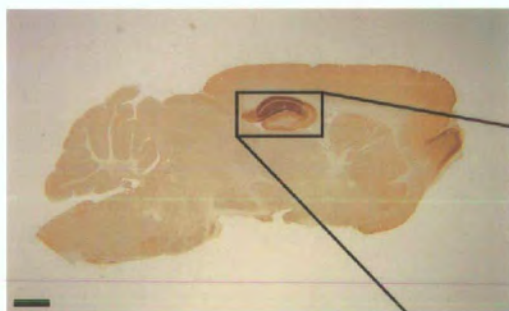
D

	Control	Stargazer	Stargazin-specific staining
Hippocampus			
Ammon's horn			
CA1	++++	+++	+
CA3	+++	++	+
Dentate Gyrus			
Molecular layer	+++	++	+
Granule cell layer	+/++	+/++	−
Polymorphic layer	−	−	−
Cortex	++/+++	+/++	+
Caudate-putamen	++/+++	−/+	++
Cerebellum			
Granule cell layer	+++	+	++
Purkinje cell layer			
Bergmann glia (cell body)	++++	−	+++
Purkinje cells	+	−	+
Molecular layer	++	−	++
Bergmann glia (processes)	+++	−	+++

Table 6.1 Relative expression level of anti-stargazin antibody immunoreactive species in control ('stargazin-competent') and stargazer ('stargazin-less') mouse brain sections. Levels were estimated by visual comparison of DAB stained sections. Comparisons of immunoreactive species in sections from both brains revealed the distribution of stargazin-specific staining. − = staining at background levels; + = low staining; ++ = moderate staining; +++ = high staining; ++++ = very high level of staining. n = 4 − 8 sections from 2 − 4 mice.

6.2.4 Immunoaffinity purification of stargazin and stargazin-associated protein complexes

Chen et al. (2000) revealed that stargazin interacted with a number of proteins including the AMPAR subunits GluR1, GluR2 and GluR4 and the PDZ proteins PSD-93, PSD-95 and SAP-102. However, these studies were conducted in COS cells as they were unable to co-immunoprecipitate the GluR proteins with stargazin from brain extracts.

Sharp et al. (2001) were able to solubilise stargazin from mouse forebrain using CHAPS. By immunoprecipitation, they were also able to show that stargazin associated with the GluR1 subunit as well as the α1B subunit of the N-type VOCC.

The following experiments were undertaken to independently investigate whether these interactions occurred *in vivo* and to assess the specificity of these interactions with stargazin. The conditions that would enable the solubilisation of stargazin from brain tissue were determined and then whether the AMPAR subunits interacted with stargazin. Stargazer tissue was used as a negative control; a control that Sharp et al. (2001) did not employ.

Two anti-stargazin-specific antibody immunoaffinity columns were prepared, as described in section 2.4.1. Sodium deoxycholate-solubilised forebrain membrane proteins from control (+/+ and +/stg) and stg/stg mice were prepared and applied separately to the immunoaffinity columns. Anti-stargazin antibody-bound proteins were subsequently eluted off the column, using a high pH buffer, as described in section 2.4.2. The eluted samples were then analysed by immunoblotting, using the anti-stargazin antibody, the anti-AMPAR subunit-specific antibodies and the anti-NR1 (NMDAR) antibody as probes.

6.2.4.1 Detection of stargazin in solubilised forebrain samples

Samples of the detergent-solubilised forebrain membranes, the pre-centrifugation fraction, the detergent-soluble fraction and the detergent-insoluble fraction, were all analysed by immunoblotting with the anti-stargazin antibody, to determine whether the stargazin protein could be solubilised from control forebrain fractions.

A sample of forebrain membrane was removed after the forebrain membrane homogenate was incubated with the sodium deoxycholate, this was termed the 'pre-centrifugation fraction 1'. The other two samples were taken after the solubilised forebrain membranes had been ultracentrifuged; the first sample was removed from the supernatant, 'soluble fraction 2', whilst the second was derived from the resuspended insoluble pellet, 'insoluble fraction 3'.

Figure 6.5 Immunoblot showing detection of stargazin in detergent-solubilised control and stargazer forebrain membrane extracts. Fractions were removed before centrifuging (mem) and from the supernatant (sol) and pellet (insol), after centrifuging.

Stargazin (red arrow) was expressed in the membrane (mem) and soluble (sol) fractions from control forebrain. No stargazin was expressed in either the stargazer membrane or soluble fractions, or in the insoluble pellets.

207 —

81 —

52.5 —

36.2 —

mem   sol   insol   mem   sol   insol

control   stargazer
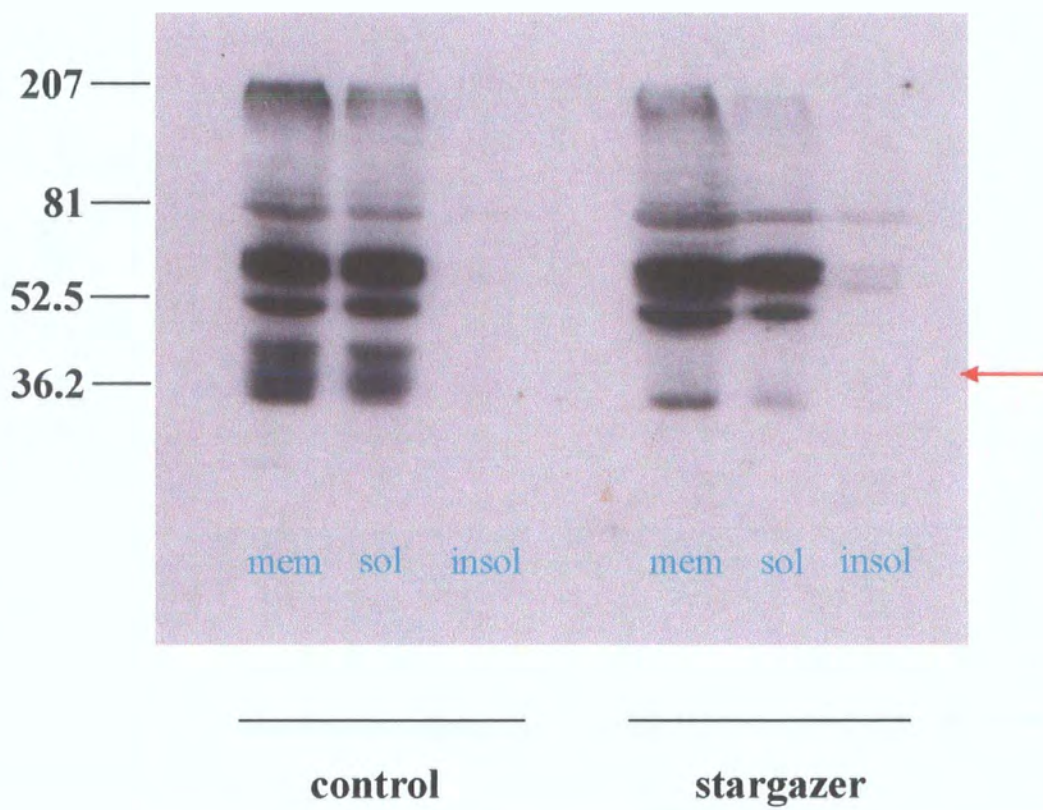
Proteins from all of the three samples were precipitated and analysed by immunoblotting. The proteins precipitated from fractions 1 and 2 were suspended in an equal volume of SDS-PAGE buffer whilst those from fraction 3 were suspended in 2 volumes of SDS-PAGE buffer. The suspended proteins were then probed by immunoblotting with 1 µg/ml anti-stargazin antibody.

The stargazin protein, NS53 protein and NS60 protein were detected in both fractions 1 and 2, that is, in the pre-centrifugation/post-sodium deoxycholate incubation sample and also in the soluble fraction. Stargazin was not detected in either the insoluble fraction from control forebrain or in the fractions from stargazer forebrain (figure 6.5).

6.2.4.2 Collection of eluted fractions

The solubilised protein preparations from control and stargazer forebrains were applied to separate anti-stargazin antibody-specific immunoaffinity columns by circulation, as described in section 2.4.2.3. Stargazin, and its interacting proteins, should bind with high affinity to the anti-stargazin antibody in the column and would, therefore, be immunopurified from the circulating soluble proteins. The stargazin and associated proteins were then eluted off the columns and the eluate was collected in 1 ml fractions. The proteins in these fractions were then precipitated, as described in section 2.6, and suspended in 0.5 volumes of SDS-PAGE buffer. The suspended proteins were loaded onto 10 % resolving gels and probed with 1 µg/ml stargazin antibody.

Figures 6.6A and 6.7 show the elution profile of stargazin from control forebrain fractions eluted off one anti-stargazin antibody immunoaffinity column. The anti-stargazin antibody detected a large band, corresponding to a weight of 35-41 kDa i.e. stargazin, in the control forebrain (positive control). This signal was absent in the stargazer forebrain membrane sample (figure 6.6A). The 35-41 kDa anti-stargazin antibody-specific immunopositive species corresponding to stargazin was, however, clearly present in the eluted fractions. The most intense signal was obtained with fraction 5, but fractions 4, 6 and 7 all gave robust signals, indicating that they

Figure 6.6 Expression of stargazin in fractions eluted off the anti-stargazin antibody immunoaffinity columns. Figure 6.6A shows the expression of stargazin from control forebrain homogenates whilst figure 6.6B shows that from stargazer forebrain homogenates. Also run on both gels were positive controls (control forebrain) and negative controls (stargazer forebrain). Stargazin was seen in fractions 4-7 from the control forebrain but not in the stargazer forebrain eluted fractions. The low weight band seen in fraction 4 (figure 6.6B) is not stargazin as the weight was lower than that of stargazin. It is more likely to be a lower band that is sometimes seen below the stargazin signal.
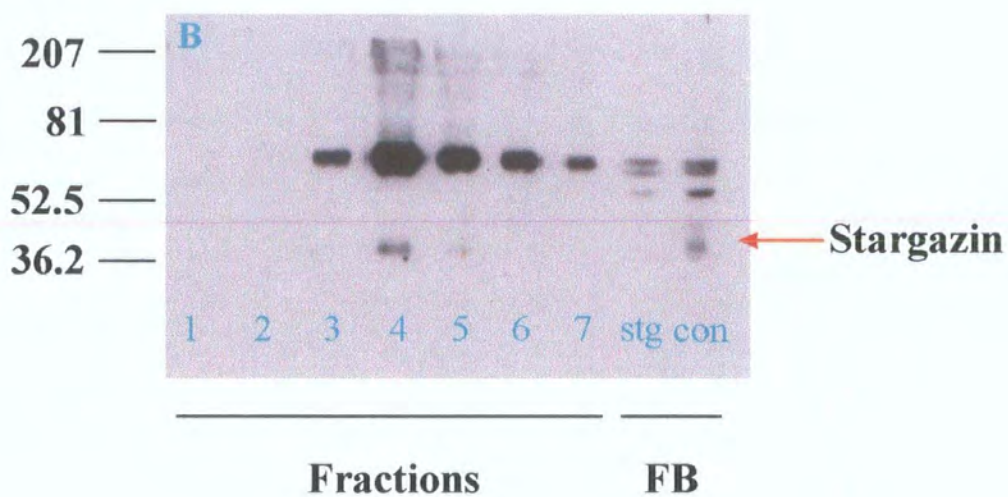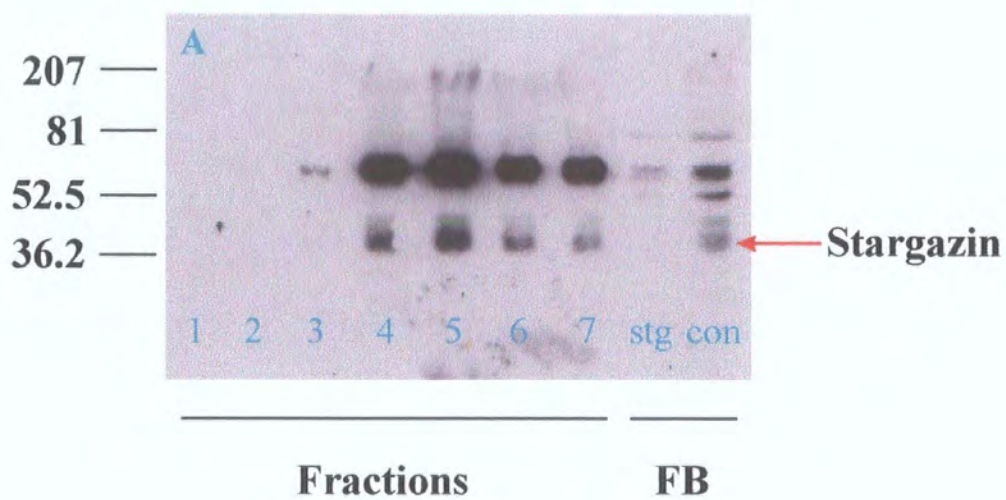
contained relatively large amounts of stargazin protein when compared to all the eluted fractions.
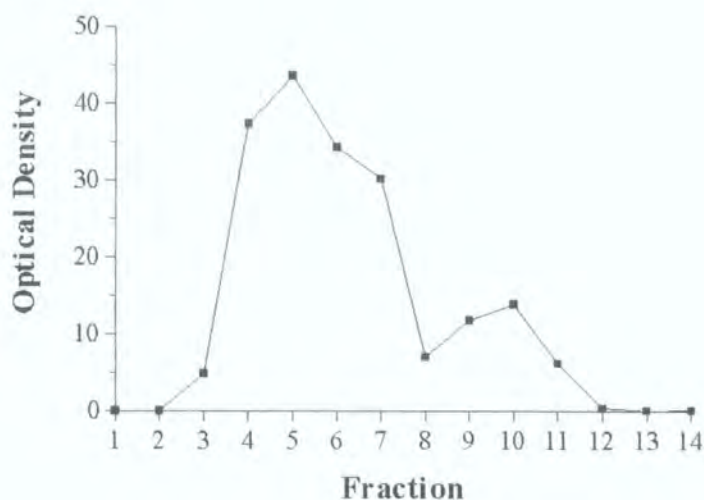
Figure 6.7 pH elution profile of stargazin (35-41 kDa) solubilised from control mouse forebrain, from the anti-stargazin antibody immunoaffinity column. Eluted fractions were collected; proteins were precipitated and probed following immunoblotting with the anti-stargazin-specific antibody. The films were then analysed using the GelDoc 2000 and BioRad Quantity One software. The optical densities were obtained and plotted against the eluate fraction number.

Figure 6.6B shows the pH profile from the second anti-stargazin antibody-specific immunoaffinity column, which had been loaded with detergent-solubilised forebrain fractions from stargazer mice. Fractions were eluted, immunoblotted and probed with the anti-stargazin antibody. The anti-stargazin antibody clearly detected stargazin protein at 35-41 kDa in the control forebrain membrane (positive control) whilst no stargazin was detected in the stargazer forebrain membrane (negative control). As expected, the eluted fractions from stargazer mice did not contain the 35-41 kDa stargazin protein, as the immunosignal associated with this protein was not detected with any of the eluted fractions. However, the NS60 immunospecies observed in both control and stargazer forebrain membranes was seen in all the eluted fractions. By obtaining the optical densities of the NS60 immunosignal in all the fractions, an elution curve was obtained (figure 6.8).
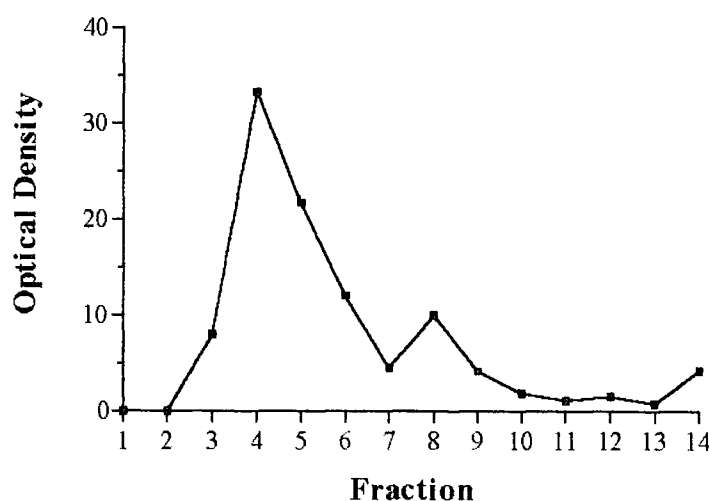
Figure 6.8 pH elution profile off the anti-stargazin antibody immunoaffinity column of the NS60 immunoreactive species solubilised from stargazer forebrain. Eluted fractions were immunoblotted and probed with the anti-stargazin antibody. Optical densities of the NS60 protein in each of the eluted fractions were obtained using BioRad Quantity One software. These were plotted in the graph above against the fraction number.

By referring to the immunoblots (figure 6.6) and the elution curves (figures 6.7 and 6.8), the fractions containing the highest amount of stargazin protein (35-41 kDa) or the NS60 protein, fractions 4 and 5, were pooled. The proteins were chloroform-methanol precipitated from the combined fractions, resuspended in SDS-Page sample buffer, immunoblotted and probed with a number of antibodies directed against candidate stargazin-associated proteins to establish whether these interactions occurred *in vivo*.

6.2.4.3 Stargazin is seen in the combined fractions

Initially, the combined eluted fractions were probed with the anti-stargazin antibody (1 μg/ml) in order to confirm that the signal observed in the individual fractions with the anti-stargazin antibody was still present when the fractions were pooled. This can be seen in figure 6.9, where both the combined eluted fractions and forebrain membranes were probed, on the same immunoblot, with the anti-stargazin antibody. The stargazin signal was observed in both the control forebrain (positive control) and the combined eluted fractions from the immunopurified solubilised protein from

Figure 6.9 Stargazin is present in combined eluted fractions. The fractions showing the highest amounts of protein were combined and then probed with the anti-stargazin antibody. The stargazin signal was still observed in the combined control (ctl) eluate fractions but not in the stargazer (stg) fractions. As a control, control (ctl) and stargazer (stg) forebrain membrane homogenates were also probed. As expected, the stargazin signal is only seen in the control forebrain.

118 —

81 —

52.5 —

36.2 —

29.9 —

ctl   stg   stg   ctl

← Stargazin

_____   _____

forebrain   combined
                   eluate
                   fractions
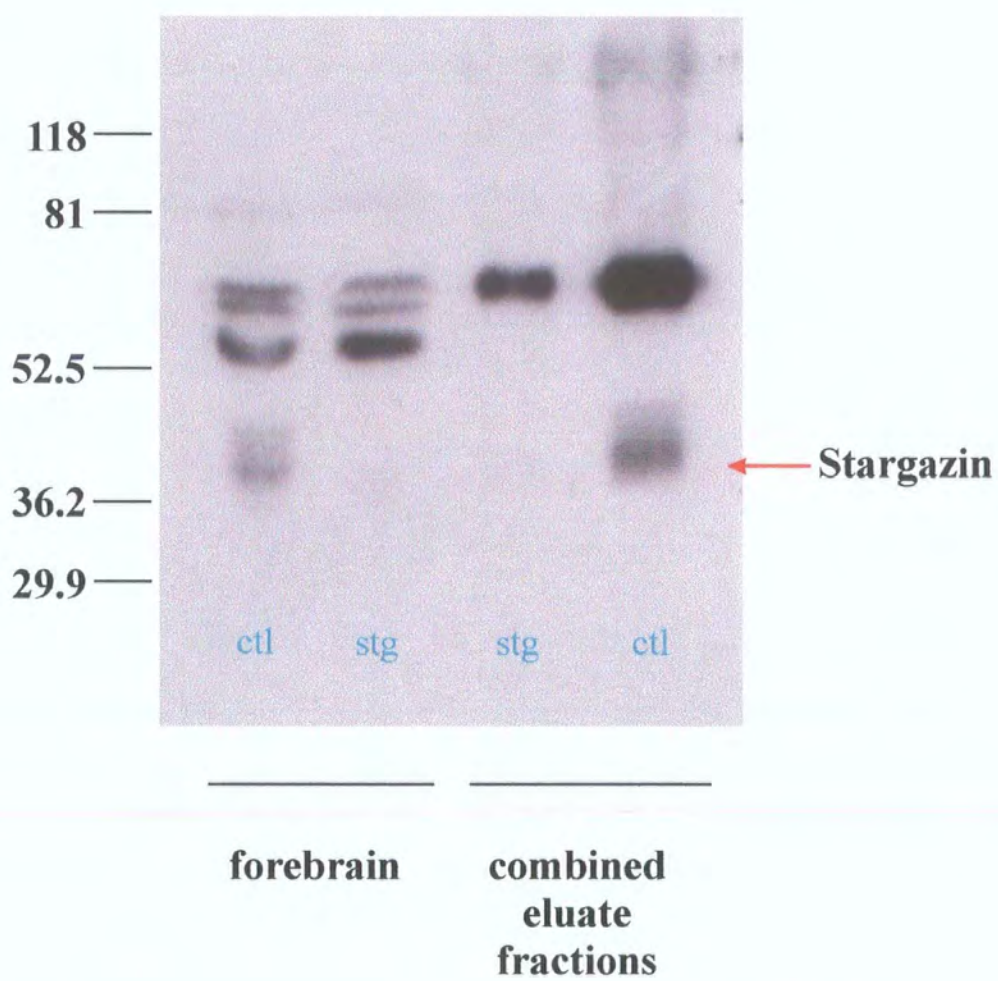
control forebrain. The 35-41 kDa, stargazin protein was not detected in either the stargazer forebrain or in the immunopurified soluble protein from stargazer forebrain. In these latter samples, only the NS53 and NS60 proteins were observed; species that were not stargazin based on the predicted molecular size (Sharp et al., 2001).

6.2.4.4 AMPAR subunits bind to co-elute with purified stargazin protein from control forebrain

The immunopurified stargazin protein from the solubilised control forebrain was analysed by immunoblotting using anti-AMPAR subunit-specific GluR1, GluR2, GluR3 and GluR4 antibodies as probes (figure 6.10). The GluR subunits all have a molecular weight of approximately 105 kDa. Cellular membranes from control mice were used as positive controls. Anti-GluR2 antibody was used at 200 ng/ml (figure 6.10A), anti-GluR3 antibody at 100 ng/ml (figure 6.10B), and anti-GluR4 antibody at 200 ng/ml (figure 6.10C).

It can be seen that the immunoreactive species at approximately 105 kDa were detected in all three cerebellar membrane samples. The GluR2 and GluR4 proteins were also detected in the purified stargazin samples but not the GluR3 protein. This would imply that whilst stargazin appeared to associate with the GluR2 and GluR4 subunits, it did not co-associate with the GluR3 subunit.

Purified proteins from solubilised control and stargazer forebrains eluted from the anti-stargazin immunoaffinity columns were probed with 0.5 µg/ml anti-GluR1 antibody (figure 6.10D). This time, however, 500 µl of the purified samples were precipitated and resuspended in 100 µl of SDS-PAGE sample buffer. Samples taken from the forebrain membrane, which were subsequently used for the purification i.e. pre-centrifugation fraction 1, were run along side the purified proteins as positive controls.

The stargazer and control forebrain membranes both showed an immunosignal at ~ 105 kDa, which corresponded to that of the GluR1 subunit. The purified proteins

Figure 6.10 Purification of stargazin complexes from control mouse brain. DOC-solubilised control forebrain membranes were applied to the anti-stargazin immunoaffinity column. Eluted column fractions were combined (P) and screened for AMPAR subunit expression. In all cases, cerebellar membranes (CB) were probed at the same time, on the same gel.

Combined fractions and cerebellar membranes were screened with anti-GluR2 antibody (A), anti-GluR3 antibody (B), anti-GluR4 antibody (C) or anti-GluR1 antibody (D). A signal was seen with the fractions probed with the GluR2 and GluR4 antibodies, but not the GluR3 antibody.

A signal was also seen with the GluR1 antibody in both fractions from DOC-solubilised control forebrains (ctl) and from DOC-solubilised stargazer forebrains (stg) (D). Here, the controls were stargazer forebrain (stg) and control forebrain (ctl) which both show a strong GluR1 signal.
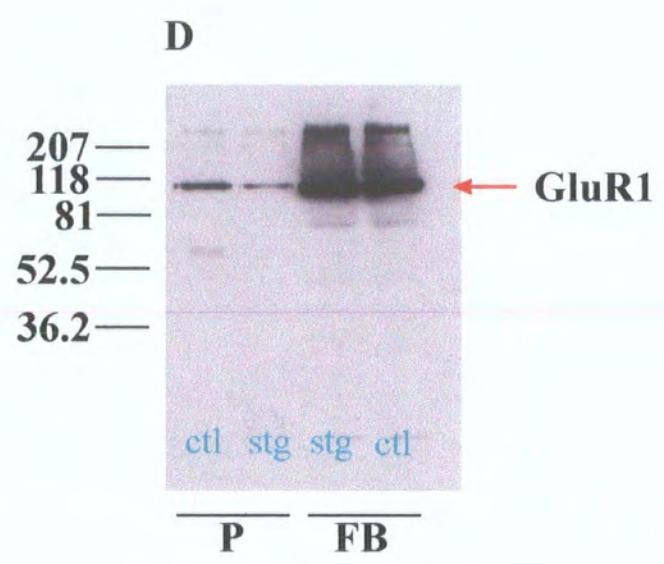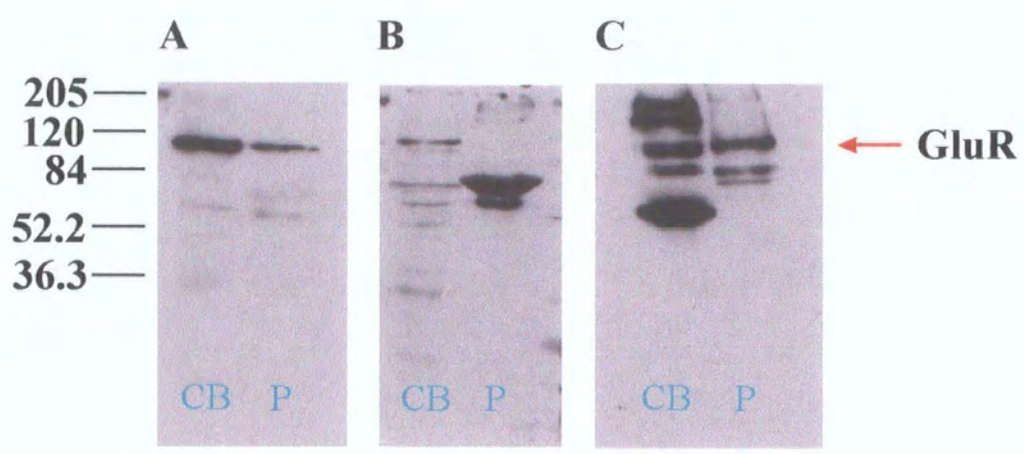
from the control forebrain also showed a band of the same size, indicating that stargazin interacted with the GluR1 subunit also.

A weak signal was also seen, however, with the anti-stargazin immunoaffinity column purified proteins obtained from stargazer forebrain. Since stargazer mice are effectively null mutants for stargazin, i.e. they do not express stargazin protein as shown previously (section 6.1 and figures 6.5 and 6.6), the GluR1 subunit must weakly interact with NS53 or NS60, which were co-purified with stargazin from control brain and purified in the absence of stargazin from stargazer tissue. These possibly represent other γ-subunit isoforms with which the anti-stargazin antibody cross-reacts.

A similar result was observed in figure 6.11, where the immunoaffinity purified proteins from both solubilised stargazer and control forebrains, were probed with 0.5 µg/ml anti-GluR1 antibody, 1 µg/ml anti-GluR2 antibody and 2 µg/ml anti-NR1 antibody. Control forebrain membranes were used as the positive controls.

The anti-GluR1 and anti-GluR2 antibodies detected weak bands at approximately 105 kDa in both the forebrain membranes and the control purified samples, indicating an interaction between stargazin and the GluR1 and GluR2 subunits (figures 6.11A and 6.11B respectively). The anti-NR1 antibody detected a protein at approximately 120 kDa, which corresponded to the NMDAR NR1 subunit. This protein was detected only in the forebrain membrane control (figure 6.11C), however, if the exposure time of the hyperfilm on the ECL-treated nitrocellulose was increased (to 5 minutes), NR1 was also detected in the purified proteins from both control and stargazer forebrains (figure 6.11D).

6.3 Discussion

An anti-mouse stargazin antibody was generated and characterised. This antibody was used to detect stargazin protein in cerebellar and forebrain membranes. Letts et al. (1998) had suggested that some stargazin mRNA was not prematurely transcriptionally arrested and thereby implied that some stargazin protein may be

Figure 6.11 Association of glutamate receptor subunits with stargazin. DOC-solubilised control (ctl) and stargazer (stg) forebrain extracts were applied to anti-stargazin immunoaffinity columns. Peak eluted fractions were combined and probed for GluR1 (A), GluR2 (B) or NR1 (C and D) immunoreactivity, with forebrain membranes from +/+ and +/stg mice as the control (FB).

The forebrain membranes showed strong signals with all antibodies. A signal was also seen when the eluted control fractions were probed with the AMPAR subunit specific antibodies. However, a signal in the eluted stargazer fractions was seen with these antibodies, indicating that the stargazin antibody is not specific.

Initially, no signal was detected in either the control or the stargazer fractions with the anti-NR1 antibody, indicating no direct association (C). However, when left to expose for longer (5 minutes), the NR1 species was detected in both fractions.

It is likely that the antibody is also picking out other γ proteins and that these proteins are binding to the subunits in the stargazer tissue (a tissue with no stargazin).
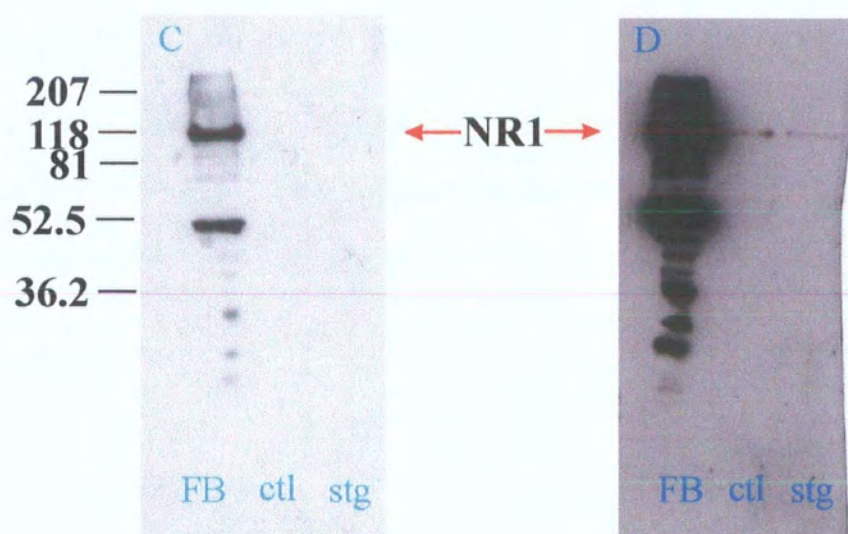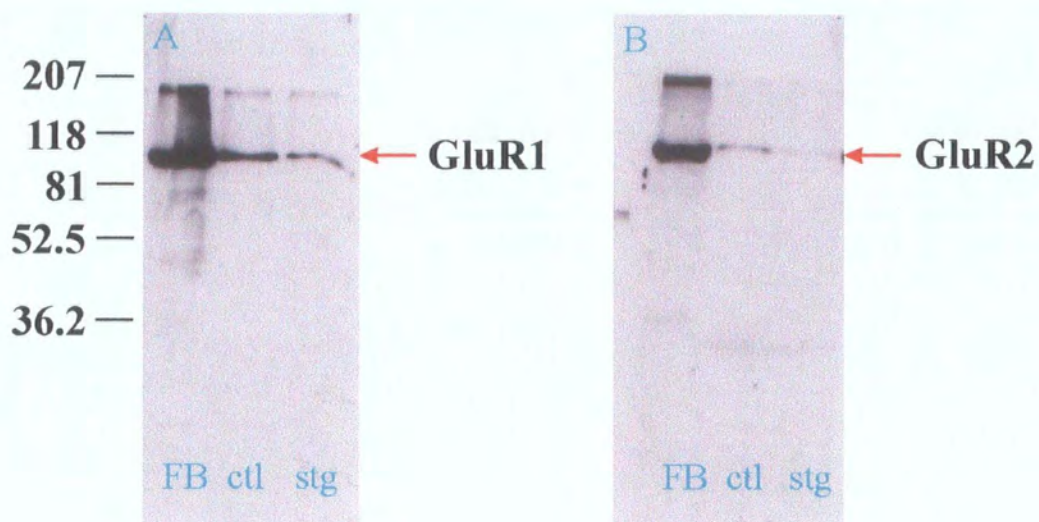
synthesised by stargazer mice. However, stargazin protein was not detected in either stargazer forebrain or stargazer cerebellar membranes in immunoblotting studies utilising the anti-stargazin antibody. These results revealed that stargazer mouse is a null mutant for stargazin protein.

The antibody was also employed in comparative immunohistochemical studies to identify the anatomical distribution of stargazin protein in control mouse brain. Finally, this antibody was used to generate anti-stargazin immunoaffinity purification columns to purify stargazin in order to begin to proteomically map the repertoire of proteins that associate with stargazin *in vivo*.

6.3.1 Distribution of stargazin and other γ isoforms

It was previously shown that stargazin mRNA was expressed in adult mouse brain but not in heart, spleen, lung, liver, kidney, testis or skeletal muscle (Letts et al., 1998). Similar observations were made in rat, except that low levels of stargazin mRNA were detected in the testes (Chu et al., 2001). The distribution of human γ_2 mRNA differs slightly from that in the mouse. Whilst the highest level of expression is seen in the brain, and in the cerebellum in particular, lower levels were expressed in the liver, testes, spinal cord, small intestine and stomach (Burgess et al., 2001; Green et al., 2001).

In mouse brain, *in situ* hybridisation studies revealed expression of stargazin mRNA in the cerebellum, the CA3 and dentate gyrus of the hippocampal formation, the cerebral cortex, the thalamus and the olfactory bulbs. Within the hippocampus, stargazin mRNA was found in the pyramidal cells whilst in the cerebellum, it was expressed in granule cells, Purkinje cells and in stellate cells (Chen et al., 2000; Klugbauer et al., 2000; Letts et al., 1998).

The immunohistochemical studies performed here revealed a broadly similar distribution of stargazin protein, with high levels of immunostaining in both the hippocampus and cerebellum, along with the striatum and cortex. In the hippocampus, stargazin-specific immunostaining was detected in the CA3 region and in the molecular layer of the dentate gyrus. Within the cerebellum, however,

206

stargazin immunoreactivity was heavily expressed within the granule cell layer and the Bergmann glia, not in Purkinje cells (section 6.2.3). These results were supported by the work of Sharp et al. (2001), who also reported a similar pattern of immunostaining within the mouse brain, using an anti-human γ_2 antibody.

As both stargazer cerebellar and forebrain membranes have been shown to be devoid of stargazin protein (section 6.2.2; Tiwari et al., 2001; Sharp et al., 2001), it was expected that no immunostaining would be visible in the stargazer brain sections. However, as can be seen in section 6.2.3, Sharp et al. (2001) and Ives et al (2003), some immunostaining was visible in the stargazer sections, although this was very much reduced when compared to the control sections. It is feasible that the other bands observed on immunoblots (NS53 and NS60, section 6.2.2) and the low level of immunostaining in stargazer brain sections were due to the anti-stargazin antibody detecting stargazin-like proteins.

So far, 8 isoforms of the γ subunit have been identified in mouse, rat and human tissue. Phylogenetic analyses of protein sequences have revealed that the γ isoforms can be divided into 3 main subfamilies. The γ_1 and γ_6 isoforms form one subfamily, γ_5 and γ_7 form another subfamily whilst the remaining subunits (γ_2, γ_3, γ_4 and γ_8) form a third subfamily, which can be further subdivided into two more subfamilies – {γ_2 and γ_3} and {γ_4 and γ_8} (Burgess et al., 2001; Chu et al., 2001; Klugbauer et al., 2000; Burgess et al., 1999).

Mouse γ_2 (stargazin) and γ_3/γ_4 share a high degree of amino acid similarity, particularly at their C-termini, and their mRNAs have been shown to occur in the same brain regions (Chu et al., 2001; Green et al., 2001; Chen et al., 2000; Klugbauer et al., 2000). It is possible that the immunostaining observed in stargazer brain sections was due to other isoforms being detected by antibodies. Indeed, immunoblotting with the anti-human antibodies detected both γ_3 and γ_4 proteins in the cerebral cortex, striatum and hippocampus, with only a small amount of γ_4 being detected in the cerebellum (Sharp et al., 2001). Therefore, whilst the decreased immunostaining apparent in the various regions of stargazer brain was due to the loss

207

of stargazin (γ_2) – specific immunostaining, the remaining immunostaining observed could be due to co-expression of γ_3 and γ_4 subunits.

6.3.2 Solubilisation of brain proteins

As the expression levels of AMPAR subunits were compromised in stargazer mice (section 5.2.2) and since stargazer is null for stargazin protein (section 6.2.2; Tiwari et al., 2001), it could be suggested that stargazin interacted with AMPAR subunits. Indeed, Chen et al. (2000) reported that stargazin associated with AMPAR subunits. Before any such association could be identified in brain extracts, it was necessary to solubilise proteins from brain tissue.

Sodium deoxycholate (DOC) was used to solubilise the cytoskeletal proteins from both control and stargazer forebrains (section 6.2.4), as the conditions used here are harsh enough to break the bonds anchoring the proteins to the plasma membrane but are not so harsh as to break the bonds between associating proteins. Sodium deoxycholate has been used in the past to solubilise a number of receptors and their associated proteins. For example, sodium deoxycholate was found to solubilise both NMDAR NR1 and NR2 subunits from rat forebrains and the interactions between the NR1 and NR2A or NR2B subunits were preserved (Blahos and Wenthold, 1996). DOC was also used on rat hippocampal membranes, where it was found that 70 % of NR1 subunits and 50 % of NR2A and NR2B subunits were solubilised. Similarly, PSD-95, SAP102 and SAP97 were also solubilised from the same tissue preparation. Immunoprecipitation experiments revealed that NR1 co-precipitated with NR2A, with NR2B and with PSD-95 and that both NR2A and NR2B co-immunoprecipitated with PSD-95 (Takagi et al., 2000). NR1 subunits were detected in DOC-solubilised rat thalamic and cerebellar membranes, whilst, as expected, NR2C subunits were found only in the solubilised cerebellar membranes. Immunoprecipitation by anti-NR2D antibodies revealed that NR1, NR2A and NR2B subunits co-associated with NR2D subunits in DOC-solubilised rat cortex and thalamus (Dunah et al., 1998).

AMPAR subunits have also been shown to be detected in DOC-solubilised membranes. Takagi et al. (2000) showed that ~ 85% of GluR2/3 subunits were expressed in DOC-solubilised rat hippocampal membranes. Immunoprecipitation

experiments utilising DOC-solubilised rat cortical membranes revealed that anti-GRIP antibodies co-associated with GluR1 and GluR2/3 subunits but not NR1 or PSD-95. Similarly, immunoprecipitation with anti-GluR2/3 antibodies revealed an association with GRIP and with GluR1 but not with either NR1 or PSD-95 (Wyszynski et al., 2002; Ye et al., 2000; Shen et al., 2000; Wyszynski et al., 1999). These data indicated that DOC-solublising strategies have been employed to solubilise AMPARs from brain tissue and that the protein-protein interactions were maintained.

However, DOC is not the only detergent to be successfully used in the solubilisation of proteins from cell membranes. Solubilisation of AMPAR subunits and their associating proteins has been undertaken using Triton X-100. GluR1 and SAP97 were solubilised from rat brain membranes and the interaction between them was confirmed by immunoprecipitation studies. SAP90 and SAP102 were more efficiently extracted using DOC whilst NR1 or NR2A/B subunits in rat brain membranes were found to be Triton X-100-insoluble (Colledge et al., 2000; Valtschanoff et al., 2000; Leonard et al., 1998; Blahos and Wenthold, 1996). Rubio and Wenthold (1999) reported that GluR1, GluR2/3 and, to a lesser extent, GluR4 could be immunoprecipitated from solubilised rat forebrains. The interactions between the GluR1 and GluR2/3 subunits were maintained, along with the interaction between the GluR4 and GluR2/3 subunits.

Whilst DOC was more effective than Triton X-100 in solublising NMDAR subunit-containing complexes from rat forebrain membranes, more NR1 and NR2A/B subunits were found in the soluble fraction if the membranes were solubilised with SDS, indicating that DOC was less able to extract all the NMDAR subunits bound to the membranes (Blahos and Wenthold, 1996). Immunoprecipitation studies employing SDS-solubilised rat brain membranes revealed that the interactions between NR1 and NR2B subunits, NR1 and NR2D subunits, NR1 and SAP102, NR2D and NR2A subunits, and NR2D and NR2B subunits were all preserved (Dunah et al., 1998; Leonard et al., 1998; Muller et al., 1996). However, no such interactions were observed in rat cortex, hippocampus or cerebellum even though each NMDAR subunit was solubilised from the three membranes (Suen et al., 1998).

Similarly, whilst GluR1 and GluR2/3 subunits were solubilised by SDS, the interactions between GluR1 and GluR2/3 subunits were disrupted, indicating that SDS dissociated the GluR subunits from each other (Leonard et al., 1998).

6.3.3 Identification of stargazin-associated proteins *in vivo*

Chen et al. (2000) were able to show that stargazin was able to co-immunoprecipitate GluR1, GluR2 and GluR4. Interactions between stargazin and the synaptic PDZ-containing proteins PSD-95, PSD-93, SAP97 and SAP102 were also observed. No such association was detected between stargazin and the NMDAR subunit NR1 or the potassium channel Kv1.4. This work, however, was undertaken using transfected COS cells. They were also able to show that stargazin was enriched in Triton X-100 insoluble brain postsynaptic density fractions, along with GluR4, NR1 and PSD-95.

Work presented here revealed the presence of stargazin in deoxycholate-solubilised control forebrain membranes (section 6.2.4.1). Unlike Chen et al. (2000), who were unable to co-immunoprecipitate stargazin with the AMPAR subunits from brain extracts, GluR1, GluR2 and GluR4 were all shown to co-immunoprecipitate with immunopurified stargazin protein, indicating that an interaction between stargazin and these AMPAR subunits did actually occur *in vivo*. No such interaction was detected with the GluR3 antibody (section 6.2.4.4).

Sharp et al. (2001) subsequently partly verified this observation. They, however, used CHAPS-solubilised forebrain membranes and found GluR1 to co-immunoprecipitate with stargazin. These authors did not confirm whether this interaction was specific for stargazin or not. In our hands, CHAPS proved to be ineffective in solubilising stargazin from forebrain as the majority of stargazin was found in the insoluble fraction (C.L. Thompson, personal communication).

However, when a separate anti-stargazin antibody immunoaffinity column was used to repeat this purification strategy using DOC-solubilised proteins from stargazer forebrains, weak immunoreactive signals were detected for the AMPAR subunits GluR1 and GluR2 (section 6.2.4.4). Since stargazer mice are 'stargazin-less', this was unexpected. However, the NS53 and NS60 immunoreactive species were still

210

observed in both solubilised membranes and eluates from this immunoaffinity column, when probed with the anti-stargazin antibody. It is possible that these proteins were interacting with the AMPAR proteins in the stargazer samples. The possibility that the anti-stargazin antibody was detecting other γ subunits, however, cannot be discounted, particularly as this antibody still gave some, albeit very weak, immunostaining of stargazer brain sections.

Surprisingly, these experiments, if pushed to their limits, also revealed NR1 in both control and stargazer forebrain membranes. It may be possible that this weak interaction in control membranes was due to the known interaction between stargazin and PSD-95, which is involved in the synaptic expression of the NMDAR subunits (Choi et al., 2002; Chetkovich et al., 2002; Chen et al., 2000; Kornau et al., 1995). As no stargazin protein was detected in stargazer brain membranes, this is unlikely to be the case with stargazer membranes. It is possible, however, that the other γ isoforms (the stargazin-like proteins) identified with this antibody could be interacting with the NR1 subunit.

6.3.4 Conclusion

Stargazer was shown to be a null mutant for stargazin as no stargazin protein was detected by immunoblotting in either stargazer forebrain or cerebellar membranes using the anti-mouse stargazin antibody. This antibody was then used to determine the regional and cellular distribution of stargazin in adult brains, and immunostaining was observed in the same regions of the brain as stargazin mRNA. However, whilst Sharp et al. (2001) detected stargazin protein in basket cell termini within the Purkinje cell layer, and Klugbauer et al. (2000) detected stargazin mRNA in Purkinje cells, immunostaining here was detected within the granule cell layer and Bergmann glia cell bodies and processes in the Purkinje cell layer and molecular layer respectively.

An immunoaffinity column was prepared with this antibody and GluR1, GluR2 and GluR4 were all shown to associate with stargazin *in vivo*. However, this antibody detected other proteins in both control and stargazer tissue by immunoblotting (NS53 and NS60 proteins) and detected other γ isoforms in brain sections in

211

immunohistochemical studies. It is possible, therefore, that this antibody is not specific for stargazin but may also detect γ_3 and γ_4 subunits. The generation of antibodies to other γ subunits, or to other sections of stargazin, may resolve this issue.

Stargazin has been reported to be involved in the trafficking of AMPARs to the cell surface (Chen et al., 2000). As stargazin, which is lacking in stargazer, was shown here to associate with AMPAR subunits and the AMPAR subunits GluR1, GluR2 and GluR4 have all been shown to be significantly decreased in stargazer cerebellar membranes (section 5.2.2), it is possible that these subunits are not trafficked to the cell surface, thereby having an increased turnover rate. In order to assess the validity of this hypothesis, initial studies looking at cell surface expression of the GluR2 subunit were undertaken, and these are described in chapter 7.

Surface expression of GluR2
in cultured cerebellar granule cells

7.1 Introduction

Stargazin has been shown to be co-associated with AMPARs *in vivo*, both here (section 6.2.4) and by others (Sharp et al., 2001; Chen et al., 2000). As stargazer is a null mutant for stargazin (section 6.2.2), it could be suggested that the decrease in stargazin would lead to a decrease in the expression of AMPAR subunits. Indeed, immunoblotting studies have shown differences in expression levels of the AMPAR subunits between control and stargazer cerebellum, with the largest decrease observed with the GluR2 subunit (section 5.2.2.2). This decrease in expression was confirmed using immunohistochemistry (section 5.2.1)

Receptor expression has been shown to be controlled at the level of individual synapses (Zhao et al., 1998; Rubio and Wenthold, 1997). A number of proteins have been shown to be involved in the trafficking of AMPARs to the cell surface, where the receptor complex is anchored by proteins such as glutamate receptor interacting protein (GRIP)/AMPA binding protein (ABP) (DeSouza et al., 2002; Burette et al., 2001; Wyszynski et al., 1999; Srivastava et al., 1998) and N-ethylmaleimide-sensitive factor (NSF) (Braithwaite et al., 2002; Luscher et al., 1999; Noel et al., 1999).

The proteins involved in the trafficking of AMPARs to the cell surface are described below, along with methods of measuring receptor levels at the cell surface.

7.1.1 Proteins involved in the trafficking of AMPARs to the cell surface

GluR1 subunits have been shown to associate with SAP97 (synapse associated protein 97) in the dendritic cytoplasm and somata of cultured neurons but not at the

synapse or with internalised GluR1 subunits. This led to the suggestion that SAP97 associated with the AMPAR before the SAP97-receptor complex was delivered to the cell surface, where SAP97 then dissociated from the AMPAR (Sans et al., 2001, Valtschanoff et al., 2000).

SAP97 itself is a PDZ-rich protein which is homologous to PSD-95 (Leonard et al., 1998). Whilst PSD-95 was shown to bind to NMDA subunits and Shaker-type K^+ channels (Kornau et al., 1995; Kim et al., 1995), it was thought that PSD-95 was not able to interact with AMPAR subunits. However, in hippocampal neurons over-expressing PSD-95, an increased GluR1 immunofluorescence was observed and the amplitude and frequencies of AMPAR-mediated mEPSCs were augmented, indicating that these receptors were functional (El-Husseini et al., 2000).

During the course of this PhD, a number of papers were published reporting an interaction between stargazin and PSD-95 (Schnell et al., 2002; El-Husseini Ael et al., 2002; Chetkovich et al., 2002; Choi et al., 2002; Chen et al., 2000). Stargazin was also associated with AMPAR subunits (section 6.2.4.4; Sharp et al., 2001; Chen et al., 2000) and the disruption of binding between stargazin and PSD-95 lead to a lack of AMPAR synaptic clustering and a decrease in mEPSCs. These data all indicate that PSD-95 (and other MAGUKs such as SAP102) indirectly associate with synaptic AMPARs through an interaction with stargazin.

7.1.2 Determination of the level of cell surface expression of receptor subunits

It is possible that, since stargazin has been reported to be involved in the trafficking of AMPARs to the cell surface, the surface expression of the receptor is compromised. A number of methods to determine the levels of both NMDAR and AMPAR subunit expression at the cell surface have been described.

Hall and Soderling (1997) used both chymotrypsin, which cleaved surface-expressed proteins, and bis (sulfosuccinimidyl) suberate (BS^3), which cross-linked surface-expressed proteins, to determine the surface expression levels of the NMDAR subunits NR1 and NR2B. Using both treatments, the authors calculated that

40 – 50 % of NR1 subunits and > 90 % of NR2B subunits were expressed at the cell surface (Hall and Soderling, 1997a). Chymotrypsin was also used to show the level of surface expression of NMDAR subunits was enhanced following incubation with NMDAR antagonists (Crump et al., 2001). BS^3 was also used to estimate the level of surface expression of GluR1 + GluR2 subunits and GluR2 + GluR4 subunits in transfected cells. In both cases, BS^3 reduced the total subunit population by 25 – 40 % (Hall et al., 1997).

NHS-ss-biotin (sulfosuccinimidyl 2-(biotinamido)ethyl-1,3-dithiopropionate) has also been used to determine the surface expression of receptor subunits. Cell-surface biotinylation of transfected HEK-293 cells revealed that whilst the NR1 subunit was located at plasma membrane in the presence and absence of NR2A subunits, the NR2A subunit was only trafficked to the cell surface in the presence of NR1 (Garcia-Gallo et al., 2001). Biotinylation was used to estimate the amount of $[^3H]$ AMPA binding sites expressed in both transfected BHK-570 cells (Hall et al., 1997) and in cultured hippocampal neurons (Hall and Soderling, 1997b). In the latter, 52 % of total $[^3H]$ AMPA were detected at the cell surface whilst in the former, ~ 30 – 40 % of total binding site population was detected, both of which provided an estimate of the surface expression of GluR1-3 subunits.

7.1.3 Work undertaken in this chapter

It was necessary to evaluate whether a compromised stargazin expression affected the cell surface expression of AMPAR subunits. It is not possible to study this using fixed slices or membrane preparations, as a dynamic system is required. In order to determine the level of surface expression, cerebellar granule cells were cultured from age-matched, littermate neonatal control (+/+ and +/stg) and stg/stg mice. These mice had been identified by genotyping using the genomic DNA amplification system used earlier (section 3.2.1) to identify breeding pairs. Cultured granule cells were then treated with the membrane impermeant, cross-linking agent BS^3 and the level of expression of the GluR2 subunit in both control and stg/stg granule cells was determined.

7.2 Results

7.2.1 PCR of neonatal DNA

The PCR amplification strategy used to identify adult heterozygous mice required for breeding purposes was also used to identify the genotype of P3 neonatal mice. It is necessary to determine whether a neonatal mouse is +/+, +/stg or stg/stg as neonates are used for culturing purposes at P5-6 whereas the phenotype does not begin to be expressed until P14.

Genomic DNA was obtained from tail biopsies, as outlined in section 2.13.1, from each of the (P3) neonatal mice born to +/stg parents. Individual mice were tagged in order to be identified later. The genomic DNA was then amplified using the PCR amplification strategy and the PCR products separated on an agarose gel and visualised in the BioRad GelDoc 2000 System, as described in section 2.13.2.

As can be seen in figure 7.1, a single PCR product of 600bp was amplified from +/+ mice, a 300 bp PCR product amplified from stg/stg mice and both 300 bp and 600 bp PCR products from +/stg mice. In addition, an 800 bp product was observed in +/stg mice only, which was not investigated further but probably represents a hybrid of the 300 bp/600 bp products.

7.2.2 Cerebellar granule cell cultures

Cerebellar granule cells (CGCs) from +/+ mice and +/stg mice were cultured together (control cells) whilst those from stg/stg mice were cultured separately but at the same time as the control cerebellar granule cells. Cells from +/+ and +/stg mice were cultured together as controls as no significant differences in any parameters investigated had been observed. All mice used were from the same litter and were age-matched/littermate matched mice. The method used for the culturing of the cells was as described in section 2.14.

Granule cells were removed from the cerebella when the mice were at age P5-6 and allowed to remain in the dish until they reached DIV 11. The cells were cultured in 5 mM K^+ containing media and followed a developmental pathway expected of cerebellar granule cells in culture (Ives et al., 2002a). The stg/stg granule cells

216

Figure 7.1 Agarose gel analysis of amplicons obtained from a genomic PCR amplification of mouse tail biopsy obtained from littermate offspring of +/stg parents, using UV light following ethidium bromide staining. A 100 base pair marker is in lane M, and the 300 base pair, 600 base pair and 800 base pair products indicated. The low molecular weight band identified by the red arrow was due to excess PCR primers. Lanes 1-10 are products from 10 neonatal mice. Positive controls (lanes 11-13) are from mice of known genetic background; negative controls are in lane 14. The key below indicates whether the sample comes from a +/+, +/stg or stg/stg mouse:

Sample	Genotype	Sample	Genotype
1	+/stg	6	stg/stg
2	+/+	7	+/+
3	stg/stg	8	+/+
4	+/stg	9	+/stg
5	stg/stg	10	+/stg

Sample	Control	
11	Positive	DNA from known stg/stg
12	Positive	DNA from known +/stg
13	Positive	DNA from known +/+
14	Negative	No DNA

800 →
600 →

300 →

M 1 2 3 4 5 6 7 8 9 10 11 12 13 14
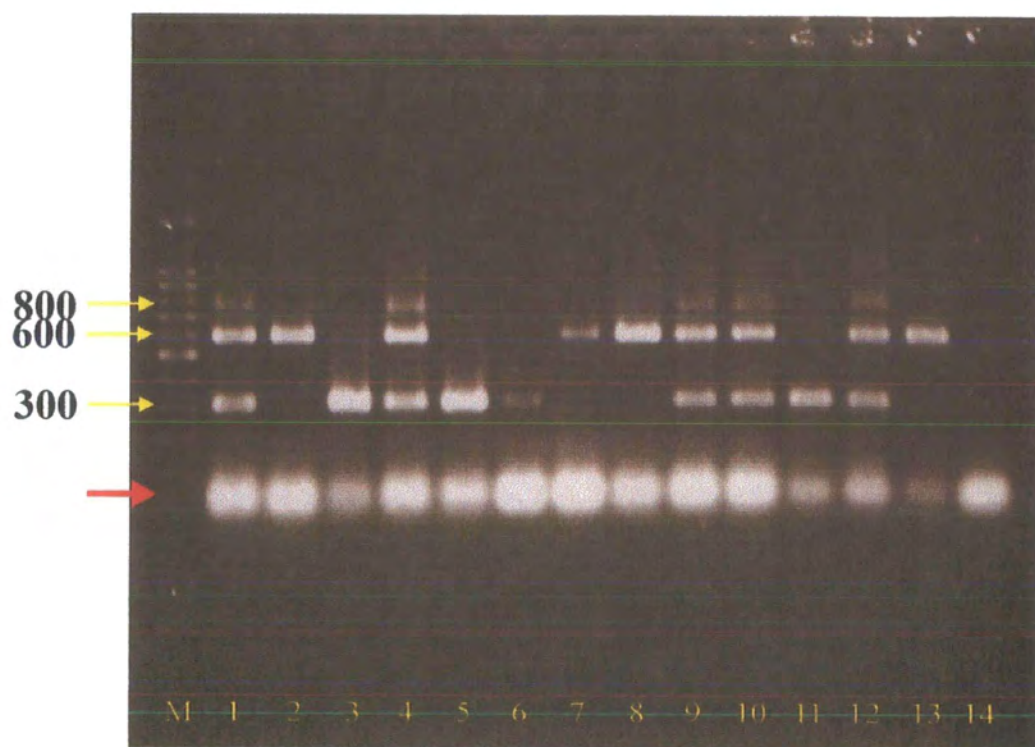
Samples   **Controls**

survived equally well as control granule cells; the stg/stg cells migrated and clustered and extended processes.

7.2.2.1 GluR2 expression in CGCs

Cerebellar granule cells were cultured from both control (+/+ and +/stg) and stargazer mice (stg/stg). The cells were cultured for 11 DIV, at which point the cells were collected for quantitative immunoblotting.

The media were removed from the petri dishes and the cells washed three times with PBS, 37°C. Solubilising buffer, comprising of 50 mM tris, 2 mM EDTA, pH 6.8, 2 % (w/v) SDS, 0.5 ml, warmed to 37°C, was then added to each dish and the cells scraped off. The lysate was then triturated, using a syringe and needle, before heating at 95°C for 5 minutes, flash freezing in liquid N_2 and stored at –20°C until required. The lysates were then rapidly defrosted and the proteins chloroform-methanol precipitated in the same manner as brain homogenates (section 2.6).

Figure 7.2 shows the relative expression level of GluR2 and actin in cultured control and stargazer granule cells. A single band with a molecular weight of 105 kDa, corresponding to the GluR2 protein was seen in both control and stargazer CGCs as well as in both control and stargazer membranes. The immunoblot was also probed for the expression of actin protein, which is the lower band marked on the figure.

As CGCs were probed for GluR2 immunoreactivity and subsequently for actin immunoreactivity, the levels of expression (in both control and stargazer CGCs) could be determined by computer-assisted densitometry. The optical densities of the subunit signals were measured and adjusted using the optical densities obtained from the actin signals. The results obtained from the stargazer CGCs were normalised to those obtained from control CGCs, as described in section 2.7.3.

Figure 7.2 GluR2 and actin expression in cultured control (+/+ and +/stg) and stargazer cerebellar granule cells, as determined by immunoblotting. Proteins of a range of concentrations (2.5 μg/10 μl, 5 μg/10 μl and 10 μl/10 μg) were obtained from control (+/+ and +/stg) and stargazer (stg/stg) cerebellar granule cells, before being probed with anti-GluR2 and anti-β-actin antibodies.

The immunoreactive species recognised by the anti-GluR2 antibody has a molecular weight of ~105 kDa, in accordance with the predicted weight of GluR2. The immunoreactive species recognised by the anti-β-actin antibody has a molecular weight of 45 kDa, in accordance with its predicted weight. As can be seen, the GluR2 protein is present in both the control and stargazer cerebellar granule cell, although it is much reduced in the stg/stg cells.

Also shown on the immunoblot are the positive controls (10 μg/10 μl) – adult control (+/+ and +/stg, ctl) and stargazer (stg) cerebellar membranes.

Broad range (21 kDa – 205 kDa) molecular weight markers were used and have been indicated to the left of the immunoblot.

| 205 — |
| 113 — |
| 75 — |

GluR2

| 53.9 — |

Actin

| 34.8 — |
| 28.8 — |

ctl   stg   10   5   2.5   10   5   2.5

CB   Cerebellar Granule Cells
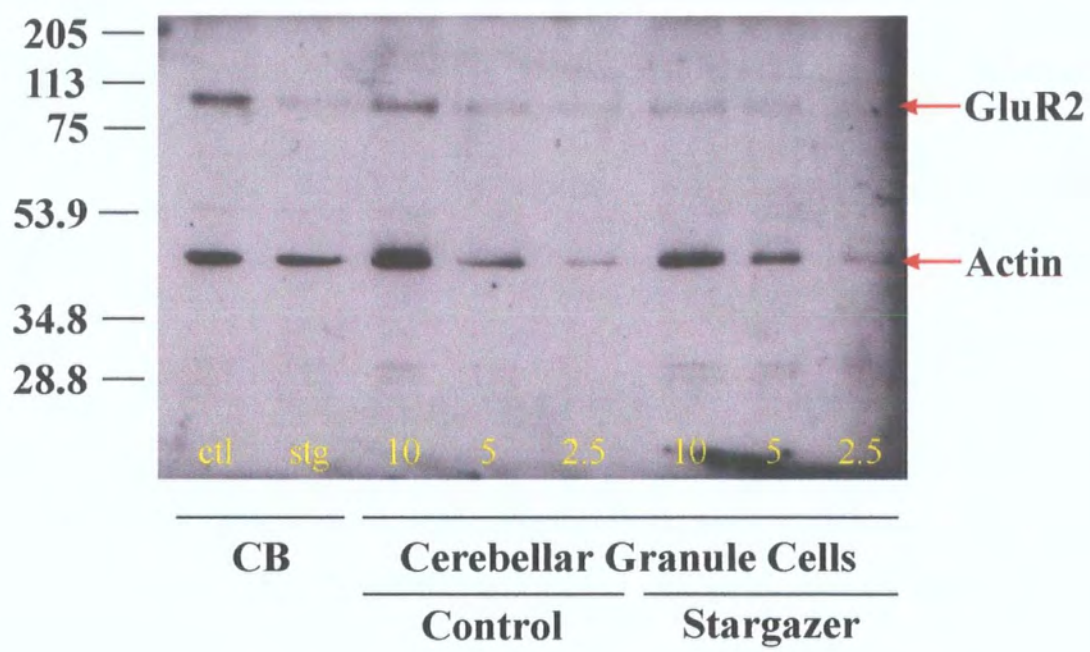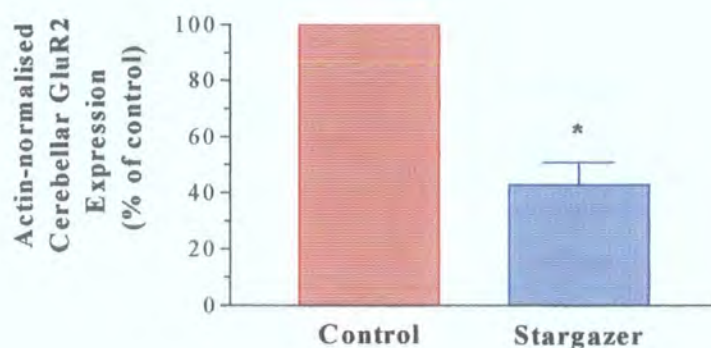
Control   Stargazer

Figure 7.3 Expression levels of GluR2 subunit in cultured control (+/+ and +/stg) and stargazer (stg/stg) cerebellar granule cells. Immunoblots, probed with anti-GluR2 subunit-specific and anti-actin specific antibodies, were analysed by densitometric analysis. GluR2 : actin ratio of stargazer granule cells was expressed as a percentage of control expression. Results are mean ± sem. The level of GluR2 expression was significantly reduced in stargazer granule cells, when compared to control granule cells, as determined by the Student's *t*-test (* = P < 0.05) (n = 3 samples of cells from 2 – 3 petri dishes from each of 2 cultures for both control and stargazer).

As can be seen in figure 7.3 above, GluR2 expression was significantly decreased in stargazer granule cells when compared to control granule cells. The level of expression of GluR2 in stargazer CGCs was 42.9 ± 8.0 % of control levels. Whilst this was not as low as was observed in stargazer cerebellar membranes, it reflected the decrease in GluR2 immunohistochemical staining observed in stargazer granule cell layer.

7.2.2.2 Quantification of surface expression of GluR2 in cultured CGCs

Cultured CGCs, derived from age-matched, littermate control and stargazer mouse neonates, were analysed to determine the relative level of surface expressed AMPAR GluR2 subunit, essentially as described by Hall et al. (Hall and Soderling, 1997b, Hall et al., 1997) and Archibald et al. (1998).

Preliminary experiments with control cerebellar membranes demonstrated that an incubation of 10 minutes at 37°C with 1 mg/ml BS^3 was sufficient to yield an almost

Figure 7.4 BS^3 treatment of cultured cerebellar granule cells. Cultured control (+/+ and +/stg, ctl) and stargazer (stg/stg, stg) granule cells were incubated with either vehicle (SS) or the cross-linker BS^3 (BS) before being collected and the proteins precipitated. The proteins (5 µg/10 µl and 10 µg/10 µl) were then immunoprobed for GluR2 (A) and actin (B).

As can be seen in A, vehicle-treated stargazer granule cells showed a decreased expression of GluR2, as would be expected. BS^3 treatment reduced the level of the 105 kDa GluR2 protein and this resulted in a decreased signal with the antibody, in both the control and stargazer granule cells.

10 µg/10 µl control (+/+ and +/stg) cerebellar membranes were also used as a positive control.

Broad range (20.7 kDa – 207 kDa) molecular weight markers were used and the respective molecular weights have been indicated to the left of the immunoblots.

A

207 —
118 —
81 —

52.5 —

36.2 —

29.9 —

SS BS SS BS SS BS SS BS

ctl   stg   ctl   stg   CB

10μg/10μl   5μg/10μl

← GluR2

B

207 —
118 —
81 —

52.5 —

36.2 —

29.9 —

SS BS SS BS SS BS SS BS

ctl   stg   ctl   stg   CB

10μg/10μl   5μg/10μl
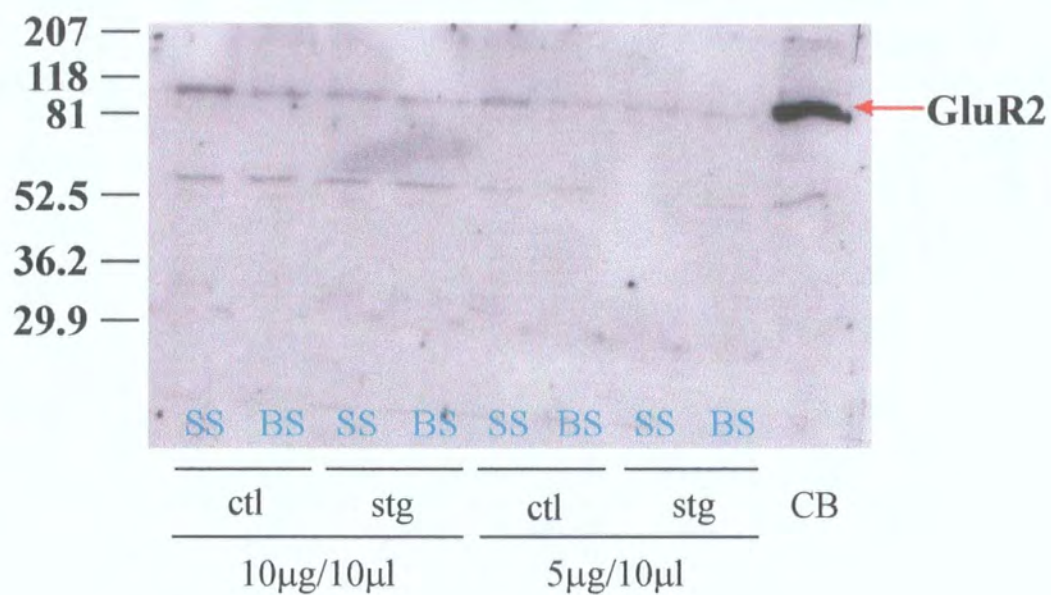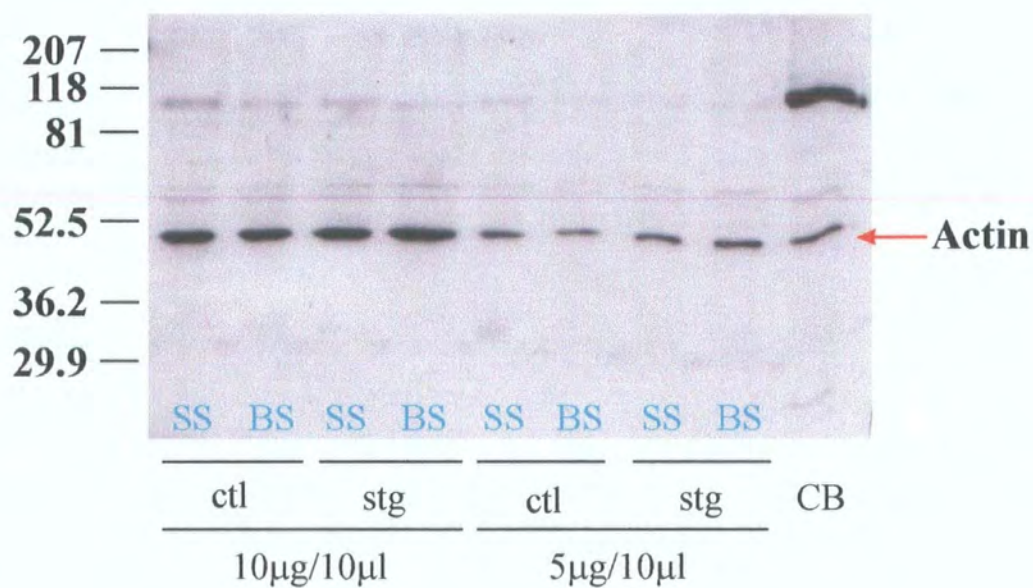
← Actin

complete reduction in GluR2 immunoreactivity. Cultured control and stargazer CGCs were treated with either saline solution (SS) or 1 mg/ml BS^3, before harvesting and collecting, as described in section 2.15. The SS- and BS^3-treated cell proteins were chloroform-methanol precipitated, as described in section 2.6 and separated by gel electrophoresis, as outlined in section 2.7, before being probed with anti-GluR2 and anti-actin antibodies (see figure 7.4).

The anti-GluR2 antibody detected the 105 kDa GluR2 subunit in SS-treated control and stargazer cultured CGCs. Immunoblots revealed the expression levels of GluR2 in cultured stargazer granule cells were decreased when compared to control granule cells. Following BS^3-treatment, the residual GluR2 signal revealed the intracellular GluR2. The optical densities obtained from the immunoblots were then used to calculate the level of cell surface expression of the GluR2 subunit in stargazer CGCs, relative to control CGCs.

The expression of GluR2 in SS-treated cells, both control and stargazer, was determined thus, using the appropriate optical densities:

Control cells ($OD_{SS\ cntl}$): $OD_{SS\ GluR2}$ / $OD_{SS\ Actin}$ ($\equiv 100\ \%$)

Stargazer cells ($OD_{SS\ stg}$): $OD_{SS\ GluR2}$ / $OD_{SS\ Actin}$

Stg GluR2 expression (normalised to control): ($OD_{SS\ stg}$ / $OD_{SS\ cntl}$) * 100

The results of such experiments and calculations can be seen in figure 7.5 below.
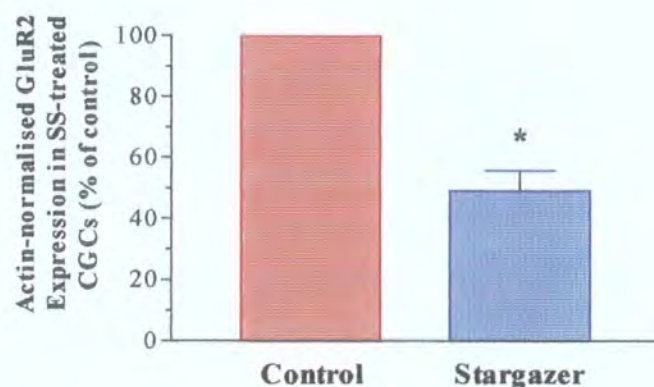
Figure 7.5 Expression of GluR2 subunit in vehicle-treated (SS) cultured cerebellar granule cells. Immunoblots were probed with anti-GluR2 and anti-actin antibodies and were analysed by densitometric analysis. GluR2 : actin ratio of stargazer granule cells was expressed as a percentage of control expression, which was given an arbitrary value of 100%. Results are expressed as mean ± sem. Expression in stargazer granule cells was significantly reduced when compared to the level of expression in control granule cells, as determined using the Student's *t*-test (* = P < 0.05) (n = 2 samples of cells from 2 – 3 petri dishes from each of 2 cultures for both control and stargazer).

As can be seen in figure 7.5 above, a decreased expression of the GluR2 subunit was observed in SS-treated cultured stargazer CGCs when compared to SS-treated cultured control CGCs. The level of expression of GluR2 in SS-treated cultured cerebellar granule cells derived from stargazer neonates was 49.1 ± 6.6 % of that determined in SS-treated cultured cerebellar granule cells derived from age-matched, littermate control neonates. This was a significant decrease with a P value of 0.0286 and mirrored the results observed with untreated CGCs (section 7.2.2.1).

In order to assess the relative amount of GluR2 subunit expressed at the granule cell surface, the membrane impermeant protein-modifying agent, BS^3, was used. BS^3 effectively cross-linked cell surface expressed proteins, thereby decreasing the availability of the 105 kDa GluR2 protein to the anti-GluR2 antibody. BS^3 either disrupts the part of the GluR2 subunit that the antibody recognises and/or cross-links the GluR2 subunit to neighbouring proteins so that it no longer has a molecular mass of 105 kDa when analysed by immunoblotting. The residual signal at 105 kDa represents the GluR2 found intracellularly, as shown in figure 7.4.

226

In order to determine the extracellular levels of GluR2, the BS^3 values need to be subtracted from the total values (i.e. from the values obtained from SS-treated cells). This was calculated for control CGCs thus:

Total expression ($OD_{SS\ cntl}$): $OD_{SS\ GluR2}$ / $OD_{SS\ Actin}$ (as determined above)

Intracellular GluR2 ($OD_{BS\ cntl}$): $OD_{BS\ GluR2}$ / $OD_{BS\ Actin}$

Extracellular GluR2: $[(OD_{SS\ cntl} - OD_{BS\ cntl}) / OD_{SS\ cntl}] * 100$

The same calculations were used to determine the extracellular GluR2 level in stargazer granule cells by replacing the ODs used above (i.e. the optical densities of immunoreactive species in control cells determined on immunoblots) with those obtained for the stargazer cells so that the following results were obtained:

Total expression ($OD_{SS\ stg}$): $OD_{SS\ GluR2}$ / $OD_{SS\ Actin}$ (as determined above)

Intracellular GluR2 ($OD_{BS\ stg}$): $OD_{BS\ GluR2}$ / $OD_{BS\ Actin}$

Extracellular GluR2: $[(OD_{SS\ stg} - OD_{BS\ stg}) / OD_{SS\ stg}] * 100$
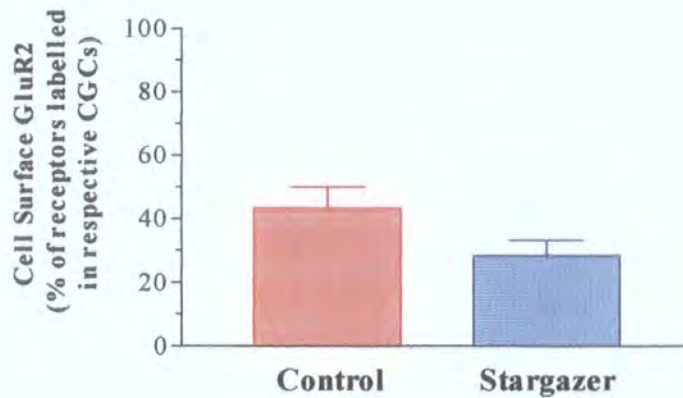
Figure 7.6 Cell surface expression of GluR2 in control and stargazer CGCs. Immunoblots probed with anti-GluR2 and anti-β actin antibodies were analysed by densitometric analysis. Values obtained represent extracellular GluR2 expressed as a percentage of the receptors labelled in SS-treated control and stargazer cells respectively. Results are mean ± sem; n = 2 samples of cells from 2 – 3 petri dishes from each of 2 cultures for both control and stargazer. No significant difference was found between control and stargazer CGCs using the Student's t-test (P > 0.05).

The results of such calculations can be seen in figure 7.6, where the levels of GluR2 expressed at the surface of cultured control CGCs and cultured stargazer CGCs can be examined. The extracellular GluR2 level in control granule cells was 43.4 ± 6.7 % of the GluR2 detected in SS-treated control cells whilst that in stargazer granule cells was 28.4 ± 4.8 % of the total GluR2 expression calculated in SS-treated stargazer cells. No significant difference between the two cell preparations was calculated.

However, stargazer CGCs contained only 49.1 % of the total GluR2 protein detected control CGCs. Therefore, only 28.4 % of the 49.1 % of the GluR2 protein found in control cells was expressed at the cell surface of stargazer cells. In order to take this lower level of protein into consideration, one more calculation must be performed. The final calculation used was thus:

Absolute stg GluR2 levels: $(OD_{SS\ stg} * OD_{BS\ stg}) / 100$

As this was a normalised value, the value for control cells was 100 %.
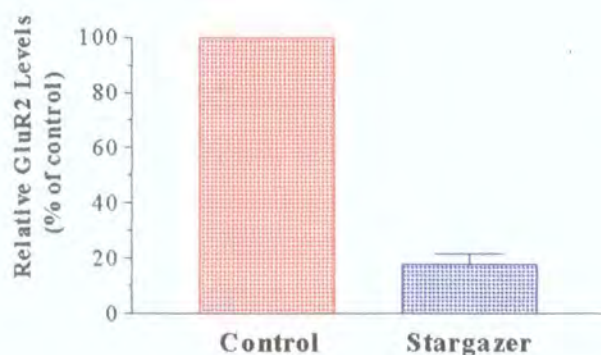
Figure 7.7 Expression of extracellular GluR2 in stargazer CGCs compared
to total GluR2 in control CGCs. Levels of the GluR2 subunit at the cell
surface of cultured stargazer cerebellar granule cells were expressed as a
percentage of total GluR2 expression in cultured control granule cells.
Results are mean ± sem, n = 2 samples of cells from 2 − 3 petri dishes from
each of 2 cultures for both control and stargazer.

As can be seen in figure 7.7, the level of surface GluR2 expressed in cultured
stargazer CGCs was only 17.8 ±4.0 % of the total GluR2 exhibited by control cells.
This was significantly less than the level of surface expression observed in control
granule cells (P = 0.0408).

7.3 Discussion

Cerebellar granule cells were cultured from age-matched, littermate control (+/+ and
+/stg) and stg/stg mice. GluR2 expression was determined and shown to be
decreased in cerebellar granule cells derived from stg/stg, when compared to control
cells. These data mirror the results observed earlier with cerebellar membranes
(section 5.2.2). The cultured granule cells were then used to determine the level of
cell surface expression of the GluR2 subunit, using the membrane impermeable
cross-linking agent, BS³.

7.3.1 Culture media is important in the expression of receptor subunits

Cultured rat cerebellar granule cells develop a survival requirement, around DIV 2 − 4, which can be satisfied by either culturing the cells in media containing a depolarising concentration of 25 mM K^+ or with the addition of glutamate receptor antagonists, such as NMDA, to the culture media (Balazs et al., 1988b; Balazs et al., 1988a; Gallo et al., 1987). Mice cerebellar granule cells, however, show no such requirement and have been shown to survive in culture media containing low and high concentrations of K^+ (5 − 25 mM) (Mogensen et al., 1994).

The expression of receptor subunits have, however, been shown to be affected by the concentration of K^+ in the culture media. Mouse cerebellar granule cells cultured under non-depolarising media (i.e. with 5 mM K^+), a GABAR profile similar to that observed in adult cerebellar membranes was detected, that is α_{1-3}, α_6, β_{2-3}, γ_2 and δ subunits were expressed. Under depolarising conditions (i.e. 25 mM K^+-containing media), the expression of certain GABAR subunits was altered. Low levels of α_1, α_6 and β_2 were observed whilst expression of α_3, α_5 and β_3 were increased (Ives et al., 2002b).

GABAR α_6 expression was shown to be decreased, by both immunoblotting and immunohistochemistry, in stargazer cerebellar membranes. A deficit in benzodiazepine-insensitive binding, an indication of α_6 subunit-containing receptors, was also exhibited by stargazer cerebellar membranes (section 3.2.4.2; Thompson et al., 1998). α_6 expression has been shown to be decreased in stg/stg granule cells cultured in low K^+ media, as was the deficit in benzodiazepine-insensitive binding (Ives et al., 2003), indicating that stg/stg granule cells cultured in 5 mM K^+-containing media reproduce the decrease in GABAR α_6 subunit expression observed in adult stargazer cerebellar membranes.

The expression of stargazin protein was also determined in both control and stg/stg granule cells cultured in non-depolarising media. Stargazin, whilst present in the granule cell layer of the cerebellum (section 6.2.3; Ives et al., 2003), is absent from stargazer cerebellar membranes (section 6.2.2; Sharp et al., 2001). Whilst stargazin

was shown to be present in control granule cells, it was not detected in cultured stg/stg granule cells (Ives et al., 2003).

Finally, the level of expression of the GluR2 subunit of the AMPA receptor was determined in both cultured control and stg/stg granule cells. The GluR2 protein is significantly decreased in stargazer cerebellar membranes (section 5.2.2.3). This finding was also found to be replicated in cultured stg/stg cerebellar granule cells (section 7.2.2). It would therefore appear that culturing murine granule cells in low K^+-containing media replicates the properties seen *in vivo*.

7.3.2 Determination of the amount of surface expression of receptor subunit proteins

The level of surface expression of the GluR2 subunit was then determined in the cultured cerebellar granule cells. The method used involved the cross-linking of the surface proteins with BS^3, a membrane-impermeable, irreversible, amine-reactive cross-linking reagent. This method was employed to determine the surface expression of NMDA receptors in hippocampal neurons, where 60 % of NR1 subunits and over 90 % of NR2B subunits expressed were located at the cell surface (Hall and Soderling, 1997b). AMPAR subunits in primary cultures of hippocampal neurons were also analysed using BS^3 (Hall and Soderling, 1997a). The level of expression of GluR1 was 39 % of control whilst that of GluR2/3 was 57 % of control, indicating that 61 % of GluR1 and 43 % of GluR2/3 were expressed at the cell surface.

In both instances, the level of surface expression of each of the receptor subunits was also determined using chymotrypsin, with the results obtained being similar to those produced with BS^3 treatment. Immunoreactivities for the intracellular proteins actin, tubulin and calcium/calmodium-dependent protein kinase II (CaMKII) were unaffected by both treatments, indicating that only transmembrane proteins were either susceptible to cleavage by chymotrypsin or cross-linking by BS^3 (Hall and Soderling, 1997b; Hall and Soderling, 1997a).

231

Ives et al. (2002) used both BS^3 and chymotrypsin to determine the expression of GABA receptor subunits at the surface of cerebellar granule cells. Cerebellar granule cells, cultured from P6 - 7 $C3B6Fe^+$ mice in 5 mM K^+-containing media, were subsequently treated with either chymotrypsin or BS^3 before the cells were harvested and probed for the expression of GABAR subunits. Similar results were obtained with both treatments, with 74 % of α_1 subunits, 51 % of α_6 subunits and 83 % of β_2/β_3 subunits being expressed at the cell surface. The level of expression of the intracellular proteins actin and neuron-specific enolase did not change following incubation with BS^3, indicating that, again, only extracellular proteins were cross-linked.

The levels of expression at the cell surface of GABA receptor subunits were also determined in stargazer granule cells (Ives et al., 2003). Control (+/+ and +/stg) and stg/stg granule cells were cultured in low K^+ media for 9 - 10 days before treatment with BS^3. Both control and stg/stg granule cells exhibited α_6 subunit expression, although the level of expression was reduced in stg/stg cells, as expected. Similarly, the δ subunit was found in both control and stg/stg granule cells. Treatment with BS^3 revealed that the cell surface levels of α_6 were reduced whilst the δ subunit was found exclusively in an intracellular compartment of stg/stg cells.

Applying the same method to cultured granule cells here revealed that the level of total GluR2 in stg/stg cells was 43 % of control (section 7.2.2.1), reflecting the decrease seen in GluR2 levels in adult stargazer cerebellar membranes (section 5.2.2.3). Treatment of the cells with SS, the vehicle for BS^3, revealed that the vehicle had no effect on the level of GluR2 subunit, with total GluR2 levels in SS-treated stg/stg cells being 49.1 % of the level found in SS-treated control cells (section 7.2.2.2).

Treatment of the cultured cells with BS^3 revealed the level of expression of GluR2 at the cell surface of both control and stg/stg cells, which were 43 % and 28 % respectively, expressed as a percentage of total GluR2 expressed in control and stg/stg cells (section 7.2.2.2). The level expressed at the surface of control cells corresponded to the level of surface expressed GluR2/3 found by Hall et al. (1997).

The level of GluR2 found to be expressed at the cell surface of stg/stg granule cells was a percentage of total GluR2 expressed in stg/stg cells. As the total level of GluR2 protein expressed in stg/stg cells was much less than that expressed in control cells, the proportion of GluR2 expressed at the cell surface of stg/stg cells was calculated to be only 18 % of the total GluR2 labelling observed in control granule cells (section 7.2.2.2).

7.3.3 Conclusion

The genomic PCR technique used to determine the genotype of adult mice was used to determine the genotype of P3 neonatal mice, which were then used for cell culturing purposes at P5 – 6. Cerebellar granule cells from control (+/+ and +/stg) and stg/stg age-matched, littermate mice were obtained and cultured for 11 DIV. GluR2 protein was shown to be decreased in stg/stg granule cells by immunoblotting, to a similar degree as that observed in adult stargazer cerebellar membranes.

Cell surface expression of GluR2 was determined using the cross-linking reagent BS[3] and was also found to be significantly reduced in stg/stg granule cells, indicating that the compromised stargazin expression decreased cell surface expression of the GluR2 subunit. Further work, however, is needed to determine whether only the GluR2 subunit is reduced at the cell surface, or whether the levels of GluR1 and GluR4, which also associate with stargazin, are also reduced at the cell surface. Furthermore, it is not yet known whether the GluR2-containing receptor is stable at the stg/stg cell surface or the reduction observed is due to an increase in the rate of endocytosis.

Chapter 8

Summary and future aims

$GABA_A$ receptors, NMDA receptors and AMPA receptors were all studied in the brain of the ataxic, epileptic mouse, stargazer. A genomic DNA amplification system was utilised to identify the genotype of +/+, +/stg and stg/stg mice, which were either subsequently used to maintain the breeding programme or for primary cerebellar granule cell cultures.

Initial studies revealed no apparent differences in GABAR α_1 or α_6 subunit expression levels between +/+ and +/stg mice. Levels of α_6 subunit were significantly decreased in stargazer cerebellar membranes, when compared to control (+/+ and +/stg) cerebellar membranes. Autoradiographical studies revealed a decrease in benzodiazepine-insensitive receptors in stargazer cerebellum, i.e. in α_6-containing receptors. Interestingly, the same studies also revealed an increase in benzodiazepine-insensitive binding in the stargazer dentate gyrus, implying an increase in $\alpha_4\gamma$-containing receptors and a potential decrease in extrasynaptic $\alpha_4\delta$-containing receptors. Further work is currently being undertaken by other members of the group to elucidate the role of stargazin in the trafficking and assembly of GABARs.

Antibodies were generated to the NMDAR subunits and characterised using control tissue. These antibodies were then used to determine the level and anatomical distribution of expression of the NMDAR subunits in control and stargazer brains. No significant differences were found by either immunoblotting or by immunohistochemistry. These data appeared to be confirmed by radioligand binding studies, where no apparent difference was found in the binding of [^{3}H] MK-801 to NMDARs in control and stargazer brain sections and synaptic membranes.

An anti-stargazin antibody was also generated and was used to determine the expression of stargazin protein. Whilst stargazin protein was detected in both control

234

forebrain and cerebellar tissues, no stargazin was detected in stargazer, thereby demonstrating that stargazer was a null mutant for stargazin.

AMPA receptor subunits were also studied in control and stargazer brains. No differences were observed in the anatomical distributions of the receptor subunits; however, immunoblotting studies using cerebellar membranes did reveal significant decreases in the expression of the GluR1, GluR2 and GluR4 subunits, with the largest decrease observed in the levels of the GluR2 subunit. Interestingly, the anatomical distribution of the GluR2 subunit appeared to mirror that of stargazin.

Sodium deoxycholate was used to successfully solubilise stargazin from brain extracts. Co-immunoprecipitation studies using anti-stargazin immunoaffinity columns revealed that stargazin associated with the AMPAR GluR1, GluR2 and GluR4 subunits *in vivo*. However, control experiments using solubilised proteins from stargazer tissue also revealed weak interactions between the antibody and GluR subunits.

Since the generation of the anti-stargazin antibody, more γ isoforms have been described by a number of other groups. It is possible, therefore, that the antibody was recognising other γ isoforms, especially as some immunostaining was still observed in stargazer brain sections. The peptide, against which the anti-stargazin antibody was raised, consisted of the final 15 amino acids of the γ_2 subunit (DSLHANTANRRTTPV). The γ_1 and γ_{5-7} isoforms do not contain this sequence, however, there is some similarity between the C-terminus of γ_2 and the C-termini of γ_3, γ_4 and γ_8. These isoforms contain the NR-R/K-TTPV motif whilst the γ_{2-4} isoforms also share a histidine residue at position -11 and γ_2 and γ_8 both possess a threonine residue and an aspargine residue at positions -8 and -9 respectively.

The use of the antibodies here revealed staining to be present both in the hippocampus and the cerebellum of the brain of stargazer mouse, implying some cross-reactivity of the anti-stargazin antibodies. Whilst γ_3 mRNA has been shown to be present in the murine hippocampus, neither γ_3 mRNA nor γ_3 protein has been detected in the cerebellum. γ_4 mRNA and protein have both been identified within

the murine cerebellum but not within the murine hippocampus. γ_8 mRNA has been shown to be present in both rat and human brain tissue, where it has been detected in both the hippocampus and the cerebellum. It is possible, therefore, that the anti-stargazin antibodies used here were detecting the γ_3 and γ_8 isoforms within the stargazer hippocampus and the γ_4 and γ_8 isoforms within stargazer cerebellum. Indeed, since γ_4 protein has been shown to have a molecular mass of 53 kDa, it is possible that the NS53 species observed on the immunoblots here was the γ_4 isoform. However, further studies are required to establish the protein expression of the other γ isoforms within both control and stargazer brains.

As the sequences of other γ isoforms have been elucidated, it may be possible to design a peptide that is more stargazin-specific. Alternatively, immunoaffinity columns using a second anti-γ isoform antibody could be prepared. Proteins would be purified down the anti-stargazin immunoaffinity column but the material would then be placed down the second anti-γ isoform immunoaffinity column. Any proteins also binding to this second γ isoform would then be pulled out of the purified preparation, leaving only stargazin-associated complexes in the preparation.

Work by other groups has shown that stargazin is involved in the trafficking and synaptic localisation of AMPAR subunits. Since stargazin was shown here to associate with AMPAR subunits *in vivo*, it is possible that there is a decreased cell surface expression of these subunits. To determine whether this was the case, control and stargazer cerebellar granule cells were cultured. These cells were then treated with the membrane-impermeant cross-linking reagent BS^3, to allow the surface expression of proteins to be evaluated. It was shown that, not only do stargazer cerebellar granule cells contain less GluR2 protein than control cells, the proportion of GluR2 subunits expressed at the cell surface is also significantly reduced. More experiments would need to be undertaken to determine whether expression of the other AMPAR subunits are also reduced at the cell surface.

Although this type of experiment reveals the amount of protein expressed at the cell surface, it does not explain whether there appears to be less GluR2 because of an increased turnover rate. One way of determining if this was the case would be to

236

undertake pulse-chase labelling of the cells. Proteins in the granule cells would be labelled with ^{35}S-methionine and then immunoprecipitated with anti-GluR2 antibodies. The amount of ^{35}S immunoprecipitated would decrease over time, giving an indication of the turnover rate of the protein in control and stargazer granule cells.

Stock Solutions

PBS

136.9 mM NaCl
2.68 mM KCl
10.1 mM Na_2HPO_4
1.76 mM KH2PO4
pH 7.4

Protease Inhibitor Cocktail

Inhibits serine, cystein, aspartic proteases and aminopeptidases

4-(2-aminoethyl)benzene sulfonyl fluoride
Pepstatin-A
Trans-epoxysuccinyl-L-leucylamido(4-guanidino)butane (E-64)
Bistatin
Leupeptin
Aprotinin

Immunoblotting Solutions

Running Buffer

1.5 M Tris
8 mM EDTA
pH 8.8
0.4 % (w/v) SDS

Electrode Buffer

0.01 M Tris
0.8 M Glycine
2.3 mM EDTA
pH 8.8
0.2 % (w/v) SDS

Transfer Buffer

25 mM Tris
192 mM Glycine
20 % (v/v) Methanol
pH > 8

Luminol

> 1.25 mM Luminol
> 0.1 M Tris-HCl
> pH 8.5

ECL Reagent

Luminol	10 ml
68 mM p-coumaric acid (in DMSO)	100 µl
H_2O_2 (30 % stock)	3 µl

70% Ethanol

Ethanol	70 ml
dH_2O (final volume)	100 ml

4 % Paraformaldehyde in 0.1 M Phosphate Buffer

4 % (w/v) Paraformaldehyde

Paraformaldehyde	40 g
dH_2O	500 ml
1 M NaOH	3 drops

Heat to 60°C in a fume hood. When cool, filter using 1M Whatman filter paper.

0.2 M Phosphate buffer, pH 7.2

0.2 M Na_2HPO_4	400 ml
0.2 M NaH_2PO_4	100 ml

Paraformaldehyde in phosphate buffer

4 % Paraformaldehyde	500 ml
0.2 M Phosphate buffer, pH 7.2	500 ml

PCR Solutions

TBE (10X)

Tris	108 g
Orthoboric Acid	55 g
0.5 M EDTA, pH 8.0	40 ml
dH_2O (final volume)	1 L

PCR Loading Buffer

> 10 mM Tris-HCl, pH 7.5
> 50 mM EDTA
> 0.25 % (w/v) Bromophenol Blue
> 30 % (v/v) Glycerol

Cell Culture Solutions

HEBSS

> 138.8 mM NaCl
> 5.0 mM KCl
> 25 mM HEPES
> 4.2 mM $NaHCO_3$
> 1.0 mM $NaH_2PO_4.H_2O$
> pH 7.4

$MgSO_4$ solution

> 3.82 % (w/v) $MgSO_4$

Solution 1H

HEBSS	50 ml
Glucose	0.125 g
BSA	0.15 g
$MgSO_4$	0.5 ml

4 % BSA solution

HEBSS	5 ml
BSA	0.2 g
$MgSO_4$	40 µl

Trypsin solution

Solution 1H	10 ml
Bovine Pancreas Trypsin	2.5 mg

Concentrated Trypsin Inhibitor

Solution 1H	10 ml
$MgSO_4$	0.1 ml
1300 Kunitz units/10 ml DNase I	100 µl
Soybean Trypsin Inhibitor	8 mg

Dilute Trypsin Inhibitor

Solution 1H	10 ml
Concentrated Trypsin Inhibitor	1.6 ml

References

Ahmed MS, Mather A, Enna SJ (1999) Binding of [^{3}H] desglycinyl remacemide to rat brain membranes: association with the benzomorphan attachment site of the N-methyl-D-aspartic acid receptor channel. Brain Res 827:46-50.

Aizawa M, Ito Y, Fukuda H (1997) Pharmacological profiles of generalized absence seizures in lethargic, stargazer and γ-hydroxybutyrate-treated model mice. Neurosci Res 29:17-25.

Aizenman E, Lipton SA, Loring RH (1989) Selective modulation of NMDA responses by reduction and oxidation. Neuron 2:1257-1263.

Akazawa C, Shigemoto R, Bessho Y, Nakanishi S, Mizuno N (1994) Differential expression of five N-methyl-D-aspartate receptor subunit mRNAs in the cerebellum of developing and adult rats. J Comp Neurol 347:150-160.

Anson LC, Chen PE, Wyllie DJ, Colquhoun D, Schoepfer R (1998) Identification of amino acid residues of the NR2A subunit that control glutamate potency in recombinant NR1/NR2A NMDA receptors. J Neurosci 18:581-589.

Arai A, Silberg J, Kessler M, Lynch G (1995) Effect of thiocyanate on AMPA receptor mediated responses in excised patches and hippocampal slices. Neuroscience 66:815-827.

Araujo F, Tan S, Ruano D, Schoemaker H, Benavides J, Vitorica J (1996) Molecular and pharmacological characterization of native cortical γ-aminobutyric acid$_A$ receptors containing both α_1 and α_3 subunits. J Biol Chem 271:27902-27911.

Archibald K, Perry MJ, Molnar E, Henley JM (1998) Surface expression and metabolic half-life of AMPA receptors in cultured rat cerebellar granule cells. Neuropharmacology 37:1345-1353.

Attwell PJ, Rahman S, Ivarsson M, Yeo CH (1999) Cerebellar cortical AMPA-kainate receptor blockade prevents performance of classically conditioned nictitating membrane responses. J Neurosci 19:RC45.

Bahr BA, Hoffman KB, Kessler M, Hennegriff M, Park GY, Yamamoto RS, Kawasaki BT, Vanderklish PW, Hall RA, Lynch G (1996) Distinct distributions of α-amino-3-hydroxy-5-methyl-4-isoxazolepropionate (AMPA) receptor subunits and a related 53,000 M(R) antigen (GR53) in brain tissue. Neuroscience 74:707-721.

Balazs R, Jorgensen OS, Hack N (1988a) N-methyl-D-aspartate promotes the survival of cerebellar granule cells in culture. Neuroscience 27:437-451.

Balazs R, Hack N, Jorgensen OS (1988b) Stimulation of the N-methyl-D-aspartate receptor has a trophic effect on differentiating cerebellar granule cells. Neurosci Lett 87:80-86.

Bampton ET, Gray RA, Large CH (1999) Electrophysiological characterisation of the dentate gyrus in five inbred strains of mouse. Brain Res 841:123-134.

Bao S, Chen L, Qiao X, Thompson RF (1999) Transgenic brain-derived neurotrophic factor modulates a developing cerebellar inhibitory synapse. Learn Mem 6:276-283.

Barnard EA, Skolnick P, Olsen RW, Mohler H, Sieghart W, Biggio G, Braestrup C, Bateson AN, Langer SZ (1998) International Union of Pharmacology. XV. Subtypes of γ-aminobutyric acid$_A$ receptors: classification on the basis of subunit structure and receptor function. Pharmacol Rev 50:291-313.

Baude A, Sequier JM, McKernan RM, Olivier KR, Somogyi P (1992) Differential subcellular distribution of the α6 subunit versus the α1 and β2/3 subunits of the GABA$_A$/benzodiazepine receptor complex in granule cells of the cerebellar cortex. Neuroscience 51:739-748.

Baude A, Molnar E, Latawiec D, McIlhinney RA, Somogyi P (1994) Synaptic and nonsynaptic localization of the GluR1 subunit of the AMPA-type excitatory amino acid receptor in the rat cerebellum. J Neurosci 14:2830-2843.

Baude A, Nusser Z, Molnar E, McIlhinney RA, Somogyi P (1995) High-resolution immunogold localization of AMPA type glutamate receptor subunits at synaptic and non-synaptic sites in rat hippocampus. Neuroscience 69:1031-1055.

Belelli D, Lambert JJ, Peters JA, Gee KW, Lan NC (1996) Modulation of human recombinant $GABA_A$ receptors by pregnanediols. Neuropharmacology 35:1223-1231.

Belzung C, Le Guisquet AM, Crestani F (2000) Flumazenil induces benzodiazepine partial agonist-like effects in BALB/c but not C57BL/6 mice. Psychopharmacology (Berl) 148:24-32.

Benke D, Michel C, Mohler H (1997) $GABA_A$ receptors containing the α4-subunit: prevalence, distribution, pharmacology, and subunit architecture in situ. J Neurochem 69:806-814.

Benke D, Honer M, Michel C, Mohler H (1996) $GABA_A$ receptor subtypes differentiated by their gamma-subunit variants: prevalence, pharmacology and subunit architecture. Neuropharmacology 35:1413-1423.

Benke D, Fritschy JM, Trzeciak A, Bannwarth W, Mohler H (1994) Distribution, prevalence, and drug binding profile of γ-aminobutyric acid type A receptor subtypes differing in the beta-subunit variant. J Biol Chem 269:27100-27107.

Benke D, Mertens S, Trzeciak A, Gillessen D, Mohler H (1991a) Identification and immunohistochemical mapping of $GABA_A$ receptor subtypes containing the δ-subunit in rat brain. FEBS Lett 283:145-149.

Benke D, Mertens S, Trzeciak A, Gillessen D, Mohler H (1991b) GABA$_A$ receptors display association of γ2-subunit with α1- and β2/3-subunits. J Biol Chem 266:4478-4483.

Bennett JA, Dingledine R (1995) Topology profile for a glutamate receptor: three transmembrane domains and a channel-lining reentrant membrane loop. Neuron 14:373-384.

Bernard V, Somogyi P, Bolam JP (1997) Cellular, subcellular, and subsynaptic distribution of AMPA-type glutamate receptor subunits in the neostriatum of the rat. J Neurosci 17:819-833.

Billinton A, Ige AO, Bolam JP, White JH, Marshall FH, Emson PC (2001) Advances in the molecular understanding of GABA$_B$ receptors. Trends Neurosci 24:277-282.

Birnir B, Tierney ML, Dalziel JE, Cox GB, Gage PW (1997) A structural determinant of desensitization and allosteric regulation by pentobarbitone of the GABA$_A$ receptor. J Membr Biol 155:157-166.

Black JL, 3rd, Lennon VA (1999) Identification and cloning of putative human neuronal voltage-gated calcium channel γ-2 and γ-3 subunits: neurologic implications. Mayo Clin Proc 74:357-361.

Blahos J, 2nd, Wenthold RJ (1996) Relationship between N-methyl-D-aspartate receptor NR1 splice variants and NR2 subunits. J Biol Chem 271:15669-15674.

Bleakman R, Schoepp DD, Ballyk B, Bufton H, Sharpe EF, Thomas K, Ornstein PL, Kamboj RK (1996) Pharmacological discrimination of GluR5 and GluR6 kainate receptor subtypes by (3S,4aR,6R,8aR)-6-[2-(1(2)H-tetrazole-5-yl)ethyl]decahydroisdoquinoline-3 carboxylic-acid. Mol Pharmacol 49:581-585.

Bochet P, Audinat E, Lambolez B, Crepel F, Rossier J, Iino M, Tsuzuki K, Ozawa S (1994) Subunit composition at the single-cell level explains functional properties of a glutamate-gated channel. Neuron 12:383-388.

Bonnert TP, McKernan RM, Farrar S, le Bourdelles B, Heavens RP, Smith DW, Hewson L, Rigby MR, Sirinathsinghji DJ, Brown N, Wafford KA, Whiting PJ (1999) θ, a novel γ-aminobutyric acid type A receptor subunit. Proc Natl Acad Sci U S A 96:9891-9896.

Boulter J, Hollmann M, O'Shea-Greenfield A, Hartley M, Deneris E, Maron C, Heinemann S (1990) Molecular cloning and functional expression of glutamate receptor subunit genes. Science 249:1033-1037.

Braithwaite SP, Xia H, Malenka RC (2002) Differential roles for NSF and GRIP/ABP in AMPA receptor cycling. Proc Natl Acad Sci U S A 99:7096-7101.

Brandoli C, Sanna A, De Bernardi MA, Follesa P, Brooker G, Mocchetti I (1998) Brain-derived neurotrophic factor and basic fibroblast growth factor downregulate NMDA receptor function in cerebellar granule cells. J Neurosci 18:7953-7961.

Brooks-Kayal AR, Shumate MD, Jin H, Rikhter TY, Coulter DA (1998) Selective changes in single cell GABA(A) receptor subunit expression and function in temporal lobe epilepsy. Nat Med 4:1166-1172.

Brose N, Gasic GP, Vetter DE, Sullivan JM, Heinemann SF (1993) Protein chemical characterization and immunocytochemical localization of the NMDA receptor subunit NMDA R1. J Biol Chem 268:22663-22671.

Burette A, Khatri L, Wyszynski M, Sheng M, Ziff E, Weinberg R (2001) Differential cellular and subcellular localization of AMPA receptor-binding protein and glutamate receptor-interacting protein. J Neurosci 21:495-503.

Burgess DL, Gefrides LA, Foreman PJ, Noebels JL (2001) A cluster of three novel Ca^{2+} channel γ subunit genes on chromosome 19q13.4: evolution and expression profile of the gamma subunit gene family. Genomics 71:339-350.

Burgess DL, Davis CF, Gefrides LA, Noebels JL (1999) Identification of three novel Ca^{2+} channel γ subunit genes reveals molecular diversification by tandem and chromosome duplication. Genome Res 9:1204-1213.

Chadwick DW, Betts TA, Boddie HG, Crawford PM, Lindstrom P, Newman PK, Soryal I, Wroe S, Holdich TA (2002) Remacemide hydrochloride as an add-on therapy in epilepsy: a randomized, placebo-controlled trial of three dose levels (300, 600 and 1200 mg/day) in a Q.I.D. regimen. Seizure 11:114-123.

Chafetz RS, Nahm WK, Noebels JL (1995) Aberrant expression of neuropeptide Y in hippocampal mossy fibers in the absence of local cell injury following the onset of spike-wave synchronization. Brain Res Mol Brain Res 31:111-121.

Chapman AG, Smith SE, Meldrum BS (1991) The anticonvulsant effect of the non-NMDA antagonists, NBQX and GYKI 52466, in mice. Epilepsy Res 9:92-96.

Charton JP, Herkert M, Becker CM, Schroder H (1999) Cellular and subcellular localization of the 2B-subunit of the NMDA receptor in the adult rat telencephalon. Brain Res 816:609-617.

Chazot PL, Coleman SK, Cik M, Stephenson FA (1994) Molecular characterization of N-methyl-D-aspartate receptors expressed in mammalian cells yields evidence for the coexistence of three subunit types within a discrete receptor molecule. J Biol Chem 269:24403-24409.

Chen L, Chetkovich DM, Petralia RS, Sweeney NT, Kawasaki Y, Wenthold RJ, Bredt DS, Nicoll RA (2000) Stargazin regulates synaptic targeting of AMPA receptors by two distinct mechanisms. Nature 408:936-943.

Chetkovich DM, Chen L, Stocker TJ, Nicoll RA, Bredt DS (2002) Phosphorylation of the Postsynaptic Density-95 (PSD-95)/Discs Large/Zona Occludens-1 binding site of stargazin regulates binding to PSD-95 and synaptic targeting of AMPA receptors. J Neurosci 22:5791-5796.

Chizh BA; Headley PM; Tzschentke TM (2001) NMDA receptor antagonists as analgesics: focus on the NR2B subtype. Trends Pharmacol Sci 22:636-642.

Choi J, Ko J, Park E, Lee JR, Yoon J, Lim S, Kim E (2002) Phosphorylation of stargazin by PKA regulates its interaction with PSD-95. J Biol Chem 277:12359-12363.

Chu PJ, Robertson HM, Best PM (2001) Calcium channel γ subunits provide insights into the evolution of this gene family. Gene 280:37-48.

Ciabarra AM, Sullivan JM, Gahn LG, Pecht G, Heinemann S, Sevarino KA (1995) Cloning and characterization of chi-1: a developmentally regulated member of a novel class of the ionotropic glutamate receptor family. J Neurosci 15:6498-6508.

Clarke CE, Cooper JA, Holdich TA (2001) A randomized, double-blind, placebo-controlled, ascending-dose tolerability and safety study of remacemide as adjuvant therapy in Parkinson's disease with response fluctuations. Clin Neuropharmacol 24:133-138.

Colledge M, Dean RA, Scott GK, Langeberg LK, Huganir RL, Scott JD (2000) Targeting of PKA to glutamate receptors through a MAGUK-AKAP complex. Neuron 27:107-119.

Collingridge GL, Kehl SJ, McLennan H (1983) Excitatory amino acids in synaptic transmission in the Schaffer collateral-commissural pathway of the rat hippocampus. J Physiol 334:33-46.

Craig AM, Blackstone CD, Huganir RL, Banker G (1993) The distribution of glutamate receptors in cultured rat hippocampal neurons: postsynaptic clustering of AMPA-selective subunits. Neuron 10:1055-1068.

Crozier RA, Black IB, Plummer MR (1999) Blockade of NR2B-containing NMDA receptors prevents BDNF enhancement of glutamatergic transmission in hippocampal neurons. Learn Mem 6:257-266.

Crump FT, Dillman KS, Craig AM (2001) cAMP-dependent protein kinase mediates activity-regulated synaptic targeting of NMDA receptors. J Neurosci 21:5079-5088.

Dai WM, Egebjerg J, Lambert JD (2001) Characteristics of AMPA receptor-mediated responses of cultured cortical and spinal cord neurones and their correlation to the expression of glutamate receptor subunits, GluR1-4. Br J Pharmacol 132:1859-1875.

Das S, Sasaki YF, Rothe T, Premkumar LS, Takasu M, Crandall JE, Dikkes P, Conner DA, Rayudu PV, Cheung W, Chen HS, Lipton SA, Nakanishi N (1998) Increased NMDA current and spine density in mice lacking the NMDA receptor subunit NR3A. Nature 393:377-381.

Deransart C, Marescaux C, Depaulis A (1996) Involvement of nigral glutamatergic inputs in the control of seizures in a genetic model of absence epilepsy in the rat. Neuroscience 71:721-728.

des Portes V, Coulpier M, Melki J, Dreyfus PA (1994) Early detection of mouse wobbler mutation: a model of pathological motoneurone death. Neuroreport 5:1861-1864.

DeSouza S, Fu J, States BA, Ziff EB (2002) Differential Palmitoylation Directs the AMPA Receptor-Binding Protein ABP to Spines or to Intracellular Clusters. J Neurosci 22:3493-3503.

Di Pasquale E, Keegan KD, Noebels JL (1997) Increased excitability and inward rectification in layer V cortical pyramidal neurons in the epileptic mutant mouse *Stargazer*. J Neurophysiol 77:621-631.

Didier M, Xu M, Berman SA, Bursztajn S (1995) Differential expression and co-assembly of NMDA ζ1 and ε subunits in the mouse cerebellum during postnatal development. Neuroreport 6:2255-2259.

Donevan SD, Rogawski MA (1998) Allosteric regulation of α-amino-3-hydroxy-5-methyl-4-isoxazole-propionate receptors by thiocyanate and cyclothiazide at a common modulatory site distinct from that of 2,3-benzodiazepines. Neuroscience 87:615-629.

Doriat JF, Koziel V, Humbert AC, Daval JL (1999) Repeated seizure-associated long-lasting changes of N-methyl-D-aspartate receptor properties in the developing rat brain. Int J Dev Neurosci 17:369-376.

Duggan MJ, Pollard S, Stephenson FA (1991) Immunoaffinity purification of GABA$_A$ receptor a-subunit iso-oligomers. Demonstration of receptor populations containing α1α2, α1α3, and α2α3 subunit pairs. J Biol Chem 266:24778-24784.

Dunah AW, Luo J, Wang YH, Yasuda RP, Wolfe BB (1998) Subunit composition of *N*-methyl-D-aspartate receptors in the central nervous system that contain the NR2Dsubunit. Mol Pharmacol 53:429-437.

Dunah AW, Yasuda RP, Wang YH, Luo J, Davila-Garcia M, Gbadegesin M, Vicini S, Wolfe BB (1996) Regional and ontogenic expression of the NMDA receptor subunit NR2D protein in rat brain using a subunit-specific antibody. J Neurochem 67:2335-2345.

Durand GM, Bennett MV, Zukin RS (1993) Splice variants of the N-methyl-D-aspartate receptor NR1 identify domains involved in regulation by polyamines and protein kinase C. Proc Natl Acad Sci U S A 90:6731-6735.

Durand GM, Gregor P, Zheng X, Bennett MV, Uhl GR, Zukin RS (1992) Cloning of an apparent splice variant of the rat N-methyl-D-aspartate receptor NMDAR1 with altered sensitivity to polyamines and activators of protein kinase C. Proc Natl Acad Sci U S A 89:9359-9363.

Ebert B, Madsen U, Lund TM, Lenz SM, Krogsgaard-Larsen P (1994a) Molecular pharmacology of the AMPA agonist, (S)-2-amino-3-(3-hydroxy-5-phenyl-4-isoxazolyl)propionic acid [(S)-APPA] and the AMPA antagonist, (R)-APPA. Neurochem Int 24:507-515.

Ebert B, Lenz S, Brehm L, Bregnedal P, Hansen JJ, Frederiksen K, Bogeso KP, Krogsgaard-Larsen P (1994b) Resolution, absolute stereochemistry, and pharmacology of the S-(+)- and R-(-)-isomers of the apparent partial AMPA receptor agonist (R,S)-2-amino-3-(3-hydroxy-5-phenylisoxazol-4-yl)propionic acid [(R,S)-APPA]. J Med Chem 37:878-884.

El-Husseini AE, Schnell E, Chetkovich DM, Nicoll RA, Bredt DS (2000) PSD-95 involvement in maturation of excitatory synapses. Science 290:1364-1368.

El-Husseini Ael D, Schnell E, Dakoji S, Sweeney N, Zhou Q, Prange O, Gauthier-Campbell C, Aguilera-Moreno A, Nicoll RA, Bredt DS (2002) Synaptic strength regulated by palmitate cycling on PSD-95. Cell 108:849-863.

Endo S, Olsen RW (1993) Antibodies specific for alpha-subunit subtypes of $GABA_A$ receptors reveal brain regional heterogeneity. J Neurochem 60:1388-1398.

Fadda E, Danysz W, Wroblewski JT, Costa E (1988) Glycine and D-serine increase the affinity of N-methyl-D-aspartate sensitive glutamate binding sites in rat brain synaptic membranes. Neuropharmacology 27:1183-1185.

Favaron M, Manev RM, Rimland JM, Candeo P, Beccaro M, Manev H (1993) NMDA-stimulated expression of BDNF mRNA in cultured cerebellar granule neurones. Neuroreport 4:1171-1174.

Ferrante RJ, Andreassen OA, Dedeoglu A, Ferrante KL, Jenkins BG, Hersch SM, Beal MF (2002) Therapeutic effects of coenzyme Q10 and remacemide in transgenic mouse models of Huntington's disease. J Neurosci 22:1592-1599.

Ferrer-Montiel AV, Montal M (1996) Pentameric subunit stoichiometry of a neuronal glutamate receptor. Proc Natl Acad Sci U S A 93:2741-2744.

Filliat P, Pernot-Marino I, Baubichon D, Lallement G (1998) Behavioral effects of NBQX, a competitive antagonist of the AMPA receptors. Pharmacol Biochem Behav 59:1087-1092.

Fletcher EJ, Martin D, Aram JA, Lodge D, Honore T (1988) Quinoxalinediones selectively block quisqualate and kainate receptors and synaptic events in rat neocortex and hippocampus and frog spinal cord in vitro. Br J Pharmacol 95:585-597.

Foster AC, Wong EH (1987) The novel anticonvulsant MK-801 binds to the activated state of the N-methyl-D-aspartate receptor in rat brain. Br J Pharmacol 91:403-409.

Foster AC, Kemp JA, Leeson PD, Grimwood S, Donald AE, Marshall GR, Priestley T, Smith JD, Carling RW (1992) Kynurenic acid analogues with improved affinity and selectivity for the glycine site on the N-methyl-D-aspartate receptor from rat brain. Mol Pharmacol 41:914-922.

Friedman LK (1998) Selective reduction of GluR2 protein in adult hippocampal CA3 neurons following status epilepticus but prior to cell loss. Hippocampus 8:511-525.

Friedman LK, Veliskova J (1998) GluR2 hippocampal knockdown reveals developmental regulation of epileptogenicity and neurodegeneration. Brain Res Mol Brain Res 61:224-231.

Friedman LK, Pellegrini-Giampietro DE, Sperber EF, Bennett MV, Moshe SL, Zukin RS (1994) Kainate-induced status epilepticus alters glutamate and GABA$_A$ receptor gene expression in adult rat hippocampus: an in situ hybridization study. J Neurosci 14:2697-2707.

Fritschy JM, Benke D, Mertens S, Oertel WH, Bachi T, Mohler H (1992) Five subtypes of type A γ-aminobutyric acid receptors identified in neurons by double and triple immunofluorescence staining with subunit-specific antibodies. Proc Natl Acad Sci U S A 89:6726-6730.

Fujikawa N, Tominaga-Yoshino K, Okabe M, Ogura A (2000) Depolarization-dependent survival of cultured mouse cerebellar granule neurons is strain-restrained. Eur J Neurosci 12:1838-1842.

Gallagher MJ, Huang H, Pritchett DB, Lynch DR (1996) Interactions between ifenprodil and the NR2B subunit of the N-methyl-D-aspartate receptor. J Biol Chem 271:9603-9611.

Gallo V, Kingsbury A, Balazs R, Jorgensen OS (1987) The role of depolarization in the survival and differentiation of cerebellar granule cells in culture. J Neurosci 7:2203-2213.

Gao WQ, Zheng JL, Karihaloo M (1995) Neurotrophin-4/5 (NT-4/5) and brain-derived neurotrophic factor (BDNF) act at later stages of cerebellar granule cell differentiation. J Neurosci 15:2656-2667.

Garcia-Gallo M, Renart J, Diaz-Guerra M (2001) The NR1 subunit of the N-methyl-D-aspartate receptor can be efficiently expressed alone in the cell surface of mammalian cells and is required for the transport of the NR2A subunit. Biochem J 356:539-547.

Geter-Douglass B, Witkin JM (1999) Behavioral effects and anticonvulsant efficacies of low-affinity, uncompetitive NMDA antagonists in mice. Psychopharmacology (Berl) 146:280-289.

Gomperts SN, Rao A, Craig AM, Malenka RC, Nicoll RA (1998) Postsynaptically silent synapses in single neuron cultures. Neuron 21:1443-1451.

Graham SH, Chen J, Lan JQ, Simon RP (1996) A dose-response study of neuroprotection using the AMPA antagonist NBQX in rat focal cerebral ischemia. J Pharmacol Exp Ther 276:1-4.

Green P, Warre R, Hayes P, McNaughton N, Medhurst A, Pangalos M, Duckworthdagger D, Randall A (2001) Kinetic modification of the α_{1I} subunit-mediated T-type Ca^{2+} channel by a human neuronal Ca^{2+} channel γ subunit. J Physiol 533:467-478.

Griebel G, Belzung C, Perrault G, Sanger DJ (2000) Differences in anxiety-related behaviours and in sensitivity to diazepam in inbred and outbred strains of mice. Psychopharmacology (Berl) 148:164-170.

Grooms SY, Opitz T, Bennett MV, Zukin RS (2000) Status epilepticus decreases glutamate receptor 2 mRNA and protein expression in hippocampal pyramidal cells before neuronal death. Proc Natl Acad Sci U S A 97:3631-3636.

Guilarte TR, McGlothan JL, Nihei MK (2000) Hippocampal expression of N-methyl-D-aspartate receptor (NMDAR1) subunit splice variant mRNA is altered by developmental exposure to Pb(2+). Brain Res Mol Brain Res 76:299-305.

Hadingham KL, Harkness PC, McKernan RM, Quirk K, Le Bourdelles B, Horne AL, Kemp JA, Barnard EA, Ragan CI, Whiting PJ (1992) Stable expression of mammalian type A γ-aminobutyric acid receptors in mouse cells: demonstration of functional assembly of benzodiazepine-responsive sites. Proc Natl Acad Sci U S A 89:6378-6382.

253

Hadingham KL, Wingrove PB, Wafford KA, Bain C, Kemp JA, Palmer KJ, Wilson AW, Wilcox AS, Sikela JM, Ragan CI, et al. (1993) Role of the β subunit in determining the pharmacology of human γ-aminobutyric acid type A receptors. Mol Pharmacol 44:1211-1218.

Hafidi A, Hillman DE (1997) Distribution of glutamate receptors GluR 2/3 and NR1 in the developing rat cerebellum. Neuroscience 81:427-436.

Haggerty GC, Brown G (1996) Neurobehavioral profile of subcutaneously administered MK-801 in the rat. Neurotoxicology 17:913-921.

Hall RA, Soderling TR (1997a) Quantitation of AMPA receptor surface expression in cultured hippocampal neurons. Neuroscience 78:361-371.

Hall RA, Soderling TR (1997b) Differential surface expression and phosphorylation of the N-methyl-D-aspartate receptor subunits NR1 and NR2 in cultured hippocampal neurons. J Biol Chem 272:4135-4140.

Hall RA, Hansen A, Andersen PH, Soderling TR (1997) Surface expression of the AMPA receptor subunits GluR1, GluR2, and GluR4 in stably transfected baby hamster kidney cells. J Neurochem 68:625-630.

Harris EW, Ganong AH, Monaghan DT, Watkins JC, Cotman CW (1986) Action of 3-((+/-)-2-carboxypiperazin-4-yl)-propyl-1-phosphonic acid (CPP): a new and highly potent antagonist of N-methyl-D-aspartate receptors in the hippocampus. Brain Res 382:174-177.

Hashimoto K, Fukaya M, Qiao X, Sakimura K, Watanabe M, Kano M (1999) Impairment of AMPA receptor function in cerebellar granule cells of ataxic mutant mouse *stargazer*. J Neurosci 19:6027-6036.

Hatta K, Yamamato T, Hori T, Okuwa M, Moroji T (1991) 3-((+/-)2-carboxypiperazin-4-yl)propyl-1-phosphonic acid (CPP) more potently antagonizes the high-affinity Mg^{2+} binding site on the N-methyl-D-aspartate/phencyclidine receptor ion channel complex than the L-glutamate recognition site. Neurosci Lett 124:229-231.

Hauge SA, Tracy JA, Baudry M, Thompson RF (1998) Selective changes in AMPA receptors in rabbit cerebellum following classical conditioning of the eyelid-nictitating membrane response. Brain Res 803:9-18.

Hawkins LM, Chazot PL, Stephenson FA (1999) Biochemical evidence for the co-association of three N-methyl-D-aspartate (NMDA) R2 subunits in recombinant NMDA receptors. J Biol Chem 274:27211-27218.

Hawkins LM, Beaver KM, Jane DE, Taylor PM, Sunter DC, Roberts PJ (1995) Characterization of the pharmacology and regional distribution of (S)-[3H]-5-fluorowillardiine binding in rat brain. Br J Pharmacol 116:2033-2039.

Hawkinson JE, Espitia SA (1997) Effects of thiocyanate and AMPA receptor ligands on (S)-5-fluorowillardiine, (S)-AMPA and (R,S)-AMPA binding. Eur J Pharmacol 329:213-221.

Hayes NL, Nowakowski RS (2002) Dynamics of cell proliferation in the adult dentate gyrus of two inbred strains of mice. Brain Res Dev Brain Res 134:77-85.

Henneberger C, Grantyn R, Rothe T (2000) Rapid genotyping of newborn gene mutant mice. J Neurosci Methods 100:123-126.

Hevers W, Korpi ER, Luddens H (2000) Assembly of functional α6β3γ2δ GABA(A) receptors in vitro. Neuroreport 11:4103-4106.

Hollmann M, Maron C, Heinemann S (1994) N-glycosylation site tagging suggests a three transmembrane domain topology for the glutamate receptor GluR1. Neuron 13:1331-1343.

Hollmann M, Boulter J, Maron C, Beasley L, Sullivan J, Pecht G, Heinemann S (1993) Zinc potentiates agonist-induced currents at certain splice variants of the NMDA receptor. Neuron 10:943-954.

Honer M, Benke D, Laube B, Kuhse J, Heckendorn R, Allgeier H, Angst C, Monyer H, Seeburg PH, Betz H, Mohler H (1998) Differentiation of glycine antagonist sites of N-Methyl-D-aspartate receptor subtypes. Preferential interaction of CGP 61594 with NR1/2B receptors. J Biol Chem 273:11158-11163.

Honore T, Davies SN, Drejer J, Fletcher EJ, Jacobsen P, Lodge D, Nielsen FE (1988) Quinoxalinediones: potent competitive non-NMDA glutamate receptor antagonists. Science 241:701-703.

Hooper WD, Eadie MJ, Blakey GE, Lockton JA, Manun'Ebo M (2001) Evaluation of a pharmacokinetic interaction between remacemide hydrochloride and phenobarbitone in healthy males. Br J Clin Pharmacol 51:249-255.

Hu RQ, Cortez MA, Man HY, Wang YT, Snead OC, 3rd (2001) Alteration of GluR2 expression in the rat brain following absence seizures induced by gamma-hydroxybutyric acid. Epilepsy Res 44:41-51.

Huettner JE (1989) Indole-2-carboxylic acid: a competitive antagonist of potentiation by glycine at the NMDA receptor. Science 243:1611-1613.

Huettner JE, Bean BP (1988) Block of N-methyl-D-aspartate-activated current by the anticonvulsant MK-801: selective binding to open channels. Proc Natl Acad Sci U S A 85:1307-1311.

Huh KH, Endo S, Olsen RW (1996) Diazepam-insensitive $GABA_A$ receptors in rat cerebellum and thalamus. Eur J Pharmacol 310:225-233.

Hume RI, Dingledine R, Heinemann SF (1991) Identification of a site in glutamate receptor subunits that controls calcium permeability. Science 253:1028-1031.

Hyman C, Juhasz M, Jackson C, Wright P, Ip NY, Lindsay RM (1994) Overlapping and distinct actions of the neurotrophins BDNF, NT-3, and NT-4/5 on cultured dopaminergic and GABAergic neurons of the ventral mesencephalon. J Neurosci 14:335-347.

Ikeda K, Nagasawa M, Mori H, Araki K, Sakimura K, Watanabe M, Inoue Y, Mishina M (1992) Cloning and expression of the ε4 subunit of the NMDA receptor channel. FEBS Lett 313:34-38.

Isaac JT, Crair MC, Nicoll RA, Malenka RC (1997) Silent synapses during development of thalamocortical inputs. Neuron 18:269-280.

Ishii T, Moriyoshi K, Sugihara H, Sakurada K, Kadotani H, Yokoi M, Akazawa C, Shigemoto R, Mizuno N, Masu M, et al. (1993) Molecular characterization of the family of the N-methyl-D-aspartate receptor subunits. J Biol Chem 268:2836-2843.

Ives J, Drewery D, Thompson C (2002a) Neuronal activity and its influence on developmentally regulated GABA(A) receptor expression in cultured mouse cerebellar granule cells. Neuropharmacology 43:715.

Ives JH, Drewery DL, Thompson CL (2002b) Differential cell surface expression of $GABA_A$ receptor α1, α6, β2 and β3 subunits in cultured mouse cerebellar granule cells influence of cAMP-activated signalling. J Neurochem 80:317-327.

Ives JH, Drewery DL, Lucocq J, Sieghart W, Tiwari P, Doran B, Wright M, Thompson CL (2003) $GABA_A$ receptor assembly and trafficking is impaired in cerebellar granule cells of the ataxic mouse, stargazer: evidence that stargazin directly interacts with $GABA_A$ receptor subunits *in vivo* (manuscript in preparation).

Janssens N, Lesage AS (2001) Glutamate receptor subunit expression in primary neuronal and secondary glial cultures. J Neurochem 77:1457-1474.

Jay SD, Ellis SB, McCue AF, Williams ME, Vedvick TS, Harpold MM, Campbell KP (1990) Primary structure of the γ subunit of the DHP-sensitive calcium channel from skeletal muscle. Science 248:490-492.

Jechlinger M, Pelz R, Tretter V, Klausberger T, Sieghart W (1998) Subunit composition and quantitative importance of hetero-oligomeric receptors: $GABA_A$ receptors containing $\alpha 6$ subunits. J Neurosci 18:2449-2457.

Jia Z, Agopyan N, Miu P, Xiong Z, Henderson J, Gerlai R, Taverna FA, Velumian A, MacDonald J, Carlen P, Abramow-Newerly W, Roder J (1996) Enhanced LTP in mice deficient in the AMPA receptor GluR2. Neuron 17:945-956.

Jin DH, Jung YW, Ko BH, Moon IS (1997) Immunoblot analyses on the differential distribution of NR2A and NR2B subunits in the adult rat brain. Mol Cells 7:749-754.

Jones MW, Peckham HM, Errington ML, Bliss TV, Routtenberg A (2001) Synaptic plasticity in the hippocampus of awake C57BL/6 and DBA/2 mice: interstrain differences and parallels with behavior. Hippocampus 11:391-396.

Jones A, Korpi ER, McKernan RM, Pelz R, Nusser Z, Makela R, Mellor JR, Pollard S, Bahn S, Stephenson FA, Randall AD, Sieghart W, Somogyi P, Smith AJ, Wisden W (1997) Ligand-gated ion channel subunit partnerships: $GABA_A$ receptor α_6 subunit gene inactivation inhibits δ subunit expression. J Neurosci 17:1350-1362.

Kadotani H, Hirano T, Masugi M, Nakamura K, Nakao K, Katsuki M, Nakanishi S (1996) Motor discoordination results from combined gene disruption of the NMDA receptor NR2A and NR2C subunits, but not from single disruption of the NR2A or NR2C subunit. J Neurosci 16:7859-7867.

Kang MG, Chen CC, Felix R, Letts VA, Frankel WN, Mori Y, Campbell KP (2001) Biochemical and biophysical evidence for γ_2 subunit association with neuronal voltage-activated Ca^{2+} channels. J Biol Chem 276:32917-32924.

Katsumori H, Minabe Y, Osawa M, Ashby CR, Jr. (1998) Acute effects of various GABA receptor agonists and glutamate antagonists on focal hippocampal seizures in freely moving rats elicited by low-frequency stimulation. Synapse 28:103-109.

Kawai M, Horikawa Y, Ishihara T, Shimamoto K, Ohfune Y (1992) 2-(Carboxycyclopropyl)glycines: binding, neurotoxicity and induction of intracellular free Ca^{2+} increase. Eur J Pharmacol 211:195-202.

Kawasaki-Yatsugi S, Ichiki C, Yatsugi S, Shimizu-Sasamata M, Yamaguchi T (1998) YM90K, an AMPA receptor antagonist, protects against ischemic damage caused by permanent and transient middle cerebral artery occlusion in rats. Naunyn Schmiedebergs Arch Pharmacol 358:586-591.

Keinanen K, Wisden W, Sommer B, Werner P, Herb A, Verdoorn TA, Sakmann B, Seeburg PH (1990) A family of AMPA-selective glutamate receptors. Science 249:556-560.

Kemp JA, Foster AC, Leeson PD, Priestley T, Tridgett R, Iversen LL, Woodruff GN (1988) 7-Chlorokynurenic acid is a selective antagonist at the glycine modulatory site of the N-methyl-D-aspartate receptor complex. Proc Natl Acad Sci U S A 85:6547-6550.

Kempermann G, Gage FH (2002) Genetic influence on phenotypic differentiation in adult hippocampal neurogenesis. Brain Res Dev Brain Res 134:1-12.

Kempermann G, Kuhn HG, Gage FH (1997) Genetic influence on neurogenesis in the dentate gyrus of adult mice. Proc Natl Acad Sci U S A 94:10409-10414.

Kessler M, Terramani T, Lynch G, Baudry M (1989) A glycine site associated with N-methyl-D-aspartic acid receptors: characterization and identification of a new class of antagonists. J Neurochem 52:1319-1328.

Khan ZU, Gutierrez A, De Blas AL (1996) The $\alpha 1$ and $\alpha 6$ subunits can coexist in the same cerebellar $GABA_A$ receptor maintaining their individual benzodiazepine-binding specificities. J Neurochem 66:685-691.

Khan ZU, Gutierrez A, De Blas AL (1994) The subunit composition of a $GABA_A$/benzodiazepine receptor from rat cerebellum. J Neurochem 63:371-374.

Kieburtz K, Feigin A, McDermott M, Como P, Abwender D, Zimmerman C, Hickey C, Orme C, Claude K, Sotack J, Greenamyre JT, Dunn C, Shoulson I (1996) A controlled trial of remacemide hydrochloride in Huntington's disease. Mov Disord 11:273-277.

Kim E, Niethammer M, Rothschild A, Jan YN, Sheng M (1995) Clustering of Shaker-type K^+ channels by interaction with a family of membrane-associated guanylate kinases. Nature 378:85-88.

Kim JJ, Thompson RF (1997) Cerebellar circuits and synaptic mechanisms involved in classical eyeblink conditioning. Trends Neurosci 20:177-181

Kleckner NW, Dingledine R (1988) Requirement for glycine in activation of NMDA-receptors expressed in Xenopus oocytes. Science 241:835-837.

Kloog Y, Nadler V, Sokolovsky M (1988) Mode of binding of [^{3}H] dibenzocycloalkenimine (MK-801) to the N-methyl-D-aspartate (NMDA) receptor and its therapeutic implication. FEBS Lett 230:167-170.

Klugbauer N, Dai S, Specht V, Lacinova L, Marais E, Bohn G, Hofmann F (2000) A family of γ-like calcium channel subunits. FEBS Lett 470:189-197.

Kodama M, Yamada N, Sato K, Kitamura Y, Koyama F, Sato T, Morimoto K, Kuroda S (1999) Effects of YM90K, a selective AMPA receptor antagonist, on amygdala-kindling and long-term hippocampal potentiation in the rat. Eur J Pharmacol 374:11-19.

Koerner C, Danober L, Boehrer A, Marescaux C, Vergnes M (1996) Thalamic NMDA transmission in a genetic model of absence epilepsy in rats. Epilepsy Res 25:11-19.

Kornau HC, Schenker LT, Kennedy MB, Seeburg PH (1995) Domain interaction between NMDA receptor subunits and the postsynaptic density protein PSD-95. Science 269:1737-1740.

Kudo Y, Akita K, Ishida M, Shinozaki H (1991) A significant increase in intracellular Ca^{2+} concentration induced by (2S,3R,4S)-2-(carboxycyclopropyl)glycine, a new potent NMDA agonist, in cultured rat hippocampal neurons. Brain Res 567:342-345.

Kullmann DM, Asztely F, Walker MC (2000) The role of mammalian ionotropic receptors in synaptic plasticity: LTP, LTD and epilepsy. Cell Mol Life Sci 57:1551-1561.

Kumar SS, Bacci A, Kharazia V, Huguenard JR (2002) A developmental switch of AMPA receptor subunits in neocortical pyramidal neurons. J Neurosci 22:3005-3015.

Kurschner VC, Petruzzi RL, Golden GT, Berrettini WH, Ferraro TN (1998) Kainate and AMPA receptor binding in seizure-prone and seizure-resistant inbred mouse strains. Brain Res 780:1-8.

Kutsuwada T, Kashiwabuchi N, Mori H, Sakimura K, Kushiya E, Araki K, Meguro H, Masaki H, Kumanishi T, Arakawa M, et al. (1992) Molecular diversity of the NMDA receptor channel. Nature 358:36-41.

Laube B, Kuhse J, Betz H (1998) Evidence for a tetrameric structure of recombinant NMDA receptors. J Neurosci 18:2954-2961.

Laube B, Hirai H, Sturgess M, Betz H, Kuhse J (1997) Molecular determinants of agonist discrimination by NMDA receptor subunits: analysis of the glutamate binding site on the NR2B subunit. Neuron 18:493-503.

Laurie DJ, Bartke I, Schoepfer R, Naujoks K, Seeburg PH (1997) Regional, developmental and interspecies expression of the four NMDAR2 subunits, examined using monoclonal antibodies. Brain Res Mol Brain Res 51:23-32.

Laurie DJ, Seeburg PH, Wisden W (1992) The distribution of 13 GABA$_A$ receptor subunit mRNAs in the rat brain. II. Olfactory bulb and cerebellum. J Neurosci 12:1063-1076.

Leeson PD, Baker R, Carling RW, Curtis NR, Moore KW, Williams BJ, Foster AC, Donald AE, Kemp JA, Marshall GR (1991) Kynurenic acid derivatives. Structure-activity relationships for excitatory amino acid antagonism and identification of potent and selective antagonists at the glycine site on the N-methyl-D-aspartate receptor. J Med Chem 34:1243-1252.

Lehmann J, Schneider J, McPherson S, Murphy DE, Bernard P, Tsai C, Bennett DA, Pastor G, Steel DJ, Boehm C, et al. (1987) CPP, a selective N-methyl-D-aspartate (NMDA)-type receptor antagonist: characterization in vitro and in vivo. J Pharmacol Exp Ther 240:737-746.

Leonard AS, Davare MA, Horne MC, Garner CC, Hell JW (1998) SAP97 is associated with the alpha-amino-3-hydroxy-5-methylisoxazole-4-propionic acid receptor GluR1 subunit. J Biol Chem 273:19518-19524.

Letts VA, Felix R, Biddlecome GH, Arikkath J, Mahaffey CL, Valenzuela A, Bartlett FS, 2nd, Mori Y, Campbell KP, Frankel WN (1998) The mouse stargazer gene encodes a neuronal Ca^{2+}-channel γ subunit. Nat Genet 19:340-347.

Letts VA, Valenzuela A, Kirley JP, Sweet HO, Davisson MT, Frankel WN (1997) Genetic and physical maps of the stargazer locus on mouse chromosome 15. Genomics 43:62-68.

Lowry OH, Rosebrough NJ, Farr AL, Randall RJ (1951) Protein measurement with the folin phenol reagent. J Biol Chem 193:265-275.

Lu W, Man H, Ju W, Trimble WS, MacDonald JF, Wang YT (2001) Activation of synaptic NMDA receptors induces membrane insertion of new AMPA receptors and LTP in cultured hippocampal neurons. Neuron 29:243-254.

Luo J, Bosy TZ, Wang Y, Yasuda RP, Wolfe BB (1996) Ontogeny of NMDA R1 subunit protein expression in five regions of rat brain. Brain Res Dev Brain Res 92:10-17.

Luo J, Wang Y, Yasuda RP, Dunah AW, Wolfe BB (1997) The majority of N-methyl-D-aspartate receptor complexes in adult rat cerebral cortex contain at least three different subunits (NR1/NR2A/NR2B). Mol Pharmacol 51:79-86.

Luscher C, Xia H, Beattie EC, Carroll RC, von Zastrow M, Malenka RC, Nicoll RA (1999) Role of AMPA receptor cycling in synaptic transmission and plasticity. Neuron 24:649-658.

Lynch DR, Guttmann RP (2002) Excitotoxicity: perspectives based on N-methyl-D-aspartate receptor subtypes. J Pharmacol Exp Ther 300:717-723.

Maisonpierre PC, Belluscio L, Friedman B, Alderson RF, Wiegand SJ, Furth ME, Lindsay RM, Yancopoulos GD (1990) NT-3, BDNF, and NGF in the developing rat nervous system: parallel as well as reciprocal patterns of expression. Neuron 5:501-509.

Mano I, Teichberg VI (1998) A tetrameric subunit stoichiometry for a glutamate receptor-channel complex. Neuroreport 9:327-331.

Mansour M, Nagarajan N, Nehring RB, Clements JD, Rosenmund C (2001) Heteromeric AMPA receptors assemble with a preferred subunit stoichiometry and spatial arrangement. Neuron 32:841-853.

Mares P, Mikulecka A, Pometlova M (1997) Anticonvulsant action of 2,3-dihydroxy-6-nitro-7-sulfamoyl-benzo(f)quinoxaline in immature rats: comparison with the effects on motor performance. J Pharmacol Exp Ther 281:1120-1126.

Martin LJ, Furuta A, Blackstone CD (1998) AMPA receptor protein in developing rat brain: glutamate receptor-1 expression and localization change at regional, cellular, and subcellular levels with maturation. Neuroscience 83:917-928.

Martin LJ, Blackstone CD, Levey AI, Huganir RL, Price DL (1993) AMPA glutamate receptor subunits are differentially distributed in rat brain. Neuroscience 53:327-358.

Matsui T, Sekiguchi M, Hashimoto A, Tomita U, Nishikawa T, Wada K (1995) Functional comparison of D-serine and glycine in rodents: the effect on cloned NMDA receptors and the extracellular concentration. J Neurochem 65:454-458.

Mayer ML, Vyklicky L, Jr., Clements J (1989) Regulation of NMDA receptor desensitization in mouse hippocampal neurons by glycine. Nature 338:425-427.

Meguro H, Mori H, Araki K, Kushiya E, Kutsuwada T, Yamazaki M, Kumanishi T, Arakawa M, Sakimura K, Mishina M (1992) Functional characterization of a heteromeric NMDA receptor channel expressed from cloned cDNAs. Nature 357:70-74.

Mellor JR, Merlo D, Jones A, Wisden W, Randall AD (1998) Mouse cerebellar granule cell differentiation: electrical activity regulates the $GABA_A$ receptor $\alpha6$ subunit gene. J Neurosci 18:2822-2833.

Mennini T, Mancini L, Reggiani A, Trist D (1997) GV 150526A, 7-Cl-kynurenic acid and HA 966 antagonize the glycine enhancement of N-methyl-D-aspartate-induced [^{3}H] noradrenaline and [^{3}H] dopamine release. Eur J Pharmacol 336:275-281.

Mihalek RM, Banerjee PK, Korpi ER, Quinlan JJ, Firestone LL, Mi ZP, Lagenaur C, Tretter V, Sieghart W, Anagnostaras SG, Sage JR, Fanselow MS, Guidotti A, Spigelman I, Li Z, DeLorey TM, Olsen RW, Homanics GE (1999) Attenuated sensitivity to neuroactive steroids in γ-aminobutyrate type A receptor delta subunit knockout mice. Proc Natl Acad Sci U S A 96:12905-12910.

Mogensen HS, Hack N, Balazs R, Jorgensen OS (1994) The survival of cultured mouse cerebellar granule cells is not dependent on elevated potassium-ion concentration. Int J Dev Neurosci 12:451-460.

Molnar E, Baude A, Richmond SA, Patel PB, Somogyi P, McIlhinney RA (1993) Biochemical and immunocytochemical characterization of antipeptide antibodies to a cloned GluR1 glutamate receptor subunit: cellular and subcellular distribution in the rat forebrain. Neuroscience 53:307-326.

Monaghan DT, Larsen H (1997) NR1 and NR2 subunit contributions to N-methyl-D-aspartate receptor channel blocker pharmacology. J Pharmacol Exp Ther 280:614-620.

Monyer H, Burnashev N, Laurie DJ, Sakmann B, Seeburg PH (1994) Developmental and regional expression in the rat brain and functional properties of four NMDA receptors. Neuron 12:529-540.

Monyer H, Sprengel R, Schoepfer R, Herb A, Higuchi M, Lomeli H, Burnashev N, Sakmann B, Seeburg PH (1992) Heteromeric NMDA receptors: molecular and functional distinction of subtypes. Science 256:1217-1221.

Monyer H, Seeburg PH, Wisden W (1991) Glutamate-operated channels: developmentally early and mature forms arise by alternative splicing. Neuron 6:799-810.

Moss FJ, Viard P, Davies A, Bertaso F, Page KM, Graham A, Canti C, Plumpton M, Plumpton C, Clare JJ, Dolphin AC (2002) The novel product of a five-exon *stargazin*-related gene abolishes $Ca_V2.2$ calcium channel expression. EMBO J 21:1514-1523.

Mothet JP, Parent AT, Wolosker H, Brady RO, Jr., Linden DJ, Ferris CD, Rogawski MA, Snyder SH (2000) D-serine is an endogenous ligand for the glycine site of the N-methyl-D-aspartate receptor. Proc Natl Acad Sci U S A 97:4926-4931.

Mugnaini M, Dal Forno G, Corsi M, Bunnemann B (2000) Receptor binding characteristics of the novel NMDA receptor glycine site antagonist [^{3}H] GV150526A in rat cerebral cortical membranes. Eur J Pharmacol 391:233-241.

Muller BM, Kistner U, Kindler S, Chung WJ, Kuhlendahl S, Fenster SD, Lau LF, Veh RW, Huganir RL, Gundelfinger ED, Garner CC (1996) SAP102, a novel postsynaptic protein that interacts with NMDA receptor complexes in vivo. Neuron 17:255-265.

Murphy DE, Schneider J, Boehm C, Lehmann J, Williams M (1987) Binding of [^{3}H] 3-(2-carboxypiperazin-4-yl)propyl-1-phosphonic acid to rat brain membranes: a selective, high-affinity ligand for N-methyl-D-aspartate receptors. J Pharmacol Exp Ther 240:778-784.

Nahm WK, Noebels JL (1998) Nonobligate role of early or sustained expression of immediate-early gene proteins c-fos, c-jun, and Zif/268 in hippocampal mossy fiber sprouting. J Neurosci 18:9245-9255.

Namba T, Morimoto K, Sato K, Yamada N, Kuroda S (1994) Antiepileptogenic and anticonvulsant effects of NBQX, a selective AMPA receptor antagonist, in the rat kindling model of epilepsy. Brain Res 638:36-44.

Neelands TR, Macdonald RL (1999) Incorporation of the π subunit into functional γ-aminobutyric acid$_A$ receptors. Mol Pharmacol 56:598-610.

Nicoll RA, Malenka RC (1999) Leaky synapses. Neuron 23:197-198.

Nielsen BS, Banke TG, Schousboe A, Pickering DS (1998) Pharmacological properties of homomeric and heteromeric GluR1o and GluR3o receptors. Eur J Pharmacol 360:227-238.

Niethammer M, Kim E, Sheng M (1996) Interaction between the C terminus of NMDA receptor subunits and multiple members of the PSD-95 family of membrane-associated guanylate kinases. J Neurosci 16:2157-2163.

Nishi M, Hinds H, Lu HP, Kawata M, Hayashi Y (2001) Motoneuron-specific expression of NR3B, a novel NMDA-type glutamate receptor subunit that works in a dominant-negative manner. J Neurosci 21:RC185.

Noebels JL, Qiao X, Bronson RT, Spencer C, Davisson MT (1990) Stargazer: a new neurological mutant on chromosome 15 in the mouse with prolonged cortical seizures. Epilepsy Res 7:129-135.

Noel J, Ralph GS, Pickard L, Williams J, Molnar E, Uney JB, Collingridge GL, Henley JM (1999) Surface expression of AMPA receptors in hippocampal neurons is regulated by an NSF-dependent mechanism. Neuron 23:365-376.

Nowak L, Bregestovski P, Ascher P, Herbet A, Prochiantz A (1984) Magnesium gates glutamate-activated channels in mouse central neurones. Nature 307:462-465.

Nusser Z, Sieghart W, Somogyi P (1998a) Segregation of different GABA$_A$ receptors to synaptic and extrasynaptic membranes of cerebellar granule cells. J Neurosci 18:1693-1703.

Nusser Z, Hajos N, Somogyi P, Mody I (1998b) Increased number of synaptic GABA(A) receptors underlies potentiation at hippocampal inhibitory synapses. Nature 395:172-177.

Nusser Z, Sieghart W, Stephenson FA, Somogyi P (1996) The α_6 subunit of the GABA$_A$ receptor is concentrated in both inhibitory and excitatory synapses on cerebellar granule cells. J Neurosci 16:103-114.

Oguro K, Oguro N, Kojima T, Grooms SY, Calderone A, Zheng X, Bennett MV, Zukin RS (1999) Knockdown of AMPA receptor GluR2 expression causes delayed neurodegeneration and increases damage by sublethal ischemia in hippocampal CA1 and CA3 neurons. J Neurosci 19:9218-9227.

Ohmori J, Sakamoto S, Kubota H, Shimizu-Sasamata M, Okada M, Kawasaki S, Hidaka K, Togami J, Furuya T, Murase K (1994) 6-(1H-imidazol-1-yl)-7-nitro-2,3(1H,4H)-quinoxalinedione hydrochloride (YM90K) and related compounds: structure-activity relationships for the AMPA-type non-NMDA receptor. J Med Chem 37:467-475.

Olivera S, Rodriguez-Ithurralde D, Henley JM (1999) Acetylcholinesterase potentiates [^{3}H] fluorowillardiine and [^{3}H] AMPA binding to rat cortical membranes. Neuropharmacology 38:505-512.

Olverman HJ, Jones AW, Watkins JC (1988) [^{3}H] D-2-amino-5-phosphonopentanoate as a ligand for N-methyl-D-aspartate receptors in the mammalian central nervous system. Neuroscience 26:1-15.

O'Neill MJ, Hicks C, Ward M (1996) Neuroprotective effects of 7-nitroindazole in the gerbil model of global cerebral ischaemia. Eur J Pharmacol 310:115-122.

Palmer GC, Murray RJ, Wilson TC, Eisman MS, Ray RK, Griffith RC, Napier JJ, Fedorchuk M, Stagnitto ML, Garske GE (1992) Biological profile of the metabolites and potential metabolites of the anticonvulsant remacemide. Epilepsy Res 12:9-20.

Patneau DK, Mayer ML (1990) Structure-activity relationships for amino acid transmitter candidates acting at N-methyl-D-aspartate and quisqualate receptors. J Neurosci 10:2385-2399.

Peeters BW, van Rijn CM, Vossen JM, Coenen AM (1990) Involvement of NMDA receptors in non-convulsive epilepsy in WAG/Rij rats. Life Sci 47:523-529.

Peeters BW, Van Rijn CM, Van Luijtelaar EL, Coenen AM (1989) Antiepileptic and behavioural actions of MK-801 in an animal model of spontaneous absence epilepsy. Epilepsy Res 3:178-181.

Pellegrini-Giampietro DE, Pulsinelli WA, Zukin RS (1994) NMDA and non-NMDA receptor gene expression following global brain ischemia in rats: effect of NMDA and non-NMDA receptor antagonists. J Neurochem 62:1067-1073.

Perez-Otano I, Schulteis CT, Contractor A, Lipton SA, Trimmer JS, Sucher NJ, Heinemann SF (2001) Assembly with the NR1 subunit is required for surface expression of NR3A-containing NMDA receptors. J Neurosci 21:1228-1237.

Petralia RS, Esteban JA, Wang YX, Partridge JG, Zhao HM, Wenthold RJ, Malinow R (1999) Selective acquisition of AMPA receptors over postnatal development suggests a molecular basis for silent synapses. Nat Neurosci 2:31-36.

Petralia RS, Wang YX, Mayat E, Wenthold RJ (1997) Glutamate receptor subunit 2-selective antibody shows a differential distribution of calcium-impermeable AMPA receptors among populations of neurons. J Comp Neurol 385:456-476.

Petralia RS, Yokotani N, Wenthold RJ (1994) Light and electron microscope distribution of the NMDA receptor subunit NMDAR1 in the rat nervous system using a selective anti-peptide antibody. J Neurosci 14:667-696.

Pickard L, Noel J, Duckworth JK, Fitzjohn SM, Henley JM, Collingridge GL, Molnar E (2001) Transient synaptic activation of NMDA receptors leads to the insertion of native AMPA receptors at hippocampal neuronal plasma membranes. Neuropharmacology 41:700-713.

Pickard L, Noel J, Henley JM, Collingridge GL, Molnar E (2000) Developmental changes in synaptic AMPA and NMDA receptor distribution and AMPA receptor subunit composition in living hippocampal neurons. J Neurosci 20:7922-7931.

Pirker S, Schwarzer C, Wieselthaler A, Sieghart W, Sperk G (2000) GABA$_A$ receptors: immunocytochemical distribution of 13 subunits in the adult rat brain. Neuroscience 101:815-850.

Pollard S, Thompson CL, Stephenson FA (1995) Quantitative characterization of α6 and α1α6 subunit-containing native γ-aminobutyric acid$_A$ receptors of adult rat cerebellum demonstrates two α subunits per receptor oligomer. J Biol Chem 270:21285-21290.

Pollard S, Duggan MJ, Stephenson FA (1993) Further evidence for the existence of alpha subunit heterogeneity within discrete γ-aminobutyric acid$_A$ receptor subpopulations. J Biol Chem 268:3753-3757.

Porter RH, Greenamyre JT (1995) Regional variations in the pharmacology of NMDA receptor channel blockers: implications for therapeutic potential. J Neurochem 64:614-623.

Portera-Cailliau C, Price DL, Martin LJ (1996) N-methyl-D-aspartate receptor proteins NR2A and NR2B are differentially distributed in the developing rat central nervous system as revealed by subunit-specific antibodies. J Neurochem 66:692-700.

Premkumar LS, Auerbach A (1997) Stoichiometry of recombinant N-methyl-D-aspartate receptor channels inferred from single-channel current patterns. J Gen Physiol 110:485-502.

Priestley T, Laughton P, Myers J, Le Bourdelles B, Kerby J, Whiting PJ (1995) Pharmacological properties of recombinant human N-methyl-D-aspartate receptors comprising NR1a/NR2A and NR1a/NR2B subunit assemblies expressed in permanently transfected mouse fibroblast cells. Mol Pharmacol 48:841-848.

Prince HC, Tzingounis AV, Levey AI, Conn PJ (2000) Functional downregulation of GluR2 in piriform cortex of kindled animals. Synapse 38:489-498.

Prince HK, Conn PJ, Blackstone CD, Huganir RL, Levey AI (1995) Down-regulation of AMPA receptor subunit GluR2 in amygdaloid kindling. J Neurochem 64:462-465.

Qiao X, Chen L, Gao H, Bao S, Hefti F, Thompson RF, Knusel B (1998) Cerebellar brain-derived neurotrophic factor-TrkB defect associated with impairment of eyeblink conditioning in Stargazer mutant mice. J Neurosci 18:6990-6999.

Qiao X, Hefti F, Knusel B, Noebels JL (1996) Selective failure of brain-derived neurotrophic factor mRNA expression in the cerebellum of stargazer, a mutant mouse with ataxia. J Neurosci 16:640-648.

Qiao X, Noebels JL (1993) Developmental analysis of hippocampal mossy fiber outgrowth in a mutant mouse with inherited spike-wave seizures. J Neurosci 13:4622-4635.

Ripellino JA, Neve RL, Howe JR (1998) Expression and heteromeric interactions of non-N-methyl-D-aspartate glutamate receptor subunits in the developing and adult cerebellum. Neuroscience 82:485-497.

Riva MA, Tascedda F, Molteni R, Racagni G (1994) Regulation of NMDA receptor subunit mRNA expression in the rat brain during postnatal development. Brain Res Mol Brain Res 25:209-216.

Robert A, Irizarry SN, Hughes TE, Howe JR (2001) Subunit interactions and AMPA receptor desensitization. J Neurosci 21:5574-5586.

Rogawski MA, Donevan SD (1999) AMPA receptors in epilepsy and as targets for antiepileptic drugs. Adv Neurol 79:947-963.

Rogers SW, Hughes TE, Hollmann M, Gasic GP, Deneris ES, Heinemann S (1991) The characterization and localization of the glutamate receptor subunit GluR1 in the rat brain. J Neurosci 11:2713-2724.

Rousset M, Cens T, Restituito S, Barrere C, Black JL, McEnery MW, Charnet P (2001) Functional roles of γ_2, γ_3 and γ_4, three new Ca^{2+} channel subunits, in P/Q-type Ca^{2+} channels expressed in *Xenopus* oocytes. J Physiol 532:583-593.

Rubio ME, Wenthold RJ (1999) Calnexin and the immunoglobulin binding protein (BiP) coimmunoprecipitate with AMPA receptors. J Neurochem 73:942-948.

Rubio ME, Wenthold RJ (1997) Glutamate receptors are selectively targeted to postsynaptic sites in neurons. Neuron 18:939-950.

Rudolph U, Crestani F, Mohler H (2001) $GABA_A$ receptor subtypes: dissecting their pharmacological functions. Trends Pharmacol Sci 22:188-194.

Sans N, Racca C, Petralia RS, Wang YX, McCallum J, Wenthold RJ (2001) Synapse-associated protein 97 selectively associates with a subset of AMPA receptors early in their biosynthetic pathway. J Neurosci 21:7506-7516.

Sato K, Kiyama H, Tohyama M (1993) The differential expression patterns of messenger RNAs encoding non-N-methyl-D-aspartate glutamate receptor subunits (GluR1-4) in the rat brain. Neuroscience 52:515-539.

Sattler R, Tymianski M (2001) Molecular mechanisms of glutamate receptor-mediated excitotoxic neuronal cell death. Mol Neurobiol 24:107-129.

Saxena NC, Macdonald RL (1994) Assembly of $GABA_A$ receptor subunits: role of the delta subunit. J Neurosci 14:7077-7086.

Schilling G, Coonfield ML, Ross CA, Borchelt DR (2001) Coenzyme Q10 and remacemide hydrochloride ameliorate motor deficits in a Huntington's disease transgenic mouse model. Neurosci Lett 315:149-153.

Schnell E, Sizemore M, Karimzadegan S, Chen L, Bredt DS, Nicoll RA (2002) Direct interactions between PSD-95 and stargazin control synaptic AMPA receptor number. Proc Natl Acad Sci USA 99:13902-13907.

Schoepp DD, Lodge D, Bleakman D, Leander JD, Tizzano JP, Wright RA, Palmer AJ, Salhoff CR, Ornstein PL (1995) In vitro and in vivo antagonism of AMPA receptor activation by (3S, 4aR, 6R, 8aR)-6-[2-(1(2)H-tetrazole-5-yl) ethyl] decahydroisoquinoline-3-carboxylic acid. Neuropharmacology 34:1159-1168.

Schofield PR, Darlison MG, Fujita N, Burt DR, Stephenson FA, Rodriguez H, Rhee LM, Ramachandran J, Reale V, Glencorse TA, et al. (1987) Sequence and functional expression of the GABA A receptor shows a ligand-gated receptor super-family. Nature 328:221-227.

Schwarzer C, Tsunashima K, Wanzenbock C, Fuchs K, Sieghart W, Sperk G (1997) $GABA_A$ receptor subunits in the rat hippocampus II: altered distribution in kainic acid-induced temporal lobe epilepsy. Neuroscience 80:1001-1017.

273

Scotti AL, Reuter H (2001) Synaptic and extrasynaptic γ-aminobutyric acid type A receptor clusters in rat hippocampal cultures during development. Proc Natl Acad Sci U S A 98:3489-3494.

Serafini R, Bracamontes J, Steinbach JH (2000) Structural domains of the human GABA$_A$ receptor β3 subunit involved in the actions of pentobarbital. J Physiol 524:649-676.

Sharp AH, Black JL, Dubel SJ, Sundarraj S, Shen J, Yunker AM, Copeland TD, McEnery MW (2001) Biochemical and anatomical evidence for specialized voltage-dependent calcium channel γ isoform expression in the epileptic and ataxic mouse, stargazer. Neuroscience 105:599-617.

Sheardown MJ, Suzdak PD, Nordholm L (1993) AMPA, but not NMDA, receptor antagonism is neuroprotective in gerbil global ischaemia, even when delayed 24 h. Eur J Pharmacol 236:347-353.

Sheardown MJ, Nielsen EO, Hansen AJ, Jacobsen P, Honore T (1990) 2,3-Dihydroxy-6-nitro-7-sulfamoyl-benzo(F)quinoxaline: a neuroprotectant for cerebral ischemia. Science 247:571-574.

Shen L, Liang F, Walensky LD, Huganir RL (2000) Regulation of AMPA receptor GluR1 subunit surface expression by a 4.1N-linked actin cytoskeletal association. J Neurosci 20:7932-7940.

Shi SH, Hayashi Y, Petralia RS, Zaman SH, Wenthold RJ, Svoboda K, Malinow R (1999) Rapid spine delivery and redistribution of AMPA receptors after synaptic NMDA receptor activation. Science 284:1811-1816.

Shimizu-Sasamata M, Kawasaki-Yatsugi S, Okada M, Sakamoto S, Yatsugi S, Togami J, Hatanaka K, Ohmori J, Koshiya K, Usuda S, Murase K (1996) YM90K: pharmacological characterization as a selective and potent alpha-amino-3-hydroxy-

5-methylisoxazole-4-propionate/kainate receptor antagonist. J Pharmacol Exp Ther 276:84-92.

Shingai R, Sutherland ML, Barnard EA (1991) Effects of subunit types of the cloned $GABA_A$ receptor on the response to a neurosteroid. Eur J Pharmacol 206:77-80.

Shoulson I, Penney J, McDermott M, Schwid S, Kayson E, Chase T, Fahn S, Greenamyre JT, Lang A, Siderowf A, Pearson N, Harrison M, Rost E, Colcher A, Lloyd M, Matthews M, Pahwa R, McGuire D, Lew MF, Schuman S, Marek K, Broshjeit S, Factor S, Brown D, Feigin A, Mazurkiewicz J, Ford B, Jennings D, Dilllon S, Comella C, Blasucci L, Janko K, Shulman L, Wiener W, Bateman-Rodriguez D, Carrion A, Suchowersky O, Lafontaine AL, Pantella C, Siemers E, Belden J, Davies R, Lannon M, Grimes D, Gray P, Martin W, Kennedy L, Adler C, Newman S, Hammerstad J, Stone C, Lewitt P, Bardram K, Mistura K, Miyasaki J, Johnston L, Cha JH, Tennis M, Panniset M, Hall J, Tetrud J, Friedlander J, Hauser R, Gauger L, Rodnitzky R, Deleo A, Dobson J, Seeberger L, Dingmann C, Tarsy D, Ryan P, Elmer L, Ruzicka D, Stacy M, Brewer M, Locke B, Baker D, Casaceli C, Day D, Florack M, Hodgeman K, Laroia N, Nobel R, Orme C, Rexo L, Rothenburgh K, Sulimowicz K, Watts A, Wratni E, Tariot P, Cox C, Leventhal C, Alderfer V, Craun AM, Frey J, McCree L, McDermott J, Cooper J, Holdich T, Read B (2001) A randomized, controlled trial of remacemide for motor fluctuations in Parkinson's disease. Neurology 56:455-462.

Shuttleworth CW, Connor JA (2001) Strain-dependent differences in calcium signaling predict excitotoxicity in murine hippocampal neurons. J Neurosci 21:4225-4236.

Sieghart W, Sperk G (2002) Subunit composition, distribution and function of $GABA_A$ receptor subtypes. Curr Top Med Chem 2:795-816.

Sigel E, Stephenson FA, Mamalaki C, Barnard EA (1983) A gamma-aminobutyric acid/benzodiazepine receptor complex of bovine cerebral cortex. J Biol Chem 258:6965-6971.

Slany A, Zezula J, Tretter V, Sieghart W (1995) Rat β3 subunits expressed in human embryonic kidney 293 cells form high affinity [^{35}S] t-butylbicyclophosphorothionate binding sites modulated by several allosteric ligands of γ-aminobutyric acid type A receptors. Mol Pharmacol 48:385-391.

Small DL, Murray CL, Mealing GA, Poulter MO, Buchan AM, Morley P (1998) Brain derived neurotrophic factor induction of N-methyl-D-aspartate receptor subunit NR2A expression in cultured rat cortical neurons. Neurosci Lett 252:211-214.

Sommer B, Kohler M, Sprengel R, Seeburg PH (1991) RNA editing in brain controls a determinant of ion flow in glutamate-gated channels. Cell 67:11-19.

Sommer B, Keinanen K, Verdoorn TA, Wisden W, Burnashev N, Herb A, Kohler M, Takagi T, Sakmann B, Seeburg PH (1990) Flip and flop: a cell-specific functional switch in glutamate-operated channels of the CNS. Science 249:1580-1585.

Somogyi P, Fritschy JM, Benke D, Roberts JD, Sieghart W (1996) The γ2 subunit of the GABA$_A$ receptor is concentrated in synaptic junctions containing the α1 and β2/3 subunits in hippocampus, cerebellum and globus pallidus. Neuropharmacology 35:1425-1444.

Song DK, Choe B, Bae JH, Park WK, Han IS, Ho WK, Earm YE (1998) Brain-derived neurotrophic factor rapidly potentiates synaptic transmission through NMDA, but suppresses it through non-NMDA receptors in rat hippocampal neuron. Brain Res 799:176-179.

Sperk G, Schwarzer C, Tsunashima K, Fuchs K, Sieghart W (1997) GABA$_A$ receptor subunits in the rat hippocampus I: immunocytochemical distribution of 13 subunits. Neuroscience 80:987-1000.

Sprengel R, Suchanek B, Amico C, Brusa R, Burnashev N, Rozov A, Hvalby O, Jensen V, Paulsen O, Andersen P, Kim JJ, Thompson RF, Sun W, Webster LC, Grant SG, Eilers J, Konnerth A, Li J, McNamara JO, Seeburg PH (1998) Importance of the intracellular domain of NR2 subunits for NMDA receptor function in vivo. Cell 92:279-289.

Srivastava S, Osten P, Vilim FS, Khatri L, Inman G, States B, Daly C, DeSouza S, Abagyan R, Valtschanoff JG, Weinberg RJ, Ziff EB (1998) Novel anchorage of GluR2/3 to the postsynaptic density by the AMPA receptor-binding protein ABP. Neuron 21:581-591.

Stafstrom CE, Tandon P, Hori A, Liu Z, Mikati MA, Holmes GL (1997) Acute effects of MK801 on kainic acid-induced seizures in neonatal rats. Epilepsy Res 26:335-344.

Stensbol TB, Slok FA, Trometer J, Hurt S, Ebert B, Kjoller C, Egebjerg J, Madsen U, Diemer NH, Krogsgaard-Larsen P (1999) Characterization of a new AMPA receptor radioligand, [^{3}H] 2-amino-3-(3-carboxy-5-methyl-4-isoxazolyl)propionic acid. Eur J Pharmacol 373:251-262.

Stephenson FA, Duggan MJ (1991) Molecular approaches to the stucture and function of the GABA$_A$ receptors. In: Molecular Neurobiology: A Practical Approach (Chad J, Wheal H, eds), pp 183-204. Oxford: IRL Press.

Subramaniam S, Donevan SD, Rogawski MA (1996) Block of the N-methyl-D-aspartate receptor by remacemide and its des-glycine metabolite. J Pharmacol Exp Ther 276:161-168.

Sucher NJ, Akbarian S, Chi CL, Leclerc CL, Awobuluyi M, Deitcher DL, Wu MK, Yuan JP, Jones EG, Lipton SA (1995) Developmental and regional expression pattern of a novel NMDA receptor-like subunit (NMDAR-L) in the rodent brain. J Neurosci 15:6509-6520.

Suen PC, Wu K, Xu JL, Lin SY, Levine ES, Black IB (1998) NMDA receptor subunits in the postsynaptic density of rat brain: expression and phosphorylation by endogenous protein kinases. Brain Res Mol Brain Res 59:215-228.

Suen PC, Wu K, Levine ES, Mount HT, Xu JL, Lin SY, Black IB (1997) Brain-derived neurotrophic factor rapidly enhances phosphorylation of the postsynaptic N-methyl-D-aspartate receptor subunit 1. Proc Natl Acad Sci U S A 94:8191-8195.

Sugihara H, Moriyoshi K, Ishii T, Masu M, Nakanishi S (1992) Structures and properties of seven isoforms of the NMDA receptor generated by alternative splicing. Biochem Biophys Res Commun 185:826-832.

Sun L, Margolis FL, Shipley MT, Lidow MS (1998) Identification of a long variant of mRNA encoding the NR3 subunit of the NMDA receptor: its regional distribution and developmental expression in the rat brain. FEBS Lett 441:392-396.

Sur C, Farrar SJ, Kerby J, Whiting PJ, Atack JR, McKernan RM (1999) Preferential coassembly of alpha4 and delta subunits of the γ-aminobutyric acid$_A$ receptor in rat thalamus. Mol Pharmacol 56:110-115.

Sutcliffe MJ, Wo ZG, Oswald RE (1996) Three-dimensional models of non-NMDA glutamate receptors. Biophys J 70:1575-1589.

Swedberg MD, Jacobsen P, Honore T (1995) Anticonvulsant, anxiolytic and discriminative effects of the AMPA antagonist 2,3-dihydroxy-6-nitro-7-sulfamoyl-benzo(f)quinoxaline (NBQX). J Pharmacol Exp Ther 274:1113-1121.

Tai LS, Ng TK, Mak NK, Yung KK (2001) Co-localization of AMPA-type glutamate receptor immunoreactivity in neurons of the rat subthalamic nucleus. Brain Res 895:95-103.

Takagi N, Logan R, Teves L, Wallace MC, Gurd JW (2000) Altered interaction between PSD-95 and the NMDA receptor following transient global ischemia. J Neurochem 74:169-178.

Takahashi T, Feldmeyer D, Suzuki N, Onodera K, Cull-Candy SG, Sakimura K, Mishina M (1996) Functional correlation of NMDA receptor epsilon subunits expression with the properties of single-channel and synaptic currents in the developing cerebellum. J Neurosci 16:4376-4382.

Thompson C, Drewery D, Atkins H, Stephenson F, Chazot P (2002a) Immunohistochemical localization of N-methyl-D-aspartate receptor subunits in the adult murine hippocampal formation: evidence for a unique role of the NR2D subunit. Brain Res Mol Brain Res 102:55.

Thompson CL, Ives JH, Drewery DL, Seighart W, Tiwari P, Wright MF, Lucocq JM (2002b) Stargazin and its role in the expression, assembly and trafficking of cerebellar granule cell-specific GABA$_A$ receptor subtypes. Soc Neurosci Abstr:433.413.

Thompson CL, Drewery DL, Atkins HD, Stephenson FA, Chazot PL (2000) Immunohistochemical localization of N-methyl-D-aspartate receptor NR1, NR2A, NR2B and NR2C/D subunits in the adult mammalian cerebellum. Neurosci Lett 283:85-88.

Thompson CL, Tehrani MHJ, Barnes EM, Jr., Stephenson FA (1998) Decreased expression of GABA$_A$ receptor α_6 and β_3 subunits in stargazer mutant mice: a possible role for brain-derived neurotrophic factor in the regulation of cerebellar GABA$_A$ receptor expression? Brain Res Mol Brain Res 60:282-290.

Thompson CL, Pollard S, Stephenson FA (1996) Developmental regulation of expression of GABA$_A$ receptor α_1 and α_6 subunits in cultured rat cerebellar granule cells. Neuropharmacology 35:1337-1346.

Thompson CL, Stephenson FA (1994) GABA$_A$ receptor subtypes expressed in cerebellar granule cells: a developmental study. J Neurochem 62:2037-2044.

Thompson CL, Bodewitz G, Stephenson FA, Turner JD (1992) Mapping of GABA$_A$ receptor α_5 and α_6 subunit-like immunoreactivity in rat brain. Neurosci Lett 144:53-56.

Thompson RF, Kim JJ (1996) Memory systems on the brain and localization of a memory. Proc Natl Acad Sci U S A 93:13438-13444.

Tiwari P, Ives JH, Thompson CL (2001) Impaired AMPA receptor expression in stargazer mice: evidence of stargazin-AMPAR complexes *in vivo*. British Neurosci Assoc Abstr 16:77 (29.02).

Tocco G, Annala AJ, Baudry M, Thompson RF (1992) Learning of a hippocampal-dependent conditioning task changes the binding properties of AMPA receptors in rabbit hippocampus. Behav Neural Biol 58:222-231.

Tocco G, Devgan KK, Hauge SA, Weiss C, Baudry M, Thompson RF (1991) Classical conditioning selectively increases AMPA receptor binding in rabbit hippocampus. Brain Res 559:331-336

Tortella FC, Hill RG (1996) EEG seizure activity and behavioral neurotoxicity produced by (+)-MK801, but not the glycine site antagonist L-687,414, in the rat. Neuropharmacology 35:441-448.

Tovar KR, Sprouffske K, Westbrook GL (2000) Fast NMDA receptor-mediated synaptic currents in neurons from mice lacking the $\epsilon 2$ (NR2B) subunit. J Neurophysiol 83:616-620.

Tretter V, Ehya N, Fuchs K, Sieghart W (1997) Stoichiometry and assembly of a recombinant GABA$_A$ receptor subtype. J Neurosci 17:2728-2737.

Tretter V, Hauer B, Nusser Z, Mihalek RM, Hoger H, Homanics GE, Somogyi P, Sieghart W (2001) Targeted disruption of the GABA$_A$ receptor δ subunit gene leads to an up-regulation of γ$_2$ subunit-containing receptors in cerebellar granule cells. J Biol Chem 276:10532-10538.

Trussell LO, Zhang S, Raman IM (1993) Desensitization of AMPA receptors upon multiquantal neurotransmitter release. Neuron 10:1185-1196.

Tsunashima K, Schwarzer C, Kirchmair E, Sieghart W, Sperk G (1997) GABA$_A$ receptor subunits in the rat hippocampus III: altered messenger RNA expression in kainic acid-induced epilepsy. Neuroscience 80:1019-1032.

Tsuzuki K, Isa T, Ozawa S (2000) Subunit composition of AMPA receptors expressed by single hippocampal neurons. Neuroreport 11:3583-3587.

Umemura K, Shimakura A, Nakashima M (1997) Neuroprotective effect of a novel AMPA receptor antagonist, YM90K, in rat focal cerebral ischaemia. Brain Res 773:61-65.

Usman N, Tarabykin V, Gruss P (2000) The novel PCR-based technique of genotyping applied to identification of scrambler mutation in mice. Brain Res Brain Res Protoc 5:243-247.

Valtschanoff JG, Burette A, Davare MA, Leonard AS, Hell JW, Weinberg RJ (2000) SAP97 concentrates at the postsynaptic density in cerebral cortex. Eur J Neurosci 12:3605-3614.

van Luijtelaar EL, Coenen AM (1995) Effects of remacemide and its metabolite FPL 12495 on spike-wave discharges, electroencephalogram and behaviour in rats with absence epilepsy. Neuropharmacology 34:419-425.

Vilquin JT, Vignier N, Tremblay JP, Engvall E, Schwartz K, Fiszman M (2000) Identification of homozygous and heterozygous dy2J mice by PCR. Neuromuscul Disord 10:59-62.

Vissavajjhala P, Janssen WG, Hu Y, Gazzaley AH, Moran T, Hof PR, Morrison JH (1996) Synaptic distribution of the AMPA-GluR2 subunit and its colocalization with calcium-binding proteins in rat cerebral cortex: an immunohistochemical study using a GluR2-specific monoclonal antibody. Exp Neurol 142:296-312.

Wafford KA, Kathoria M, Bain CJ, Marshall G, Le Bourdelles B, Kemp JA, Whiting PJ (1995) Identification of amino acids in the N-methyl-D-aspartate receptor NR1 subunit that contribute to the glycine binding site. Mol Pharmacol 47:374-380.

Wafford KA, Bain CJ, Le Bourdelles B, Whiting PJ, Kemp JA (1993) Preferential co-assembly of recombinant NMDA receptors composed of three different subunits. Neuroreport 4:1347-1349.

Wahl P, Madsen U, Banke T, Krogsgaard-Larsen P, Schousboe A (1996) Different characteristics of AMPA receptor agonists acting at AMPA receptors expressed in Xenopus oocytes. Eur J Pharmacol 308:211-218.

Wang YH, Bosy TZ, Yasuda RP, Grayson DR, Vicini S, Pizzorusso T, Wolfe BB (1995) Characterization of NMDA receptor subunit-specific antibodies: distribution of NR2A and NR2B receptor subunits in rat brain and ontogenic profile in the cerebellum. J Neurochem 65:176-183.

Watanabe D, Inokawa H, Hashimoto K, Suzuki N, Kano M, Shigemoto R, Hirano T, Toyama K, Kaneko S, Yokoi M, Moriyoshi K, Suzuki M, Kobayashi K, Nagatsu T, Kreitman RJ, Pastan I, Nakanishi S (1998a) Ablation of cerebellar Golgi cells disrupts synaptic integration involving GABA inhibition and NMDA receptor activation in motor coordination. Cell 95:17-27.

Watanabe M, Fukaya M, Sakimura K, Manabe T, Mishina M, Inoue Y (1998b) Selective scarcity of NMDA receptor channel subunits in the stratum lucidum (mossy fibre-recipient layer) of the mouse hippocampal CA3 subfield. Eur J Neurosci 10:478-487.

Wenthold RJ, Petralia RS, Blahos J, II, Niedzielski AS (1996) Evidence for multiple AMPA receptor complexes in hippocampal CA1/CA2 neurons. J Neurosci 16:1982-1989.

Wenthold RJ, Yokotani N, Doi K, Wada K (1992) Immunochemical characterization of the non-NMDA glutamate receptor using subunit-specific antibodies. Evidence for a hetero-oligomeric structure in rat brain. J Biol Chem 267:501-507.

Wenzel A, Fritschy JM, Mohler H, Benke D (1997) NMDA receptor heterogeneity during postnatal development of the rat brain: differential expression of the NR2A, NR2B, and NR2C subunit proteins. J Neurochem 68:469-478.

Wenzel A, Villa M, Mohler H, Benke D (1996) Developmental and regional expression of NMDA receptor subtypes containing the NR2D subunit in rat brain. J Neurochem 66:1240-1248.

Wenzel A, Scheurer L, Kunzi R, Fritschy JM, Mohler H, Benke D (1995) Distribution of NMDA receptor subunit proteins NR2A, 2B, 2C and 2D in rat brain. Neuroreport 7:45-48.

Wessel D, Flugge UI (1984) A method for the quantitative recovery of protein in dilute solution in the presence of detergents and lipids. Anal Biochem 138:141-143.

Whiting PJ, McAllister G, Vassilatis D, Bonnert TP, Heavens RP, Smith DW, Hewson L, O'Donnell R, Rigby MR, Sirinathsinghji DJ, Marshall G, Thompson SA, Wafford KA, Vasilatis D (1997) Neuronally restricted RNA splicing regulates the expression of a novel GABA$_A$ receptor subunit conferring atypical functional properties. J Neurosci 17:5027-5037.

Wilding TJ, Huettner JE (1996) Antagonist pharmacology of kainate- and α-amino-3-hydroxy-5-methyl-4-isoxazolepropionic acid-preferring receptors. Mol Pharmacol 49:540-546.

Williams K (1993) Ifenprodil discriminates subtypes of the N-methyl-D-aspartate receptor: selectivity and mechanisms at recombinant heteromeric receptors. Mol Pharmacol 44:851-859.

Wisden W, Herb A, Wieland H, Keinanen K, Luddens H, Seeburg PH (1991) Cloning, pharmacological characteristics and expression pattern of the rat GABA$_A$ receptor α$_4$ subunit. FEBS Lett 289:227-230.

Wong EH, Knight AR, Woodruff GN (1988) [^{3}H] MK-801 labels a site on the N-methyl-D-aspartate receptor channel complex in rat brain membranes. J Neurochem 50:274-281.

Wong LA, Mayer ML, Jane DE, Watkins JC (1994) Willardiines differentiate agonist binding sites for kainate- versus AMPA-preferring glutamate receptors in DRG and hippocampal neurons. J Neurosci 14:3881-3897.

Wong LA, Mayer ML (1993) Differential modulation by cyclothiazide and concanavalin A of desensitization at native α-amino-3-hydroxy-5-methyl-4-isoxazolepropionic acid- and kainate-preferring glutamate receptors. Mol Pharmacol 44:504-510.

Wroblewski JT, Fadda E, Mazzetta J, Lazarewicz JW, Costa E (1989) Glycine and D-serine act as positive modulators of signal transduction at N-methyl-D-aspartate sensitive glutamate receptors in cultured cerebellar granule cells. Neuropharmacology 28:447-452.

Wu G, Malinow R, Cline HT (1996) Maturation of a central glutamatergic synapse. Science 274:972-976.

Wyszynski M, Kim E, Dunah AW, Passafaro M, Valtschanoff JG, Serra-Pages C, Streuli M, Weinberg RJ, Sheng M (2002) Interaction between GRIP and Liprin-alpha/SYD2 Is Required for AMPA Receptor Targeting. Neuron 34:39-52.

Wyszynski M, Valtschanoff JG, Naisbitt S, Dunah AW, Kim E, Standaert DG, Weinberg R, Sheng M (1999) Association of AMPA receptors with a subset of glutamate receptor-interacting protein *in vivo*. J Neurosci 19:6528-6537.

Yamada K, Fukaya M, Shimizu H, Sakimura K, Watanabe M (2001) NMDA receptor subunits GluRϵ1, GluRe3 and GluRζ1 are enriched at the mossy fibre-granule cell synapse in the adult mouse cerebellum. Eur J Neurosci 13:2025-2036.

Yamada MK, Nakanishi K, Ohba S, Nakamura T, Ikegaya Y, Nishiyama N, Matsuki N (2002) Brain-derived neurotrophic factor promotes the maturation of GABAergic mechanisms in cultured hippocampal neurons. J Neurosci 22:7580-7585.

Yamaguchi S, Donevan SD, Rogawski MA (1993) Anticonvulsant activity of AMPA/kainate antagonists: comparison of GYKI 52466 and NBOX in maximal electroshock and chemoconvulsant seizure models. Epilepsy Res 15:179-184.

Yang W, Drewe JA, Lan NC (1995) Cloning and characterization of the human GABA$_A$ receptor α_4 subunit: identification of a unique diazepam-insensitive binding site. Eur J Pharmacol 291:319-325.

Ye B, Liao D, Zhang X, Zhang P, Dong H, Huganir RL, Torres R, Firestein BL, Staudinger J, Olson EN, Bredt DS, Gale NW, Yancopoulos GD (2000) GRASP-1: a neuronal RasGEF associated with the AMPA receptor/GRIP complex. Neuron 26:603-617.

Yeo CH (1991) Cerebellum and classical conditioning of motor responses. Ann N Y Acad Sci 627:292-304.

Zezula J, Slany A, Sieghart W (1996) Interaction of allosteric ligands with GABA$_A$ receptors containing one, two, or three different subunits. Eur J Pharmacol 301:207-214.

Zhang D, Pan ZH, Awobuluyi M, Lipton SA (2001) Structure and function of GABA$_C$ receptors: a comparison of native versus recombinant receptors. Trends Pharmacol Sci 22:121-132.

Zhao HM, Wenthold RJ, Petralia RS (1998) Glutamate receptor targeting to synaptic populations on Purkinje cells is developmentally regulated. J Neurosci 18:5517-5528.

Zhu JJ, Esteban JA, Hayashi Y, Malinow R (2000) Postnatal synaptic potentiation: delivery of GluR4-containing AMPA receptors by spontaneous activity. Nat Neurosci 3:1098-1106.

Zhu WJ, Wang JF, Krueger KE, Vicini S (1996) δ subunit inhibits neurosteroid modulation of GABA$_A$ receptors. J Neurosci 16:6648-6656.